

VOL. 641 NO. 2 JULY 9, 1993

THIS ISSUE COMPLETES VOL. 641

JOURNAL OF

CHROMATOGRAPHY

INCLUDING ELECTROPHORESIS AND OTHER SEPARATION METHODS

EDITORS

U.A.Th. Brinkman (Amsterdam)
 R.W. Giese (Boston, MA)
 J.K. Haken (Kensington, N.S.W.)
 K. Macek (Prague)
 L.R. Snyder (Orinda, CA)

EDITORS, SYMPOSIUM VOLUMES,
 E. Heftmann (Orinda, CA), Z. Deyl (Prague)

EDITORIAL BOARD

D.W. Armstrong (Rolla, MO)
 W.A. Aue (Halifax)
 P. Boček (Brno)
 A.A. Boulton (Saskatoon)
 P.W. Carr (Minneapolis, MN)
 N.H.C. Cooke (San Ramon, CA)
 V.A. Davankov (Moscow)
 Z. Deyl (Prague)
 S. Dilli (Kensington, N.S.W.)
 H. Engelhardt (Saarbrücken)
 F. Erni (Basle)
 M.B. Evans (Hatfield)
 J.L. Glajch (N. Billerica, MA)
 G.A. Guiochon (Knoxville, TN)
 P.R. Haddad (Hobart, Tasmania)
 I.M. Hais (Hradec Králove)
 W.S. Hancock (San Francisco, CA)
 S. Hjertén (Uppsala)
 S. Honda (Higashi-Osaka)
 Cs. Horváth (New Haven, CT)
 J.F.K. Huber (Vienna)
 K.P. Hupe (Waldbronn)
 T.W. Hutchens (Houston, TX)
 J. Janák (Brno)
 P. Jandera (Pardubice)
 B.L. Karger (Boston, MA)
 J.J. Kirkland (Newport, DE)
 E. sz. Kovats (Lausanne)
 A.J.P. Martin (Cambridge)
 L.W. McLaughlin (Chestnut Hill, MA)
 E.D. Morgan (Keele)
 J.D. Pearson (Kalamazoo, MI)
 H. Poppe (Amsterdam)
 F.E. Regnier (West Lafayette, IN)
 P.G. Righetti (Milan)
 P. Schoenmakers (Eindhoven)
 R. Schwarzenbach (Dübendorf)
 R.E. Shoup (West Lafayette, IN)
 R.P. Singhal (Wichita, KS)
 A.M. Sioffi (Marseille)
 D.J. Strydom (Boston, MA)
 N. Tanaka (Kyoto)
 S. Terabe (Hyogo)
 K. Unger (Mainz)
 A. Verpoorte (Leiden)
 Gy. Vigh (College Station, TX)
 J.T. Watson (East Lansing, MI)
 B.D. Westerlund (Uppsala)

EDITORS, BIBLIOGRAPHY SECTION

Z. Deyl (Prague), J. Janák (Brno), V. Schwartz (Prague)

ELSEVIER

JOURNAL OF CHROMATOGRAPHY

INCLUDING ELECTROPHORESIS AND OTHER SEPARATION METHODS

Scope. The *Journal of Chromatography* publishes papers on all aspects of **chromatography, electrophoresis** and related methods. Contributions consist mainly of research papers dealing with chromatographic theory, instrumental developments and their applications. The section *Biomedical Applications*, which is under separate editorship, deals with the following aspects: developments in and applications of chromatographic and electrophoretic techniques related to clinical diagnosis or alterations during medical treatment; screening and profiling of body fluids or tissues related to the analysis of active substances and to metabolic disorders; drug level monitoring and pharmacokinetic studies; clinical toxicology; forensic medicine; veterinary medicine; occupational medicine; results from basic medical research with direct consequences in clinical practice. In *Symposium volumes*, which are under separate editorship, proceedings of symposia on chromatography, electrophoresis and related methods are published.

Submission of Papers. The preferred medium of submission is on disk with accompanying manuscript (see *Electronic manuscripts* in the Instructions to Authors, which can be obtained from the publisher, Elsevier Science Publishers B.V., P.O. Box 330, 1000 AH Amsterdam, Netherlands). Manuscripts (in English; *four* copies are required) should be submitted to: Editorial Office of *Journal of Chromatography*, P.O. Box 681, 1000 AR Amsterdam, Netherlands, Telefax (+31-20) 5862 304, or to: The Editor of *Journal of Chromatography, Biomedical Applications*, P.O. Box 681, 1000 AR Amsterdam, Netherlands. Review articles are invited or proposed in writing to the Editors who welcome suggestions for subjects. An outline of the proposed review should first be forwarded to the Editors for preliminary discussion prior to preparation. Submission of an article is understood to imply that the article is original and unpublished and is not being considered for publication elsewhere. For copyright regulations, see below.

Publication. The *Journal of Chromatography* (incl. *Biomedical Applications*) has 40 volumes in 1993. The subscription prices for 1993 are:

J. Chromatogr. (incl. *Cum. Indexes, Vols. 601-650*) + *Biomed. Appl.* (Vols. 612-651):
Dfl. 8520.00 plus Dfl. 1320.00 (p.p.h.) (total ca. US\$ 5466.75)

J. Chromatogr. (incl. *Cum Indexes, Vols. 601-650*) only (Vols. 623-651):
Dfl. 7047.00 plus Dfl. 957.00 (p.p.h.) (total ca. US\$ 4446.75)

Biomed. Appl. only (Vols. 612-622):

Dfl. 2783.00 plus Dfl. 363.00 (p.p.h.) (total ca. US\$ 1747.75).

Subscription Orders. The Dutch guilder price is definitive. The US\$ price is subject to exchange-rate fluctuations and is given as a guide. Subscriptions are accepted on a prepaid basis only, unless different terms have been previously agreed upon. Subscriptions orders can be entered only by calendar year (Jan.-Dec.) and should be sent to Elsevier Science Publishers, Journal Department, P.O. Box 211, 1000 AE Amsterdam, Netherlands, Tel. (+31-20) 5803 642, Telefax (+31-20) 5803 598, or to your usual subscription agent. Postage and handling charges include surface delivery except to the following countries where air delivery via SAL (Surface Air Lift) mail is ensured: Argentina, Australia, Brazil, Canada, China, Hong Kong, India, Israel, Japan*, Malaysia, Mexico, New Zealand, Pakistan, Singapore, South Africa, South Korea, Taiwan, Thailand, USA. *For Japan air delivery (SAL) requires 25% additional charge of the normal postage and handling charge. For all other countries airmail rates are available upon request. Claims for missing issues must be made within six months of our publication (mailing) date, otherwise such claims cannot be honoured free of charge. Back volumes of the *Journal of Chromatography* (Vols. 1-611) are available at Dfl. 230.00 (plus postage). Customers in the USA and Canada wishing information on this and other Elsevier journals, please contact Journal Information Center, Elsevier Science Publishing Co. Inc., 655 Avenue of the Americas, New York, NY 10010, USA, Tel. (+1-212) 633 3750, Telefax (+1-212) 633 3764.

Abstracts/Contents Lists published in Analytical Abstracts, Biochemical Abstracts, Biological Abstracts, Chemical Abstracts, Chemical Titles, Chromatography Abstracts, Current Awareness in Biological Sciences (CABS), Current Contents/Life Sciences, Current Contents/Physical, Chemical & Earth Sciences, Deep-Sea Research/Part B: Oceanographic Literature Review, Excerpta Medica, Index Medicus, Mass Spectrometry Bulletin, PASCAL-CNRS, Referativnyi Zhurnal, Research Alert and Science Citation Index.

US Mailing Notice. *Journal of Chromatography* (ISSN 0021-9673) is published weekly (total 52 issues) by Elsevier Science Publishers (Sara Burgerhartstraat 25, P.O. Box 211, 1000 AE Amsterdam, Netherlands). Annual subscription price in the USA US\$ 4446.75 (subject to change), including air speed delivery. Second class postage paid at Jamaica, NY 11431. **USA**

POSTMASTERS: Send address changes to *Journal of Chromatography*, Publications Expediting, Inc., 200 Meacham Avenue, Elmont, NY 11003. Airfreight and mailing in the USA by Publications Expediting.

See inside back cover for Publication Schedule, Information for Authors and information on Advertisements.

© 1993 ELSEVIER SCIENCE PUBLISHERS B.V. All rights reserved.

0021-9673/93/\$06.00

No part of this publication may be reproduced, stored in a retrieval system or transmitted in any form or by any means, electronic, mechanical, photocopying, recording or otherwise, without the prior written permission of the publisher, Elsevier Science Publishers B.V., Copyright and Permissions Department, P.O. Box 521, 1000 AM Amsterdam, Netherlands.

Upon acceptance of an article by the journal, the author(s) will be asked to transfer copyright of the article to the publisher. The transfer will ensure the widest possible dissemination of information.

Special regulations for readers in the USA. This journal has been registered with the Copyright Clearance Center, Inc. Consent is given for copying of articles for personal or internal use, or for the personal use of specific clients. This consent is given on the condition that the copier pays through the Center the per-copy fee stated in the code on the first page of each article for copying beyond that permitted by Sections 107 or 108 of the US Copyright Law. The appropriate fee should be forwarded with a copy of the first page of the article to the Copyright Clearance Center, Inc., 27 Congress Street, Salem, MA 01970, USA. If no code appears in an article, the author has not given broad consent to copy and permission to copy must be obtained directly from the author. All articles published prior to 1980 may be copied for a per-copy fee of US\$ 2.25, also payable through the Center. This consent does not extend to other kinds of copying, such as for general distribution, resale, advertising and promotion purposes, or for creating new collective works. Special written permission must be obtained from the publisher for such copying.

No responsibility is assumed by the Publisher for any injury and/or damage to persons or property as a matter of products liability, negligence or otherwise, or from any use or operation of any methods, products, instructions or ideas contained in the materials herein. Because of rapid advances in the medical sciences, the Publisher recommends that independent verification of diagnoses and drug dosages should be made.

Although all advertising material is expected to conform to ethical (medical) standards, inclusion in this publication does not constitute a guarantee or endorsement of the quality or value of such product or of the claims made of it by its manufacturer.

This issue is printed on acid-free paper.

CONTENTS

(Abstracts/Contents Lists published in *Analytical Abstracts, Biochemical Abstracts, Biological Abstracts, Chemical Abstracts, Chemical Titles, Chromatography Abstracts, Current Awareness in Biological Sciences (CABS), Current Contents/Life Sciences, Current Contents/Physical, Chemical & Earth Sciences, Deep-Sea Research/Part B: Oceanographic Literature Review, Excerpta Medica, Index Medicus, Mass Spectrometry Bulletin, PASCAL-CNRS, Referativnyi Zhurnal, Research Alert and Science Citation Index*)

REGULAR PAPERS

Column Liquid Chromatography

- Siliceous sorbents with immobilized Carbowax 20M as column packings for liquid chromatography. I. Physico-chemical properties of siliceous materials with immobilized Carbowax 20M layer
by I. Choma, A.L. Dawidowicz, R. Dobrowolski and S. Pikus (Lublin, Poland) (Received February 19th, 1993) 205
- Siliceous sorbents with immobilized Carbowax 20M as column packings for liquid chromatography. II. Application in high-performance liquid chromatography
by I. Choma and A.L. Dawidowicz (Lublin, Poland) (Received February 19th, 1993) 211
- Detection systems with a photodiode-array detector for flow-injection and high-performance liquid chromatographic determination of phosphinate, phosphonate and diphosphonate
by T. Nakazato and N. Yoza (Fukuoka, Japan) (Received March 1st, 1993) 221
- Determination of stability constants of metal complexes from ion chromatographic measurements
by P. Janoš (Ústí nad Labem, Czech Republic) (Received March 15th, 1993) 229
- High-performance liquid chromatography of guanine and its nucleosides and nucleotides by pre-column fluorescence derivatization with phenylglyoxal reagent
by S. Yonekura, M. Iwasaki, M. Kai and Y. Ohkura (Fukuoka, Japan) (Received March 4th, 1993) 235
- Validation of improved methods for high-performance liquid chromatographic determination of phenylpropanolamine, dextromethorphan, guaifenesin and sodium benzoate in a cough-cold formulation
by T.D. Wilson (Evansville, IN, USA), W.G. Jump (Princeton, NJ, USA) and W.C. Neumann and T. San Martin (Lancaster, PA, USA) (Received March 25th, 1993) 241
- Isomeric separation of Beraprost sodium using an α_1 -acid glycoprotein column
by L.A. Sly, D.L. Reynolds and T.A. Walker (Kansas City, MO, USA) (Received March 30th, 1993) 249
- Enantiomeric separation of fluorescent, 6-aminoquinolyl-N-hydroxysuccinimidyl carbamate, tagged amino acids
by M. Pawlowska, S. Chen and D.W. Armstrong (Rolla, MO, USA) (Received February 16th, 1993) 257
- Optical resolution by high-performance liquid chromatography on benzylcarbamates of cellulose and amylose
by Y. Kaida and Y. Okamoto (Nagoya, Japan) (Received March 8th, 1993) 267
- Immobilized metal ion affinity partitioning of erythrocytes from different species in dextran-poly(ethylene glycol) aqueous phase systems
by H. Walter and K.E. Widen (Long Beach, CA, USA) and G. Birkenmeier (Leipzig, Germany) (Received March 23rd, 1993) 279
- Gas Chromatography*
- Quenching in the flame photometric detector
by W.A. Aue and X.-Y. Sun (Halifax, Canada) (Received March 8th, 1993) 291
- Thermodynamic study of polystyrene-*n*-alkane systems by inverse gas chromatography
by L. Bonifaci and G.P. Ravanetti (Mantova, Italy) (Received January 26th, 1993) 301
- High-resolution gas chromatographic-mass spectrometric determination of neutral chlorinated aromatic sulphur compounds in stack gas samples
by S. Sinkkonen, E. Kolehmainen, J. Koistinen and M. Lahtiperä (Jyväskylä, Finland) (Received March 25th, 1993) 309
- Capillary gas chromatography of acidic non-steroidal antiinflammatory drugs as *tert*.-butyldimethylsilyl derivatives
by K.-R. Kim, W.-H. Shim and Y.-J. Shin (Suwon, South Korea) and J. Park, S. Myung and J. Hong (Seoul, South Korea) (Received March 15th, 1993) 319

(Continued overleaf)

Contents (continued)

Supercritical Fluid Chromatography

Thermodynamic pitfalls in chromatography revisited: supercritical fluid chromatography by M. Roth (Brno, Czech Republic) (Received January 18th, 1993)	329
Comparison of flame ionization and inductively coupled plasma mass spectrometry for the detection of organometallics separated by capillary supercritical fluid chromatography by N.P. Vela and J.A. Caruso (Cincinnati, OH, USA) (Received February 24th, 1993)	337
Characterization of fuels by multi-dimensional supercritical fluid chromatography and supercritical fluid chromatography– mass spectrometry by P.E. Andersson, M. Demirbüker and L.G. Blomberg (Stockholm, Sweden) (Received March 23rd, 1993) . . .	347
High-speed supercritical fluid extraction method for routine measurement of polycyclic aromatic hydrocarbons in en- vironmental soils with dichloromethane as a static modifier by J. Dankers, M. Groenenboom, L.H.A. Scholtis and C. van der Heiden (Breda, Netherlands) (Received March 22nd, 1993)	357

Electrophoresis

Isotachopheresis superimposed on capillary zone electrophoresis by J.L. Beckers (Eindhoven, Netherlands) (Received March 8th, 1993)	363
Capillary electrophoresis with on-line sample pretreatment for the analysis of biological samples with direct injection by I. Morita (Hiroshima and Tokyo, Japan) and J.-I. Sawada (Tokyo, Japan) (Received March 16th, 1993)	375
Characterization of each isoform of a F(ab') ₂ by capillary electrophoresis by R. Vincentelli and N. Bihoreau (Les Ulis, France) (Received March 29th, 1993)	383

SHORT COMMUNICATIONS

Column Liquid Chromatography

New graph of binary mixture solvent strength in adsorption liquid chromatography by V.R. Meyer (Berne, Switzerland) and M.D. Palamareva (Sofia, Bulgaria) (Received March 23th, 1993)	391
Time- and cost-saving approach for liquid chromatography–mass spectrometry vacuum systems by J.T. Snodgrass, M.J. Hayward and M.L. Thomson (Princeton, NJ, USA) (Received April 15th, 1993)	396

Gas Chromatography

4-(Trifluoromethyl)-2,3,5,6-tetrafluorobenzyl bromide as a new electrophoric derivatizing reagent by M. Saha, J. Saha and R.W. Giese (Boston, MA, USA) (Received April 7th, 1993)	400
--	-----

BOOK REVIEW

Chromatographic retention indices—an aid to identification of organic compounds (by V. Pacáková and L. Feltl), reviewed by J.M. Takács (Budapest, Hungary)	405
---	-----

AUTHOR INDEX	408
------------------------	-----

Siliceous sorbents with immobilized Carbowax 20M as column packings for liquid chromatography

I. Physico-chemical properties of siliceous materials with immobilized Carbowax 20M layer

Irena Choma*, Andrzej L. Dawidowicz, Ryszard Dobrowolski and Stanisław Pikus

Faculty of Chemistry, Maria Curie-Skłodowska University, M. Curie-Skłodowska Square 3, 20-031 Lublin (Poland)

(First received April 15th, 1992; revised manuscript received February 19th, 1993)

ABSTRACT

For better stability the gas chromatographic stationary phase Carbowax 20M is often immobilized on different support materials. Some physico-chemical properties of siliceous supports with thermally immobilized Carbowax 20M are described. The results obtained point to the formation of acidic groups (centres) in the Carbowax layer during its immobilization procedure.

INTRODUCTION

The polyethylene glycol (PEG) Carbowax 20M is one of the most popular stationary phases used in gas chromatography (GC) [1–3], mainly from its very high selectivity towards many organic compounds. For instance, Carbowax 20M and all PEGs are superior to methylsilicone stationary phase for the separation of polar compounds differing only slightly in boiling temperatures [4]. The main disadvantages of Carbowax 20M result from its low thermal stability and low resistance to the destructive action of oxygen [1,2,4,5]. To minimize these shortcomings, various immobilization procedures are used. Thermal immobilization was described by Aue and co-workers [6–8]. In addition to the preparation conditions, they formulated a hypothesis concerning the mechanism of the bond-

ing of a Carbowax 20M chain to the siliceous surface [8,9].

Several years ago, Aue and co-workers' method was applied to the modification of controlled-porosity glasses differently enriched in boron atoms [10–12]. The sorbents obtained were characterized by means of the adsorption isotherms calculated from the GC data. A model of Carbowax 20M bonding, in agreement with that suggested by Aue and co-workers, was proposed [11]. It was also demonstrated that sorbents with thermally immobilized Carbowax 20M can be used as fillings of columns for HPLC [12]. These sorbents are characterized by good selectivity and reproducibility of capacity factors. They can be used for many analytical purposes, *e.g.*, in the analysis of phenols, steroids and benzodiazepines [12,13].

In spite of all earlier investigations, still very little is known about the structure of the immobilized Carbowax 20M layer and about the properties and application of such sorbents,

* Corresponding author.

especially in HPLC. The aim of this work was to obtain some physico-chemical and chromatographic properties of Carbowax 20M and to shed some more light on the structure of the immobilized layer.

The first part of this paper concerns the physico-chemical properties of sorbents with a Carbowax layer. These sorbents are compared with the initial materials (applied as supports of the investigated phase) and sorbents with adhesively deposited Carbowax 20M.

The second part considers mainly the chromatographic properties of chosen sorbents used as packings for (A) liquid adsorption chromatography in normal- and reversed-phase systems and (B) gel permeation chromatography. Additionally, sorbents with Carbowax 20M are compared with LiChrosorb DIOL, a sorbent of similar polarity. Finally, the properties of sorbents before and after chromatographic examination are discussed.

EXPERIMENTAL

Materials

Controlled-porosity glasses (CPGs) were prepared from Vycor-type glass consisting of 55% SiO₂, 35% B₂O₃ and 10% Na₂O. Separate portions of this material (120–150- μ m fractions) were converted into porous form by appropriate thermal treatment and leaching in sulphuric acid and sodium hydroxide solution. The details of the CPG preparation procedure have been described elsewhere [14,15]. In order to obtain packings for HPLC columns, porous glasses were additionally crushed and from the ground material a fraction of about 8 μ m was collected. Table I gives the physico-chemical properties of the prepared porous glasses (called CPG II and CPG III) and LiChrosorb Si-100 silica gel (Merck, Darmstadt, Germany). Carbowax 20M was bonded to all the siliceous materials as described [6,7,16,17]. Finally, the following materials were obtained: CPG II C; CPG III C and Si-100 C (where C represents the presence of bonded Carbowax 20M).

After the preparation procedure (but before the HPLC column packing procedure) the sorbents obtained were placed in a stainless-steel

column (300 \times 8 mm) thermostated at 60°C and washed with 250 ml each of hexane, chloroform and methanol at a flow-rate of 1 ml/min.

Methods

Specific surface area measurements were carried out using a Sorptomatic 1800 instrument (Carlo Erba, Milan, Italy). Mean pore diameters of the prepared sorbents were calculated on the basis of nitrogen adsorption-desorption hysteresis curve measured with the same instrument.

The amounts of bonded Carbowax 20M were calculated utilizing elemental analysis data. For this purpose a Model 185 CHN analyser (Hewlett-Packard, Palo Alto, CA, USA) was used.

Particle size fractionation was carried out using a Multi-Plex Laboratory Classifier 100 MZR (Alpina, Germany).

Potentiometric titrations were performed using an automatic titrator set (Radiometer, Copenhagen, Denmark). A PHM-64 digital pH meter with a G 202 C glass electrode and a K 4018 calomel reference electrode were used together with standard thermostated vessels. Titrations were carried out using 0.1 M NaOH and 0.1 M HCl at 298 \pm 0.5 K in a nitrogen atmosphere; 0.1 M NaCl was used as the supporting electrolyte. For each point on the potentiometric titration curve the equilibrium state with respect to the display of the pH meter was achieved. The surface charge density was evaluated as described elsewhere [18].

X-ray patterns of the investigated materials were obtained on a DRON-3 diffractometer using a Cu K α radiation lamp with a nickel filter.

RESULTS AND DISCUSSION

Table I gives the physico-chemical properties of two porous glasses CPG II and CPG III and LiChrosorb Si 100 silica gel. In addition to values of the specific surface areas (S_{BET}) and pore diameters (D_{max}) corresponding to the maximum of the pore-size distribution function, the values of the pore volumes ($V_{\text{p}}^{\text{ads}}$) and mean diameters ($D_{\text{c}}^{\text{ads}}$) calculated from the desorption (top rows) and adsorption (bottom rows) branches of the

TABLE I
PHYSICO-CHEMICAL PROPERTIES OF THE MATERIALS USED AS SUPPORTS OF IMMOBILIZED CARBOWAX 20M

S_{BET} = Specific surface area; D_{max} = pore diameter corresponding to the maximum of the pore size distribution function; $V_{\text{p}}^{\text{ads}}$ and $D_{\text{c}}^{\text{ads}}$ = pore volumes and mean diameters calculated from desorption (top rows) and adsorption (bottom rows) branch of the nitrogen isotherm.

Support	S_{BET} (m^2/g)	$V_{\text{p}}^{\text{des}}$ (cm^3/g)	$D_{\text{c}}^{\text{des}}$ (\AA)	D_{max} (\AA)
CPG II	228	1.01	180	150
		0.98	170	
CPG III	347	1.16	134	100
		1.13	131	
Si-100	318	1.32	165	140
		1.26	160	

nitrogen isotherm are also given. D_{c} values were calculated assuming that the pores had cylindrical shapes. Table II gives the related physico-chemical values for the sorbents obtained by immobilization of Carbowax 20M on CPG II and CPG III and on silica gel Si-100. The values of the amount of the polymer calculated per gram of the support or per square metre of its surface are also given. On the basis of the latter values, the thicknesses of the Carbowax layers (d_{t}) were calculated assuming that the density of Carbowax is 1.33 g/cm^3 .

As can be seen, the physico-chemical prop-

erties of the initial siliceous materials are very similar to one another. It was our intention to choose similar sorbents and to demonstrate that there is no essential difference whether silica gel or porous glass of similar properties is used as a support.

The similar values of $D_{\text{c}}^{\text{des}}$ and $D_{\text{c}}^{\text{ads}}$ and of $V_{\text{p}}^{\text{des}}$ and $V_{\text{p}}^{\text{ads}}$ indicate that there are no bottle-shaped pores. The materials with immobilized Carbowax 20M possess much lower specific surface areas and pore volumes; however, these data should be treated with some reserve, because in the calculations the same values were assumed for the areas occupied by a single adsorbed molecule (nitrogen) on pure siliceous surfaces and on supports with immobilized Carbowax. In addition, it is not certain whether nitrogen dissolves in the polymer layer to some extent. The D_{max} values for sorbents with immobilized Carbowax 20M are slightly lower than those for the initial sorbents. This is related to the presence of a Carbowax layer on the surface of the pores. The mean diameters D_{c} are larger for the sorbents with immobilized Carbowax 20M because the smallest pores are probably filled with polymer. The amount of immobilized Carbowax 20M is highest for CPG II C, which is especially evident when w/S values are taken into account. The values of w/S for CPG III C and Si-100 C are almost the same.

As was mentioned in the Introduction, Carbowax 20M possesses a low thermal stability, especially in the presence of oxygen. It is com-

TABLE II
PHYSICO-CHEMICAL PROPERTIES OF THE SORBENTS WITH IMMOBILIZED CARBOWAX 20M

w/w and w/S = polymer amounts calculated per gram and per square metre of the support; d_{t} = thickness of the Carbowax layer; other parameters as in Table I.

Sorbent	S_{BET} (m^2/g)	$V_{\text{p}}^{\text{des}}$ (cm^3/g)	$D_{\text{c}}^{\text{des}}$ (\AA)	D_{max} (\AA)	w/w ($\times 100$) (g/g)	w/S ($\times 100$) (g/m^2)	d_{t} (\AA)
CPG II C	57	0.37	250	130	58.58	0.256	19.2
		0.35	240				
CPG III C	92	0.39	175	100	53.49	0.154	11.6
		0.38	170				
Si-100 C	119	0.62	210	130	46.80	0.147	11.1
		0.61	205				

monly known that even a minimum content of oxygen in the carrier gas can cause oxidation and destruction of the Carbowax layer used as a stationary phase in a GC column [5]. It may lead to the formation of aldehyde, carboxyl [1,4,19] and oxirane groups [20] and consequently can change the surface properties. Similar phenomena may occur during thermal immobilization. Therefore, the modified materials were investigated in order to check whether such processes took place during their preparation procedure. For this purpose the potentiometric titration method was applied.

Potentiometric titration of a suspension of a solid provides much information about the structure and character of a solid surface [21], mainly about the charge surface density (σ) on the solid surface–electrolyte interface. Potentiometric titration of the following materials was performed: porous glass (CPG III), porous glass with immobilized Carbowax 20M (CPG III C), porous glass with adhesively deposited Carbowax 20M (CPG III C_{adh}) (with the same amount of stationary phase as for the materials with an immobilized Carbowax layer) and, for comparison, bulk Carbowax 20M and bulk Carbowax 20M additionally heated in a nitrogen atmosphere at 270°C (*i.e.*, at the same temperature as during the immobilization process). For both heated and non-heated Carbowax 20M the titration curves coincided with that obtained for the titration of pure electrolyte. This means that the samples possess zero charge in the investigated pH range. For the other samples values of the surface charge density (σ) were calculated according to ref. 18. Adhesively deposited Carbowax 20M dissolves in the electrolyte and probably only a monolayer of the polymer remains on the surface of porous glass, so the σ values were recalculated per gram of glass support, Q . Fig. 1 shows the Q vs. pH dependences for the three samples, (A) CPG III, (B) CPG III C_{adh} and (C) CPG III C.

In the pH range 2.5–5.5, CPG III and CPG III C_{adh} are characterized by virtually zero charge. Above pH 5.5 a gradual increase in negative charge is observed, suggesting the presence of acidic groups. The negative charge Q increases slightly quicker for CPG III than for CPG III

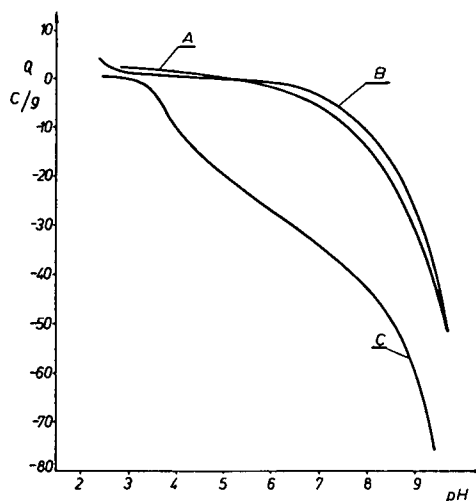


Fig. 1. Charge surface density vs. pH recalculated per gram of the support, Q , for (A) CPG III, (B) CPG III C_{adh} and (C) CPG III as a function of pH.

C_{adh} . This may result from the presence of the surface Carbowax layer which remains after dissolution of the excess amount of the deposited polymer. The course of curve C in Fig. 1 (glass with thermally immobilized Carbowax 20M) is completely different from those for curves A and B. The segment parallel to zero charge density is very short and at pH 3.5 a rapid increase in negative charge is observed, indicating the presence of strongly acidic groups. From pH 4 to about 8 a monotonic increase in negative charge is seen, suggesting the presence of several surface acidic groups of different strengths ranging from pK 4 to 8. It is probable that the mechanism of bonding of these groups (carboxyl?) to the surface is different, *e.g.*, by being attached directly or through the chains of various lengths. Similar shapes of the curves have been observed in the case of oxidized activated carbons [22]. The changes in the surface charge connected with the acidic groups being created during the immobilization process can be better presented as the difference (ΔQ) between the values for materials with thermally immobilized and adhesively deposited Carbowax 20M (Fig. 2). The rapid increase in the charge at pH 3.5 indicates a relatively high content of strongly acidic (pK 3.5) groups. This may mean that some of them are very close or even are clustered. From the

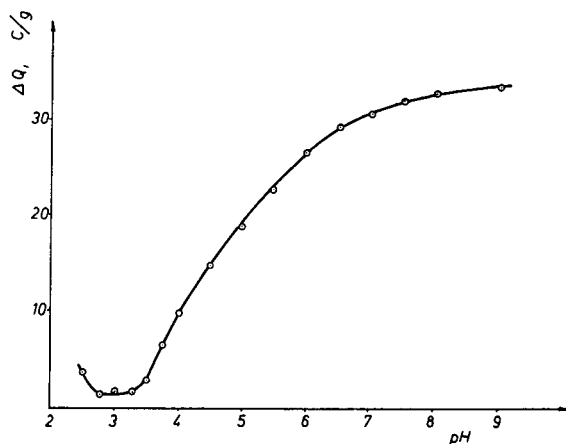


Fig. 2. Difference ΔQ between the surface charge densities recalculated per gram of the support for the material with thermally immobilized Carbowax 20M (see Fig. 1, curve C) and the material with adhesively deposited Carbowax 20M (see Fig. 1, curve B).

change in the surface charge and from the amount of the polymer, it is possible to estimate that one monoprotic acidic group lies every 40-mers ($\text{CH}_2\text{CH}_2\text{O}-$) in the Carbowax chain.

As was mentioned above, thermal immobilization of Carbowax 20M causes the partial oxidation and degradation of the polymer chain. It can be expected that carboxyl, aldehyde and oxirane groups are created. Moreover, it seems that not only temperature (270°C) and traces of oxygen are the main factors causing the formation of dissociating groups. The catalytic influence of the siliceous surface is very significant, as shown by the fact that Carbowax 20M heated at 270°C in the same nitrogen atmosphere but without the presence of silica does not show any ionic groups; as already mentioned, the titration curves for heated Carbowax and the electrolyte overlap one another.

In order to obtain additional information about the structure of the Carbowax layer immobilized on a siliceous surface, the X-ray patterns for Carbowax 20M, porous glass with an immobilized Carbowax 20M layer, porous glass with adhesively deposited Carbowax layer and pure porous glass supports were obtained (Fig. 3). The X-ray pattern for porous glass CPG III does not show any diffraction peaks because of the amorphous structure of the material. The

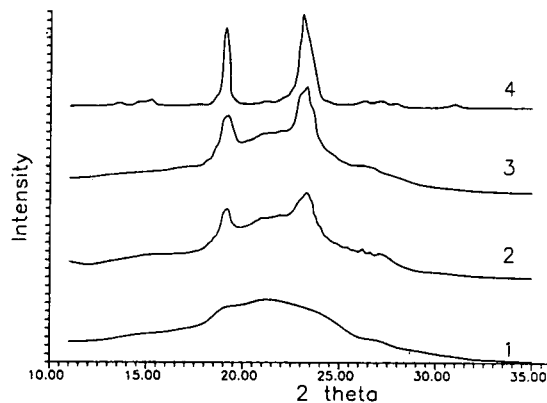


Fig. 3. X-ray diffraction patterns for: (1) CPG III, (2) CPG III C, (3) CPG III C_{adh} and (4) Carbowax 20M. The intensity of the X-ray diffraction patterns for Carbowax has been decreased about 15-fold.

diffractogram of Carbowax 20M possesses two strong peaks at $2\theta = 19.1^\circ$ and 23.2° . The same peaks are observed in the X-ray patterns of porous glass with immobilized and adhesively deposited Carbowax 20M (CPG III C and CPG III C_{adh}). It can be concluded that part of the immobilized and also part of the adhesively deposited Carbowax 20M are in a crystalline form, just as in bulk Carbowax. This means that some of the Carbowax 20M chains in the materials CPG III C and CPG III C_{adh} are positioned parallel. Quantitative diffraction analysis revealed about 4 wt.% of a crystalline form in CPG III C and about 5% in CPG III C_{adh} , which after recalculation gives about 11.5% and 14.5% of a crystalline form in immobilized and adhesively deposited Carbowax layers, respectively.

In contrast to the results obtained by potentiometric titration, from which different properties of materials with immobilized Carbowax and those with adhesively deposited polymer can be deduced, the X-ray patterns do not exhibit any essential differences between these materials.

CONCLUSIONS

Thermal immobilization of Carbowax 20M leads to changes in the physico-chemical properties of the initial material.

Potentiometric titration indicates the presence of acidic groups in the layer of immobilized

Carbowax. This suggests a destruction process in the polymer during immobilization. In addition to oxygen and temperature, the catalytic influence of the siliceous surface seems to be a very important factor in Carbowax degradation.

Part of the immobilized Carbowax 20M exists in a crystalline form as in the bulk Carbowax.

ACKNOWLEDGEMENT

We gratefully acknowledge many helpful suggestions by and discussions with Dr. W.J. Gelsema, Utrecht University, Netherlands.

REFERENCES

- 1 M. Horká, K. Janák and K. Tesarik, *Chem. Listy*, 83 (1989) 125.
- 2 J.A. Yancey, *J. Chromatogr. Sci.*, 24 (1986) 117
- 3 G. Castello and G. D'Amato, *J. Chromatogr.*, 90 (1974) 291
- 4 P.H. Silvis, J.W. Walsh and D.M. Shelow, *Am. Lab.*, 2 (1987) 41.
- 5 J.R. Conder, N.A. Fruitwala and M.K. Shingari, *J. Chromatogr.*, 269 (1983) 171.
- 6 M.M. Daniewski and W.A. Aue, *J. Chromatogr.*, 147 (1978) 119.
- 7 W.A. Aue, M.M. Daniewski, J. Müller and J.P. Laba, *Anal. Chem.*, 49 (1977) 1465.
- 8 W.A. Aue, C.R. Hastings and Sh. Kapila, *J. Chromatogr.*, 77 (1973) 299.
- 9 M.M. Daniewski and W.W. Aue, *J. Chromatogr.*, 147 (1978) 395.
- 10 I. Choma and A.L. Dawidowicz, in A. Waksmundzki (Editor), *Postępy Chromatografii w Polsce w Ostatnich Latach*, UMCS, Lublin, 1984, p. 177.
- 11 A.L. Dawidowicz, I. Choma and W.M. Buda, *Z. Phys. Chem.*, 268 (1987) 273.
- 12 I. Choma and A.L. Dawidowicz, *Chem. Anal. (Warsaw)*, 33 (1988) 313.
- 13 I. Choma, A.L. Dawidowicz and R. Lodkowski, *J. Chromatogr.*, 600 (1992) 109
- 14 A.L. Dawidowicz, A. Waksmundzki and A. Deryło, *Chem. Anal. (Warsaw)*, 24 (1979) 811.
- 15 W. Haller, *J. Phys. Chem.*, 42 (1965) 686.
- 16 M.M. Daniewski, *Habilitation Thesis*, Warsaw, 1978.
- 17 J.A. Jonnsson, L. Mathiesson and Z. Suprynowicz, *J. Chromatogr.*, 207 (1981) 69.
- 18 G.A. Parks and P.L. de Bruyn, *J. Phys. Chem.*, 66 (1962) 967.
- 19 H.E. Persinger and J.T. Shank, *J. Chromatogr. Sci.*, 11 (1973) 190.
- 20 M. Verzele, *J. High Resolut. Chromatogr. Chromatogr. Commun.*, 2 (1979) 647.
- 21 A.L. Dawidowicz, W. Janusz, J. Szczypa and A. Waksmundzki, *J. Colloid Interface Sci.*, 115 (1987) 555.
- 22 R. Dobrowolski, *Ph.D. Thesis*, UMCS, Lublin, 1988.

Siliceous sorbents with immobilized Carbowax 20M as column packings for liquid chromatography

II. Application in high-performance liquid chromatography

Irena Choma* and Andrzej L. Dawidowicz

Faculty of Chemistry, Maria Curie-Skłodowska University, M. Curie-Skłodowska Square 3, 20-031 Lublin (Poland)

(First received April 15th, 1992; revised manuscript received February 19th, 1993)

ABSTRACT

The chromatographic properties of siliceous supports with thermally immobilized Carbowax 20M as packings for high-performance liquid chromatography are described. Such materials were examined as sorbents in normal- and reversed-phase chromatographic systems and as macromolecular sieves for size-exclusion chromatography of biopolymers. Additionally, the stability of the Carbowax layer was determined.

INTRODUCTION

Carbowax 20M is one of the most popular stationary phases applied in gas chromatography (GC) [1], owing to its very high selectivity in relation to many compounds, especially to those differing only slightly in polarity or boiling temperatures. The application range of Carbowax 20M has been increased by introducing various immobilization procedures [2–10]. Such phases are mainly employed in GC and sorbents with immobilized Carbowax 20M have hardly been used in HPLC.

This paper deals with chromatographic properties of siliceous sorbents with thermally immobilized Carbowax 20M as packings for HPLC.

Synthesized materials were investigated as sorbents in normal- and reversed-phase systems and as macromolecular sieves for the size-exclusion chromatography of biopolymers. In addition, the stability of packings with thermally immobilized Carbowax 20M is discussed.

EXPERIMENTAL

Materials

The preparation and synthesis of materials used in this experiment were described in Part I [11]. LiChrosorb DIOL (Merck, Darmstadt, Germany) taken additionally for the comparison (abbreviated here to Si-Diol), was characterized by the following data: $S_{\text{BET}} = 229 \text{ m}^2/\text{g}$, $V_{\text{p}}^{\text{des}} = 0.90 \text{ cm}^3/\text{g}$, $V_{\text{p}}^{\text{ads}} = 0.88 \text{ cm}^3/\text{g}$, $D_{\text{c}}^{\text{des}} = 157 \text{ \AA}$, $D_{\text{c}}^{\text{ads}} = 154 \text{ \AA}$ and $D_{\text{max}} = 108 \text{ \AA}$. The particle

* Corresponding author.

size of Si-Diol and other sorbents was 10 μm . The plate numbers (N) (calculated from the band width at half-height of the nitrobenzene peak using hexane as mobile phase) and the peak asymmetry factors A_s (calculated for the same peak at 5% of the peak height) were as follows:

	CPG II	CPG III	Si-100	CPG II C	CPG III C	Si-100 C	Si-Diol
$N =$	5600	5350	4300	4350	3900	2400	1600
$A_s =$	1.35	1.80	1.00	1.25	1.00	1.00	1.00

Protein standards (Kit MS II) were purchased from Serva (Heidelberg, Germany).

Methods

HPLC investigations were carried out using a Liquochrom 2010 liquid chromatograph (MIM, Budapest, Hungary) with a UV detector (254 nm).

The mobile phases used were pure hexane, methanol–2-propanol–hexane (10:30:60) and methanol–water (50:50, 40:60 and 30:70). In size-exclusion chromatography, 0.1 M NaH_2PO_4 buffer (pH 6.8) was applied. The flow-rate was 1 ml/min. Stainless-steel columns (250 \times 4 mm I.D.) were packed using the balanced density slurry method.

Methods for the determination of specific surface areas, mean pore diameters and amounts of Carbowax were described in Part I [11].

RESULTS AND DISCUSSION

Immobilized Carbowax 20M in a normal-phase HPLC system

As mentioned in Part I [11], sorbents with thermally immobilized Carbowax 20M can be successfully employed in HPLC [12–14]. In order to elucidate their mechanism in a normal-phase system, the separation of aromatic hydrocarbons performed on columns filled with materials with an immobilized Carbowax layer were compared with analogous separations obtained on columns packed with pure silica sorbents.

Table I gives capacity factors (k') of aromatic hydrocarbons analysed on the sorbents CPG II, CPG III, Si-100, CPG II C, CPG III C, Si-100 C, Si-Diol (see Part I [11]). For better illustration, Fig. 1 shows related chromatograms obtained on the chosen sorbents. As can be seen, both retention times and k' values obtained on the sorbents with immobilized Carbowax 20M are much lower than those obtained on the initial materials, *i.e.*, CPG II, CPG III and Si-100. This is most evident for polar nitrobenzene. The peaks are well separated, narrow and symmetrical; however, naphthalene and diphenyl elute in a common band. A very similar separation to those obtained on the materials with immobilized Carbowax was obtained using Si-Diol as a column filling.

As was mentioned in the Introduction, sor-

TABLE I

CAPACITY FACTORS (k') OF AROMATIC HYDROCARBONS ON COLUMNS PACKED WITH THE INVESTIGATED SORBENTS

Mobile phase: hexane.

Compound	k'						
	CPG II C	CPG III C	Si-100 C	Si-Diol	CPG II	CPG III	Si-100
Benzene	0.07	0.15	0.07	0.16	0.19	0.32	0.29
Naphthalene	0.19	0.34	0.25	0.32	0.37	0.57	0.50
Diphenyl	0.19	0.34	0.25	0.32	0.56	0.84	0.69
Anthracene	0.50	0.82	0.70	0.57	0.69	1.01	0.90
Nitrobenzene	1.14	1.91	1.50	0.93	4.59	6.25	5.10

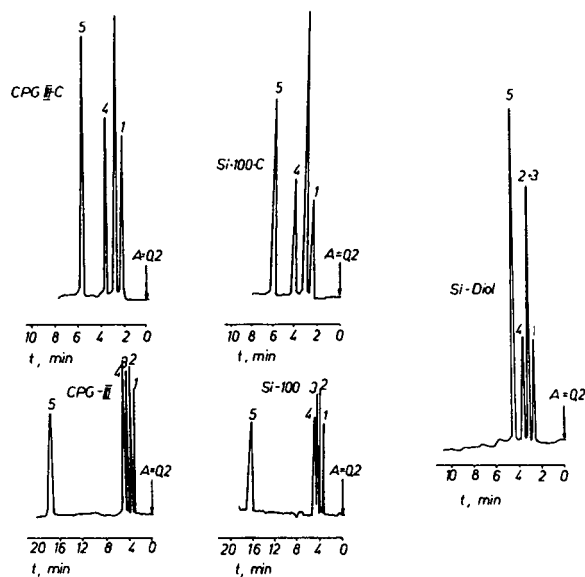


Fig. 1. Separation of aromatic hydrocarbons on sorbents CPG II C, CPG III C, Si-100, Si-100 C and Si-Diol with the normal-phase system. Column, 250 × 4 mm I.D.; mobile phase, hexane; flow-rate, 1 cm³/min. Compounds: 1 = benzene; 2 = naphthalene; 3 = diphenyl; 4 = anthracene; 5 = nitrobenzene.

bents with bonded or adhesively deposited Carbowax 20M are especially recommended for GC separations of polar compounds [1,15]. However, amino compounds are an exception. According to many publications [15,16], caution

should be exercised when analysing substances with amino groups on polyethylene glycol (PEG)-phases, because of the possibility of reactions of these substances with aldehyde groups that can be formed as a result of PEG chain degradation. There is a great possibility that aldehyde, carboxyl or oxirane groups exist in the polymer layer because the sorbents used in the present work were obtained by means of thermal immobilization. Potentiometric titration (see Part I [11]) indicated the presence of a carboxyl or oxirane groups which may also be associated with the presence of aldehyde groups. Hence, the separation of amino compounds allows one to obtain some information about the probable presence of aldehyde groups.

Table II gives the capacity factors of nitroanilines, aniline, nitrobenzene and benzene separated using columns filled with CPG II C, CPG III C and Si-100 C. For comparison analogous data obtained using the columns packed with the pure siliceous materials CPG II, CPG III and Si-100 are also given. As can be seen, the retention sequences are identical for the initial supports, *i.e.*, for CPG II, CPG III and Si-100. *o*-Nitroaniline elutes before aniline and other nitroanilines. This suggests that an intra-hydrogen bond is formed between the amino and nitro groups in the *ortho* position. It was found that *m*- and *p*-nitroaniline elute

TABLE II

CAPACITY FACTORS (k') OF NITROANILINES, ANILINE, BENZENE AND NITROBENZENE ON COLUMNS PACKED WITH THE INVESTIGATED SORBENTS

Mobile phase: methanol–2-propanol–hexane (10:30:60).

Compound	k'					
	CPG II	CPG II C	CPG III	CPG III C	Si-100	Si-100 C
Benzene	0.25	0.38	0.21	0.35	0.17	0.38
Nitrobenzene	0.34	0.80	0.33	0.88	0.27	0.86
Aniline	0.59	—	0.72	1.80	0.53	1.72
<i>o</i> -Nitroaniline	0.39	2.02	0.42	2.07	0.33	2.21
<i>m</i> -Nitroaniline	0.59	4.21	0.72	4.08	0.53	4.54
<i>p</i> -Nitroaniline	0.59	5.45	0.72	5.33	0.53	6.14

together with aniline, which seems to show that only the amino group interacts with the silica surface and that the mesomeric effect of the nitro group does not influence protonation of hydrogen atoms connected with nitrogen. The sorbents with a bonded Carbowax layer possess entirely different properties from the pure siliceous initial materials. This is confirmed by the increase in capacity factors, by the increase in selectivities (all substances are completely separated) and by the different order of the elution (aniline elutes before *o*-nitroaniline and then *m*-nitroaniline and *p*-nitroaniline elute). It is probable that in the interaction with the PEG layer *o*-nitroaniline employs both functional groups. The same applies to *m*- and *p*-nitroaniline. The sequence of nitroanilines is related to the increasing mesomeric effect. The chromatographic properties of the sorbents with a Carbowax layer are very similar.

The lack of the aniline peak for CPG II C (even when aniline was injected alone) is of great interest; see the absence of the capacity factor for aniline on this sorbent (Table II). It is probable that CPG II C possesses much more reactive groups than the other sorbents with immobilized Carbowax 20M. It may be connected with a greater amount of immobilized Carbowax 20M relative to the support surface (w/S) in the case of the sorbent CPG II C (see Part I [11]).

The same phenomenon can be observed in the separation of toluidines. Table III gives the capacity factors of the mixture of toluidines and

TABLE III
CAPACITY FACTORS (k') OF TOLUIDINES AND ANILINE ON COLUMNS FILLED WITH CPG II C, CPG III C AND Si-100 C

Mobile phase: methanol–2-propanol–hexane (10:30:60).

Compound	k'		
	CPG II C	CPG III C	Si-100 C
<i>o</i> -Toluidine	1.20	1.20	1.18
<i>m</i> -Toluidine	–	1.42	1.38
<i>p</i> -Toluidine	–	1.42	1.38
Aniline	–	1.71	1.73

aniline obtained for the sorbents CPG II C, CPG III C and Si-100 C. As with nitroanilines, the separations of toluidines on CPG III C and Si-100 C are very similar (the k' values are almost identical). For CPG II C only the *o*-toluidine peak is obtained and has a k' value comparable to those on CPG III C and Si-100 C. The other toluidines and aniline “disappear”. These results seem to indicate a strong interaction between amino groups of the analyte compounds with aldehyde, carboxyl or oxirane groups of the sorbents. These interactions can be weakened by the presence of other functional groups (*e.g.*, nitro groups), decreasing the basic properties of the amino group (as with *m*- and *p*-nitroanilines) or by steric hindrance as with *o*-toluidine and *o*-nitroaniline (screening effect or intra-chelate).

Immobilized Carbowax 20M in reversed-phase HPLC

As was mentioned earlier, Carbowax 20M is a medium-polarity stationary phase. However, in immobilized polyethylene glycol chains some of the ether oxygen atoms are engaged in interactions with the support surface (for silica gel with hydroxyl groups bonded with surface silica atoms, and for porous glass with boron atoms and with hydroxyl groups connected with both Si and B atoms [17]). The polarity of such a polyethylene glycol layer is lower than that of

TABLE IV
CAPACITY FACTORS (k') OF AROMATIC COMPOUNDS ON A COLUMN PACKED WITH Si-100 C AT VARIOUS METHANOL–WATER MOBILE PHASE COMPOSITIONS

Compound	k'		
	Methanol–water (50:50)	Methanol–water (40:60)	Methanol–water (30:70)
Benzene	0.24	0.37	0.50
Phenol	0.24	0.37	0.50
Toluene	0.24	0.37	0.50
Nitrobenzene	0.24	0.37	0.50
Naphthalene	0.69	0.96	1.40
Diphenyl	0.79	1.23	1.89
Anthracene	1.53	2.81	5.12

bulk PEG [18]. The aim here was to investigate whether the decrease in the polarity of Carbowax 20M is sufficient to be able to use siliceous sorbents with a PEG layer as packings for RP chromatography. A positive answer can be expected because PEGs covalently bonded to the silica gel surface (via γ -glycidoxypropylsilane) have been successfully used in the high-performance hydrophobic interaction chromatography of proteins [7,19].

In order to resolve the above problem, a mixture of benzene, phenol, toluene, nitrobenzene, naphthalene, diphenyl and anthracene was separated using a column filled with Si-100 C employing methanol–water as the mobile phase.

Table IV gives the capacity factors of the analyte substances obtained with various proportions of the mobile phase components *i.e.*, methanol–water (50:50, 40:60 and 30:70). Fig. 2 shows the corresponding chromatograms. Larger amounts of methanol do not allow the separation of naphthalene from diphenyl.

As can be seen, with methanol–water (30:70) there is a complete separation of the last three eluting substances in the investigated mixture (substances which are characterized by the longest retention times), but benzene, phenol, toluene and nitrobenzene still elute in one peak. This seems to indicate that the hydrophobic properties of the immobilized Carbowax layer

are much weaker than those of sorbents with chemically bonded alkyl or aryl radicals. This conclusion is in agreement with the observations of Chang and co-workers [7,19], who called Carbowax phases “soft” in contrast to “hard phases” represented by chemically bonded alkyl radicals. The present investigations (in which one of the most popular mobile phases used in RP chromatography was applied) show how different the properties of Carbowax are in relation to alkyl or aryl phases.

In order to elucidate the chromatographic possibilities of sorbents with immobilized Carbowax 20M, more detailed experiments are needed, using other test substances and mobile phases.

Silica gel with immobilized Carbowax 20M as sorbents for size-exclusion chromatography

Sorbents with adhesively deposited Carbowax 20M are commonly used as column fillings in the size-exclusion chromatography (SEC) of biopolymers [20,21]. The Carbowax layer blocks adsorption centres on the support surface, preventing adsorption of proteins and peptides. It is worth adding that polyethylene glycol is readily water-wettable, *i.e.*, by the main component of mobile phases used in SEC of biopolymers. However, the lifetime of columns with adhesively deposited PEG is short because of strong phase bleeding [21]. Darling *et al.* [22] described an attempt at thermal treatment of the adhesively deposited Carbowax 20M layer. The sorbent obtained showed adsorption properties towards proteins, so the experiment was not successful.

The procedure of Carbowax layer immobilization proposed by Aue and co-workers [9,10] is more effective and probably destroys the structure of the PEG layer to a lesser extent than the simple thermal treatment employed by Darling *et al.* Hence the problem appears to be to establish how proteins behave during elution on a column packed with siliceous materials with thermally immobilized Carbowax 20M.

Fig. 3 shows the calibration graph for protein standards (see Table V) obtained with the columns filled with Si-100 C. It also shows, for comparison, the calibration graph obtained with the column packed with Si-Diol. It should be

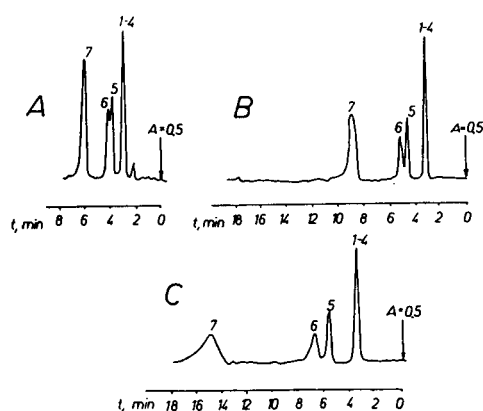


Fig. 2. Separation with the reversed-phase system on a column packed with Si-100 C. Mobile phase, methanol–water: (a) 50:50; (b) 40:60; (c) 30:70 (v/v). Compounds: 1–4 = benzene, phenol, toluene and nitrobenzene in a single peak; 5 = naphthalene; 6 = diphenyl; 7 = anthracene.

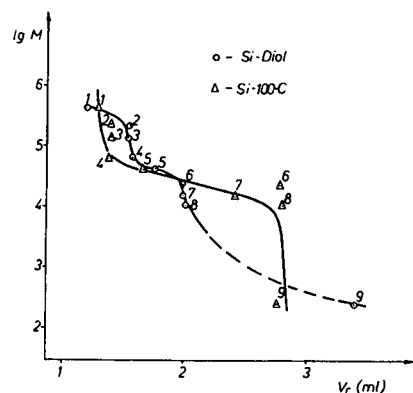


Fig. 3. Calibration graphs obtained for a column filled with Si-100 C (solid line) and Si-Diol (dashed line) using peptide standards numbered as in Table V. Mobile phase: 0.1 M NaH_2PO_4 (pH 6.8).

stressed that the separation conditions applied in these experiments were selected on the basis of literature data concerning the separation of biopolymers on diol phases [23,24].

A decidedly better calibration graph was obtained using Si-100 C as a column filling. Only chymotrypsinogen was an exception and eluted with a much larger elution volume than expected. This protein possesses a very high isoelectric point ($pI = 9.5$), indicating the presence of positively charged groups (primary amino groups) in the molecule. Consequently, chymotrypsinogen can interact very strongly with the negatively charged sorbent surface. However, several other proteins are also characterized by high pI values (that for cytochrome *c* is even

TABLE V

ISOELECTRIC POINTS (pI) AND AVERAGE MOLECULAR MASSES (\bar{M}) OF PROTEINS

No.	Protein	\bar{M}	pI
1.	Ferritin	450 000	4.4
2.	Catalase	240 000	—
3.	Aldolase	160 000	9.5
4.	Bovine serum albumin (BSA)	67 000	4.4–4.8
5.	Ovalbumin	45 000	4.7
6.	Chymotrypsinogen	25 000	9.5
7.	Myoglobin	17 800	7.1
8.	Cytochrome <i>c</i>	12 300	10.6
9.	DNP-L-Alanine	255	—

higher), but their retention volumes seem to be only slightly enhanced. The ionic strength of the mobile phase used was 0.2 and it has been shown [24,25] that this ionic strength is high enough to prevent electrostatic interactions. There must be another explanation for the extremely high elution volume for chymotrypsinogen. Hydrophobic interactions may be responsible for such a behaviour of chymotrypsinogen. In contrast to the hydrophilic myoglobin and cytochrome *c*, chymotrypsinogen is a highly hydrophobic protein. Hydrophobic interactions can be diminished by addition of an organic modifier (e.g., ethylene glycol) to the mobile phase [24,25]. With a column packed with the examined sorbent, the addition of 10% of ethylene glycol to the mobile phase caused, instead of a decrease, an increase in the retention volumes of chymotrypsinogen, myoglobine and cytochrome *c*. The same addition of ethylene glycol to the mobile phase hardly influenced the retention of biopolymers injected onto the Si-Diol column. Surprisingly, both before and after addition of ethylene glycol, the calibration graph obtained for Si-Diol was far from the ideal calibration graphs reported for this material in other publications [23,24,26]. Increases in the retention volumes on addition of organic modifiers to the aqueous eluent were observed by De Ligny *et al.* [27] in the SEC of proteins on Sephadex and were explained in terms of adsorption and partitioning. Therefore, considering the elution of chymotrypsinogen on the investigated materials, the influence of adsorption effects or specific partition phenomenon also cannot be excluded.

Stability of siliceous sorbents with thermally immobilized Carbowax 20M

Aue and co-workers, who developed the method for the thermal immobilization of Carbowax 20M, called the polymer layer they obtained a “non-extractable layer”, because it remains on the support surface after very exhaustive extraction [8–10]. As described under Experimental, we were forced to change Aue and co-workers’ method, introducing additionally a sorbent washing procedure performed in the thermostated columns. The applied washing procedure was even more effective than that

TABLE VI
PHYSICO-CHEMICAL PROPERTIES OF SORBENTS AFTER USE IN CHROMATOGRAPHIC COLUMNS

Symbols the same as in Tables I and II in Part I [11].

Sorbent	S_{BET} (m^2/g)	V_p^{ads} (cm^3/g)	D_c^{ads} (\AA)	D_{max} (\AA)	w/w ($\times 100$) (g/g)	w/S ($\times 100$) (g/m^2)	d_t (\AA)
CPG III C	216	0.83	154	100	15.17	0.044	3.3
		0.81	150				
Si-100 C	277	1.20	173	140	8.45	0.027	2.0
		1.20	173				

used by Aue and co-workers. Assuming that the excess amount of Carbowax 20M was washed from the surface and that PEG chains directly interacting with the support surface remained on the surface only, there is still the question of whether the immobilized layer is stable and whether or not it bleeds during the chromatographic process.

The most heavily used columns, *i.e.*, Si-100 C and CPG III C, were unpacked and CHN elemental analysis was performed to establish the amount of Carbowax remaining. The results are given in Table VI. When compared with Table II in Part I [11], it can be seen that the amount of the bonded Carbowax and consequently the thickness of the polymer layer had

TABLE VII
CAPACITY FACTORS (k') OF THREE GROUPS OF SUBSTANCES ON COLUMNS FILLED WITH CPG III C AND Si-100 C AT THE BEGINNING OF THE INVESTIGATION AND AFTER A LONG PERIOD (ABOUT 2 MONTHS) OF OPERATION OF THE COLUMNS

Group I substances, mobile phase = hexane; group II and III substances, mobile phase = methanol–2-propanol–hexane (10:30:60).

Group	Compound	k'			
		CPG III C		SI-100 C	
		At the beginning	At the end	At the beginning	At the end
I	Benzene	0.15	0.18	0.07	0.24
	Naphthalene	0.34	0.42	0.25	0.48
	Diphenyl	0.34	0.42	0.25	0.48
	Anthracene	0.82	0.89	0.70	0.88
	Nitrobenzene	1.91	1.70	1.50	1.61
II	Benzene	0.32	0.35	0.32	0.38
	Nitrobenzene	0.82	0.88	0.83	0.86
	Aniline	1.73	1.80	1.77	1.72
	<i>o</i> -Nitroaniline	1.87	2.07	2.28	2.21
	<i>m</i> -Nitroaniline	3.86	4.08	4.94	4.54
	<i>p</i> -Nitroaniline	4.99	5.33	6.78	6.14
III	<i>o</i> -Toluidine	1.21	1.21	1.18	1.24
	<i>m</i> -Toluidine	1.42	1.42	1.38	1.41
	<i>p</i> -Toluidine	1.42	1.42	1.38	1.41
	Aniline	1.71	1.71	1.73	1.71

decreased threefold (for CPG III C) or fivefold (for Si-100 C). The specific surface areas and pore volumes increased and the values of $D_{\text{cyl}}^{\text{ads}}$ and $D_{\text{cyl}}^{\text{des}}$ decreased, which means that the narrowest pores were unblocked.

Table VII gives the capacity factors of three groups of substances measured on the columns filled with Si-100 C and CPG III C at long intervals of time. Despite the loss of Carbowax between the separated measurements, the capacity factors were fairly stable. A possible explanation of the observed phenomenon is the assumption that not all Carbowax chains are bonded with the surface in the same way or with the same strength. It is highly improbable that the bulk polymer remains in the Carbowax layer after the washing procedure. However, it is possible that some Carbowax chains are connected with the support surface all over the length of the chain and some of them are bonded only partially. The remaining parts of the latter could protrude over the layer parallel to each other and form a crystalline structure, as confirmed by X-ray diffraction (see Part I [11]). These not entirely bonded chains could be solvolysed only during the chromatographic process. The X-ray patterns measured after the chromatographic studies using CPG III C and Si-100 C did not reveal any crystalline form.

It is probable that in the Carbowax 20M layer remaining on the surface after prolonged operation of the column all chains are bonded through their lengths and they are non-extractable. The mean thickness of the layer (3.3 Å for CPG III C and 2 Å for Si-100 C) is an argument for this interpretation. Aue *et al.* [28] reported that the thickness of the Carbowax 20M layer obtained on silica gel of specific surface area 140 m²/g is 2 Å. Unfortunately they did not discuss this value, which conflicts with the value they obtained on Chromosorb W (15 Å) [8]. The latter value is similar to those obtained here for materials after the washing procedure but before being used in HPLC columns.

CONCLUSIONS

Siliceous materials with immobilized Carbowax 20M can be applied in normal-phase

HPLC. There are limitations connected with analyses of amines and other compounds that react with aldehyde, carboxyl or oxirane groups (as in GC analysis).

The results obtained show that the hydrophobic properties of the bonded Carbowax layer are weaker than those of typical RP sorbents. Further experiments on the determination of the optimum mobile phase composition (ensuring better selectivity of the RP system with immobilized Carbowax) seem to be desirable.

The materials with immobilized Carbowax 20M seem to be more effective than the sorbents with the diol phase for the separation of proteins.

The retention data for materials with an immobilized Carbowax layer are constant despite the partial removal of the stationary phase during operation of the column. Probably after a long period of column operation a real non-extractable layer of Carbowax remains on the support surface. It is also possible that directly after synthesis the sorbents contain Carbowax chains bonded with the surface in a different way and with various strengths. Weakly bonded PEG chains are removed from the sorbent surface during HPLC column operation. This problem requires further investigation.

REFERENCES

- 1 J.A. Yancey, *J. Chromatogr. Sci.*, 24 (1986) 117.
- 2 L. Blomberg and K. Markides, *J. High Resolut. Chromatogr. Chromatogr. Commun.*, 8 (1985) 632.
- 3 K. Grob, *Making and Manipulating Capillary Columns for Gas Chromatography*, Hüthig, Heidelberg, 1986.
- 4 J. Buijten, L. Blomberg, K. Markides and T. Wännman, *J. Chromatogr.*, 268 (1983) 387.
- 5 L. Bystricky, *J. High Resolut. Chromatogr. Chromatogr. Commun.*, 9 (1986) 240.
- 6 M. Cigánek, M. Dressler and J. Teplý, *Chromatographia*, 27 (1989) 109.
- 7 J.P. Chang and J.G. An, *Chromatographia*, 25 (1988) 350.
- 8 W.A. Aue, C.R. Hastings and Sh. Kapila, *J. Chromatogr.*, 77 (1973) 299.
- 9 M.M. Daniewski and W.A. Aue, *J. Chromatogr.*, 147 (1978) 119.
- 10 W.A. Aue, M.M. Daniewski, J. Müller and J.P. Laba, *Anal. Chem.*, 49 (1977) 1465.
- 11 I. Choma, A.L. Dawidowicz, R. Dobrowolski and S. Pikus, *J. Chromatogr.*, 641 (1993) 205.

- 12 I. Choma and A.L. Dawidowicz, *Chem. Anal. (Warsaw)*, 33 (1988) 313.
- 13 I. Choma, A.L. Dawidowicz and R. Lodkowski, *J. Chromatogr.*, 600 (1992) 109.
- 14 I. Choma, *Ph.D. Thesis*, UMCS, Lublin, 1990.
- 15 M. Horká, K. Janák and K. Tesarik, *Chem. Listy*, 83 (1989) 125.
- 16 H.E. Persinger and J.T. Shank, *J. Chromatogr. Sci.*, 11 (1973) 190.
- 17 A.L. Dawidowicz, I. Choma, W.M. Buda, *Z. Phys. Chem.*, 268 (1987) 273.
- 18 W.A. Aue and M.M. Daniewski, *J. Chromatogr.*, 151 (1978) 11.
- 19 J.P. Chang, Z. Rassi and C. Horváth, *J. Chromatogr.*, 319 (1985) 396.
- 20 G. Hawk, J.A. Cameron and L.B. Dufault, *Prep. Biochem.*, 2 (1972) 193.
- 21 C. Persiani, P. Cukor and K. French, *J. Chromatogr. Sci.*, 14 (1976) 417.
- 22 T. Darling, J. Albert, P. Russel, D.M. Albert and T.W. Reid, *J. Chromatogr.*, 131 (1977) 383.
- 23 F.E. Regnier and K.M. Gooding, *Anal. Biochem.*, 103 (1980) 1.
- 24 D.E. Schmidt, Jr., R.W. Giese, D. Conron and B.L. Karger, *Anal. Chem.*, 52 (1980) 177.
- 25 H.G. Barth, *J. Chromatogr. Sci.*, 18 (1980) 409.
- 26 *Supelco Rep.*, 5, No. 20 (1986) 3.
- 27 C.L. De Ligny, W.J. Gelsema and A.M.P. Roozen, *J. Chromatogr.*, 294 (1984) 223.
- 28 W.A. Aue, C.R. Hastings and Sh. Kapila, *Anal. Chem.*, 45 (1973) 725.

Detection systems with a photodiode-array detector for flow-injection and high-performance liquid chromatographic determination of phosphinate, phosphonate and diphosphonate

Tetsuya Nakazato and Norimasa Yoza*

Department of Chemistry, Faculty of Science, Kyushu University, Hakozaki, Fukuoka 812 (Japan)

(First received October 20th, 1992; revised manuscript received March 1st, 1993)

ABSTRACT

Spectrophotometric detection systems for flow-injection analysis and high-performance liquid chromatography were designed for the determination of phosphinate, phosphonate, diphosphonate and isohypophosphate of lower oxidation numbers. Preoxidation and/or hydrolysis of these compounds to orthophosphate by peroxodisulphate in an oxidation reactor (140°C) were followed by a colour reaction with a molybdenum(VI) reagent in a second reactor. A photodiode-array detector (200–800 nm) was used to obtain the spectrophotometric characteristics of the coloured species. An unpredicted absorption spectrum was observed for the reaction product between phosphinate and molybdenum(VI). Both advantages and disadvantages of using an anion-exchange column (TSKgel SAX) for the separation of monomers and dimers, including orthophosphate and diphosphate (pyrophosphate), are discussed.

INTRODUCTION

As shown in Table I, various inorganic phosphorus compounds of different oxidation states are known. Orthophosphate and diphosphate (pyrophosphate) of oxidation number +5 are the most popular and important compounds in industrial applications and biological metabolism [1]. High-performance liquid chromatographic (HPLC) and flow-injection analysis (FIA) methods for these P^V compounds are well established [2]. Various chromogenic reagents have been successfully used to design detection systems for P^V compounds: an Mo^{VI} reagent [2], an Mo^V–

Mo^{VI} reagent [3], an Mo^{VI}–ascorbic acid reagent [4] and an Mo^{VI}–malachite green reagent [5]. All these reagents gave no direct colour reactions with P^I and P^{III} compounds (see Table I). Phosphinate and phosphonate have been determined using other detection systems for FIA [6] and HPLC [7–9].

Diphosphonate, a dimer of phosphonate of oxidation number +3, has recently been shown to act as an excellent phosphorylating agent. The versatile utility of diphosphonate has been demonstrated with a few examples of chemical syntheses [10,11], novel analogues of ADP and triphosphate. In order to investigate the kinetic and mechanistic aspects of the reactions of diphosphonate, the development of HPLC and FIA methods for the rapid and sensitive determination of phosphonate, diphosphonate and other oxo acids of lower oxidation states in Table I

* Corresponding author.

TABLE I
SYMBOLS AND STRUCTURAL CHARACTERISTICS OF PHOSPHORUS COMPOUNDS USED

Symbol ^a	Nomenclature ^b	Structure ^c	Oxidation state ^d
A	Orthophosphate	$\begin{array}{c} \text{O} \\ \parallel \\ ^-\text{O}-\text{P}-\text{O}^- \\ \\ \text{O}^- \end{array}$	P ^V
B	Phosphonate, phosphite	$\begin{array}{c} \text{O} \\ \parallel \\ \text{H}-\text{P}-\text{O}^- \\ \\ \text{O}^- \end{array}$	P ^{III}
C	Phosphinate, hypophosphite	$\begin{array}{c} \text{O} \\ \parallel \\ \text{H}-\text{P}-\text{H} \\ \\ \text{O}^- \end{array}$	P ^I
D	Diphosphate, pyrophosphate	$\begin{array}{c} \text{O} \quad \text{O} \\ \parallel \quad \parallel \\ ^-\text{O}-\text{P}-\text{O}-\text{P}-\text{O}^- \\ \quad \\ \text{O}^- \quad \text{O}^- \end{array}$	P ^V P ^V
E	Diphosphonate, pyrophosphite	$\begin{array}{c} \text{O} \quad \text{O} \\ \parallel \quad \parallel \\ \text{H}-\text{P}-\text{O}-\text{P}-\text{H} \\ \quad \\ \text{O}^- \quad \text{O}^- \end{array}$	P ^{III} P ^{III}
F	Isohypophosphate	$\begin{array}{c} \text{O} \quad \text{O} \\ \parallel \quad \parallel \\ \text{H}-\text{P}-\text{O}-\text{P}-\text{O}^- \\ \quad \\ \text{O}^- \quad \text{O}^- \end{array}$	P ^{III} P ^V

^a These are used in the figures throughout.

^b Including trivial names.

^c Indicate completely dissociated forms.

^d Sometimes used as abbreviated notations in the text.

have been attempted in our laboratory [12,13]. As described above, molybdenum reagents for the detection of P^V compounds gave no colour reactions with the lower oxo acids, and therefore preoxidation of the lower oxo acids was needed for the detection of these compounds with molybdenum reagents. Sodium hydrogensulphite has been successfully used as an oxidant. However, the corrosive sulphite is harmful to laboratory instruments and may not be healthy for operators.

This work was initiated in an attempt to improve the laboratory and environmental aspects by using an alternative oxidant, peroxodisulphate [14,15], which has been examined for the oxidation and hydrolysis of phosphorus compounds in environmental samples [16,17]. The Mo^{VI} reagent used in this work was easy to prepare, stable on storage at room temperature and reacted rapidly with orthophosphate to form a molybdophosphate that could be detected at a wavelength of ca. 400 nm. A photodiode-array

detector in an FIA system provided absorption spectra over the range 200–800 nm for a coloured complex passing through a flow cell. The detector was useful to confirm the oxidation and/or hydrolysis of phosphorus compounds and to monitor an unpredicted reaction between phosphinate and molybdenum(VI) in the absence of the oxidant.

A separation column was used to achieve good separations of the monomers phosphinate, phosphonate and orthophosphate and of the dimers diphosphonate and pyrophosphate. Both the advantages and disadvantages of using an anion-exchange column (TSKgel SAX) for the separation of the monomers and dimers are discussed.

EXPERIMENTAL

Chemicals

Orthophosphate (KH_2PO_4), phosphonate ($\text{Na}_2\text{PHO}_3 \cdot 5\text{H}_2\text{O}$), phosphinate ($\text{NaPH}_2\text{O}_2 \cdot \text{H}_2\text{O}$) and pyrophosphate ($\text{Na}_4\text{P}_2\text{O}_7 \cdot 10\text{H}_2\text{O}$) were of JIS-S grade (Kishida, Osaka, Japan). Diphosphonate ($\text{Na}_2\text{P}_2\text{H}_2\text{O}_5$) was prepared according to the literature [10]. Water was purified with a Milli-Q system (Millipore, Bedford, MA, USA).

Reagents and eluents

Eluents. Water was used as a carrier of injected samples for the FIA mode in Figs. 1 and 2. For the HPLC mode in Fig. 2, eluents for isocratic elution consisted of 0.02–0.10 M potassium sulphate and 0.1% (v/v) Na_4EDTA (4Na) and/or Na_2EDTA .

Colour reagent. Sulphuric acid (0.3 M) containing 4.3 mM ammonium molybdate [$(\text{NH}_4)_6\text{Mo}_7\text{O}_{24} \cdot 4\text{H}_2\text{O}$] or 0.03 M Mo^{VI} , which was prepared according to the literature [2], was used as a colour reagent. This Mo^{VI} reagent was stable for at least 6 months at room temperature.

Oxidant. A 0.5% potassium peroxodisulphate solution was used to oxidize monomeric lower oxo acids to orthophosphate for the FIA mode in Fig. 2. A 1.0% solution was used to oxidize all lower oxo acids to orthophosphate for the FIA and HPLC modes in Fig. 2. The solutions were stable for at least 3 months at room temperature.

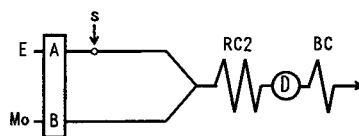


Fig. 1. Flow-injection system with Mo^{VI} reagent. E = water; Mo = Mo^{VI} reagent; pump A, 1.0 ml/min; B, 0.5 ml/min; S = sample injector (100 μl); RC2 = colour reaction coil (10 m \times 0.5 mm I.D., PTFE, room temperature); D = spectrophotometric detector (200–800 nm); BC = back-pressure coil (3 m \times 0.25 mm I.D., PTFE).

Equipment

The main components of the FIA system in Fig. 1 were pump A (Jasco 880 U) for the eluent, pump B (Kyowa Seimitsu KHU-W-52) for Mo^{VI} reagent, a sample injector (Rheodyne Model 7125), a reactor (RC2) made of a PTFE tubing and a spectrophotometric detector (Jasco Uvidec-100-IV) used to measure absorbance at 400 nm. A photodiode-array detector (Shimadzu SPDM6AS) was also used to measure absorption spectra at 200–800 nm.

The main components of the FIA–HPLC system in Fig. 2 were pump A (Jasco 880 PU) for the eluent and two-channel pumps B and C (Kyowa Seimitsu KHU-W-52) for the oxidant and the Mo^{VI} reagent. The two reactors (RC1 and RC2) were made of PTFE tubing and RC1 was held in a thermostated reaction bath (Sanuki R-3000C). The separation column was packed

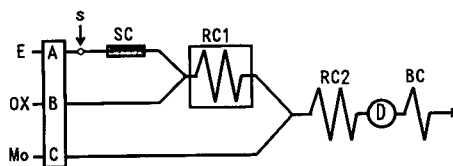


Fig. 2. FIA–HPLC system with an oxidant and Mo^{VI} reagent. E = water (FIA) or $\text{K}_2\text{SO}_4 + \text{Na}_4\text{EDTA}$ (HPLC); OX = $\text{K}_2\text{S}_2\text{O}_8$; Mo = Mo^{VI} reagent; pump A, 1.0 ml/min; B, 0.5 ml/min; C, 0.8 ml/min, except 0.5 ml/min in Fig. 5; S = sample injector (100 μl); SC = separation column (25 cm \times 4 mm I.D., TSKgel SAX); RC1 = oxidation and hydrolysis reaction coil (10 m \times 0.5 mm I.D., PTFE, 140°C); RC2 = colour reaction coil (10 m \times 0.5 mm I.D., PTFE, room temperature); D = spectrophotometric detector; BC = back-pressure coil (3 m \times 0.25 mm I.D., PTFE). The separation column (SC) is used for the HPLC mode and is demounted for the FIA mode.

with an anion exchanger (TSKgel SAX). The column was used for the HPLC mode and was demounted for FIA mode. The other components were similar to those in Fig. 1.

RESULTS AND DISCUSSION

Effect of temperature of colour reactor on FIA signal intensities and absorption spectra

As mentioned above, orthophosphate reacts with Mo^{VI} and $\text{Mo}^{\text{V}}\text{-Mo}^{\text{VI}}$ reagents to form molybdophosphate (yellow) ($\text{H}_3\text{PMo}_{12}\text{O}_{40}$) and the so-called heteropoly blue, respectively [2]. The heteropoly blue method is more advantageous than the yellow molybdophosphate method with respect to sensitivity. We examined the detection of lower oxo acids with the combined use of the $\text{Mo}^{\text{V}}\text{-Mo}^{\text{VI}}$ reagent and peroxydisulphate as an oxidant. It was found, however, that the $\text{Mo}^{\text{V}}\text{-Mo}^{\text{VI}}$ reagent was deactivated by peroxydisulphate and was unable to detect not only the lower oxo acids, but also orthophosphate. The following experiments were carried out with the Mo^{VI} reagent. A two-channel FIA system (Fig. 1) without the use of peroxydisulphate and a three-channel FIA–HPLC system (Fig. 2) with the oxidant were employed.

Prior to the oxidation experiments with peroxydisulphate, the reactivities of orthophosphate, phosphonate and phosphinate with the Mo^{VI} reagent were studied by employing the FIA system in Fig. 1. The reactor (RC2) temperature

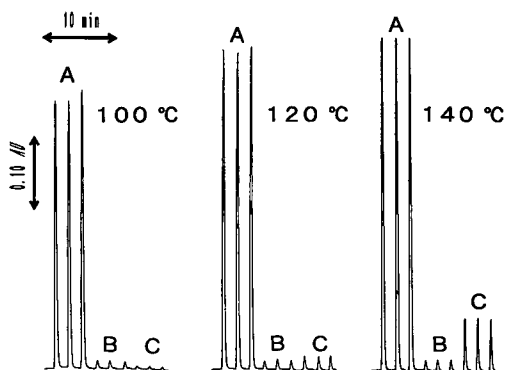


Fig. 3. Effect of colour reactor (RC2) temperature on FIA signal intensities of (A) orthophosphate, (B) phosphonate and (C) phosphinate. Manifold as in Fig. 1; measurement wavelength, 400 nm; sample, each 1×10^{-3} M.

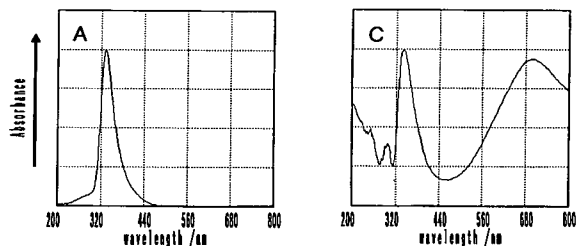


Fig. 4. Absorption spectra of coloured complexes measured by the photodiode-array detector. A and C correspond to signals A and C at 140°C in Fig. 3. The scale on the absorbance axis is arbitrary and relative to the highest maximum.

for the colour reaction was varied over the range 100–140°C. As expected, the peak intensities for the lower oxo acids were lower than those for orthophosphate at temperatures below 120°C (Fig. 3). The small signals for the lower oxo acids may be ascribed mainly to the impurity (orthophosphate) in commercial chemicals [18]. On the other hand, the appearance of the marked peak C for phosphinate at 140°C was unpredicted. The spectrum over the range 200–800 nm of the coloured species A and C at 140°C were recorded with a photodiode-array detector with a flow cell ($8 \mu\text{l}$) [19]. It is evident from Fig. 4 that the spectrum for phosphinate (C), with an additional absorption maximum at longer wavelength, is different from the typical spectrum of molybdophosphate (A), characteristic of orthophosphate and orthophosphate-producing compounds. Two possible speculations to be investigated in the future are that (1) phosphinate reacts with molybdenum(VI) at high temperature to form a phosphinate complex and (2) phosphinate acts as a reductant for molybdenum(VI) to form a mixed polymer of

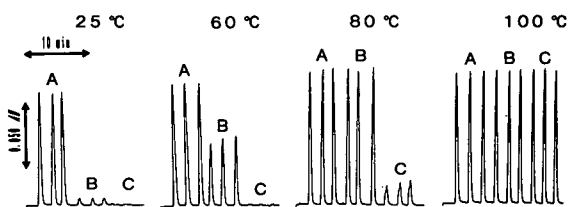


Fig. 5. Effect of oxidation reactor (RC1) temperature on FIA signals of (A) orthophosphate, (B) phosphonate and (C) phosphinate. Manifold, FIA mode in Fig. 2; oxidant, 0.5% $\text{K}_2\text{S}_2\text{O}_8$; measurement wavelength, 400 nm; sample, each 1×10^{-3} M.

molybdenum(V) and molybdenum(VI) or a reduced complex of molybdophosphate.

Effect of temperature of oxidation reactor on oxidation of lower oxo acids

The oxidative capability of peroxydisulphate for the lower oxo acids was examined by employing the three-channel FIA system in Fig. 2. Preoxidation of the lower oxo acids by peroxydisulphate was effected before the resulting orthophosphate was allowed to mix with the Mo^{VI} reagent. As shown in Fig. 5, the peak intensities of phosphonate and phosphinate, relative to that of orthophosphate, increases with increasing temperature of the oxidation reactor (RC1). Complete oxidation and quantitative colour formation were achieved at 100°C .

Similar experiments were carried out with the dimers pyrophosphate and diphosphonate, which needed to be prehydrolysed and/or preoxidized with peroxydisulphate. The two dimers, in addition to the monomers, were quantitatively detected at 140°C . Only incomplete colour formation was achieved for pyrophosphate at 100°C , probably owing to the rate-determining slow hydrolysis of pyrophosphate. At 140°C , the absorption spectra for phosphonate, diphosphonate and pyrophosphate, given by the photodiode-array detector, were identical with that in Fig. 4A, indicating that all species were completely converted into orthophosphate.

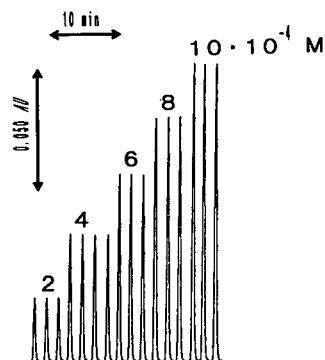


Fig. 6. FIA calibration of diphosphonate. Manifold, FIA mode in Fig. 2; RC1 temperature, 140°C ; oxidant, 1.0% $\text{K}_2\text{S}_2\text{O}_8$; measurement wavelength, 400 nm; the concentration range is from 2×10^{-4} to 10×10^{-4} M. Each sample was injected in triplicate or quadruplicate.

The FIA calibration profile for diphosphonate is presented in Fig. 6. It shows good linearity (correlation coefficient ≥ 0.999), reproducibility (R.S.D. of measurement $< 1.0\%$) and detection limit (ca. 10^{-5} M).

HPLC separation of monomers

In the previous sections we have mentioned the effectiveness of peroxydisulphate as the oxidant in the FIA mode (Fig. 2). We now describe the application of FIA as a detection system in the HPLC separation of phosphorus compounds. An anion-exchange separation column was fitted and a mixed solution of EDTA and potassium sulphate was used as the eluent (Fig. 2): The pH values of the eluents could be adjusted by varying the ratio of Na_4EDTA and Na_2EDTA , maintaining the total EDTA concentration (0.1%, w/w) constant.

Figs. 7 and 8 show the HPLC profiles for a mixed solution of orthophosphate, phosphonate and phosphinate obtained by varying either the sulphate concentration (Fig. 7) or pH (Fig. 8). The three species could be detected quantitative-

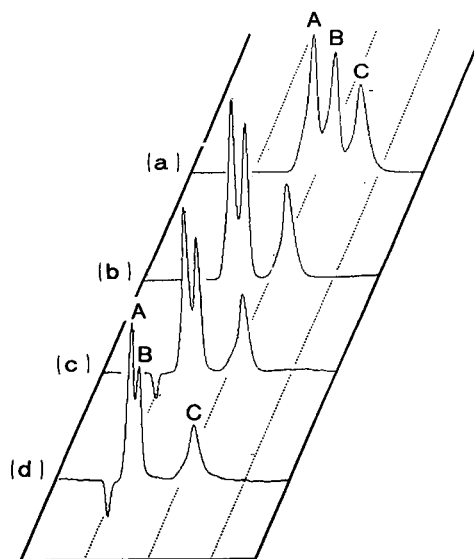


Fig. 7. Effect of potassium sulphate concentration on the separation of (A) orthophosphate, (B) phosphonate and (C) phosphinate. Manifold, HPLC mode in Fig. 2; eluent, 0.1% (w/w) Na_4EDTA + (a) 0.02, (b) 0.05, (c) 0.07 and (d) 0.10 M K_2SO_4 ; separation column, TSKgel SAX; measurement wavelength, 400 nm; sample, each 1×10^{-3} M.

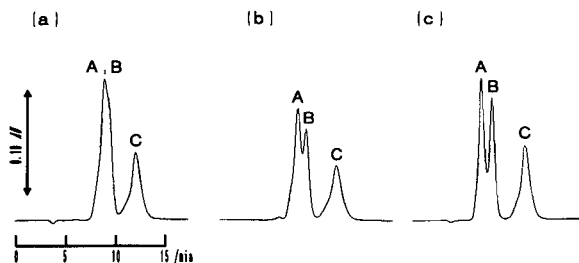
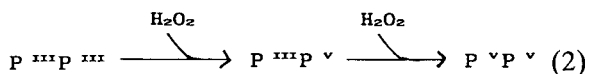
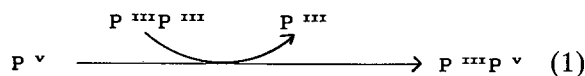


Fig. 8. Effect of pH on the separation of (A) orthophosphate, (B) phosphonate and (C) phosphinate. Manifold, HPLC mode in Fig. 2; eluent, 0.05 M K_2SO_4 + 0.1% EDTA; pH, (a) 5, (b) 7 and (c) 10; separation column, TSKgel SAX; measurement wavelength, 400 nm; sample, each 1×10^{-3} M.

ly. The separation of phosphinate from other species was satisfactory, but only incomplete resolution between orthophosphate and phosphonate could be achieved in spite of the variations in the eluent composition. The TSKgel SAX with the trimethylammonium ion as an anion-exchange group may not be a good choice for the separation of the monomers. We obtained a preliminary result that TSKgel IC-Anion-PW with the diethylmethylammonium ion as an anion-exchange group gives complete resolution of the three monomers whose retention times increase in the order phosphinate < orthophosphate < phosphonate. Detailed results will be reported elsewhere.

HPLC separation of dimers

It has been reported [10,11] that diphosphonate, $P^{III}P^{III}$, acts as a phosphorylating agent (eqn. 1) and is oxidizable by hydrogen peroxide (eqn. 2) to give isohypophosphate, $P^{III}P^V$, and pyrophosphate, P^VP^V . This section deals with the HPLC analysis of the phosphorus compounds involved in eqns. 1 and 2.



An HPLC profile for an authentic mixture of P^V , P^{III} , P^VP^V and $P^{III}P^{III}$ is shown in Fig. 9. The two dimers were well separated from one another and from the monomers, but the res-

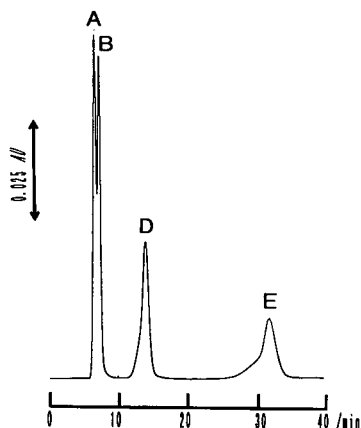


Fig. 9. HPLC profile for a mixed solution of (A) orthophosphate, (B) phosphonate, (D) pyrophosphate and (E) diphosphonate. Manifold, HPLC mode in Fig. 2; eluent, 0.11 M K_2SO_4 + 0.02% Na_4EDTA ; separation column, TSKgel SAX; measurement wavelength, 400 nm; sample components, each 1×10^{-3} M.

olution of P^{III} and P^V was incomplete, as was expected from the results in Figs. 7 and 8.

The reaction products of P^V and $P^{III}P^{III}$ in eqn. 1 were analysed under the same conditions as in Fig. 9. As shown in Fig. 10, a peak F for $P^{III}P^V$ was observed around the retention time of P^VP^V (Fig. 9). The unsymmetrical peaks such as D, E and F in Figs. 9 and 10 tended to be observed when the same column was used continuously for as long as 6 months. A similar

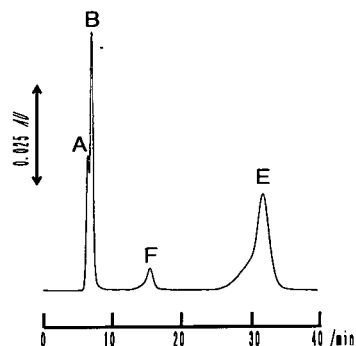


Fig. 10. Analysis of the reaction products of orthophosphate and diphosphonate. A = Orthophosphate; B = phosphonate; E = diphosphonate; F = isohypophosphate. Initial concentrations, 0.1 M orthophosphate and 0.3 M diphosphonate; incubation time, 3.8 h; incubation temperature, 50°C; manifold, HPLC mode in Fig. 2; separation column, TSKgel SAX; eluent, 0.11 M K_2SO_4 + 0.02% Na_4EDTA ; measurement wavelength, 400 nm.

experiment on the HPLC separation of $P^{III}P^V$ and P^VP^V was reported in a previous paper [11]. As only P^V units were monitored with $Mo^{V}-Mo^{VI}$ reagent in the absence of an oxidant, three peaks of P^V , $P^{III}P^V$ and P^VP^V were recorded, but the peaks for P^{III} and $P^{III}P^{III}$ could not be confirmed. On the other hand, the present method permitted the detection of all phosphorus compounds (Table I) involving any structural units of P^V , P^{III} and/or P^I .

The HPLC method also showed good quantitative capabilities with respect to linearity, reproducibility and detection limit, comparable to those in the FIA method.

CONCLUSIONS

The FIA detection system described is based on the preoxidation of lower oxo acids of phosphorus by peroxodisulphate and the coloration of the resultant orthophosphate with $Mo(VI)$ reagent. A photodiode-array detector was advantageous not only for quantitative purposes but also for the spectral characterization of the coloured reaction products. The HPLC system, *i.e.*, the combination of the FIA system and the anion-exchange separation column, was confirmed to be powerful for the quantitative analysis of mixed samples of lower oxo acids of phosphorus.

REFERENCES

- 1 E.E. Conn, P.K. Stumpf, G. Bruening and R.H. Doi, *Outlines of Biochemistry*, Wiley, New York, 1987.
- 2 N. Yoza, H. Hirano, Y. Baba and S. Ohashi, *J. Chromatogr.*, 325 (1985) 385.
- 3 N. Yoza, Y. Sagara, H. Morioka, H. Hirano, T. Handa, Y. Baba and S. Ohashi, *J. Flow Injection Anal.*, 3 (1986) 37.
- 4 N. Yoza, K. Ito, Y. Hirai and S. Ohashi, *J. Chromatogr.*, 196 (1980) 471.
- 5 S. Motomizu, T. Wakimoto and K. Tōei, *Talanta*, 30 (1983) 333.
- 6 T. Yamane and M. Kamijyo, *Bunseki Kagaku*, 38 (1989) 46.
- 7 B.J. Julin, H.W. Vandeborn and J.J. Kirkland, *J. Chromatogr.*, 112 (1975) 443.
- 8 T. Tanaka, K. Hiroy, A. Kawahara and S. Wakida, *Bunseki Kagaku*, 32 (1983) 771.
- 9 D.S. Ryder, *J. Chromatogr.*, 354 (1986) 438.
- 10 Y. Yamamoto, Y. Baba, M. Mizokuchi, M. Onoe, T. Sumiyama, M. Tsuhako, N. Yoza and S. Ohashi, *Bull. Chem. Soc. Jpn.*, 61 (1988) 3217.
- 11 N. Yoza, M. Okamatsu, N. Tokushige, T. Miyajima and Y. Baba, *Bull. Chem. Soc. Jpn.*, 64 (1991) 16.
- 12 Y. Hirai, N. Yoza and S. Ohashi, *J. Chromatogr.*, 206 (1981) 501.
- 13 Y. Baba, M. Tsuhako and N. Yoza, *J. Chromatogr.*, 507 (1990) 103.
- 14 E. Ben-Zvi, *J. Phys. Chem.*, 67 (1963) 2698.
- 15 A.G. Miroshnichenko and V.A. Lunenok-Burmakina, *Russ. J. Inorg. Chem.*, 15 (1970) 1345.
- 16 T. Korenaga and K. Okada, *Bunseki Kagaku*, 33 (1984) 683.
- 17 M. Goto, M. Nishimura, T. Tominaga and D. Ishii, *Bunseki Kagaku*, 37 (1988) 52.
- 18 Y. Hirai, *J. Flow Injection Anal.*, 1 (1984) 16.
- 19 N. Yoza, S. Nakashima, T. Nakazato, N. Ueda, H. Kodama and A. Tateda, *Anal. Chem.*, 64 (1992) 1499.

Determination of stability constants of metal complexes from ion chromatographic measurements

Pavel Janoš

Research Institute of Inorganic Chemistry, 400 60 Ústí nad Labem (Czech Republic)

(First received July 3rd, 1992; revised manuscript received March 15th, 1993)

ABSTRACT

Relations were derived between the retention of metal cations on a cation-exchange column and the composition of a mobile phase in the presence of complexing agents and, based on the derived relations, a method was suggested for measuring the stability constants of complexes of metal cations with anions of dicarboxylic (polycarboxylic) acids. The method was applied to the determination of the stability constants of complexes of some divalent cations (Zn^{2+} , Ni^{2+} , Co^{2+} , Cd^{2+} , Mn^{2+} , Fe^{2+} and Pb^{2+}) with the anions of oxalic, tartaric, citric, pyridine-2,6-dicarboxylic and malonic acids. The results are in good agreement with those obtained with other methods.

INTRODUCTION

The method of ion chromatography (IC) has been widely used for the separation and determination of metal cations. Complex-forming reactions in the mobile phase are often employed to improve the separation (see, for example, refs. 1–5) and a number of others as given in the review [6]). Although these methods are fairly common in analytical practice, comparatively few studies have been devoted to a systematic investigation of the effect of a complexing ligand on the separation of metal cations and to deriving relations between retention of the analytes and composition of the mobile phase [7–10]. Until now IC has been used, but to a lesser extent, for assessing physico-chemical characteristics.

Recently Lin and Horváth [11] published a paper dealing with the measurement of the stability constants of metal complexes, using the IC method. Independently of the mentioned work [11], we suggested in our preceding paper [12] the possibility of studying the composition

and stability of complexes with the aid of the ion chromatographic method.

In the present paper relations are derived in greater detail, describing the retention of metal cations on cation exchangers in those cases when complex-forming reactions are taking place in the mobile phase. Based on the derived relations a method for measuring the stability constants of metal complexes is suggested. The method was adopted for measuring the stability constants of complexes of divalent metal cations with the anions of oxalic, tartaric, citric, pyridine-2,6-dicarboxylic (PDCA) and malonic acids.

EXPERIMENTAL

Apparatus

The liquid chromatograph consisted of two HPP 5001 high-pressure pumps (for pumping the mobile phase and the post-column derivatization agent), an LCI 30 injection valve with a 20- μ m sampling loop, an RE 2M post-column reactor, a TZ 4261 strip-chart recorder (all made by

Laboratorní přístroje, Prague, Czech Republic) and a Model 832 870 UV–VIS spectrophotometric detector (Knauer, Berlin, Germany) operated at a wavelength of 520 nm.

The mobile phases were deaerated in an ultrasonic bath prior to their use. The flow-rates of both the mobile phase and derivatization agent in the course of measuring were 0.3 ml min⁻¹. The capacity factors of analytes were calculated by a usual method. The column dead volume was assessed from disturbances on chromatograms, brought about by the injection of samples (injection or solvent peaks). The measurements were carried out at the room temperature, 22 ± 1°C.

Columns and chemicals

A glass column 150 × 3 mm packed with octadecyl-bonded silica Separon SGX C₁₈, 5 μm, coated for 2 h with 5 mmol l⁻¹ sodium dodecyl sulphate (SDS) at a flow-rate of 0.1 ml min⁻¹, was used for the separation of metal ions. A more detailed description of the preparation of columns and of their properties is given in ref. 13. It was found that the separation on a column modified in this way is controlled by an ion-exchange mechanism [13]. A saturation column, 30 × 3 mm packed with the Separon SGX 7-μm silica, was connected between the pump and the sampling loop (all columns were supplied by Tessek, Prague, Czech Republic).

The 5 mmol l⁻¹ SDS solution was prepared from research-grade-quality reagent (Serva, Heidelberg, Germany).

In addition, the following stock solutions were prepared: 1 mol l⁻¹ sodium hydroxide and 0.1 mol l⁻¹ solutions of oxalic, tartaric, citric and malonic acids. The 1 mmol l⁻¹ solution of PDCA (Merck, Darmstadt, Germany) was prepared by dissolving in 0.1 mol l⁻¹ sodium hydroxide. Concentrations of the stock solutions were checked using conventional titrimetric (acidimetric or alkalimetric) methods. The mobile phases were prepared by combining the sodium hydroxide stock solution with the solution of each acid at requisite ratios so that the mobile phases should always contain equal quantity of Na⁺ and required amount of the complexing ligand. The

mobile phase pH was adjusted to a required constant value by adding dilute perchloric acid.

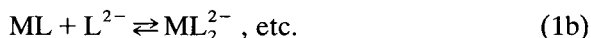
Stock solutions of the examined cations were prepared from the nitrates, chlorides or sulphates and diluted to a constant concentration within the 0.01–0.1 mmol l⁻¹ range for each run of the measurements.

A 0.2 mmol l⁻¹ solution of 4-(2-pyridyl-azo)resorcinol (PAR) containing 1 mol l⁻¹ acetic acid and 3 mol l⁻¹ ammonium hydroxide served as the post-column derivatizing agent.

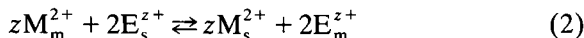
Unless stated otherwise all the reagents used were analytical grade (Lachema, Brno, Czech Republic). Redistilled water was used for preparing the solutions.

RESULTS AND DISCUSSION

With the experimental arrangement described in the preceding section the mobile phase contains, in the first place, the eluting cation E^{z+}, a complexing anion (ligand, L) and perchlorate ions supplied by adjusting pH with the aid of perchloric acid. In the present derivation we will not consider (unlike Lin and Horváth [11]) the participation of H⁺ in the ion-exchange equilibria. We are assuming that the pH value is sufficiently high that the H⁺ concentration may be neglected. (Provided that the concentration of the eluting ion is, for example, 0.1 mol l⁻¹, as shown below, this assumption holds true within almost the full range of commonly employed pH values.) At the same time we assume that the prevailing form of ligands in the solutions at the given pH is the anion L²⁻ (dissociation to the second degree). After the injection of analyte (metal cation, M²⁺) into the mobile phase formation of complexes occurs according to:



The separated metals are present in the form of free cations or in the form of neutral or negatively charged complexes that do not take part in the ion-exchange processes taking place on the column. The retention of analytes is described by:



The indexes *m* and *s* refer to mobile and stationary phases, respectively. The equilibrium constant of eqn. 2 (selectivity coefficient) is given as

$$K_M^E = \frac{[\text{M}_s^{2+}]^z [\text{E}_m^{z+}]_m^2}{[\text{M}_m^{2+}]^z [\text{E}_s^{z+}]_s^2} \quad (3)$$

The sorbent capacity, *Q*, is expressed as a sum

$$Q = z[\text{E}^{z+}]_s + 2[\text{M}^{2+}]_s \quad (4)$$

while the second term on the right-hand side usually may be neglected and it is possible to write:

$$[\text{E}^{z+}]_s = Q/z \quad (5)$$

It holds for the capacity factor *k_M*:

$$k_M = q \frac{[\text{M}^{2+}]_s}{c_M} \quad (6)$$

where *q* is the phase ratio and *c_M* is total concentration of metal in the mobile phase as given by the sum (for simplicity the ionic charges are omitted):

$$c_M = [\text{M}]_m + [\text{ML}]_m + [\text{ML}_2]_m + \dots + [\text{ML}_n]_m \quad (7)$$

Eqn. 7 can be rewritten using the overall stability constants β_1 – β_n :

$$c_M = [\text{M}]_m(1 + \beta_1[\text{L}] + \beta_2[\text{L}]^2 + \dots + \beta_n[\text{L}]^n) \quad (8)$$

On combining the eqns. 3, 5, 6 and 8 and rearranging, we obtain:

$$k_M = q \frac{(K_M^E)^{1/2} \left(\frac{Q}{z}\right)^{2/z}}{[\text{E}^{z+}]^{2/z} (1 + \beta_1[\text{L}] + \beta_2[\text{L}]^2 + \dots + \beta_n[\text{L}]^n)} \quad (9)$$

expressing both the pushing effect of eluting cation and the pulling effect of complexing anion. Usually eqn. 9 is presented in logarithmic form and the effect of complexing equilibria is expressed by means of the side equilibria coefficient α_M [7,8,10].

To be able to examine experimentally the influence of complexing equilibria on the retention of analytes, we had to vary the concen-

tration of ligand in the mobile phase and, at the same time, keep all the other variables in the mobile phase constant, particularly the concentration of eluting ion and pH. Lin and Horváth [11] used ethylene diamine and tartaric acid as the main components of the mobile phase; the concentration of the ethylenediammonium cation was kept constant, the tartrate anion concentration was varied within 0.2–5 mmol l⁻¹ and the constant value of pH was adjusted by adding either sodium hydroxide or nitric acid. Thus the mobile phase contained, in addition to the main components, an undefined amount of other ions (Na⁺, NO₃⁻). Their influence, however, is likely to be negligible.

In the present study we used a weaker driving cation, Na⁺, at a higher concentration. Mobile phases were prepared by combining sodium hydroxide solution with solutions of each acid (oxalic, tartaric, etc.) so that the Na⁺ concentration was constant while only the ligand concentration was varied. Constant pH value was adjusted with the aid of perchloric acid. Therefore, the mobile phase composition was exactly defined and the measurements were carried out at almost constant ionic strength (*ca.* 0.1 mol l⁻¹ sodium perchlorate). Perchlorate anions take part neither in complexing nor in ion-exchange reactions in the system under consideration. The measurements were carried out at a pH value at which the examined dibasic acids are almost fully dissociated [14] (oxalic and tartaric acids and PDCA at pH 6 and malonic acid at pH 6.5). For measurements in the citrate medium the pH value of 5.5 was adopted, at which the prevailing form in the solution is a HL²⁻ anion (the formal charge is -2.156 [14]).

Provided that, with a proper arrangement of experiments, we can consider the concentration of the eluting cation E^{z+} as being constant, eqn. 9 may be rewritten in the following form:

$$\frac{1}{k_M} = A(1 + \beta_1[\text{L}] + \beta_2[\text{L}]^2 + \dots + \beta_n[\text{L}]^n) \quad (10)$$

where the constant *A* is given as:

$$A = \frac{[\text{E}^{z+}]^{2/z}}{q(K_M^E)^{1/2} \left(\frac{Q}{z}\right)^{2/z}} \quad (11)$$

Eqn. 10 expresses the dependence of the capacity factor on the concentration of ligand in a mobile phase or, on the other hand, makes it possible to determine stability constants from experimentally assessed dependences $1/k_M$ vs. ligand concentration.

An example of the experimentally assessed dependence of the reciprocal value of capacity

factors on the concentration of a ligand in the mobile phase in the case of tartrate complexes is shown in Fig. 1. As may be seen from that diagram, the obtained dependences are linear within the examined concentration range. This means that we may neglect the quadratic and higher terms in brackets on the right-hand side of eqn. 10. Then the stability constants can be

TABLE I
STABILITY CONSTANTS OF METAL COMPLEXES

Ions	Log β_1	
	This work	Published values [references]
<i>Oxalate complexes</i>		
Zn ²⁺	4.07 ± 0.06	3.88 [15]; 4.87 [2]
Ni ²⁺	4.69 ± 0.46	5.16 [15]
Co ²⁺	4.08 ± 0.04	3.25 [15]
Cd ²⁺	3.35 ± 0.01	2.75 [15]
Mn ²⁺	3.35 ± 0.01	3.2 [15]; 3.20 [2]
Fe ²⁺	3.64 ± 0.03	3.05 [15]
Pb ²⁺	4.12 ± 0.57	3.32 [15]
<i>Tartrate complexes</i>		
Zn ²⁺	2.44 ± 0.06	2.29 [12] ^a ; 2.75 ± 0.03 [11] ^b ; 3.82 [15]
Ni ²⁺	2.41 ± 0.07	2.39 [12] ^a
Co ²⁺	2.24 ± 0.01	2.36 [12] ^a ; 2.48 ± 0.02 [11] ^b ; 3.225 [16] ^c
Cd ²⁺	2.15 ± 0.03	2.04 [12] ^a ; 2.27 ± 0.01 [11] ^b ; 2.913 [16] ^c
Mn ²⁺	1.94 ± 0.02	1.35 [12] ^a ; 1.89 ± 0.04 [11] ^b ; 2.49 [15]
Fe ²⁺	2.11 ± 0.01	2.29 [12] ^a ; 2.17 ± 0.01 [11] ^b ; 2.2 [15]
Pb ²⁺	2.43 ± 0.04	2.93 [12] ^a ; 2.60 [15]
<i>Citrate complexes (HL²⁻)</i>		
Zn ²⁺	4.18 ± 0.11	4.27 [15]; 4.98 [2]
Co ²⁺	4.48 ± 0.02	5.00 [15]
Cd ²⁺	3.32 ± 0.05	3.15 [15]
Mn ²⁺	3.50 ± 0.09	4.15 [15]; 3.70 [2]
Fe ²⁺	3.75 ± 0.07	4.4 [15]
Pb ²⁺	4.10 ± 0.06	4.34 [15]
<i>PDCA complexes</i>		
Mn ²⁺	4.66 ± 0.13	5.01 [2]
<i>Malonate complexes</i>		
Zn ²⁺	2.81 ± 0.03	2.96 [15]
Ni ²⁺	3.19 ± 0.10	3.24 [15]
Co ²⁺	3.01 ± 0.06	2.97 [15]
Cd ²⁺	2.75 ± 0.06	1.92 [15]
Mn ²⁺	2.71 ± 0.06	3.28 [15]
Fe ²⁺	2.85 ± 0.08	

^a IC method, ionic strength ca. 0.04 mmol l⁻¹ lithium perchlorate pH 3.60 ± 0.05.

^b IC method, 30°C, ionic strength ca. 1–13 mmol l⁻¹

^c Capillary isotachopheresis method.

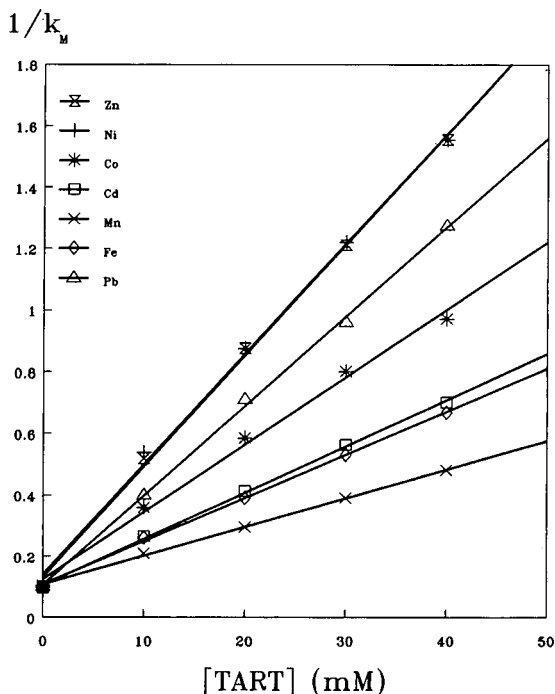


Fig. 1. Dependence of reciprocal value of the capacity factor on tartrate concentration in mobile phase. Column: 150×3 mm, Separon SGX C_{18} , $5 \mu\text{m}$, SDS coated. Mobile phase: $0.1 \text{ mol l}^{-1} \text{ Na}^+ + \text{tartrate}$, $\text{pH } 6.00 \pm 0.05$ adjusted with perchloric acid.

calculated simply as the quotient of the line slope and the y-axis intercept of the linear dependence.

In Table I the values of the stability constants as obtained by the described method are presented and compared with the corresponding published data. In most cases the agreement between our results and the literature may be considered comparatively good. The differences are caused by different experimental methods, particularly by different conditions in the course of the measuring proper (temperature, ionic strength, etc.); these conditions are not always specified in the cited papers.

CONCLUSIONS

The method of IC enables the stability constants of metal cation complexes with anions of

simple dicarboxylic or polycarboxylic acids to be measured in a simple way. In the case of complexes with larger organic ligands the possibility of more complex mechanisms of retention has to be considered. The accuracy of the stability constant determination depends, in the first place, on the accuracy of measuring the analyte retention characteristics. In the chosen system the conditions of the measurement can be optimized by changing either the mobile phase composition or, as the case may be, the column capacity (see ref. 13). A disadvantage of the column used is that it is not possible to measure at higher pH values because of the damage to the silica gel matrix of the column packing.

It has been shown that by a detailed analysis of the experimental dependences $1/k_M$ vs. ligand concentration, and using eqn. 10, the stability constants of higher complexes in certain systems may be obtained (provided that such complexes are formed under the given conditions) [17].

The relations derived in the present work may be used not only for calculating the stability constants from chromatographic measurements but also for optimizing the process of separation on the basis of published values of the stability constants.

REFERENCES

1. D. Yan and G. Schwedt, *Anal. Chim. Acta*, 178 (1985) 347.
2. D. Yan and G. Schwedt, *Fresenius' J. Anal. Chem.*, 338 (1990) 149.
3. J.M. Hwang, F.C. Chang and Y.C. Yeh, *J. Chin. Chem. Soc.*, 30 (1983) 167.
4. J. Vialle, M.C. Bertrand, M. Kolosky, O. Paise and G. Raffin, *Analisis*, 17 (1989) 376.
5. D.T. Gjerde, *J. Chromatogr.*, 349 (1988) 49.
6. K. Robards, P. Starr and E. Patsalides, *Analyst*, 116 (1991) 1247.
7. G.J. Sevenich and J.S. Fritz, *Anal. Chem.*, 55 (1983) 12.
8. J. Hradil, F. Švec, A.A. Aratskova, L.D. Belyakova and V.I. Orlov, *J. Chromatogr.*, 509 (1990) 369.
9. P. Janoš, K. Štulík and V. Pacáková, *Talanta*, 38 (1991) 1445.
10. P.R. Haddad and R.C. Foley, *J. Chromatogr.*, 500 (1990) 301.
11. F.H. Lin and Cs. Horváth, *J. Chromatogr.*, 589 (1992) 185.
12. P. Janoš and M. Broul, *Fresenius' J. Anal. Chem.*, 344 (1992) 545.

- 13 P. Janoš, K. Štulík and V. Pacáková, *Talanta*, 39 (1992) 29.
- 14 T. Hirokawa, M. Nishino, N. Aoki, Y. Kiso, Y. Sawamoto, T. Yagi and J. Akiyama, *J. Chromatogr.*, 271 (1983) D1.
- 15 S. Kotrlý and L. Šůcha, *Handbook of Chemical Equilibria in Analytical Chemistry*, Ellis Horwood, Chichester, 1985.
- 16 T. Hirokawa and Y. Kiso, *J. Chromatogr.*, 248 (1982) 341.
- 17 P. Janoš, in preparation.

High-performance liquid chromatography of guanine and its nucleosides and nucleotides by pre-column fluorescence derivatization with phenylglyoxal reagent

Sayuri Yonekura and Masatake Iwasaki

Daiichi College of Pharmaceutical Sciences, Tamagawa-cho, Minami-ku, Fukuoka 815 (Japan)

Masaaki Kai and Yosuke Ohkura*

Faculty of Pharmaceutical Sciences, Kyushu University 62, Maidashi, Higashi-ku, Fukuoka 812 (Japan)

(First received December 30th, 1992; revised manuscript received March 4th, 1993)

ABSTRACT

A pre-column fluorescence derivatization method for the high-performance liquid chromatographic determination of guanine and its nucleosides and nucleotides is described. The compounds are converted into fluorescent derivatives by reaction with phenylglyoxal in a phosphate buffer (pH 6.0) at 37°C for 15 min. The derivatives are separated on a reversed-phase column (TSKgel ODS-120T) by gradient elution of acetonitrile in mobile phase containing 5 mM phosphate buffer (pH 6.5), and then detected fluorimetrically. The derivatization results in the guanine-containing compounds eluting as single fluorescent peaks. The method is highly selective and sensitive; the limits of detection for the compounds tested are 140–720 fmol per 100- μ l injection volume.

INTRODUCTION

A sensitive quantification method for nucleic acid-related compounds is becoming increasingly important in studies of cellular proliferation and metabolism [1–3]. Nucleic acid bases and nucleos(t)ides have generally been measured by methods based on high-performance liquid chromatography (HPLC) with UV detection [4–8] or native fluorescence detection [9,10] using ion-exchange or reversed-phase columns. However, to measure these compounds in complex biological samples such as mammalian body fluids

and tissues using such methods is difficult because of their limited sensitivity and low selectivity and because many other biogenic substances interfere with the detection in the chromatography.

An HPLC method with dual-electrochemical detection has been reported for the sensitive determination of guanine-containing nucleotides [11,12]; this detection system is operated at a high applied potential (+0.95 V vs. Ag/AgCl) and permits the nucleotides to be detected at the picomole level. However, there are problems in the detection, owing to the disturbance by many detectable biogenic substances at the high voltage and also the unstable noise level depending on composition of the mobile phase for HPLC.

Selective fluorimetric detection is possible for the HPLC determination of nucleos(t)ides,

* Corresponding author.

provided that the fluorogenic reagent used for the derivatization shows a high molecular recognition specificity to one of the nucleic acid bases; chloroacetaldehyde [13–15] and bromoacetaldehyde [16,17] have been used for the selective detection of adenine nucleos(t)ides in HPLC, which permits their quantification in pico- and subpicomole quantities on-column [14,15,17].

We reported previously that phenylglyoxal (PGO) reacts with guanine-containing compounds to produce fluorescent derivatives and the reaction is applicable to the manual spectrofluorimetric determination of the compounds [18]. However, the structures of the fluorescent derivatives remained unknown, and the derivatives yielded from some of the guanine-containing compounds resulted in multiple peaks when they were subjected to reversed-phase HPLC.

This paper describes the derivatization reaction conditions that can produce single fluorescent peaks from guanine and its nucleos(t)ides in the HPLC of their derivatives, and an HPLC method with pre-column derivatization utilizing these reaction conditions for the selective and sensitive determination of these compounds.

EXPERIMENTAL

Chemicals and solutions

Nucleic acid bases and nucleos(t)ides were purchased from Seikagaku Kogyo (Tokyo, Japan). PGO monohydrate was from Aldrich (Milwaukee, WI, USA). Water was deionized and then distilled prior to use. Other chemicals were of analytical reagent grade.

A guanine solution (1.0 $\mu\text{mol/ml}$) was prepared by dissolving guanine hydrochloride in 0.1 *M* sodium hydroxide and diluting twenty-fold with water. The solution was diluted with water to 100 nmol/ml, and then stored in a refrigerator (-20°C). The stock solutions (100 nmol/ml each) of other nucleic acid bases and nucleos(t)ides were prepared with water. A mixture of guanine and its nucleos(t)ides (5 nmol/ml each) and/or a 5 nmol/mol solution of each compound were used within a day for the experiments of the derivatization and HPLC separation. PGO solution (0.1 *M*) was prepared in dimethyl sulphoxide (DMSO).

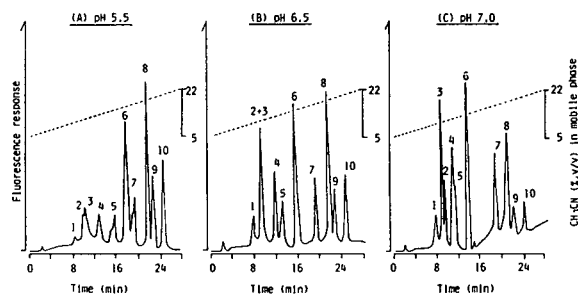


Fig. 1. Chromatograms of a standard mixture of guanine and its nucleos(t)ides (250 pmol of each per injection volume). HPLC conditions were as described in the Experimental section, but the pH of the phosphate buffer in the mobile phase was changed to (A) 5.5, (B) 6.5 and (C) 7.0. Peaks: 1 = GTP; 2 = GDP; 3 = dGTP; 4 = dGDP; 5 = GMP; 6 = dGMP; 7 = cGMP; 8 = guanine; 9 = guanosine; 10 = deoxyguanosine.

Derivatization procedure

A 200- μl portion of sample solution was placed in a test tube, to which were added 100 μl each of 0.1 *M* PGO and 50 mM phosphate buffer (pH 6.0). The mixture was warmed at 37°C for 15 min. A 100- μl portion of the final reaction mixture was used for HPLC.

HPLC system and its operating conditions

The HPLC system consisted of a Hitachi 638-30 chromatograph equipped with a programming controller for gradient elution, a Rheodyne 7125 syringe-loading sample injector valve (100- μl loop) and a Hitachi F-1000 spectrofluorimeter fitted with a 25- μl flow cell. The column was a TSKgel ODS-120T (particle size 5 μm ; 150 mm \times 4.6 mm I.D.; Tosoh, Japan). The column temperature was ambient ($24 \pm 4^\circ\text{C}$). For the separation of the fluorescent derivatives, a gradient elution of acetonitrile (5–22%, v/v) in an aqueous mobile phase containing 5 mM phosphate buffer (pH 6.5) was carried out over 28 min at a flow-rate of 1.0 ml/min (see Fig. 1). The fluorescence intensity of the eluate was monitored at 510 nm (emission) with excitation at 360 nm.

RESULTS AND DISCUSSION

HPLC separation

A standard mixture of guanine, guanosine, deoxyguanosine, GMP, cGMP, dGMP, GDP,

dGDP, GTP and dGTP (ten species in all) was subjected to the fluorescence derivatization and the derivatives were then separated by reversed-phase HPLC. The derivatives were retained on the ODS column and eluted within 28 min by a linear gradient elution of acetonitrile in the mobile phase (Fig. 1). All of the eluates from their peaks showed almost identical fluorescence excitation (maxima, around 360 nm) and emission (maxima, around 510 nm) spectra.

The pH of the buffer in the mobile phase affected the retention time and peak heights (Fig. 1). At the investigated pH in the range 3.5–8.5, the complete separation of the derivatives of the ten species of guanine and its nucleos(t)ides could not be attained. With increasing pH of the buffer, the derivatives of the nucleotides were eluted earlier than those of guanine and nucleosides. A relatively good separation was achieved at pH 6.5 or 7.0 (Fig. 1B and C). The fluorescent peaks resulting from the nucleotides were higher at higher pH than at lower pH. In contrast, the peaks due to guanine and its nucleosides fluoresced more intensely at weakly acidic pH.

At pH 6.5, higher concentrations of the phosphate buffer in the range 2.5–10 mM caused early elution of all the derivatives, though no significant change in the separation profile was found at different concentrations of buffer. However, the maximum peak heights were attained at phosphate buffer concentration 2.5–5.0 mM. In this study, 5 mM phosphate buffer (pH 6.5) in the mobile phase was employed for the HPLC separation.

Fluorescence derivatization

The optimum conditions that could afford a single fluorescent derivative from each of the guanine-containing compounds were different from those previously reported for the manual spectrofluorimetric method [18]. Under the previously described conditions, *i.e.* heating with PGO in 11 mM maleate buffer (pH 4.0) at 60°C for 30 min, the phosphate moieties of the nucleotides were partially hydrolysed, and two or more fluorescent peaks from each nucleotide were observed in the chromatogram. For example, derivatization of GTP as described previous-

ly [18] resulted in three peaks due to GTP, GDP and GMP.

However, modification of the reaction conditions to milder ones resulted in single fluorescent peaks for each guanine-containing compound. The optimum derivatization conditions were reaction with PGO at 37°C for 15 min in 12.5 mM phosphate buffer. In this experiment, the derivatization of GTP and dGTP (5 nmol/ml solution) resulted in minor peaks corresponding to GDP and dGDP, respectively, as well as the major peaks due to the nucleotides. The heights of these minor peaks were approximately 3% of the height of the major peaks of GTP and dGTP. This may be the result of spontaneous degradation of the nucleotides during sample preparation and storage, because the 100 nmol/ml solutions of GTP and dGTP, after storage at –20°C for 1 week, contained the corresponding nucleotide diphosphates at the 3% level, as determined when the non-derivatized samples were subjected to reversed phase ion-pair HPLC [8] with UV detection (254 nm).

Under the above-mentioned conditions, the pH of the reaction mixture had greatly affected the fluorescence production (Fig. 2). Maximum and stable peak heights were attained at phosphate buffer pH 6.0. The concentration of the phosphate buffer (pH 6.0) also influenced the fluorescence derivatization (Fig. 3). Most peak heights were greatest at a concentration range of 10–15 mM in the reaction mixture. Thus, 50 mM

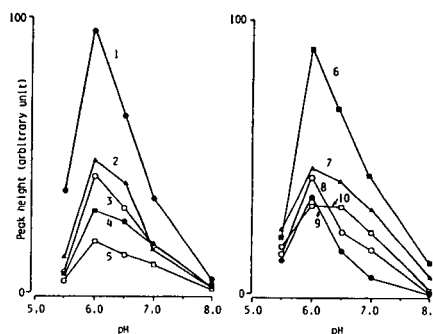


Fig. 2. Effect of the pH of the phosphate buffer in the reaction mixture on the fluorescence derivatization. HPLC conditions were as in Fig. 1B. Curves: 1 = guanine; 2 = GDP; 3 = cGMP; 4 = GMP; 5 = GTP; 6 = dGMP; 7 = dGDP; 8 = deoxyguanosine; 9 = guanosine; 10 = dGTP.

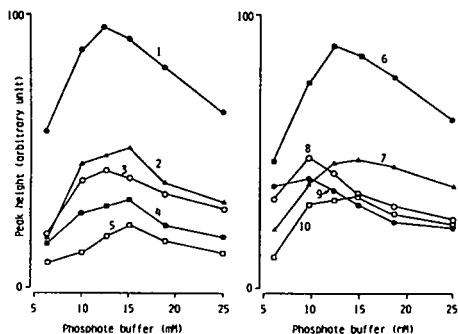


Fig. 3. Effect of the concentration of phosphate buffer (pH 6.0) in the reaction mixture on the fluorescence derivatization. HPLC conditions were as in Fig. 1B. For curves, see Fig. 2.

phosphate buffer (pH 6.0) was used for the derivatization reaction.

The reaction temperature of 37°C was effective in obtaining single fluorescent peaks from the compounds and the reaction time of 15 min generally provided the compounds with the highest peaks (Fig. 4). On the other hand, higher temperatures in the range 20–60°C allowed the derivatization to proceed more rapidly, and at 60°C the maximum peak heights were achieved by heating for 5 min. However, the peak heights were approximately 60% of these obtained by heating at 37°C for 15 min.

The organic solvent used to dissolve PGO also

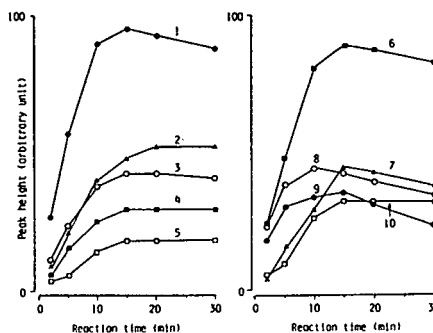


Fig. 4. Effect of reaction time at 37°C on the fluorescence derivatization. HPLC conditions were as in Fig. 1B. For curves, see Fig. 2.

influenced the production of the fluorescent derivatives (Table I). Of the solvents tested, DMSO resulted in guanine-containing compounds with the highest peaks. A DMSO concentration of 25% (v/v) in the reaction mixture served to give the greatest production of the fluorescent derivatives.

Other nucleic acid bases and nucleos(t)ides (500 pmol each on-column; adenine, cytosine, uracil, thymine, hypoxanthine, xanthine, adenosine, cytidine, uridine, thymidine, ATP, CTP, UTP, ADP, AMP, CDP, CMP, dATP, dADP and dATP) did not provide any fluorescent derivatives when treated under the present derivatization conditions.

TABLE I

EFFECT OF ORGANIC SOLVENT USED TO DISSOLVE PGO ON THE FORMATION OF THE FLUORESCENT DERIVATIVES OF GUANINE AND ITS NUCLEOS(T)IDES

Compound	Peak height				
	DMSO	N,N-Dimethyl-formamide	Acetonitrile	Methyl cellosolve	Methanol
GTP	19	0	1	3	7
dGTP	34	1	1	7	14
GDP	51	3	3	10	18
dGDP	48	3	14	14	19
GMP	31	4	7	21	14
dGMP	93	51	34	51	31
cGMP	45	6	17	25	14
Guanine	100 ^a	62	68	64	45
Guanosine	37	12	5	38	27
Deoxyguanosine	45	8	12	42	29

^a The peak height for guanine obtained with DMSO was taken as 100.

Reproducibility, calibration graph and detection limit

The reaction products of guanine and its nucleos(t)ides were relatively stable because the peak heights (90–98%) of the derivatives did not change when the final reaction mixture was kept for 1 h in an ice-water bath after the reaction. The relative standard deviations of the peak heights for the compounds (50 pmol each on each column) were 4.0–6.0% ($n = 10$ in each instance).

Peak heights were used for the quantification. The calibration graphs of the guanine-containing compounds (0–250 pmol on-column) were all linear. The limits of detection at a signal-to-noise ratio of 3 for the compounds were in the range 140–720 fmol per 100- μ l injection volume.

CONCLUSIONS

The present method is highly selective for guanine-containing compounds, and offers the necessary sensitivity to permit the determination of biogenic guanine-containing nucleos(t)ides in mammalian tissues. In addition, fluorescence derivatization with PGO should be useful for the fluorescence labelling of high-molecular-mass nucleic acids, DNA and RNA. This work is now in progress in our laboratories.

REFERENCES

- 1 F. Pane, G. Oriani, K.C.T. Kuo, C.W. Gehrke, F. Salvatore and L. Sacchetti, *Clin. Chem.*, 38 (1992) 671.
- 2 M.M. Barrowman, S. Cockcroft and B.D. Gomperts, *Nature (London)*, 319 (1986) 504.
- 3 M. Rodbell, *Nature (London)*, 284 (1980) 17.
- 4 R. Bouliou and C. Bory, *J. Chromatogr.*, 339 (1985) 380.
- 5 P. Rotllan, A. Liras and P. Llorente, *Anal. Biochem.*, 159 (1986) 377.
- 6 F. Arezzo, *Anal. Biochem.*, 160 (1987) 57.
- 7 A. Werner, W. Siems, H. Schmidt, I. Rapoport and G. Gerber, *J. Chromatogr.*, 421 (1987) 257.
- 8 V. Stocchi, L. Cucchiaroni, F. Canestrari, M.P. Piacentini and G. Fornaini, *Anal. Biochem.*, 167 (1987) 181.
- 9 S.P. Assenza and P.R. Brown, *J. Chromatogr.*, 289 (1984) 355.
- 10 T.A. Ratko and J.M. Pezzuto, *J. Chromatogr.*, 324 (1985) 484.
- 11 J.B. Kafil, H.-Y. Cheng and T.A. Last, *Anal. Chem.*, 58 (1986) 285.
- 12 T. Yamamoto, H. Shimizu, T. Kato and T. Nagatsu, *Anal. Biochem.*, 142 (1984) 395.
- 13 M.R. Perston, *J. Chromatogr.*, 275 (1983) 178.
- 14 B. Levitt, R.J. Head and D.P. Westfall, *Anal. Biochem.*, 137 (1984) 93.
- 15 S. Sonoki, Y. Tanaka, S. Hisamatsu and T. Kobayashi, *J. Chromatogr.*, 475 (1989) 311.
- 16 M. Yoshioka, Z. Tamura, M. Senda and T. Miyazaki, *J. Chromatogr.*, 344 (1985) 345.
- 17 H. Fujimori, T. Sasaki, K. Hibi, M. Senda and M. Yoshioka, *J. Chromatogr.*, 515 (1990) 363.
- 18 M. Kai, Y. Ohkura, S. Yonekura and M. Iwasaki, *Anal. Chim. Acta*, 207 (1988) 243.

Validation of improved methods for high-performance liquid chromatographic determination of phenylpropanolamine, dextromethorphan, guaifenesin and sodium benzoate in a cough-cold formulation

T.D. Wilson*

Bristol-Myers Squibb, Evansville, IN 47720 (USA)

W.G. Jump

Bristol-Myers Squibb, Princeton, NJ 08540 (USA)

W.C. Neumann and T. San Martin

Lancaster Laboratories, Lancaster, PA 17601 (USA)

(First received January 21st, 1993; revised manuscript received March 25th, 1993)

ABSTRACT

Improved methods for the HPLC determination of phenylpropanolamine·HCl, dextromethorphan·HBr, guaifenesin and sodium benzoate in an oral liquid cough-cold product have been validated. The methods were shown to be accurate, precise, selective and rugged as would be required for regulatory submission and more efficient in terms of sample and standard preparation than previous methods. Phenylpropanolamine and dextromethorphan were analyzed simultaneously on a silica based SCX column using a buffered mobile phase with detection at 263 nm, while sodium benzoate and guaifenesin were measured together using a reversed-phase C₁₈ column, an aqueous-organic mobile phase of controlled ionic strength and detection at 273 nm. A column heater was also used, set at 40°C and 35°C for these respective determinations.

INTRODUCTION

The quantitative analysis of components in liquid oral cough-cold products has been previously accomplished by diverse methods from spectrophotometric to chromatographic. Previous HPLC methods have measured these constituents either individually or in combination. LC assays that have been reported on individual components of interest to the present investiga-

tion include: phenylpropanolamine (PPA) [1–6], dextromethorphan (DM) [7–11], sodium benzoate (B) [12,13] and guaifenesin (G) [14]. These methods commonly provided determinations for additional active components not of interest to the present cough-cold product, Naldecon DX Pediatric Syrup (Bristol-Myers Squibb, Evansville, IN, USA). Simultaneous HPLC assays have been described on phenylpropanolamine-sodium benzoate-guaifenesin [15,16], phenylpropanolamine-dextromethorphan [17], phenylpropanolamine-guaifenesin [18] and dextromethorphan-guaifenesin [19],

* Corresponding author.

usually along with other components. Among these latter studies, two were internal standard methods using C_{18} columns [18,19], one was an internal standard, phenyl column method [16] and one was an external standard method which used a C_{18} column along with a standard addition method to measure accuracy [17]. The final simultaneous assay method used external standards with accuracy validated by means of spiked placebos employing a C_8 column with an ion-pairing mobile phase [15]. It was desired to validate two more efficient (in terms of sample and standard preparation) external standard methods in the present study, one of which could be used to assay guaifenesin and sodium benzoate and the other to assay phenylpropanolamine·HCl and dextromethorphan·HBr in the cough-cold preparation, simultaneously.

Reagents and drugs

HPLC-grade solvents for chromatography included acetonitrile and methanol from J.T. Baker (Phillipsburg, NJ, USA) and reagent-grade water, processed at Lancaster Labs (Lancaster, PA, USA). Reagent-grade glacial acetic acid, hydrochloric acid (12 M), sodium hydroxide (pellets) and hydrogen peroxide (30%) were from Fisher Scientific (Fair Lawn, NJ, USA) while ammonium dihydrogen phosphate was from J.T. Baker and diethylamine was from Aldrich (Milwaukee, WI, USA). Drugs used in the investigation include guaifenesin (lot G-3), dextromethorphan·HBr (lot H) and phenylpropanolamine·HCl (lot H) from the United States Pharmacopeial Convention (Rockville, MD, USA) and sodium benzoate (lot KX06814HW) from Aldrich. The drug product Naldecon DX Pediatric Syrup (lot MHM44) and the product placebo (Lot E91L047 549-GN-152) were from Bristol-Myers Squibb.

Instrumentation

HPLC analysis was conducted using a modular HP 1050 system (Hewlett-Packard, Palo Alto, CA, USA) consisting of a pump run at 2.0 ml/min for the PPA-DM assay and 1.3 ml/min for the B-G assay. The variable-wavelength UV

detector was set at 263 nm for the PPA-DM assay and 273 nm for the B-G assay. The autosampler injected 20 μ l in the PPA-DM assay and 25 μ l in the B-G assay. Columns utilized included Waters (Milford, MA, USA) μ Bondapak C_{18} , 10 μ m particle size, 30 cm \times 3.9 mm for the B-G assay and Whatman (Clifton, NJ, USA) PXS SCX, 10 μ m particle size, 25 cm \times 4.6 mm for the PPA-DM assay. A Model CH-30 column heater was used from Flatron Systems, Eppendorf N.A. (Madison, WI, USA), while chromatographic data were acquired and analyzed using a Chrom Perfect system (Justice Innovations, Palo Alto, CA, USA).

Mobile phases

A buffered aqueous-organic mixture consisting of 0.1 M $(NH_4)(H_2PO_4)$ -MeOH (30:70, v/v) with an apparent pH of 6.2 was used in the PPA-DM assay with the column temperature controlled at 40°C while the B-G assay employed water-diethylamine-glacial acetic acid-acetonitrile (739:1:10:250, v/v, apparent pH 4.1) with the column temperature controlled at 35°C.

Procedure

Standard preparation

Phenylpropanolamine-dextromethorphan assay. A mixed standard solution was prepared containing 1.25 mg/ml, 1.00 mg/ml and 1.00 mg/ml of phenylpropanolamine·HCl, dextromethorphan·HBr and sodium benzoate reference standards, respectively in water. A 10-ml volume of this solution was added to a 50-ml volumetric flask containing 200.0 mg of guaifenesin reference standard which was then diluted to volume with water to give the mixed working standard for the PPA-DM assays.

Guaifenesin-sodium benzoate assay. A 5-ml volume of the diluted mixed standard from the phenylpropanolamine-dextromethorphan assay above was further diluted to 100.0 ml with water to give the mixed standard for the B-G assay.

Sample preparation

Phenylpropanolamine–dextromethorphan assay. A 10-ml volume of sample was transferred to a 50-ml volumetric flask using a TC ('to contain') pipet which was rinsed several times with water. The rinsings were added to the flask and it was diluted to volume with water and mixed.

Guaifenesin–sodium benzoate assay. A 5-ml volume of the sample preparation from the phenylpropanolamine–dextromethorphan assay above was further diluted to 100.0 ml with water to give the final sample dilution for the B–G assay.

System suitability

Phenylpropanolamine–dextromethorphan assay. System precision was shown by 6 replicate injections of the mixed working standard which must give an R.S.D. of $\leq 2.0\%$ by peak area. The resolution factor between the DM and PPA peaks must be ≥ 6.0 . The tailing factor for both PPA and DM peaks must be ≤ 2.0 .

Guaifenesin–sodium benzoate assay. Precision was shown by 6 replicate injections of the final mixed standard which must give an R.S.D. of $\leq 2.0\%$ by peak area. The resolution factor between guaifenesin and sodium benzoate must be ≥ 4.0 . The tailing factor for both guaifenesin and benzoate must be ≤ 2.0 .

Accuracy—linearity of recovery

Phenylpropanolamine–dextromethorphan assay. Samples were prepared at 80, 100 and 120% of the label sample amounts of PPA, DM, B and G in triplicate containing an appropriate volume of the placebo solution and were assayed by the described method.

Guaifenesin–sodium benzoate assay. The synthetic samples prepared above containing placebo plus 80, 100 or 120% of sodium benzoate, guaifenesin, phenylpropanolamine·HCl and dextromethorphan·HBr, were diluted with water to the prescribed volume in triplicate and were assayed.

Precision

Phenylpropanolamine–dextromethorphan assay. System precision measurements were made

from 10 replicate injections of a single sample preparation. Method precision—ruggedness was measured by assaying six sample preparations from a composite by two analysts in different labs each using new standards and mobile phase.

Guaifenesin–sodium benzoate assay. System and method precision were determined as for the PPA–DM assay.

Selectivity

Phenylpropanolamine–dextromethorphan assay. Method selectivity was shown by stressing samples of the product (containing the three actives and the benzoate preservative) which were diluted 10 in 50 with water by means of heat (reflux, 24 h), light (Rayonet Photochemical Reactor Model RMR-500, Southern New England Ultraviolet Co., Hamden, CT, USA, 5 days), peroxide (5 ml 5% H₂O₂ brought to reflux and cooled), acid (5 ml 1 M HCl brought to reflux and cooled, neutralized and diluted to volume) and base (5 ml 1 M NaOH brought to reflux and cooled, neutralized and diluted to volume). In addition placebos were evaluated chromatographically to ensure there was no interference in the assay.

Guaifenesin–sodium benzoate assay. Method selectivity was tested using the same stressed (heat, light, peroxide, acid and base) diluted solutions as for the PPA–DM assay as well as the corresponding placebo.

RESULTS AND DISCUSSION

Drug product stability studies require potency assay validation data for submission to regulatory authorities in support of each method. The validation minimally requires proof of accuracy (linearity of recovery from spiked placebos), precision (system and method) and selectivity (through stressed drug substance or drug product) along with some indication of ruggedness (interlab, interanalyst or interday adequacy of performance). In order to facilitate rapid sample preparation and analysis of multicomponent products, it would be desirable to combine the procedures for as many components as possible into simultaneous methods. For these multi-

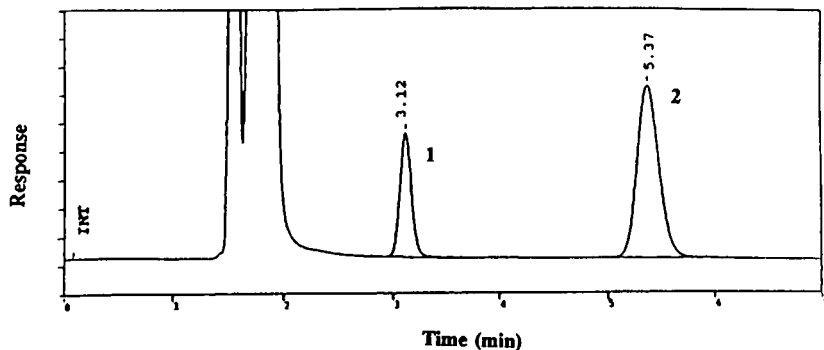


Fig. 1. Chromatogram (peak response vs. time) of a standard preparation for the PPA–DM assay showing peaks for phenylpropanolamine (1) and dextromethorphan (2) at 3.1 and 5.4 min, respectively.

component products, methods validation requirements are complicated by the necessity of validating the assay for each component knowing the possibility that degradation products from one component or excipient could interfere with the analysis of another component.

Method selectivity

The method for PPA and DM analysis used a 10- μm 25-cm SCX column with an ammonium phosphate monobasic buffered mobile phase which would produce ionizing conditions at the apparent pH of 6.2 for both bases phenylpropanolamine and dextromethorphan with respective pK_a values of 9.4 and 8.2. The chromatogram of a standard preparation is shown in Fig. 1 with PPA showing the lower retention of the two compounds (3.1 min). The large solvent front peak from 1.5 to 2.5 minutes also contains the

other components guaifenesin and benzoate, as would be seen in placebo chromatograms using this method. When the drug product was stressed with heat, light, peroxide, acid or base, no interference was seen with the PPA or DM peaks. Fig. 2, for example, shows the separation of two sets of minor light-induced degradation products at 2.8 and 4.3 min, well removed from the main peaks.

A chromatogram of the standard preparation in the B–G method is shown in Fig. 3. The peak seen at 12 min in all chromatograms in the B–G method is dextromethorphan. Selectivity in the reversed-phase method for guaifenesin and sodium benzoate was also demonstrated by lack of interference from degradation products in chromatograms of acid, base, heat, peroxide and light-stressed samples. Fig. 4 is a chromatogram of a peroxide stressed sample showing the stress-

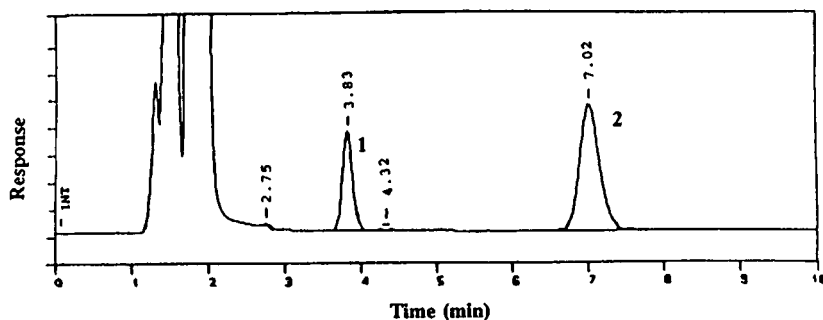


Fig. 2. Chromatogram of a light stressed sample using the PPA–DM assay procedure showing minor stress-induced peaks at 2.8 and 4.3 min. Peaks 1 and 2 as in Fig. 1.

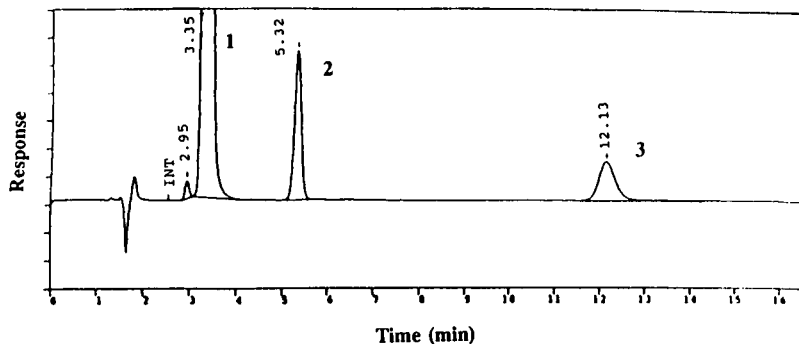


Fig. 3. Chromatogram of a standard preparation for the B–G assay showing peaks for guaifenesin (1) at 3.4 min, benzoate (2) at 5.3 min and dextromethorphan (3) at 12.1 min.

induced degradation products separated from the guaifenesin peak at 3.4 min and the benzoate peak at 5.3 min.

Method accuracy

Accuracy of the described methods is shown by linearity of recovery data for the individual components. Table I gives results for the PPA–DM method with percent recoveries at the 80, 100 and 120% label claim values. Mean recoveries of 100.6 and 100.7% were found for PPA and DM, respectively, along with very acceptable mean R.S.D. recoveries of 1.0 and 0.8%. Similarly for the B–G method with results shown in Table II, mean recoveries of 100.1 and 102.4% were found for guaifenesin and sodium benzoate respectively. Their mean R.S.D. recoveries were also good at 0.4% each. The somewhat elevated benzoate recovery is not

considered a systematic error and is in an acceptable range.

Precision and ruggedness

LC method precision measurements can be made to show both system and method reproducibility. In the current study system precision was measured by ten replicate injections of a single sample preparation into both the PPA–DM and the B–G systems. Results of this study shown in Table IIIA, reveal excellent precision with R.S.D. values no greater than 0.3% for each component.

By way of comparison, method precision was demonstrated by analysis of six replicate sample preparations in both the PPA–DM and the B–G systems. Results found in Table IIIB again show high orders of reproducibility in the sample preparation and analysis procedure with R.S.D.

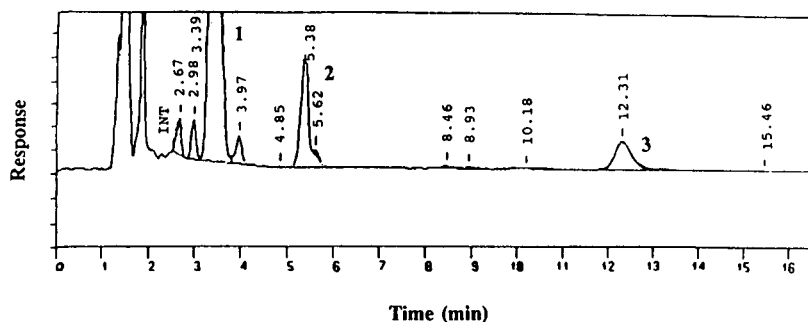


Fig. 4. Chromatogram of a peroxide-stressed sample using the B–G assay procedure. Guaifenesin (1), benzoate (2) and dextromethorphan (3) are seen as in Fig. 3 while the other small integrated peaks are peroxide-induced decomposition products.

TABLE I

LINEARITY OF RECOVERY RESULTS FOR PHENYLPROPANOLAMINE AND DEXTROMETHORPHAN IN SYNTHETIC SAMPLE STUDIES

Phenylpropanolamine · HCl					Dextromethorphan HBr				
Added (%)	Mean found (%) (n = 2)	Recovery (%)	Mean recovery (%)	R.S.D. recovery (%)	Added (%)	Mean found (%) (n = 2)	Recovery (%)	Mean recovery (%)	R.S.D. recovery (%)
80.00	80.24	100.2	101.4	1.2	80.16	80.49	100.4	101.2	1.1
79.87	82.13	102.8			79.36	81.32	102.5		
79.87	80.81	101.2			80.00	80.59	100.7		
100.00	99.48	99.5	100.5	0.9	100.20	100.09	99.9	100.5	0.6
99.84	101.07	101.2			99.20	100.36	101.2		
99.84	100.60	100.8			100.00	100.50	100.5		
120.00	118.78	99.0	100.0	0.9	120.24	119.60	99.5	100.3	0.8
119.81	120.61	100.7			119.04	120.28	101.0		
119.81	120.25	100.4			120.00	120.56	100.5		
Mean R.S.D. recovery (%)				1.0					0.8
Slope				0.971					0.985
Intercept				3.419					2.155
Correlation coefficient				0.9987					0.9991

values all less than 0.6% for all four components.

One means of showing method ruggedness (robustness) is to determine variability resulting from a reanalysis of samples by a second analyst

using a new standard preparation and new mobile phase with another instrument. Table IIC shows results for this ruggedness test on the four component cough-cold product. Differences in mean values found for each of the four

TABLE II

LINEARITY OF RECOVERY RESULTS FOR GUAIFENESIN AND SODIUM BENZOATE IN SYNTHETIC SAMPLE STUDIES

Guaifenesin					Sodium benzoate				
Added (%)	Mean found (%) (n = 2)	Recovery (%)	Mean recovery (%)	R.S.D. recovery (%)	Added (%)	Mean found (%) (n = 2)	Recovery (%)	Mean recovery (%)	R.S.D. recovery (%)
79.6	79.59	100.0	100.2	0.3	79.36	81.47	102.7	103.0	0.4
79.2	79.63	100.5			79.04	81.78	103.5		
81.4	81.37	100.0			79.36	80.67	102.9		
99.8	99.31	99.5	100.1	0.6	99.20	101.26	102.1	102.3	0.3
100.0	100.18	100.2			98.80	101.01	102.2		
98.8	99.35	100.6			99.20	101.85	102.7		
119.6	119.52	99.9	99.9	0.2	119.04	121.10	101.7	102.0	0.4
119.0	119.06	100.1			118.56	120.78	101.9		
120.6	120.20	99.7			119.04	122.06	102.5		
Mean R.S.D. recovery (%)				0.4					0.4
Slope				0.993					1.010
Intercept				0.756					1.319
Correlation coefficient				0.9998					0.9996

TABLE III

PRECISION RESULTS FOR COMPONENTS IN COUGH-COLD PRODUCT

Sample	Phenylpropanolamine · HCl	Dextromethorphan · HBr	Guaifenesin	Sodium benzoate
<i>(A) System precision results found in terms of mg of each component per 5 ml product</i>				
1	6.22	4.97	99.20	5.05
2	6.22	4.97	99.22	5.06
3	6.21	4.96	99.13	5.06
4	6.22	4.96	99.59	5.06
5	6.20	4.95	99.74	5.09
6	6.21	4.96	99.13	5.04
7	6.19	4.96	99.14	5.06
8	6.22	4.96	99.17	5.07
9	6.20	4.95	99.18	5.08
10	6.18	4.93	99.38	5.08
Mean	6.21	4.96	99.29	5.07
R.S.D. (%)	0.2	0.2	0.2	0.3
<i>(B) Method precision results in terms of mean recoveries (n = 2) in mg of each component per 5 ml</i>				
1	6.22	4.94	99.17	5.07
2	6.20	4.94	99.18	5.08
3	6.21	4.94	99.93	5.10
4	6.23	5.00	99.55	5.08
5	6.25	4.98	99.16	5.07
6	6.25	4.99	99.21	5.06
Mean	6.23	4.97	99.37	5.08
R.S.D. (%)	0.3	0.6	0.3	0.3
<i>(C) Robustness test results, precision of replicate sample analysis by second analyst, means of n = 2</i>				
1	6.23	4.98	100.78	5.15
2	6.22	4.97	98.99	5.05
3	6.21	4.96	99.21	5.08
4	6.25	5.01	99.08	5.04
5	6.27	5.01	99.77	5.09
6	6.22	4.97	99.57	4.96
Mean	6.23	4.98	99.40	5.08
R.S.D. (%)	0.4	0.4	0.8	1.3

components between the two sets of six replicates (Table IIIB vs. Table IIIC) were no more than 0.2%, indicating ease of method transfer between labs.

System suitability

The chromatographic systems met the system suitability criteria of precision, resolution and tailing factors as described in the Experimental section indicating that they were performing satisfactorily and reproducibly.

The above findings on method selectivity, accuracy, precision and ruggedness, fulfill the requirements for validation of a stability-indicating HPLC method for regulatory submission. Improvements incorporated in these methods over

previous methods were made in the areas of sample preparation, instrumentation parameters and actual chromatography. Sampling viscous syrups with a TC pipet employing the usual rinsing procedure was found to aid in method precision and accuracy as did dilution to the 0.2 mg/ml level for guaifenesin, 0.0125 mg/ml for PPA and 0.01 mg/ml for both DM and B. These changes made possible use of ordinary 20–25- μ l loop autoinjectors with increased efficiency. Detector wavelength optimization at 273 nm for the B–G assay and 263 nm for the PPA–DM assay was also useful in this regard. Common mixed standards with dilution from the PPA–DM level to the B–G assay levels combined with a similar sample dilution for each assay provided an en-

hanced efficiency and time savings. Use of the column heater at 35–40°C gave reproducible retention times and peaks of decreased tailing factor.

CONCLUSIONS

The developed methods for phenylpropanolamine–dextromethorphan and for benzoate–guaifenesin make possible the rapid, accurate and precise measurement of these ingredients in the cough-cold product under investigation. They will provide sufficient quality data to support product stability claims as required for marketing a safe and effective composition.

REFERENCES

- 1 P. Taylor, P.D. Braddock and S. Ross, *Analyst*, 109 (1984) 619.
- 2 S.M. El-Gizawy and A.N. Ahmed, *Analyst*, 112 (1987) 867.
- 3 D. R. Heidemann, *J. Pharm. Sci.*, 70 (1981) 820.
- 4 J.H. Mike, B.L. Ramos and T.A. Zupp, *J. Chromatogr.* 518 (1990) 167.
- 5 J. Araujo, J.F. Boyer and M.L. Probecker, *STP Pharma*, 4 (1988) 598.
- 6 S.K. Pant, B.K. Maitin and C.L. Jain, *Indian Drugs*, 28 (1990) 105.
- 7 A. Menyharth, F.P. Mahn and J.E. Heveran, *J. Pharm. Sci.*, 63 (1974) 430.
- 8 E.J. Kubiak and J.W. Munson, *J. Pharm. Sci.*, 69 (1980) 1380.
- 9 J.L. Murtha, T.N. Julian and G.W. Radebaugh, *J. Pharm. Sci.*, 77 (1988) 715.
- 10 A. Manz and Harry Jacin, *Liquid Chromatographic Analysis of Food and Beverages, Proceedings of a Symposium on Analysis of Foods and Beverages, Honolulu, HI, April 1–6, 1979*, Vol. 2, Academic Press, New York, 1979, p. 397.
- 11 P. Linares, M.C. Gutierrez, F. Lazaro, M.D.L. DeCastro and M. Valcarcel, *J. Chromatogr.*, 558 (1991) 147.
- 12 Anonymous, *Milchwissenschaft*, 43 (1988) 366.
- 13 B. Mandrou, H. Fabre, Y. Mou and C. Diez-Marques, *Ann. Fals. Exp. Chim.*, 82 (1989) 325.
- 14 L. Carnevale, *J. Pharm. Sci.*, 72 (1983) 196.
- 15 G.W. Schieffer, W.O. Smith, G.S. Lubey and D.G. Newby, *J. Pharm. Sci.*, 73 (1984) 1856.
- 16 N. Muhammad and J.A. Bodnar, *J. Liq. Chromatogr.*, 3 (1980) 113.
- 17 J.E. Kountourellis, C.E. Markopoulou and P.P. Georgakopoulos, *Anal. Lett.*, 23 (1990) 883.
- 18 G.W. Schieffer and D.E. Hughes, *J. Pharm. Sci.*, 72 (1983) 55.
- 19 W.O. McSharry and I.V. Savage, *J. Pharm. Sci.*, 69 (1980) 212.

Isomeric separation of Beraprost sodium using an α_1 -acid glycoprotein column

Laurie A. Sly, Donald L. Reynolds and Thomas A. Walker*

Development Resources, Marion Merrell Dow Inc., P.O. Box 9627, Kansas City, MO 64134 (USA)

(First received March 9th, 1993; revised manuscript received March 30th, 1993)

ABSTRACT

The separation of the four stereoisomers present in Beraprost sodium, a prostacyclin analogue, has been accomplished using an α_1 -acid glycoprotein stationary phase (Chiral AGP column). The stereoisomers are baseline resolved with a runtime of less than ten minutes. This chiral separation is used to quantitate the four Beraprost sodium stereoisomers present in the bulk drug, tableted formulations and in pharmacological and toxicological studies. The mobile phase variables that were found to have an effect on the stereoisomeric separation were studied and include: ionic strength, type and concentration of organic modifier, mobile phase pH and column temperature. Optimum stereoisomer separation was achieved on the Chiral AGP column. Calibration curves were linear for all four stereoisomers over the range of 0.024 to 4.04 $\mu\text{g/ml}$ using fluorescence detection (correlation coefficients were greater than 0.999). A detection limit of 0.004 $\mu\text{g/ml}$ was found for each stereoisomer. This assay has been used to determine the ratio of the four stereoisomers in the bulk drug as well as in the final formulated tablets.

INTRODUCTION

The separation of enantiomers has become an important area of analytical chemistry, especially in the pharmaceutical industry. The ability to separate and quantitate enantiomers in a drug composed of a racemic mixture is being addressed by the regulatory agencies of the United States, Japan and the European Economic Community [1–5]. Areas where a chiral separation must be used for a racemic mixture are: bulk drug stability, drug product stability, pharmacology, toxicology and pharmacokinetic studies. Without the development of a chiral separation, critical information about the drug would not be available.

A new class of prostaglandin derivatives was discovered in 1976 [prostacyclin (PGI_2)] [6]. PGI_2 was found to be an inhibitor of platelet aggregation and also had potent vasodilating

properties [7]. These properties lead to investigating its use of atherosclerosis [8], diabetes [9] and uremia [10]. The instability of PGI_2 in acidic or neutral conditions has been a major problem in studying this drug. The half-life of PGI_2 in an aqueous solution at pH 7.0 and 25°C is about 2 min [11]. Due to the instability of PGI_2 , research has been ongoing in the search for an analogue that is more stable and yet maintains the same anti-platelet and vasodilating properties.

The compound used in this study, Beraprost sodium {Sodium ($1R^*$, $2R^*$, $3aS^*$, $8bS^*$)-2,3,3a,8b-tetrahydro-2-hydroxy-1-[(*E*)-(3*S**,4*RS*)-3-hydroxy-4-methyl-1-octen-6-ynyl]-1*H*-cyclopenta[*b*]benzofuran-5-butyrates}, is a prostacyclin analogue that is significantly more stable in aqueous solutions yet has the same properties as those found for the original PGI_2 [12–16]. Beraprost sodium (Fig. 1) is composed of two diastereomers with each diastereomer containing a pair of enantiomers. The ability to separate and quantitate the isomers present in a racemic mixture is important in pharmaceutical products,

* Corresponding author.

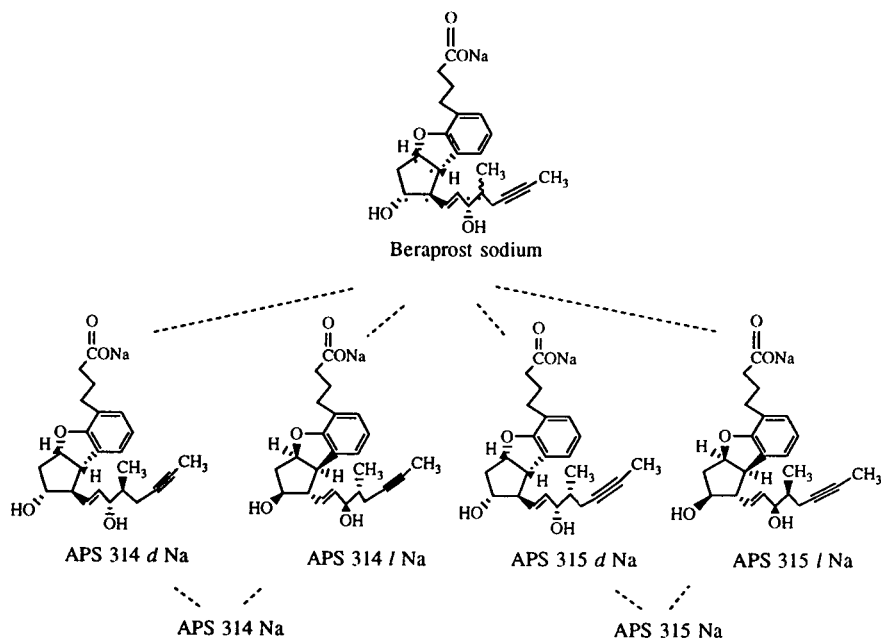


Fig. 1. Structure of Beraprost sodium and its four stereoisomers.

especially in terms of both bulk drug and formulation stability and purity [1].

A chiral separation of the four stereoisomers present in Beraprost sodium (BPS) has been accomplished. This separation uses a commercially available protein column (Chiral AGP) that is composed of an α_1 -acid glycoprotein which is covalently bound to silica gel. The AGP column was introduced as a chiral selector in liquid chromatography in 1983 by Hermansson [17]. The molecular mass of AGP is 41 000 and the protein is comprised of polypeptide and carbohydrate moieties that account for approximately 55% and 45% of its mass, respectively. The isoelectric point in phosphate buffer has been found to be 2.7 [18].

AGP is an extremely stable protein that tolerates organic solvents and high temperatures, and a wide pH range without being denatured [19]. Direct chiral separations of racemic mixtures can be performed on the AGP column for diverse types of compounds including primary, secondary and tertiary amines, acids and non-protolytic compounds. The exact retention mechanism on an AGP column is not known. However, the column does show reversed-phase

characteristics which allow many possibilities for changing enantioselectivity and retention through changes in mobile phase composition. Retention also appears to be due to a combination of hydrogen bonding, hydrophobic, electrostatic (coulombic) and charge transfer interactions [20,21].

The sample capacity of the AGP column has been investigated [21,22]. It was found that a 10-fold increase in the amount of metoprolol injected (0.5 to 5 nmol) resulted in a 10% decrease in retention with no effect on peak symmetry. The α value was unchanged over the range of sample studied. From this study, it was recommended that 3 to 5 nmol of analyte be injected into the analytical column.

The ruggedness (stability) of the Chiral AGP column has also been studied. A mobile phase consisting of 10.0 mM phosphate buffer, pH 7.0 with isopropanol (IPA)–water (6:94) was used for the separation of bupivacaine and mepivacaine as test compounds. Capacity factors of the test compounds were almost unaffected after the passage of approximately 40 000 column volumes (about 40 l) of mobile phase [19]. The AGP column also appears to be stable with high

concentrations of organic modifiers, buffers, and at elevated column temperatures without noticeable deterioration [19].

Not only have clean analytical samples been run on the Chiral AGP column, so have samples derived from biological matrices. The determination of enantiomers at low concentrations in plasma and urine has been accomplished [23,24]. The AGP column has been used for determining the enantiomers of atenolol, a β -receptor blocking agent, in human plasma at 1 ng/ml level for each enantiomer [25].

This paper will discuss the various mobile phase parameters that were studied and what affect each parameter had on the separation of the four stereoisomers present in Beraprost sodium. Detection limits and quantitation limits as well as calibration data will also be presented.

EXPERIMENTAL

Reagents and instrumentation

Beraprost sodium and the four stereoisomers (APS 314*d*, APS 314*l*, APS 315*d*, APS 315*l*) were obtained from Toray Industries (Kamakura, Japan). Acetonitrile, methanol and IPA (all HPLC-grade) were obtained from Burdick and Jackson (Muskegon, MI, USA). Phosphoric acid, sodium dibasic phosphate, and sodium hydroxide were obtained from Mallinckrodt (Paris, KY, USA). HPLC-grade water was obtained by passing deionized water through a Nanopure II water purification system (Barnstead, Dubuque, IA, USA). The instrumentation consisted of a Waters Model 600E system controller, Waters Model 600 solvent delivery system, Waters Model 700 Satellite WISP autosampler (Waters, Milford, MA, USA), a Linear Model LC-304 fluorescence detector (Linear Instruments, Reno, NV, USA), Waters Model 484 variable wavelength UV detector and Beckman PeakPro Chromatography data system (Beckman, Fullerton, CA, USA). The Chrom Tech (100 \times 4.0 mm, 5 μ m) Chiral AGP column was purchased from ASTEC (Whippany, NJ, USA).

Procedures

Standard analyte samples were weighed out in a humidity controlled glove box. (Beraprost

sodium is a potent vasodilator and very hygroscopic, therefore care must be taken when handling dry samples of bulk drug.) HPLC-grade water was added to the volumetric flask before taking the standards out of the glove box. Standards were then diluted to volume with HPLC-grade water and mixed. Calibration data was obtained by making at least four measurements at each data point (peak area vs. amount of analyte injected). Flow-rates of 1.0 ml/min were used for all separations. Fluorescence detection performed using an excitation wavelength of 282 nm and an emission wavelength of 304 nm. Injection volumes of 100 μ l were used.

RESULTS AND DISCUSSION

The mobile phase parameters that had a significant effect on the resolution of Beraprost sodium isomers on the Chiral AGP column are: type and concentration of organic modifier, ionic strength, mobile phase pH and column temperature. Each parameter was studied to evaluate their influence on the separation of the Beraprost sodium stereoisomers.

Organic modifier

The type and concentration of organic modifier had a profound affect on stereoisomer retention and resolution. Small changes in the concentration of methanol, IPA and acetonitrile produced large changes in stereoisomer retention. Stereoisomer separations performed using IPA showed better peak shapes than mobile phases containing methanol. Acetonitrile provided similar stereoisomer separations to the IPA mobile phases. However enantioselectivities and resolution were better with the IPA mobile phases. Small changes in CH₃CN concentration did not affect the separations nearly as much as did slight changes in the amount of IPA; a mobile phase containing 2% CH₃CN was equivalent to a mobile phase that contained 1% IPA. However, when a combination of CH₃CN–IPA were used, peak shape and resolution were superior when compared to mobile phases that contained only CH₃CN or IPA. Fig. 2 shows the effect of CH₃CN concentration on the stereoisomer retention while Fig. 3 compares the

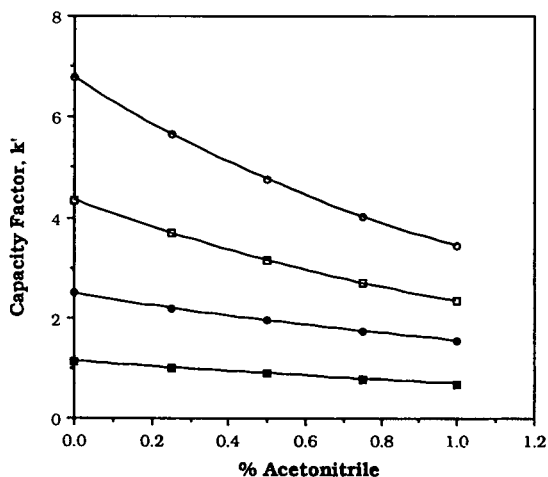


Fig. 2. Effect of acetonitrile concentration on the retention of Beraprost sodium stereoisomers on a Chiral AGP column. Mobile phase: 20.0 mM Na_2HPO_4 , pH 7.0, CH_3CN -1.5% IPA-water. ■ = APS 314l; ● = APS 315l; □ = APS 314d; ○ = APS 315d.

separation of stereoisomers when two different concentration produced a significant difference in stereoisomer retention and in the time required for the separation. This shows that the organic modifier must be carefully measured to avoid changes in the stereoisomer separation.

Mobile phase ionic strength

Retention of each stereoisomer was directly proportional to mobile phase ionic strength (Fig. 4). As the concentration of buffer was increased, retention of the stereoisomers also increased. For example, when a mobile phase containing a 5.0 mM phosphate buffer at pH 7.0 was used, retention times for the stereoisomers were between 1 and 4 min. When the phosphate buffer concentration was increased to 60.0 mM, retention times for the stereoisomers increased to between 2 and 20 min. The increase in stereoisomer retention with increasing ionic strength may be attributed to salting out of the stereoisomers onto the stationary phase.

Mobile phase pH

Research has shown that mobile phase pH has a strong influence on the retention and enantioselectivity of basic, acidic and non-protolytic compounds [26]. In one study, anionic analytes

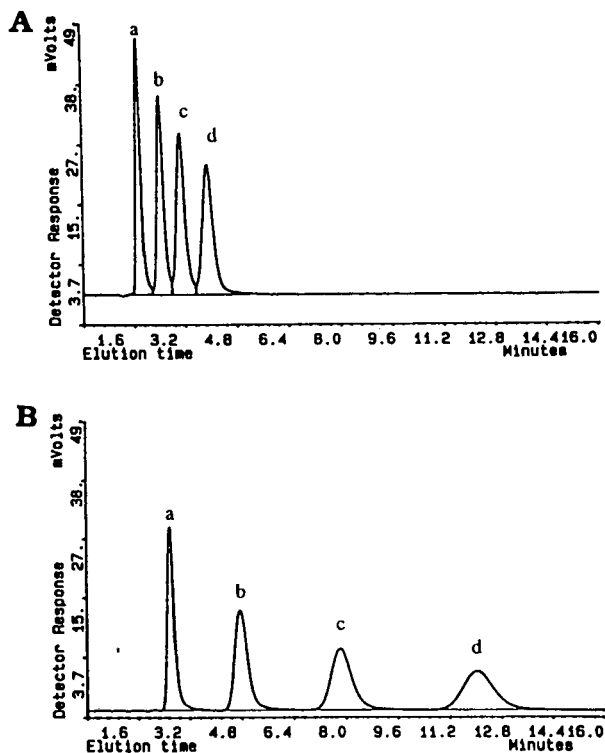


Fig. 3. Separation of Beraprost sodium stereoisomers on a Chiral AGP column using different concentrations of IPA. Mobile phase: 20.0 mM Na_2HPO_4 , pH 7.0-0.5% CH_3CN -water (v/v/v), (A) 1.0% (v/v) IPA added to the mobile phase, (B) 0.5% (v/v) added to the mobile phase, a = APS 314l, b = APS 315l, c = APS 314d, d = APS 315d.

showed increased retention with decreasing mobile phase pH [27]. However, this study covered a pH range of 6.1 to 7.0 and did not investigate what effect lower pH mobile phases would have on anionic analyte retention.

Similar results were found for the BPS stereoisomers (Fig. 5). As the mobile phase pH was decreased from 7.0 to 3.0, retention of the stereoisomers increased until about pH 4.0 and then decreased. Enantioselectivity also decreased over this pH range. The increase in stereoisomer retention from pH 7 to 4 can be explained as follows. As the pK_a of the stereoisomers is approached, the stereoisomers become more hydrophobic and interact more strongly with the hydrophobic stationary phase. The stereoisomers had the highest retention times just below their pK_a values where the

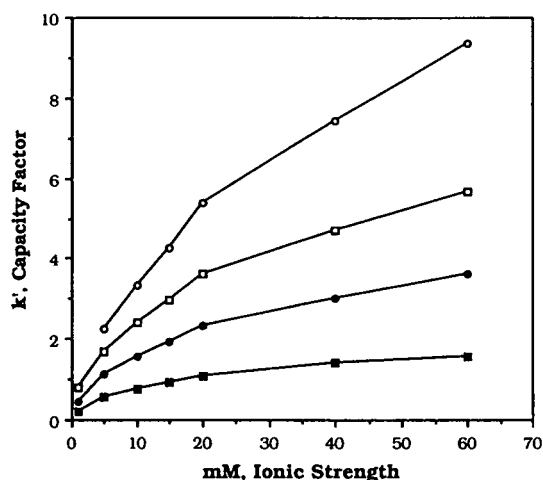


Fig. 4. Effect of ionic strength on stereoisomer retention: sodium phosphate buffer, pH 7.0, CH₃CN–IPA–water (0.5:1.0:98.5) mobile phase. ■ = APS 314l; ● = APS 315l; □ = APS 314d; ○ = APS 315d.

stereoisomers are mostly neutral. The decrease in stereoisomer retention below pH 4.0 can be explained by fewer ionic interactions and less hydrogen bonding taking place between the stereoisomers and the stationary phase as the stationary phase approaches its isoelectric point (pH 2.7).

Stereoisomer resolution as well as peak shape was best at a mobile phase pH of 7.0. Although

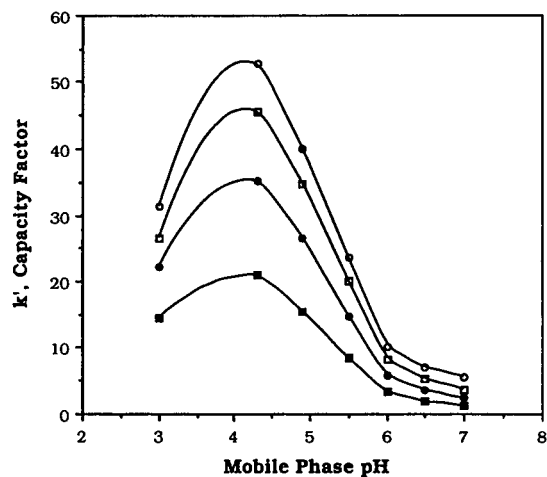


Fig. 5. Effect of mobile phase pH on stereoisomer retention: a 20.0 mM Na₂HPO₄, CH₃CN–IPA–water (0.5:1.0:98.5, v/v/v) mobile phase. ■ = APS 314l; ● = APS 315l; □ = APS 314d; ○ = APS 315d.

the stereoisomers were still resolved at some lower mobile phase pH values, peak shape was unacceptable.

Column temperature

The effect of column temperature on the retention, enantioselectivities, and resolution of several basic drugs using an AGP column has been reported [26]. At higher column temperatures, enantioselectivity decreased while column efficiency increased. The increase in efficiency was attributed to faster transfer kinetics between the stationary phase and the stereoisomers.

Similar results were found for the four Bera-prost sodium stereoisomers. Retention and selectivities of the stereoisomers decreased with increasing temperature, however, peak shape was improved (Fig. 6). Optimal peak shape was observed at a column temperature of 35°C.

Flow-rate

Several flow-rates were studied to determine if resolution would be affected. The flow-rates studied were 0.8, 0.9, 1.0 and 1.1 ml/min. Resolution was improved with lower flow-rates, however, peak tailing increased. A flow-rate of 1.0 ml/min provided the best compromise between resolution and peak tailing.

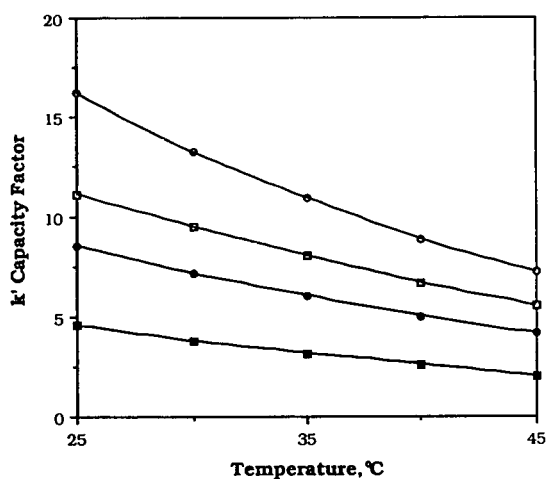


Fig. 6. Effect of column temperature on stereoisomer retention: a 20.0 mM Na₂HPO₄, CH₃CN–IPA–water (0.5:1.0:98.5, v/v/v) mobile phase. ■ = APS 314l; ● = APS 315l; □ = APS 314d; ○ = APS 315d.

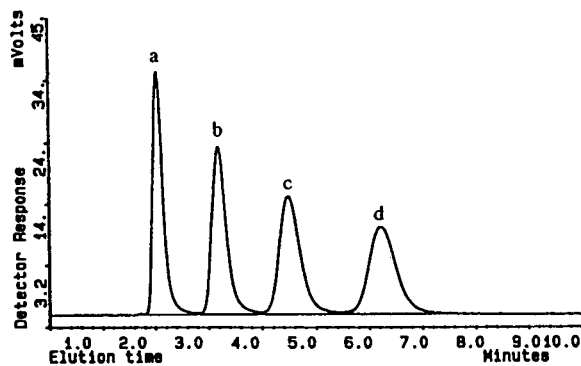


Fig. 7. Optimized separation of Beraprost sodium stereoisomers on the Chiral AGP column: a 20.0 mM Na_2HPO_4 , CH_3CN -IPA-water (0.5:1.0:98.5, v/v/v) mobile phase; column temperature; 35°C. a = APS 314l, b = APS 315l, c = APS 314d, d = APS 315d.

Separation

The optimized separation for the Beraprost sodium stereoisomers is shown in Fig. 7. The mobile phase was composed of Na_2HPO_4 (20.0 mM, pH 7.0 adjusted with NaOH) and a solvent composition of CH_3CN -IPA-water (0.5:1.0:98.5, v/v/v). A flow-rate of 1.0 ml/min and a column temperature of 35°C were used. The four stereoisomers were baseline resolved with a runtime of ten min.

TABLE II

EFFECT OF SAMPLE LOADING ON PEAK TAILING AND RESOLUTION

BPS Na ^a ($\mu\text{g}/\text{ml}$)	Peak tailing ^b				Resolution ^c		
	314l	315l	314d	315d	l/l	l/d	d/d
45.5	1.71	1.74	1.81	1.95	1.96	1.64	1.71
40.9	1.68	1.69	1.77	1.87	2.03	1.70	1.77
36.4	1.65	1.64	1.70	1.81	2.11	1.77	1.86
29.1	1.61	1.58	1.61	1.67	2.22	1.87	1.98
23.7	1.57	1.49	1.54	1.59	2.30	1.97	2.09
18.2	1.53	1.45	1.46	1.47	2.41	2.07	2.20
14.6	1.50	1.41	1.40	1.38	2.47	2.13	2.26
9.10	1.45	1.33	1.30	1.28	2.61	2.27	2.40
4.6	1.42	1.29	1.27	1.22	2.73	2.36	2.49
0.45	1.38	1.22	1.15	1.14	2.85	2.48	2.51
0.05	1.29	1.11	0.98	1.06	2.93	2.38	2.31

^a BPS Na = Beraprost sodium.

^b Calculated using USP XXII peak tailing method.

^c Calculated using USP XXII resolution method.

TABLE I

METHOD PRECISION AT DIFFERENT CONCENTRATIONS OF BERAPROST SODIUM

Determined using four injections at each concentration.

$\mu\text{g}/\text{ml}$	R.S.D. (%)			
	314l	315l	314d	315d
4.04	0.42	0.34	0.23	0.32
3.06	0.22	0.19	0.22	0.26
1.97	0.25	0.56	0.70	0.82
0.985	0.45	0.21	0.75	0.20
0.747	0.74	0.67	0.99	1.10
0.245	1.13	0.73	2.09	5.03
0.202	1.16	1.82	2.03	4.34
0.149	1.82	0.89	2.40	2.82
0.118	1.85	0.38	1.40	1.30
0.049	4.65	3.81	6.97	3.49
0.024	4.97	10.31	4.30	5.48

Calibration curves and sample loading

Calibration curves were established over the range 0.024 $\mu\text{g}/\text{ml}$ to 4.04 $\mu\text{g}/\text{ml}$. A minimum of four injections of each standard was performed. Intraday assay accuracy ranged from 97.4 to 101.9% with a precision of $\pm 1.29\%$.

Interday assay accuracy ranged from 97.9 to 101.4% with a precision of $\pm 2.15\%$ (Table I). Correlation coefficients of greater than 0.999 and detection limits of $0.004 \mu\text{g/ml}$ with a signal-to-noise ratio of 3:1 were found for each stereoisomer. This chromatographic system has been shown to be extremely rugged and reliable with over 1000 injections being done with minimal changes in retention or resolution.

The amount of sample injected onto the AGP stationary phase influenced both peak tailing and resolution (Table II). Peak tailing and resolution were better when smaller amounts of analyte was injected. Therefore, the AGP column is sensitive to the amount of injected analyte. This should be taken into account when determining how much analyte can be chromatographed.

Uses for the chiral HPLC assay

Beraprost sodium is by definition a racemic compound that contains four stereoisomers. The bulk drug and formulated tablets, as part of the release specifications, are assayed using this chiral HPLC method to insure that the ratio of stereoisomers is 1:1:1:1. This chiral HPLC assay is also used to determine the stereoisomer ratio for current and proposed bulk drug and formulated tablet stability studies.

ACKNOWLEDGEMENTS

Part of this work has been presented at *16th International Symposium on Column Liquid Chromatography (HPLC '92)*, Baltimore, MD, June 1992, the *Midwest Regional American Chemical Society Meeting*, Lawrence, KS, November 1992, and the *7th Annual Meeting and Exposition, American Association of Pharmaceutical Scientists*, San Antonio, TX, November, 1992.

REFERENCES

- 1 W.H. De Camp, *Chirality*, 1 (1989) 2.
- 2 *Guideline for Submitting Supporting Documentation in Drug Applications for the Manufacture of Drug Substances*, Office of Drug Evaluation and Research (HFS-100), Food and Drug Administration, Rockville, MD, 1987, pp. 3–4.
- 3 W.H. De Camp, in W.J. Lough (Editor), *Chiral Liquid Chromatography*, Chapman & Hall, New York, 1990, Ch. 2.
- 4 M.N. Cayen, *Chirality*, 3 (1991) 94.
- 5 H. Shindo and J. Caldwell, *Chirality*, 3 (1991) 91.
- 6 S. Moncada, R.J. Gryglewski, S. Bunting and J.R. Vane, *Nature*, 263 (1976) 663.
- 7 S. Moncada and J.R. Vane, *J. Med. Chem.*, 23 (1980) 591–593.
- 8 A. Dembinska-Kiec, T. Gryglewski, A. Zmuda and R.J. Gryglewski, *Prostaglandins*, 14 (1977) 1025.
- 9 M. Johnson, H.E. Harrison, A.T. Raferty and J.B. Elder, *Lancet*, i (1979) 325.
- 10 K. Silberbauer, H. Sinzinger and M. Winter, *Artery*, 4 (1978) 554.
- 11 F. Hirayama, M. Kurihara and K. Uekama, *Int. J. Pharm.*, 35 (1987) 193.
- 12 K. Ohno, H. Nagase, K. Matsumoto, H. Nishiyama and S. Nishio, *Adv. Prostaglandin Thromboxane Leukotriene Res.*, 15 (1985) 279.
- 13 T. Umetsu, T. Murata, Y. Tanaka, E. Osada and S. Nishio, *Jpn. J. Pharmacol.*, 43 (1987) 81.
- 14 S. Nishio, H. Matsuura, N. Kanai, Y. Fukatsu, T. Hirano, N. Nishikawa, K. Kameoka and T. Umetsu, *Jpn. J. Pharmacol.*, 47 (1988) 1.
- 15 N. Toda, *Cardiovascular Drug Review*, 6 (3) (1988) 222.
- 16 K. Nogimori, N. Kajikawa, S. Nishio and N. Yajima, *Prostaglandins*, 37(2) (1989) 205.
- 17 J. Hermansson, *J. Chromatogr.*, 269 (1983) 71.
- 18 K. Schmid, in F.W. Putnam (Editor), *The Plasma Proteins*, Academic Press, New York, 1975, p. 184.
- 19 J. Hermansson, *Trends Anal. Chem.*, 8(7) (1989) 251.
- 20 S. Allenmark, *J. Liq. Chromatogr.*, 9 (1986) 425.
- 21 I.W. Wainer, in W.J. Lough (Editor), *Chiral Liquid Chromatography*, Chapman and Hall, New York, 1990, Ch. 7.
- 22 G. Schill, I. Wainer and S. Barkan, *J. Liq. Chromatogr.*, 9 (1986) 641.
- 23 J. Hermansson, M. Eriksson and O. Nyquist, *J. Chromatogr.*, 336 (1984) 321.
- 24 D. Ofori-Adjei, O. Ericsson, B. Lindstrom, J. Hermansson, K. Adjepon-Yamoah and F. Sjoqvist, *Therap. Drug Monitor.*, 8 (1986) 457.
- 25 M. Enquist and J. Hermansson, *Chirality*, 1 (1989) 3.
- 26 J. Hermansson and M. Eriksson, *J. Liq. Chromatogr.*, 9 (1986) 621.
- 27 G. Schill, I.W. Wainer and S.A. Barkan, *J. Chromatogr.*, 365 (1986) 73.

Enantiomeric separation of fluorescent, 6-aminoquinolyl-N-hydroxysuccinimidyl carbamate, tagged amino acids

Maria Pawlowska, Shushi Chen and Daniel W. Armstrong*

Department of Chemistry, University of Missouri–Rolla, Rolla, MO 65401 (USA)

(Received February 16th, 1993)

ABSTRACT

A new derivatizing reagent, 6-aminoquinolyl-N-hydroxysuccinimidyl carbamate (AQC), has been used successfully for chromatographic enantioseparation of 31 amino acids on cyclodextrin bonded stationary phases. AQC reacts with both primary and secondary amino acids to produce stable and highly fluorescent derivatives suitable for efficient and sensitive chromatographic determinations. The derivatization reaction proceeds without detectable racemization. The detection limit is in the femtomole range and approximately 0.0075% of the D-enantiomer in an excess of the L-enantiomer is detectable. High resolution values are needed when determining trace enantiomeric impurities.

INTRODUCTION

Chemical derivatization prior to chromatography has become a common procedure in amino acid analysis. As widely documented in the review literature, numerous pre-column reactions have been reported that enhance the sensitivity and selectivity of chromatographic amino acid determinations (for reviews, see refs. 1–3 and references therein).

Recently we reported sensitive and effective methods for enantiomeric determinations of both secondary [4] and primary [5,6] amino acids on cyclodextrin bonded columns after pre-column derivatization with 9-fluorenylmethyl chloroformate (FMOC) and 9-fluorenylmethoxycarbonylglycine chloride (FMOC-Gly-Cl) reagents. Labeling with highly fluorogenic reagents

enabled the quantitation of enantiomeric trace components in complex biological matrixes [6,7] and the determination of trace enantiomeric impurities in “optically pure” commercial amino acids standards [4].

This paper presents the enantioseparation of a number of amino acids on different cyclodextrin bonded stationary phases using a new “fluorescent-tagging-agent”, 6-aminoquinolyl-N-hydroxysuccinimidyl carbamate (AQC) [8–10]. AQC is a highly electrophilic compound that reacts with nucleophiles such as amines and amino acids. It has been recently used for highly selective and sensitive achiral separation of amino acids in the reversed-phase mode and for quantitation of amino acids from human lysozyme [8–10]. The derivatization reaction is shown in Fig. 1. Both primary and secondary amino acids react rapidly with AQC to produce highly fluorescent and stable urea compounds. The by-products of the derivatization reaction do not appear to interfere

* Corresponding author.

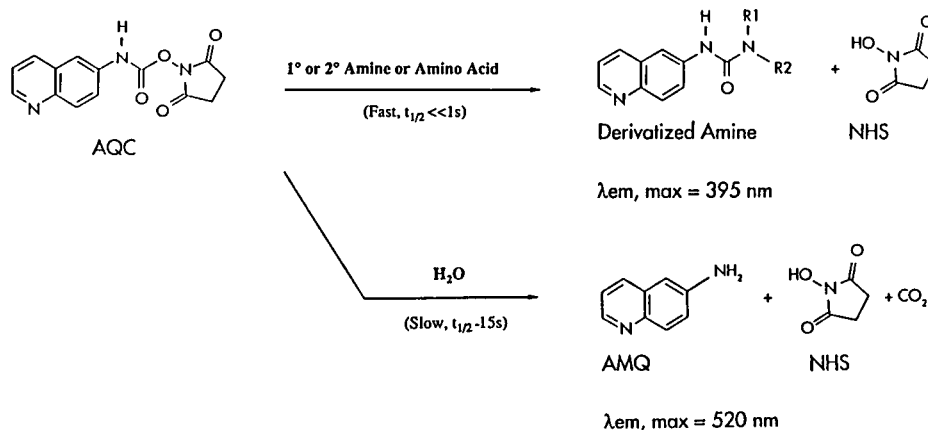


Fig. 1. Derivatization chemistry.

either chromatographically or spectroscopically with the analyte of interest. As can be seen in Fig. 1 the excess reagent is hydrolyzed to yield N-hydroxysuccinimide (NHS) and 6-aminoquinoline (AMQ) which has significantly different fluorescence spectral properties.

EXPERIMENTAL

Chemicals

All native amino acids and boric acid used in this work were purchased from Sigma (St. Louis, MO, USA). The derivatizing reagent AQC was obtained from Waters (Bedford, MA, USA). Calcium sodium EDTA was purchased from Aldrich (Milwaukee, WI, USA). All HPLC-grade solvents including acetonitrile, methanol, triethylamine and acetic acid were obtained from Fisher Scientific (Pittsburgh, PA, USA).

Methods

Derivatization procedures. The AQC derivatized amino acids were obtained according to ref. 8 by dissolving 500 pmol of each amino acid in 35 μl of sodium borate buffer (0.2 M, pH 8.8) in a vial; vortex several seconds and then add 10 μl of AQC solution to it (3 mg per 1 ml of acetonitrile). The vial was heated in an oven for 10 min at 50°C. The resulting solution was injected into a column without further purification.

The FMOC-Gly derivatization of Phe and Leu was performed as reported previously in ref. 7.

Chromatographic experiments. Separations were performed at ambient temperature with a Waters dual pump solvent delivery module Model 590. The spectrophotometric detector (Waters, Model 440) with UV wavelength of 266 nm or fluorescence scanning detector (Waters, Model 470) were used for monitoring the effluent. The excitation and emission wavelengths were 250 and 395 nm, respectively. For FMOC-Gly derivatives the excitation and emission wavelengths were 266 and 315 nm, respectively. The flow-rate in all cases was 1 ml/min. All columns used in this work were obtained from Advanced Separation Technologies (Whippany, NJ, USA). The mobile phase was a mixture of acetonitrile, methanol, acetic acid and triethylamine.

RESULTS

Selectivity and chiral recognition mechanism

The chromatographic data for enantioseparation of a number of AQC-derivatized amino acids obtained under optimal conditions are collected in Table I. The non-aqueous polar eluents consisting almost entirely of acetonitrile and containing small amounts of glacial acetic acid and triethylamine modifiers (in conjunction with different cyclodextrin stationary phases) have proven to be highly selective for many enantioseparation problems [4–7,11]. The selectivity of the system can be regulated by changing the total amount and relative ratio of the

TABLE I

CHROMATOGRAPHIC DATA FOR THE ENANTIORESOLUTION OF PROTEIN AQC-AMINO ACIDS ON CYCLODEXTRIN BONDED STATIONARY PHASES USING NON-AQUEOUS POLAR MOBILE PHASES

Compound	k' ^a	Configuration	α	R_s	Mobile phase ^b	Column ^c	
AQC-Arg	19.11	D	1.11	1.45	400:100:2:10	β	
AQC-His	16.03	L	1.06	0.70	450:50:3:6	SN	
AQC-Leu	9.51		1.14	1.50	450:50:1:6	α	
	5.36	D	1.19	2.44	450:50:2:10	β	
	3.74	D	1.11	1.67	475:25:4:6	γ	
	2.40	D	1.14	2.04	450:50:4:6	AC	
	4.16	D	1.29	3.03	475:25:3:6	RSP	
	2.40	D	1.91	6.22	450:50:4:6	RN	
	4.26	D	1.69	5.11	450:50:2:6	SN	
AQC-Lys	4.73	D	1.10	1.13	430:70:2:10	AC	
	3.74	D	1.20	1.27	400:100:2:10	RN	
AQC-Met	7.45	D	1.15	2.29	480:20:3:5	β	
	3.35	D	1.16	1.94	475:25:4:6	RSP	
	2.72	D	1.66	3.69	450:50:4:6	RN	
	8.63	D	1.56	4.13	475:25:3:2	SN	
AQC-Phe	6.24	D	1.18	2.34	450:50:2:6	β	
	3.85	D	1.13	1.74	475:25:4:6	γ	
	2.45	D	1.17	2.76	450:50:4:6	AC	
	3.21	D	1.20	2.42	450:50:3:2	RSP	
	3.22	D	1.55	4.66	450:50:4:6	RN	
	4.92	D	1.39	4.05	450:50:2:6	SN	
AQC-Thr	4.75	D	1.08	1.00	475:25:2:6	β	
AQC-Trp	13.37	D	1.13	2.03	480:20:3:6	β	
	5.32	D	1.11	1.52	450:50:3:6	γ	
	4.53	D	1.10	1.63	470:30:4:6	AC	
	4.88	D	1.21	2.00	450:50:2:4	RN	
AQC-Val	5.46	D	1.19	2.76	475:25:4:6	β	
	2.35	D	1.12	1.87	470:30:4:6	AC	
AQC-Ala	6.23	D	1.10	1.54	480:20:3:5	β	
	2.30	D	1.09	1.41	470:30:4:6	AC	
AQC-Asp	15.70	D	1.13	1.66	475:25:2:6	β	
	4.90	D	1.11	1.22	475:25:3:6	AC	
AQC-Glu	7.07	L	1.15	1.77	400:100:2:10	SN	
AQC-Tyr	9.84	D	1.14	1.86	450:50:2:6	β	
	5.02	D	1.15	2.00	470:30:4:6	AC	
	6.67	D	1.14	1.62	475:25:4:6	HP	
AQC-Pro	4.02	D	1.26	1.94	475:25:1.5:6	α	
	3.05	D	1.23	2.83	475:25:2:6	β	
	1.77	D	1.18	2.63	450:50:3:6	γ	
	1.24	D	1.28	3.33	450:50:4:6	AC	
	2.34	D	1.23	2.17	450:50:3:6	SN	
AQC-Ile ^d	6.63	D <i>allo</i>	7.59 D	7.90 L <i>allo</i>	9.72 L	475:25:2:6	β
	6.06		6.70	7.23	8.21	475:25:3:2	RN

^a k' = Capacity factor for the first eluted enantiomer.^b Mobile phases are mixtures of acetonitrile–methanol–acetic acid–triethylamine by volume (v/v).^c Columns α , β , γ , RSP, AC, SN, RN stand for α -, β -, γ -, *R,S*-2-hydroxypropyl, acetylated β -, *S*-naphthylethyl-carbamated, *R*-naphthylethyl-carbamated, cyclodextrin bonded stationary phases.^d Only k' parameter is shown.

modifiers and by addition of small amounts (2–20%, v/v) of methanol (which reduces the retention time of the analyte to practical levels, if necessary). As can be seen from the results in Table I the AQC derivatives of primary as well as secondary amino acids are easily separated into enantiomers on different bonded chiral stationary phases using the non-aqueous acetonitrile–methanol–acetic acid–triethylamine mixture as eluent. Figs. 2 and 3 show enantioseparations of AQC derivatives of primary and secondary amino acids obtained on different cyclodextrin bonded phases. It should be noted that in previous work, the resolution of the FMOC derivatized nipecotic acid was not possible [4]. However, as shown in Fig. 3, it is easily resolved as the AQC derivative on a γ -cyclodextrin column.

Table I gives the separation data for 15 common protein amino acids. Table II gives analogous data for 16 additional amino acids. In general, one or more columns were found that provided greater than baseline resolution ($R_s > 1.5$). Moreover, as indicated in Tables I and II, the D-enantiomer was eluted prior to the L-enantiomer in all cases except two (His and Glu). Consequently this should be a sensitive and

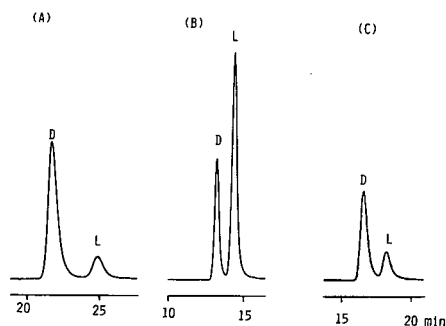


Fig. 2. Enantiomeric resolution of AQC functionalized primary amino acids obtained under optimal experimental conditions in the non-aqueous system. (A) Test compound: AQC-Phe; stationary phase: β -cyclodextrin; eluent acetonitrile–methanol–acetic acid–triethylamine (450:25:3:6, v/v). (B) Test compound: AQC-Met; stationary phase: HP- β -cyclodextrin; eluent acetonitrile–methanol–acetic acid–triethylamine (475:50:2:6, v/v). (C) Test compound: AQC-Trp; stationary phase: β -cyclodextrin; eluent acetonitrile–methanol–acetic acid–triethylamine (470:30:4:6, v/v). All columns were 250 \times 4.6 mm, the flow-rate was 1 ml/min and fluorescent detection was used (see Experimental).

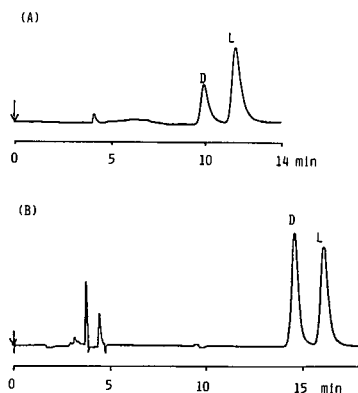


Fig. 3. Enantiomeric resolution of AQC functionalized secondary amino acids obtained under optimal experimental conditions in the nonaqueous system. (A) Test compound: AQC-Pro; stationary phase: SN- β -cyclodextrin; eluent acetonitrile–methanol–acetic acid–triethylamine (470:30:3:6, v/v). (B) Test compound: AQC-nipecotic acid; stationary phase: γ -cyclodextrin; eluent acetonitrile–methanol–acetic acid–triethylamine (450:50:3:12, v/v).

accurate method for the determination of trace level of D-amino acids in the presence of high levels of L-enantiomers [4,12,13].

It was found previously that chiral recognition of FMOC-derivatized amino acids was dependent on water concentration in the mobile phase [4,5]. Similar behavior was observed in this study for AQC-derivatized amino acids. Fig. 4 shows the change of retention characteristics of AQC-D,L-Leu obtained on the β -cyclodextrin column caused by addition of water to the mobile phase. Both methanol and water diminish the hydrogen bonding interaction between the solute and the cyclodextrin due to the competitive adsorption and solvation effects of these molecules. Hydrogen bonding solvents have considerable influence on both retention and enantioselectivity. The substitution of as little as 5% (v/v) water for methanol causes a significant decrease in the retention and selectivity (Fig. 4B). Further addition of water to the mobile phase negated the enantioselectivity exhibited by native cyclodextrin stationary phases towards almost all amino acids investigated. The only exception found was for AQC-Leu (on the β -cyclodextrin column) which was partially resolved under reversed-phase conditions as shown in Fig. 4C. Unlike the native cyclodextrin bonded phases, the deriva-

TABLE II

CHROMATOGRAPHIC DATA FOR THE ENANTIORESOLUTION OF AQC DERIVATIVES OF OTHER AMINO ACIDS AND THEIR DERIVATIVES ON CYCLODEXTRIN BONDED STATIONARY PHASES USING NON-AQUEOUS POLAR MOBILE PHASES

Compound	k' ^a	Configuration	α	R_s	Mobile phase ^b	Column ^c
Nipecotinic acid	4.94		1.10	1.46	450:50:3:2	β
	3.82		1.13	2.26	450:50:3:2	γ
	1.70		1.30	1.35	450:50:1.5:6	AC
AQC-Norval	5.20	D	1.16	2.55	475:25:2:6	β
	2.22	D	1.13	2.02	470:30:4:6	AC
	2.08	D	1.30	2.70	450:50:4:6	RN
AQC-Norleu	3.90	D	1.20	2.31	450:50:2:10	β
	2.64	D	1.16	2.52	470:30:4:6	AC
	3.29	D	1.25	2.75	475:25:4:6	RSP
	2.43	D	1.80	5.95	450:50:4:6	RN
AQC-Homophe	12.14	D	1.28	3.78	475:25:2:6	β
	4.42	D	1.15	1.95	475:25:4:6	γ
	5.00	D	1.29	3.91	470:30:4:6	AC
	5.61	D	1.45	4.57	475:25:4:6	RSP
	7.20	D	1.58	8.54	450:50:3:6	SN
AQC- α -Methyl-Phe	1.92		1.14	1.65	475:25:3:6	AC
AQC- α -Methyl- <i>m</i> -methoxy-Phe	3.20		1.09	1.42	450:50:3:2	γ
AQC- α -Amino- <i>R,S</i> -Phe-acetic acid	5.36	R	1.09	1.47	450:50:3:2	β
AQC- <i>p</i> -Nitro-Phe	3.17		1.33	1.77	450:50:2:10	RN
AQC- <i>o</i> -Methyl-Tyr	2.22	D	1.13	1.72	450:50:1.5:6	AC
AQC- <i>m</i> -Tyr	4.37		1.29	2.40	450:50:2:4	RN
AQC- α -Methyl- <i>m</i> -Tyr	2.20		1.12	1.60	475:25:5:6	AC
AQC- <i>o</i> -Tyr	3.53		1.16	1.45	460:40:5:3	RN
AQC-6-Fluoro-Trp	8.58		1.10	1.56	450:50:3:2	β
AQC-5-Hydroxy-Trp	6.10		1.18	1.86	450:50:2:4	RN
AQC-7-Methyl-Trp	7.80		1.08	1.43	450:50:3:2	γ
AQC- β -Aminoiso-butyric acid	5.85		1.10	1.42	475:25:4:6	β

^a k' is the capacity factor for the first eluted enantiomer.

^b Mobile phases are mixtures of acetonitrile–methanol–acetic acid–triethylamine by volume (v/v).

^c Columns α , β , γ , RSP, AC, SN, RN stand for α -, β -, γ -, *R,S*-2-hydroxypropyl, acetylated β -, *S*-naphthylethyl-carbamated, *R*-naphthylethyl-carbamated, cyclodextrin bonded stationary phases.

tized cyclodextrin phases exhibited enantioselectivity towards some of the AQC functionalized amino acids in water-rich systems. Table III gives retention data for a number of AQC amino acids obtained on *R,S*-hydroxypropyl derivatized β -cyclodextrin (RSP- β -CD) in the reversed-

phase mode. Fig. 5 shows the change of elution order for enantioseparation of DL-Leu on the same RSP- β -cyclodextrin column when operated with nonaqueous and aqueous eluents. As can be seen from the comparison of the results given in Table I and II vs. Table III the change in the

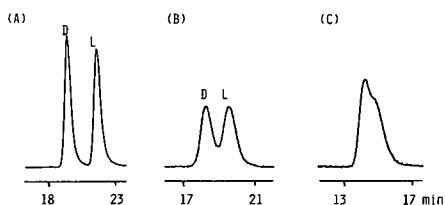


Fig. 4. The influence of the water concentration in the eluent on enantiomeric resolution of AQC-Leu. (A) Eluent: acetonitrile–methanol–acetic acid–triethylamine (475:25:3:6, v/v). (B) Eluent: acetonitrile–triethylammonium acetate (pH 7.1) (95:5, v/v) buffer. (C) Eluent: acetonitrile–triethylammonium acetate (pH 7.1) buffer (5:95, v/v). A β -cyclodextrin column (250 \times 4.6 mm) was used. The flow-rate was 1 ml/min. UV detection was used.

operation mode caused changes in elution order for most amino acids resolved with histidine being the only exception.

The retention behavior found in this study for AQC-functionalized amino acids is very similar to that reported previously for FMOC derivatives. In both cases there is little chiral recognition of derivatized amino acids on the native bonded phases under reversed-phase conditions, but the derivatized cyclodextrin phases exhibit enantioselectivity when operated with non-aqueous eluents as well as in the reversed-phase mode.

However, there is a significant difference in the chiral recognition exhibited by native

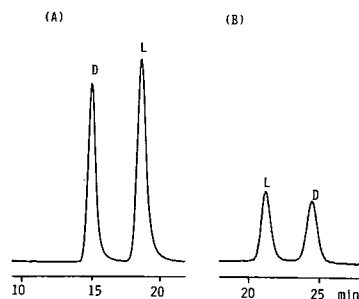


Fig. 5. Enantiomeric resolution of AQC-Leu obtained on a *R,S*-hydroxypropyl derivatized β -cyclodextrin (RSP) column. (A) Non-aqueous mobile phase: acetonitrile–methanol–acetic acid–triethylamine (475:25:3:6, v/v). (B) Reversed-phase mode with a mobile phase consisting of acetonitrile–triethylammonium acetate buffer (5:95, v/v). Notice that elution order has been reversed between two modes. The column was 250 \times 4.6 mm. The flow-rate was 1 ml/min and fluorescent detection was used.

cyclodextrin bonded phases towards FMOC and AQC derivatized amino acids in non-aqueous systems. As shown in Table I AQC derivatives can be easily resolved on native cyclodextrin bonded phases, which was not the case for FMOC-amino acids derivatives. The similarities and differences in retention behavior on the different cyclodextrin phases observed for FMOC- and AQC-functionalized amino acids confirm the chiral recognition mechanism postulated previously [5]. Briefly, this was that inclusion with the hydrophobic fluorescent group

TABLE III

CHROMATOGRAPHIC DATA FOR SEPARATION OF RACEMIC AQC-AMINO ACIDS ON CYCLODEXTRIN BONDED STATIONARY PHASES USING AQUEOUS MOBILE PHASES

Column: *R,S*-2-hydroxypropyl cyclodextrin bonded stationary phase.

Compound	k'	Configuration	α	R_s	Mobile phase ^a	
AQC-His	2.23	L	1.08	1.02	90:10	
AQC-Leu	2.37	L	1.15	1.76	90:10	
AQC-Met	5.07	L	1.15	2.14	95:5	
AQC-Val	4.81	L	1.16	1.74	95:5	
AQC-Ala	3.38	L	1.10	1.13	95:5	
AQC-Ser	2.71	L	1.07	0.88	95:5	
AQC-Homoser	2.80	L	1.16	1.86	95:5	
AQC-Ile ^b	5.32	D <i>allo</i>	5.57 D	5.57 L <i>allo</i>	5.82 L	95:5

^a Mobile phase is a ratio of buffer to acetonitrile (v/v) and buffer is 1% pH 7.1 triethylammonium acetate.

^b Only the k' for the first eluted enantiomer is shown.

(in the reversed-phase mode) resulted in good retention but poor enantioselectivity (because of insufficient polar interactions between the cyclodextrin hydroxyls and the hydrogen bonding portions of the amino acid) [4,5]. However, when using the polar organic mobile phase (in which most of the solvent is non-hydrogen-bonding acetonitrile) hydrogen bonding interactions are dominant and inclusion is minimized. In the case of AQC-derivatized amino acids there seems to be two benefits. First the smaller AQC moiety does not sterically interfere with hydrogen bonding interactions (as Fmoc sometimes does) and the 6-aminoquinolyl group itself contains two amino hydrogen bonding groups as well.

The derivatization of cyclodextrin influences significantly the enantioselectivity exhibited by the cyclodextrin phases in the aqueous as well as non-aqueous systems. Both the cyclodextrin moiety and the substituent can influence the chiral recognition, which results in unique selectivities. Under reversed-phase conditions the mechanism for enantioselectivity with the derivatized cyclodextrin bonded phase is thought to involve not only inclusion complex formation but also additional interactions between the analyte and cyclodextrin substituents. The fact that native cyclodextrins could not resolve amino acids derivatives in the reversed-phase mode indicates that the major contribution to the overall enantioselectivity of the derivatized cyclodextrin stationary phases is caused by the additional interaction of the analyte with the cyclodextrin substituent.

In non-aqueous systems the chiral recognition may arise from stereoselective hydrogen bonding between donor and acceptor sites of the analyte with the residual secondary hydroxyl groups as well as other polar moieties at the mouth of the cyclodextrin cavity. On carbamoylated β -cyclodextrin stationary phases, π - π interactions between the aromatic substituents on the cyclodextrin moiety and hydrophobic part of the chiral solutes are also possible. The discussion above is supported by the change in peak symmetry observed when changing the operation mode (and chiral recognition mechanism) from non-aqueous to aqueous systems. The measured

peak symmetry for both Fmoc- and AQC-amino acids in water-free systems was different than that found in the reversed-phase mode. As can be seen from the data presented in Table IV the change of operation mode to reversed-phase conditions improved the symmetry of the eluted peaks for all solutes investigated.

High symmetry factors have been found for Fmoc-Pro on RN- β -cyclodextrin column as well as for AQC-Met and AQC-Val on HP- β -cyclodextrin ($a \approx 1$) under reversed-phase conditions; the peak symmetry, a , was determined according to ref. 14 at 1/10 peak height, values <1 indicate tailing. It indicates that the adsorption (binding) sites are essentially of a single type (homogeneous in the adsorption energies) [15,16]. The symmetry observed for AQC-Leu on HP- β -cyclodextrin is significantly lower than that found for AQC-Met and AQC-Val on the same column. The AQC-Leu as shown above in Fig. 4C was the only exception in that it could be slightly resolved into enantiomers on a native β -cyclodextrin column. These findings suggest that in this case both the hydroxypropyl substituents and free hydroxyl groups at the mouth of the cyclodextrin cavity contribute to the chiral recognition.

In water-free systems, where steric discrimination of enantiomers has been achieved due to the external complex formation between the solute and cyclodextrin molecule, several types of adsorption (binding) conformations are possible. They would differ essentially in the accessibility for the analyte and in the type and strength of the interaction with the analyte, which may result in observed symmetry.

Advantages and practical application of the method

Labeling with AQC-reagent converts amino acids into solutes with favorable chromatographic properties. In addition, these derivatives can be resolved into enantiomers on different bonded cyclodextrin phases. AQC reacts rapidly with both primary and secondary amino groups. The by-products of the derivatization reaction are eluted from the cyclodextrin columns close to the dead volume regardless of whether reversed phase or polar organic mobile phases are used.

TABLE IV

COMPARISON OF PEAK SYMMETRY FOR FMOC AND AQC FUNCTIONALIZED AMINO ACIDS OBTAINED ON DERIVATIZED CYCLODEXTRIN BONDED STATIONARY PHASES IN NON-AQUEOUS AND AQUEOUS SYSTEMS

Solute	Non-aqueous system			Aqueous system		
	Peak symmetry ^a		Chromatographic conditions	Peak symmetry ^a		Chromatographic conditions
	D	L		D	L	
FMOC-Pro ^b	0.66	0.55	RN- β -CD ^c	0.98	0.95	RN- β -CD ^d
AQC-Leu	0.38	0.40	R,S-HP- β -CD ^e	0.83	0.63	R,S-HP- β -CD ^f
AQC-Met	0.78	0.73	R,S-HP- β -CD ^e	1.00	0.94	R,S-HP- β -CD ^f
AQC-Val	0.75	0.70	R,S-HP- β -CD ^g	0.96	0.93	R,S-HP- β -CD ^f

^a The peak symmetry was determined according to ref. 14 at 1/10 of the peak height, values <1 indicate tailing.

^b Taken from ref. 4.

^c Acetonitrile–triethylamine–glacial acetic acid (1000:6:4, v/v). CD = Cyclodextrin.

^d Water–acetonitrile–triethylamine–glacial acetic acid (850:150:6:4, v/v).

^e Acetonitrile–methanol–triethylamine–glacial acetic acid (950:50:12:6, v/v).

^f Acetonitrile–triethylamine acetate buffer (5:95, v/v).

^g Acetonitrile–methanol–triethylamine–glacial acetic acid (950:50:12:80, v/v).

As shown in Figs. 2 and 3 there is no interference when using fluorescence or UV detection.

Incorporation of the highly fluorescent aminoquinolyl group to amino acids enables high-sensitivity detection. As has been reported recently

[10] detection limits for the amino acids in reversed-phase HPLC system range from 40–300 fmol. According to our previous work [4], the applicability of non-aqueous eluents with conjunction with cyclodextrin phases offers several

TABLE V

COMPARISON OF THE DETERMINATION OF ENANTIOMERIC PURITY OF COMMERCIAL "PURE" L-AMINO ACIDS STANDARDS AND THE DETERMINATION OF ENANTIOMERIC RATIO IN THE D,L-MIXTURE USING TWO PRE-COLUMN DERIVATIZING AGENTS: AQC AND FMOC-Gly-Cl

Name	Source	Derivatizing agent			
		AQC		FMOC Gly Cl	
		%D (S.D.)	Chromatographic conditions	%D (S.D.)	Chromatographic conditions
L-Leucine	Sigma	0.049 (0.006)	RN- β -CD ^a	0.045 (0.013)	γ -CD ^b
L-Phenylalanine	Aldrich	<0.0075	RN- β -CD ^c	<0.0075	β -CD ^b
L,D-Phenylalanine	The artificial mixture	4.070 (0.096)		3.8994 (0.065)	

^a Acetonitrile–methanol–triethylamine–glacial acetic acid (900:100:16:4, v/v).

^b Acetonitrile–triethylamine–glacial acetic acid (1000:12:3, v/v).

^c Acetonitrile–methanol–triethylamine–glacial acetic acid (900:100:18:4, v/v).

advantages over water-rich systems including: faster equilibration of the column, more stable base line and more sensitive fluorescence detection due to the lack of quenching effects which occur in aqueous solutions. Consequently we were able to detect as little as 10 fmol of many of the AQC amino acids. In one case as little as 0.0075% of D-Phe in a large excess of L-enantiomer (for $k' = 2.35$) could be determined.

Because of high sensitivity and selectivity this method can be used for trace and ultra-trace determination of enantiomeric impurities. Table V shows the results of an evaluation of enantiomeric purity for L-Phe and L-Leu standards. Approximately 0.049% of D-Leu was found and quantified with a precision of 12.2% (S.D. for 4 measurements). Table V also shows the comparison data for enantiomeric trace analysis obtained after pre-column derivatization with AQC and FMOC-Gly-Cl reagents. As can be seen, excellent agreement was achieved with these two methods. Moreover the results presented in Table V indicated that both of these derivatization reactions proceed without detectable racemization. No change in enantiomeric ratio for AQC-Phe (D,L artificial mixture, see Table V) and AQC-Leu (an L standard, see Table V) was found during a 7-day period (determined both at 21°C and -5°C).

It appears that the new AQC reagent is a very effective “tagging agent” for amino acids. It causes no detectable racemization if used properly. The AQC derivatives have excellent chromatographic properties on cyclodextrin bonded phases. This, along with their spectroscopic properties and stability, make them very useful for determining trace levels of D-enantiomers in an excess of the more common L-amino acids.

ACKNOWLEDGEMENT

Support of this work by the National Institute of Health (Grant NIH BMT 2R01 GM36292-05A2) is gratefully acknowledged.

REFERENCES

- 1 P. Fuerst, L. Pollack, T.A. Graser, M. Godel and P. Stehle, *J. Chromatogr.*, 499 (1990) 557.
- 2 S. Kochhar and P. Christen, *Anal. Biochem.*, 178 (1988) 17.
- 3 S.A. Cohen and D.J. Strydom, *Anal. Biochem.*, 174 (1988) 1.
- 4 J. Zukowski, M. Pawlowska and D.W. Armstrong, *J. Chromatogr.*, 623 (1992) 33.
- 5 J. Zukowski, M. Pawlowska, M. Nagatkina and D.W. Armstrong, *J. Chromatogr.*, 629 (1993) 169.
- 6 D.W. Armstrong, M.P. Gasper, S.H. Lee, N. Ercal and J. Zukowski, *Amino Acids*, 4 (1993) 402.
- 7 D.W. Armstrong, M.P. Gasper, S.H. Lee, J. Zukowski and N. Ercal, *Chirality*, (1993) in press.
- 8 S.A. Cohen and D.M. Michaud, *Anal. Biochem.*, (1993) in press.
- 9 S.A. Cohen, K. De Antonis and D.M. Michaud, in R.H. Angeletti (Editor), *Techniques in Protein Chemistry IV*, Academic Press, San Diego, CA, 1993, in press.
- 10 D.J. Strydom and S.A. Cohen, *Bioforum*, No. 3, Millipore, Bedford, MA, 1992.
- 11 D.W. Armstrong, S. Chen, C. Chang and S. Chang, *J. Liq. Chromatogr.*, 15 (1992) 545.
- 12 T.D. Doyle, in S. Ahuja (Editor), *Chiral Separation by HPLC (ACS Symposium Series, No. 471)*, American Chemical Society, Washington, DC, 1991, p. 27.
- 13 J.A. Perry, J.D. Rateike and T.J. Szczerba, *J. Chromatogr.*, 389 (187) 57.
- 14 L.R. Snyder and J.J. Kirkland, *Introduction to Modern Liquid Chromatography*, Wiley, New York, 1979, p. 222.
- 15 J.C. Giddings, *Dynamics of Chromatography*, Marcel Dekker, New York, 1965.
- 16 A.M. Rizzi, *J. Chromatogr.*, 478 (1989) 71.

CHROM. 25 067

Optical resolution by high-performance liquid chromatography on benzylcarbamates of cellulose and amylose

Yuriko Kaida and Yoshio Okamoto*

Department of Applied Chemistry, Faculty of Engineering, Nagoya University, Chikusa-ku, Nagoya 464-01 (Japan)

(First received December 8th, 1992; revised manuscript received March 8th, 1993)

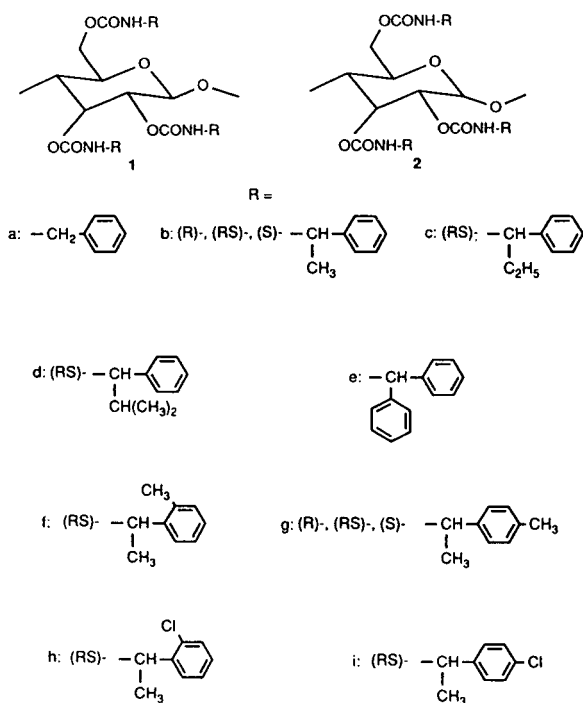
ABSTRACT

Nine benzylcarbamate derivatives of cellulose and amylose were prepared and their optical resolving abilities as chiral stationary phases for high-performance liquid chromatography were evaluated. Among the derivatives, 1-phenylethylcarbamates and 1-phenylpropylcarbamates showed characteristic high optical resolution, and the amylose derivatives resolved many racemates. The influence of the chirality of the 1-phenylethylcarbamate group was also studied. Of the cellulose derivatives, the (*R*)- and (*RS*)-derivatives showed higher optical resolving ability than the (*S*)-derivative. Of the amylose derivatives, the (*RS*)- and (*S*)-derivatives showed higher chiral recognition than the (*R*)-derivative. The optical resolving abilities of 1-phenylethylcarbamate derivatives bearing a methyl or chloro substituent on their phenyl groups were also evaluated. The chiral recognition varied depending on the nature and position of the substituents.

INTRODUCTION

Since we reported that trisphenylcarbamate derivatives of cellulose [1,2] and amylose [3] supported on silica gel show high chiral recognition, many racemates have been resolved by HPLC on the derivatives [4,5]. The optical resolution on the carbamates depends greatly on the substituents on the phenyl group [2]. Tris(1-phenylethylcarbamate)s of cellulose and amylose also show characteristic high optical resolution [6], although cellulose trimethylcarbamate and tribenzylcarbamate [6] possess poor optical resolving power. However, no systematic study has been made on the optical resolution with other benzylcarbamate derivatives of cellulose and amylose.

In this work, the optical resolving abilities of nine benzylcarbamate derivatives, benzylcarbamate (**1a**, **2a**), 1-phenylethylcarbamate (**1b**, **2b**),



* Corresponding author.

TABLE I
ELEMENTAL ANALYSES DATA FOR BENZYL CARBAMATE DERIVATIVES OF CELLULOSE (1a-i) AND AMYLOSE (2a-i)

Calculated values are shown in parentheses; DS values were calculated from the N(%) values.

Compound	C(%)	H(%)	N(%)	Cl(%)	DS	Compound	C(%)	H(%)	N(%)	C(%)	DS
1a	64.11	5.34	7.22		2.89	2a	63.94	5.05	7.13		2.85
1b-(S)	(64.17)	5.53	7.49		2.92		(64.17)	5.53	7.49		
1b-(RS)	64.42	6.08	6.78		2.99	2b-(S)	63.93	6.05	6.72		2.90
1b-(R)	65.02	6.15	6.94		2.99	2b-(RS)	64.52	6.08	6.83		2.94
	65.47	6.19	6.96			2b-(S)	64.85	6.11	6.87		2.96
	(65.67)	6.14	6.97				(65.67)	6.14	6.97		
1c	65.25	6.60	6.33		2.92	2c	66.06	6.60	6.44		2.97
	(66.96)	6.72	6.51				(66.96)	6.72	6.51		
1d	67.83	6.89	5.96		2.92	2d	67.54	6.78	5.97		2.93
	(68.12)	7.13	6.11				(68.12)	7.13	6.11		
1e	67.12	5.44	4.56		2.70	2e	72.76	5.34	5.21		2.94
	(73.00)	5.45	5.32				(73.00)	5.45	5.32		
1f	66.33	6.62	6.50		ca.3	2f	65.61	6.61	6.31		2.91
	(66.96)	6.71	6.51				(66.96)	6.71	6.51		
1g-(S)	65.26	6.63	6.39		2.94	2g-(S)	66.16	6.65	6.46		2.97
1g-(RS)	66.32	6.64	6.45		2.97	2g-(RS)	66.43	6.52	6.31		2.91
1g-(R)	66.44	6.68	6.14		2.83	2g-(R)	66.85	6.64	6.47		2.97
	(66.96)	6.71	6.51				(66.96)	6.71	6.51		
1h	55.67	4.83	6.04	15.04	ca.3	2h	55.96	4.87	6.05	15.08	ca.3
	(55.82)	4.83	5.92	14.98			(55.82)	4.83	5.92	14.98	
1i	55.73	4.83	6.01	14.87	ca.3	2i	56.09	4.81	6.00	14.86	ca.3
	(55.82)	4.83	5.92	14.98			(55.82)	4.83	5.92	14.98	

1-phenylpropylcarbamate (**1c**, **2c**), 2-methyl-1-phenylpropylcarbamate (**1d**, **2d**), 1,1-diphenylmethylcarbamate (**1e**, **2e**) and four 1-phenylethylcarbamates bearing a methyl or chloro substituent on the phenyl group (**1f–i**, **2f–i**), were evaluated. The influence of the chirality of the 1-phenylethyl group and 1-(4-tolyl)ethyl groups on optical resolution was also investigated.

EXPERIMENTAL

Benzyl isocyanate derivatives were synthesized by the reaction of the corresponding benzylamines and phosgene in toluene under reflux. 1-Phenylpropylamine was prepared from propiophenone and ammonium formate according to a convenient method [7]. 2-Methyl-1-phenylpropylamine and four 1-phenylethylamine derivatives having a methyl or chloro group on their phenyl groups were synthesized in the same way. (*R*)- and (*S*)-1-(4-tolyl)ethylamines were kindly supplied by Yamakawa Chemical.

Cellulose (Avicel, Merck, 1 g) or amylose (Nacalai Tesque, M_r 16 000, 1 g) was dissolved in an *N,N*-dimethylacetamide (15 ml)–LiCl (1.5 g) mixture with stirring at about 80°C for 24 h, and an excess of benzyl isocyanate derivatives and dry pyridine (7 ml) were added to the polysaccharide solutions. The reaction was continued for about 24 h at 100°C. Benzylcarbamates of polysaccharides were precipitated in methanol, filtered and dried *in vacuo* at 60°C; the yields were 80–98%. When racemic isocyanates were used, the enantioselective reaction did not seem to proceed, because unreacted isocyanates were almost racemic. Elemental analysis (Table I) and IR and ^1H NMR spectra indicated that almost all hydroxy groups of cellulose and amylose were converted into carbamate moieties [degree of substitution (DS) \approx 2.7–3.0].

Packing materials were prepared as reported previously [8] and were packed in a stainless-steel tube (25 cm \times 0.46 cm I.D.) by a slurry method. The theoretical plate numbers of these columns were calculated to be 3200–6400, using benzene.

Chromatographic resolution was accomplished on a JASCO BIP-I chromatograph equipped

with a JASCO 875-UV (254 nm) and a JASCO DIP-181C polarimetric detector (Hg, without filters). Separation was carried out with a hexane–2-propanol (90:10) at 25°C. The dead time (t_0) was determined with 1,3,5-tri-*tert*-butylbenzene [9]. ^1H NMR spectra were measured with JEOL GXW-270 (270 MHz) and Varian VXR500 (500 MHz) spectrometers using TMS as an internal standard. The IR spectra were taken on a JASCO IR-810 spectrophotometer in Nujol. Circular dichroism (CD) and UV spectra were measured on JASCO J-500 and J-720 spectrometers and a JASCO Ubest-55 with a 1-mm cell in tetrahydrofuran (THF) (concentration $c \approx$ 1 mg ml^{-1}) or a film prepared by casting their solutions [$c \approx$ 1 mg ml^{-1} in tetrahydrofuran (THF)] on the surface of a quartz plate. The CD intensity was calibrated on the basis of UV intensity.

RESULTS AND DISCUSSION

Fig. 1 shows the chromatogram for the resolution of Tröger base (**3**) on a column of amylose tris [(*RS*)-1-phenylethylcarbamate] (**2b**–(*RS*)). Compound **3** has been resolved on phenylcarbamates of cellulose and amylose and benzoates of cellulose [4,5]. The enantiomers eluted at retention times t_1 and t_2 . The capacity factors [$k'_1 = (t_1 - t_0)/t_0$ and $k'_2 = (t_2 - t_0)/t_0$] were 0.72 and 1.87, respectively. The separation

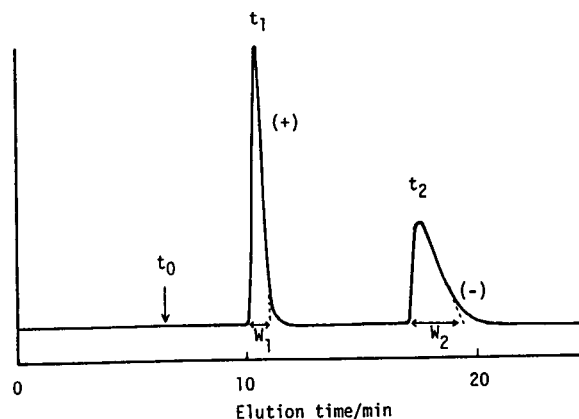


Fig. 1. Optical resolution of Tröger base (**3**) on amylose tris[(*RS*)-1-phenylethylcarbamate] (**2b**–(*RS*)). Eluent: hexane–2-propanol (90:10), 0.5 ml/min, 25°C.

TABLE II
OPTICAL RESOLUTION OF RACEMATES (3-11) ON BENZYL CARBAMATES (1a-e) OF CELLULOSE

Optical rotation of the first-eluted isomers is shown in parentheses. Eluent: hexane-2-propanol (90:10), 0.5 ml/min, 25°C.

Racemate	1a			1b			1c			1d			1e		
	k'_1	α	R_s	k'_1	α	R_s	k'_1	α	R_s	k'_1	α	R_s	k'_1	α	R_s
3	0.39(+)	ca.1		0.62(+)	ca.1		0.78(+)	ca.1		0.42(+)	ca.1		0.97(+)	ca.1	
4	0.27	1.00		0.52(-)	1.12		0.58(-)	1.09		0.30(-)	ca.1		0.50(+)	ca.1	
5	2.03	1.00		3.67(+)	1.18	2.38	4.73(+)	1.22	3.32	0.88(+)	ca.1		3.58	1.00	
6	1.28	1.00		4.30(-)	1.93	6.98	0.89(-)	1.97	8.00	1.02	1.00		1.22	1.00	
7	0.61(-)	ca.1		1.19(-)	1.09	0.68	1.43(-)	1.02		0.54(-)	ca.1		0.99(-)	ca.1	
8	0.64	1.00		1.76	1.00		2.15(+)	1.03		0.66(+)	ca.1		0.86	1.00	
9	1.47	1.00		3.17(-)	1.06		5.83	1.00		1.08	1.00		1.70	1.00	
10	0.57(-)	ca.1		0.61(+)	1.37	1.25	0.95(+)	1.56		0.32(+)	ca.1		1.20(+)	ca.1	
11	2.57(-)	ca.1		3.18(-)	1.20	1.57	5.74(-)	1.20	2.00	0.86(-)	1.04		1.54(-)	1.08	

TABLE III
OPTICAL RESOLUTION OF RACEMATES (3-11) ON BENZYL CARBAMATES (2a-e) OF AMYLOSE

Optical rotation of the first-eluted isomers is shown in parentheses. Eluent: hexane-2-propanol (90:10), 0.5 ml/min, 25°C.

Racemate	2a			2b			2c			2d			2e		
	k'_1	α	R_s	k'_1	α	R_s	k'_1	α	R_s	k'_1	α	R_s	k'_1	α	R_s
3	1.01(+)	ca.1		0.72(+)	2.60	4.20	0.86(+)	2.19	3.47	0.27	1.00		0.63(+)	ca.1	
4	0.67(+)	1.13		1.68(+)	1.15	0.83	0.61(+)	1.15	0.55	0.20(+)	ca.1		0.72(+)	ca.1	
5	4.11(+)	1.21	1.05	3.51(+)	1.41	4.02	3.32(+)	1.36	4.47	0.67(+)	1.10		5.11(-)	1.11	
6	1.43(+)	ca.1		4.30(+)	1.24	1.91	4.08(+)	1.39	2.98	0.48(+)	1.04		0.80(+)	ca.1	
7	1.14(+)	1.05		1.18(+)	ca.1		1.37(+)	ca.1		0.24(+)	ca.1		0.98(-)	ca.1	
8	3.02(-)	ca.1		2.13(+)	1.11	0.83	2.15(-)	ca.1		0.37(-)	ca.1		1.32(-)	ca.1	
9	2.01(+)	1.12		1.80(-)	1.14	0.86	2.09(-)	1.16	1.69	0.40(-)	ca.1		4.01(-)	ca.1	
10	1.92(+)	ca.1		0.75(+)	ca.1		0.68(+)	1.09		0.27(+)	1.20	1.45	1.25(+)	ca.1	
11	1.01(+)	ca.1		1.69(-)	1.24	1.37	1.88(-)	1.14	0.93	0.91(-)	ca.1		1.10(-)	1.08	

factor ($\alpha = k'_2/k'_1$) and the resolution factor [$R_s = 2(t_2 - t_1)/(W_1 + W_2)$] were determined to be 2.60 and 4.20, respectively.

Optical resolution on various aralkylcarbamates of cellulose and amylose

Table II shows the results for the optical resolution of racemates (**3–11**) on five cellulose tris(benzylcarbamate)s (**1a–e**). Among the five derivatives, 1-phenylethyl- (**1b**) and 1-phenylpropylcarbamate (**1c**) showed characteristic high optical resolution. The other derivatives, benzyl-, (**1a**), 2-methyl-1-phenylpropyl- (**1d**) and 1,1-diphenylmethylcarbamates (**1e**), showed low optical resolution in spite of the similarity of their structures to those of **1b** and **1c**. Fig. 2 shows the chromatograms for the resolution of **3** on **1a–e**. Although **3** was not resolved on any column, a clear difference was observed between the chromatograms on **1b** and **1c** and the others. The peaks observed on **1b** and **1c** are sharp, whereas on the others they are very broad. These results suggest that **1b** and **1c** may have a limited number of adsorbing sites owing to the regular structure of the cellulose derivatives, but the other derivatives may have many kinds of adsorbing sites owing to irregular structures.

The CD spectra of the films of **1a–e** are shown in Fig. 3. Intense peaks are observed for only **1b** and **1c**; the other derivatives show much weaker

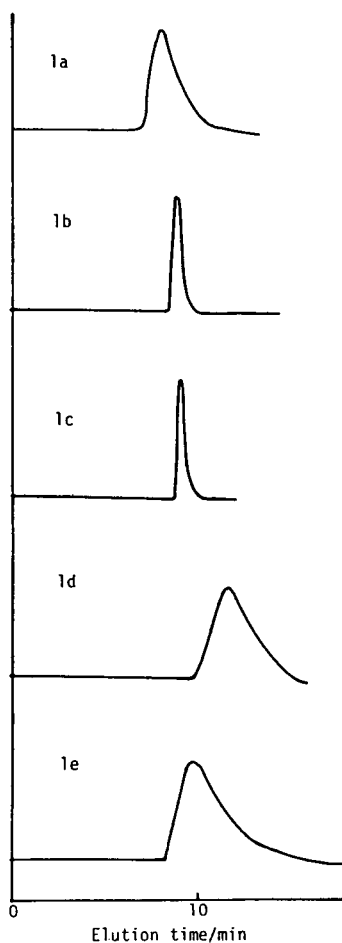
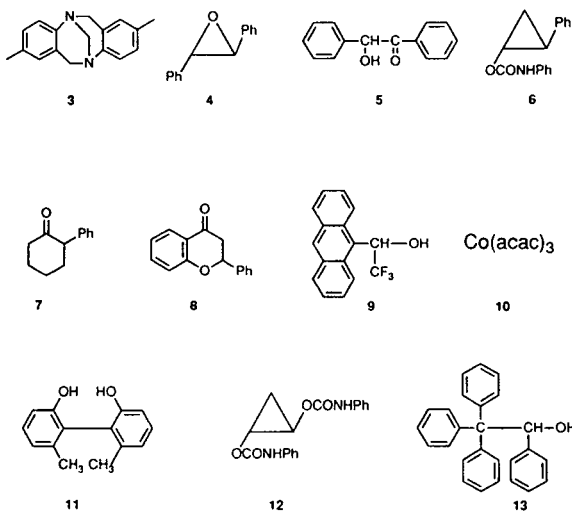


Fig. 2. Chromatograms for resolution of **3** on cellulose benzylcarbamates (**1a–e**). Eluent: hexane-2-propanol (90:10), 0.5 ml/min, 25°C.



peaks. These results support the above speculation that the higher order structure of **1b** and **1c** may be more regular than those of the other derivatives. Hence a too small group such as benzyl and too bulky groups such as 2-methyl-1-phenylpropyl and 1,1-diphenylmethyl seem to disturb the higher order structure of the carbamate derivatives.

The results for the optical resolution of **3–11** on the amylose derivatives (**2a–e**) are summarized in Table III. Similar results to those on the cellulose derivatives were obtained. 1-Phenylethyl and 1-phenylpropyl groups again appear to

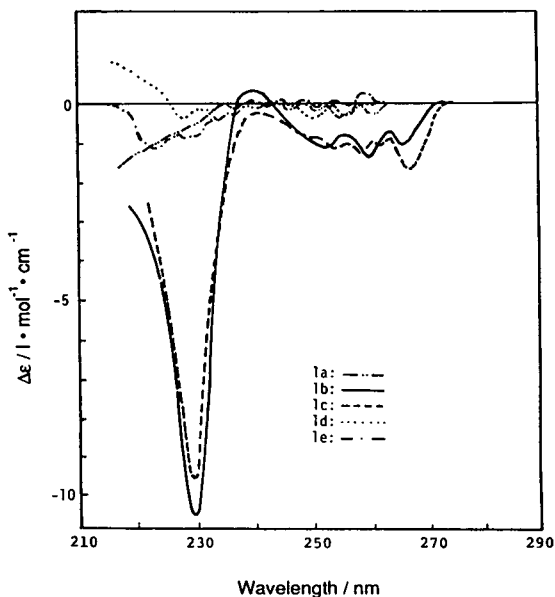


Fig. 3. CD spectra of cellulose benzylcarbamates (**1a–e**) cast from THF solutions.

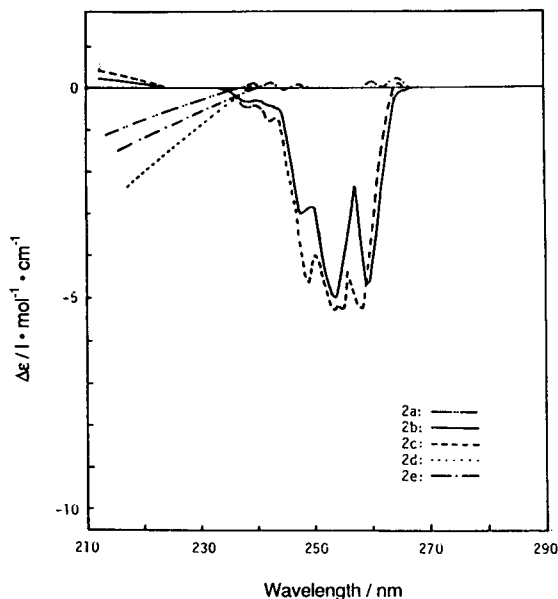


Fig. 4. CD spectra of amylose benzylcarbamates (**2a–e**) cast from THF solutions.

be suitable for keeping the regular higher order structure. The derivatives of **2b** and **2c** showed higher optical resolving abilities than the corresponding cellulose derivatives **1b** and **1c** and could resolve several racemates that were not sufficiently resolved on phenylcarbamates of cellulose and amylose. For example, **3** was resolved on **2b** and **2c** with higher α values than on other phenylcarbamates of amylose [3].

The difference in chiral recognition abilities between cellulose derivatives and amylose derivatives may be due to the differences in their higher order structures. Fig. 4 shows the CD spectra of films of **2a–e**. Intense peaks are again observed only for **2b** and **2c**, although the spectral pattern of **2b** is different from that of **1b**. This may be ascribed to the difference in the conformations between **1b** and **2b**. The chiral recognition abilities of these polysaccharide derivatives depend greatly on their conformation. For example, both phenylcarbamates of cellulose (CTPC) and amylose (ATPC) show high chiral recognition abilities, and the elution order of enantiomers on ATPC is often the reverse of that on CTPC [4]. The higher order structure of CTPC reported by Vogt and Zugenmaier on the

basis of the X-ray analysis is a left-handed threefold (3/2) helix [10] and that of ATPC is a left-handed fourfold (4/1) helix [11]. This difference in conformations between CTPC and ATPC may be responsible for the difference in chiral recognition abilities.

Optical resolution on (R)-, (RS)- and (S)-1-phenylethylcarbamates of cellulose and amylose

(R)- and (S)-1-phenylethylcarbamates of cellulose [**1b**-(R), -(S)] and amylose [**2b**-(R), -(S)] were prepared to evaluate the influence of the chirality of the side-chain on chiral recognition [6]. Tables IV and V show the optical resolution of **3–13** on (R)-, (S)- and (RS)-1-phenylethylcarbamates of cellulose [**1b**-(R), -(S), -(RS)] and amylose [**2b**-(R), -(S), -(RS)], respectively. For both the cellulose and amylose carbamates, the optical resolution depends on the chirality of the side-groups. In the cellulose derivatives, **1b**-(R) and -(RS) showed a higher optical resolving ability than **1b**-(S). The amylose derivatives showed a higher optical resolving ability than the cellulose derivatives for most racemic compounds. Especially **2b**-(RS) and -(S) can resolve many racemates effectively. The elution order of

TABLE IV

OPTICAL RESOLUTION OF RACEMATES (3–13) ON **1b**-(*R*), -(*S*) AND -(*RS*)

Optical rotation of the first-eluted isomers is shown in parentheses. Eluent: hexane–2-propanol (90:10), 0.5 ml/min, 25°C.

Racemate	1b -(<i>R</i>)			1b -(<i>S</i>)			1b -(<i>RS</i>)		
	k'_1	α	R_s	k'_1	α	R_s	k'_1	α	R_s
3	0.62(–)	1.22		0.45(–)	ca.1		0.62(+)	ca.1	
4	0.50(–)	1.21	0.84	0.37(–)	ca.1		0.52(–)	1.12	
5	4.62(–)	ca.1		2.24(+)	1.16	1.20	3.67(–)	1.18	2.38
6	4.08(–)	1.84	2.31	4.35(–)	ca.1		4.30(–)	1.93	6.98
7	1.19(–)	1.12	0.71	0.73(–)	ca.1		1.19(–)	1.09	0.68
8	1.87(+)	ca.1		1.11	1.00		1.76	1.00	
9	3.15(+)	1.13		2.03(–)	1.28	1.34	3.17(–)	1.06	
10	0.62(+)	ca.1		0.50(+)	1.19		0.61(+)	1.37	1.25
11	4.55(–)	1.32	1.22	2.55(+)	ca.1		3.18(–)	1.20	1.57
12	4.08(–)	1.84	2.31	3.58(–)	ca.1		4.30(–)	1.93	6.98
13	2.14(–)	ca.1		2.26(–)	ca.1		2.00(–)	1.09	

enantiomers was sometimes influenced by the chirality of the side-group. For instance, a reversed elution order of **9** was observed between **1b**-(*R*) and **1b**-(*S*). The amylose derivatives also exhibited a reversed elution order of enantiomers of **9**. These results indicate that not only the chirality of the glucose unit but also the chirality of the 1-phenylethyl group directly in-

fluence the chiral recognition, although the former may be more important because such a reversal of elution order cannot be observed for other racemates except for **5** and **11** on **1b** and **7**, **8** and **10** on **2b**.

Fig. 5 shows the ^1H NMR spectra of **1b**-(*R*), -(*RS*) and -(*S*) in perdeuterated dimethyl sulphoxide (DMSO-d_6) at 130°C. Changes in the spec-

TABLE V

OPTICAL RESOLUTION OF RACEMATES (3–13) ON **2b**-(*R*), -(*S*) AND -(*RS*)

Optical rotation of the first-eluted isomers is shown in parentheses. Eluent: hexane–2-propanol (90:10), 0.5 ml/min, 25°C.

Racemate	2b -(<i>R</i>)			2b -(<i>S</i>)			2b -(<i>RS</i>)		
	k'_1	α	R_s	k'_1	α	R_s	k'_1	α	R_s
3	0.74(+)	1.86	2.41	0.90(+)	2.38	4.43	0.72(+)	2.60	4.20
4	0.61(+)	1.19	0.83	0.61(+)	1.28	1.52	1.68(+)	1.15	0.83
5	3.37(+)	1.14	1.29	4.29(+)	1.98	9.10	3.51(+)	1.41	4.20
6	4.46(+)	1.18	1.01	4.79(+)	1.19	1.67	4.30(+)	1.24	1.91
7	1.10(–)	ca.1		1.50(+)	1.21	1.68	1.18(+)	ca.1	
8	2.07(+)	1.07		3.02(–)	ca.1		2.13(+)	1.11	0.83
9	1.97(+)	1.05		1.95(–)	1.88	5.67	1.80(–)	1.14	0.86
10	0.92(+)	ca.1		0.46(–)	ca.1		0.75(–)	ca.1	
11	1.93(–)	1.18	1.10	1.75(–)	1.31	1.69	1.69(–)	1.24	1.37
12	1.02(+)	1.54	1.33	1.36(+)	1.33	0.55	1.21(+)	1.40	0.79
13	4.11(–)	1.04		1.42(+)	1.26	0.84	1.43(–)	1.06	

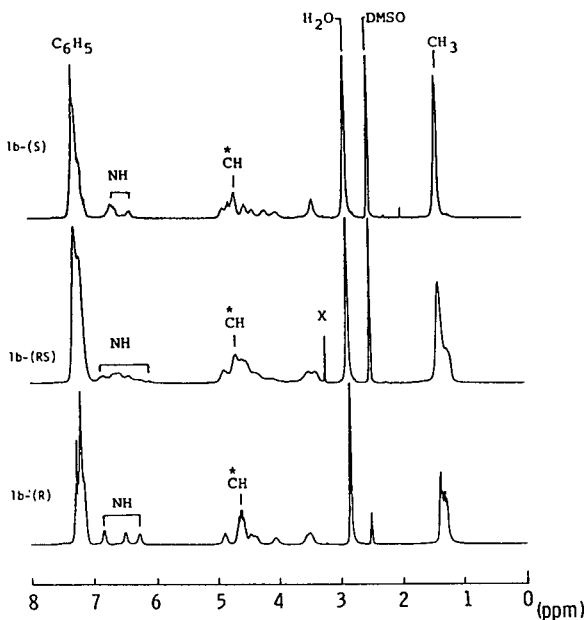


Fig. 5. ^1H NMR spectra of **1b**-(*R*), -(*RS*) and -(*S*). $\text{DMSO}-d_6$, 130°C , 270 MHz.

tral patterns were observed for the NH and main chain protons of cellulose and the methyl and methine protons of the 1-phenylethyl group. This suggests that the chirality of the 1-phenylethyl group may influence the conformation of the glucose units.

UV and CD spectra of **1b**-(*R*), -(*RS*) and -(*S*) derivatives in THF are shown in Fig. 6. The spectral pattern of **1b**-(*R*) is almost symmetrical with that of **1b**-(*S*). This implies that the arrangement of side-chains of **1b** may not be much influenced by the chirality of glucose units in the solution. Fig. 7 shows the CD spectra of the films of these derivatives cast from THF solutions. Although the three spectra show similar patterns, differences are observed in the wavelengths of the peak tops and the intensities of the peaks. The chirality of 1-phenylethyl groups may influence not only the conformation of the side-chains but also that of the glucose units in the solid film. These differences in the conformation of chiral stationary phases (CSPs) probably affect their chiral separation because the cellulose derivatives on the silica gel surface are presumed to exist in a similar state to the above film.

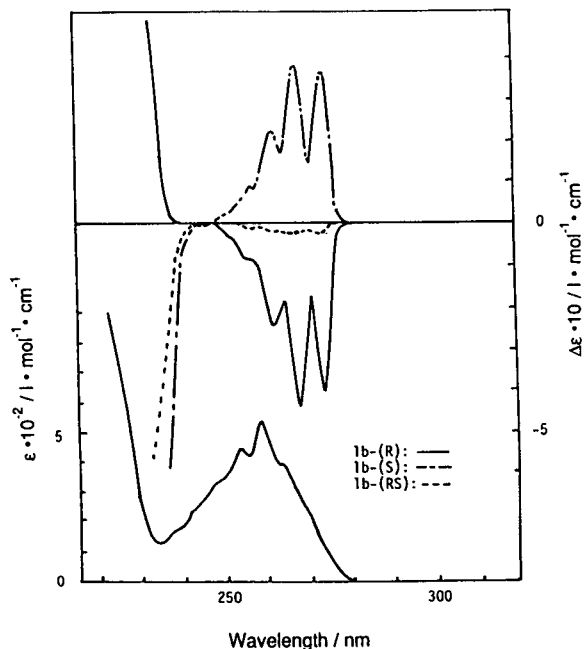


Fig. 6. CD spectra of **1b**-(*R*), -(*RS*) and -(*S*) in THF solutions.

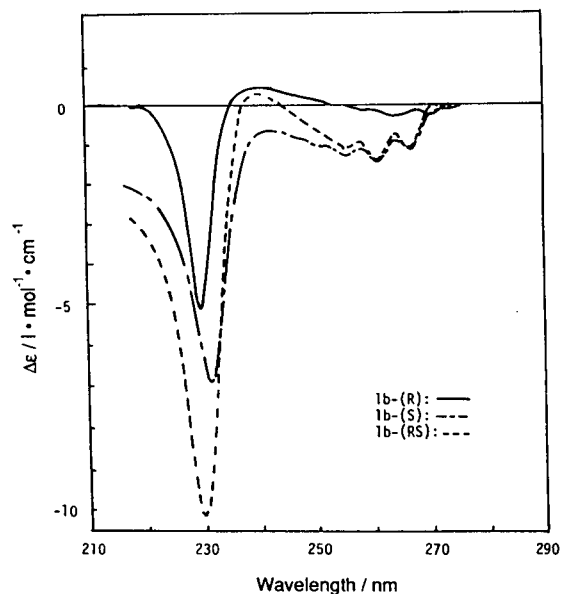


Fig. 7. CD spectra of films of **1b**-(*R*), -(*RS*) and -(*S*) cast from THF solutions.

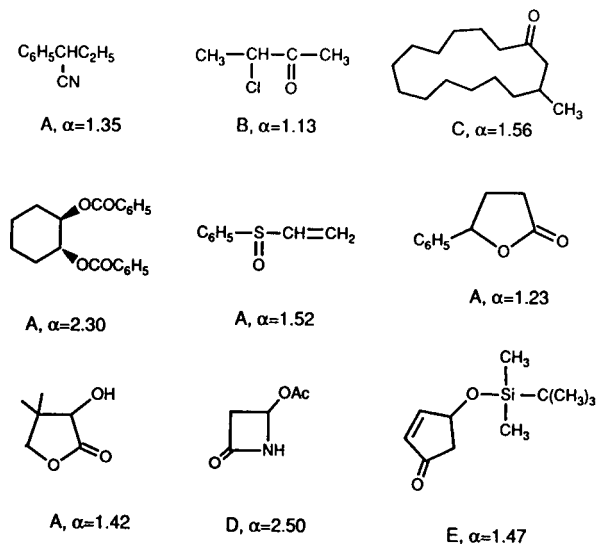


Fig. 8. Compounds resolved on **2b**-(*S*). Eluent: (A) hexane–2-propanol (90:10); (B) hexane–2-propanol (99:1); (C) hexane; (D) hexane–ethanol (80:20); (E) hexane–2-propanol (98:2).

Hence the difference in the higher order structures between the cellulose and amylose derivatives caused by the chirality of the 1-phenylethyl group may be partly responsible for the difference in the optical resolution between the cellulose and amylose derivatives. The fact that **1b**-(*R*) and -(*RS*) form lyotropic liquid crystalline phases in THF but **1b**-(*S*) does not also suggest that the higher order structures of these derivatives may differ depending on the chirality.

Among these derivatives, **2b**-(*S*) seems to show the highest optical resolving abilities for a variety of compounds, and resolves many racemic carbonyl compounds that are not sufficiently resolved on the phenylcarbamate derivatives of polysaccharides. Some examples of the compounds are shown in Fig. 8. They include β -lactams [12] and 4-hydroxy-2-cyclopentenone derivatives [13].

Optical resolution on 1-phenylethylcarbamate derivatives having a methyl or chloro substituent on their phenyl groups

The optical resolving abilities of the derivatives of 1-phenylethylcarbamates of cellulose (**1f**–**1i**) and amylose (**2f**–**2i**) having a methyl or

chloro group on their phenyl groups were also evaluated (Tables VI and VII). The chiral recognition for **3**–**11** depended greatly on the nature and position of the substituents on the phenyl groups. For example, although **2b**, **2f**, **2g** and **2i** can not resolve **10**, only **2h** can completely resolve it. CD spectra of **1b**, **1f** and **1g** are shown in Fig. 9. Different patterns are observed, although the UV spectra of these derivatives are similar, showing λ_{\max} at 208 nm (**1b**), 212 nm (**1f**) and 209 nm (**1g**). The structures of these derivatives may be affected by polarization of the charge on the phenyl groups and steric effects of the substituents. Therefore, the conformations of these derivatives may be different in the film states.

The influence of the chirality of the side-groups of **1g** and **2g** was also evaluated (Table VIII). The optical resolving abilities of these derivatives also depended on the chirality of the side-chains. Although **1b**-(*R*) and -(*RS*) showed a higher optical resolving ability than **1b**-(*S*), **1g**-(*R*) did not show a significantly higher optical resolving ability than **1g**-(*S*) and -(*RS*). The methyl group on the phenyl group appears to influence the conformation of **1g**.

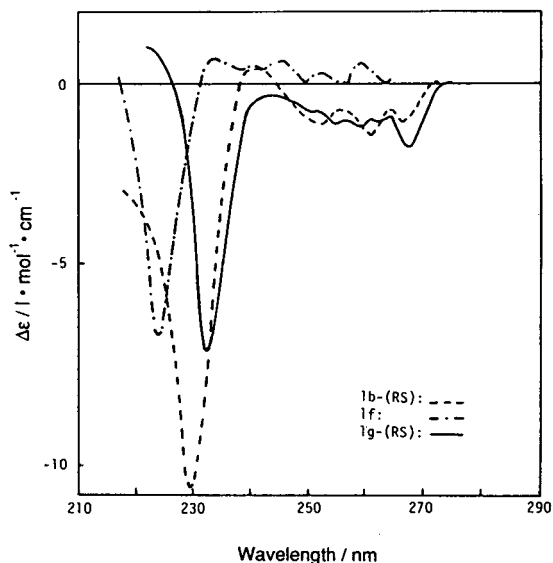


Fig. 9. CD spectra of films of **1b**-(*RS*), **1f** and **1g**-(*RS*) cast from THF solutions.

TABLE VI
OPTICAL RESOLUTION OF RACEMATES (3-11) ON 1-PHENYLETHYL CARBAMATE DERIVATIVES [1b-(RS), 1f-i] OF CELLULOSE

Optical rotation of the first-eluted isomers is shown in parentheses. Eluent: hexane-2-propanol (90:10), 0.5 ml/min, 25°C.

Racemate	1f			1g			1h			1i			R_s
	k'_1	α	R_s	k'_1	α	R_s	k'_1	α	R_s	k'_1	α	R_s	
3	0.62(+)	ca.1		0.46(+)	ca.1	0.64	0.63(+)	ca.1		0.83(+)	ca.1		
4	0.52(-)	1.12	0.58	0.31(-)	1.23	0.58	0.52(-)	ca.1	1.12	0.56(-)	ca.1		
5	3.67(+)	1.18	2.38	2.71(+)	1.25	0.72	3.72(+)	1.08	1.34	3.56(+)	1.11	3.58	1.07
6	4.30(-)	1.93	6.98	2.98(-)	1.85	4.44	6.83(-)	1.97	8.00	3.51(-)	2.24	7.09	4.68
7	1.19(-)	1.09	0.68	0.82(-)	1.07	0.44	1.25(-)	ca.1		1.63(-)	ca.1		0.53
8	1.76	1.00		1.44(+)	ca.1		2.02	1.00		1.73(+)	ca.1		
9	3.17(-)	1.06		3.26(-)	1.13	0.61	5.88	1.00		2.03(+)	1.10	0.81	1.00
10	0.61(-)	1.37	1.25	0.48(+)	1.25	0.72	0.55(+)	1.51	2.21	0.69(+)	1.29	0.88	0.87(+)
11	3.18(-)	1.20	1.57	3.48(-)	1.13	0.97	5.84(-)	1.12	1.27	3.55(-)	2.18	4.16	2.99(-)

TABLE VII
OPTICAL RESOLUTION OF RACEMATES (3-11) ON 1-PHENYLETHYL CARBAMATE DERIVATIVES [2b-(RS), 2f-i] OF AMYLOSE

Optical rotation of the first-eluted isomers is shown in parentheses. Eluent: hexane-2-propanol (90:10), 0.5 ml/min, 25°C.

Racemate	2f			2g			2h			2i			R_s
	k'_1	α	R_s	k'_1	α	R_s	k'_1	α	R_s	k'_1	α	R_s	
3	0.72(+)	2.60	4.20	0.91(+)	1.57	1.69	0.47(+)	2.14	3.38	0.73(+)	2.31	4.57	3.77
4	1.68(+)	1.15	0.83	0.65(+)	ca.1		0.55(+)	1.20	0.73	0.56(+)	1.15	0.72	ca.1
5	3.51(+)	1.41	4.02	3.34(+)	1.25	2.17	2.19(+)	1.45	4.50	3.54(+)	1.47	5.43	3.28
6	4.30(+)	1.24	1.91	4.84(+)	1.35	1.94	3.68(+)	1.15	1.27	4.05(+)	1.23	1.91	1.61
7	1.18(+)	ca.1		1.13(+)	1.07		0.99(+)	ca.1		1.47(-)	ca.1		0.83
8	2.13(+)	1.11	0.83	2.22	1.00		2.06(+)	1.04		1.78(+)	ca.1		1.00
9	1.80(-)	1.14	0.86	2.39(-)	1.20	1.00	1.92(-)	1.20	1.28	1.17(-)	1.09	0.60	1.00
10	0.75(+)	ca.1		0.80(+)	ca.1		0.53(-)	ca.1		1.04(-)	1.39	2.49	1.00
11	1.69(-)	1.24	1.37	1.95(-)	1.07		2.01(-)	1.13	0.58	1.88(-)	1.27	1.41	1.15

TABLE VIII
OPTICAL RESOLUTION OF RACEMATES (3-5, 7-12) ON 1g- AND 2g-(R), -(S) AND -(RS)

Optical rotation of the first-eluted isomers is shown in parentheses. Eluent: hexane-2-propanol (90:10), 0.5 ml/min, 25°C.

Racemate	1g-(R)			1g-(S)			1g-(RS)			2g-(R)			2g-(S)			2g-(RS)		
	k'_1	α	R_s	k'_1	α	R_s	k'_1	α	R_s	k'_1	α	R_s	k'_1	α	R_s	k'_1	α	R_s
3	0.33(+)	ca.1		0.34(+)	ca.1		0.52(-)	ca.1		0.29(-)	ca.1		0.58(+)	1.24		0.74(+)	2.14	
4	0.21(-)	ca.1		0.26(-)	ca.1		0.71(+)	1.15	0.64	0.15(+)	ca.1		0.40(+)	ca.1		0.55(+)	1.20	
5	1.31(-)	ca.1		1.11(+)	1.24		3.79(+)	1.08		0.85(+)	1.25	1.30	1.51(+)	1.20	0.97	2.91(+)	1.45	
7	0.28(-)	ca.1		0.45(-)	ca.1		1.25(-)	ca.1		0.24(-)	ca.1		0.55(+)	1.09		0.99(+)	ca.1	
8	0.63(-)	ca.1		0.69(+)	ca.1		2.02	1.00		0.52(+)	1.30	1.22	1.06(-)	1.20	0.74	2.06(+)	1.04	
9	2.01(-)	1.20	1.30	1.42(-)	1.26	1.33	5.88	1.00	2.21	0.90(-)	ca.1		1.36(-)	1.30	1.48	1.92(-)	1.20	
10	0.25(+)	ca.1		0.34(+)	1.42	1.15	0.55(+)	1.51		0.20(-)	ca.1		0.40(+)	ca.1		0.53(-)	ca.1	
11	1.50(-)	ca.1		1.43(+)	ca.1		1.46(+)	ca.1		1.19(-)	1.18		1.27(-)	ca.1		2.01(-)	ca.1	
12	1.44(-)	1.38	0.96	0.88(-)	ca.1		1.25(-)	1.25	0.86	0.50(+)	1.76	0.94	0.75(+)	1.45	0.91	0.87(+)	1.32	0.93

CONCLUSIONS

Nine benzylcarbamates of cellulose and amylose were adsorbed on silica gel and used as CSPs for HPLC. Among them, 1-phenylethyl- and 1-phenylpropylcarbamates showed high optical resolution. Too small or too bulky benzyl groups are not suitable for obtaining efficient CSPs. In the case of 1-phenylethylcarbamates, chiral recognition depends on the chirality of the 1-phenylethyl group. In the cellulose derivatives (*R*)- and (*RS*)-1-phenylethylcarbamates showed higher optical resolving ability than the (*S*)-derivative, and with amylose the (*RS*)- and (*S*)-derivatives resolved many racemates more efficiently than the (*R*)-derivative. The ^1H NMR and CD spectra of the 1-phenylethylcarbamates indicate that the conformation of the glucose units of the polysaccharides may be influenced by the chirality of the 1-phenylethyl group. The chiral recognition abilities of 1-phenylethylcarbamate derivatives of cellulose and amylose bearing a methyl or chloro substituent on the phenyl group were also evaluated. The optical resolution on these derivatives depends on the nature and position of the substituents.

ACKNOWLEDGEMENTS

The authors thank H. Hayashida and K. Hir-

ose for experimental help. Part of this work was supported by grant-in-aid for Scientific Research No. 02555184 from the Ministry of Education, Science and Culture.

REFERENCES

- 1 Y. Okamoto, M. Kawashima and K. Hatada, *J. Am. Chem. Soc.*, 106 (1984) 5357.
- 2 Y. Okamoto, M. Kawashima and K. Hatada, *J. Chromatogr.*, 363 (1987) 173.
- 3 Y. Okamoto, R. Aburatani, T. Fukumoto and K. Hatada, *Chem. Lett.*, (1987) 1857.
- 4 Y. Okamoto, Y. Kaida, R. Aburatani and K. Hatada, in S. Ahuja (Editor), *Chiral Separation of Liquid Chromatography (ACS Symposium Series, No. 471)*, American Chemical Society, Washington, DC, 1991, p. 101.
- 5 Y. Okamoto and Y. Kaida, *J. Synth. Org. Chem. Jpn.*, 51 (1993) 41.
- 6 Y. Okamoto, Y. Kaida, H. Hayashida and K. Hatada, *Chem. Lett.*, (1990) 909.
- 7 A.W. Ingersoll, *Org. Synth., Coll. Vol.*, 2 (1943) 503.
- 8 Y. Okamoto, S. Honda, I. Okamoto, H. Yuki, S. Murata, R. Noyori and H. Takaya, *J. Am. Chem. Soc.*, 103 (1981) 6971.
- 9 H. Koller, K.-H. Rimböck and A. Mannschreck, *J. Chromatogr.*, 282 (1983) 282.
- 10 U. Vogt and P. Zugenmaier, *Ber. Bunsenges. Phys. Chem.*, 89 (1985) 1217.
- 11 U. Vogt and P. Zugenmaier, presented at the *European Science Foundation Workshop on Specific Interactions in Polysaccharide Systems, Uppsala, 1983*.
- 12 Y. Kaida and Y. Okamoto, *Chirality*, 4 (1992) 122.
- 13 Y. Kaida and Y. Okamoto, *Chem. Lett.*, (1992) 85.

Immobilized metal ion affinity partitioning of erythrocytes from different species in dextran–poly(ethylene glycol) aqueous phase systems

Harry Walter* and Kim E. Widen

Laboratory of Chemical Biology—151, Veterans Affairs Medical Center, Long Beach, CA 90822-5201 (USA)

Gerd Birkenmeier

Institute of Biochemistry, University of Leipzig, D-04103 Leipzig (Germany)

(First received January 12th, 1993; revised manuscript received March 23rd, 1993)

ABSTRACT

Poly(ethylene glycol) (PEG)-bound ligands partition preferentially into the top, PEG-rich, phase of dextran (Dx)–PEG aqueous phase systems. The extraction of erythrocytes from beef, dog, horse, human, pig, rabbit, rat and sheep was examined in both non-charge-sensitive and charge-sensitive Dx–PEG phase systems containing PEG–iminodiacetate (IDA) which had been reacted with Cu(II) or Zn(II). PEG–IDA–Cu binds primarily to histidine (His) residues. Phase systems containing excess imidazole were used to obtain cell partition ratios not attributable to the metal chelate. In non-charge-sensitive phase systems having lower polymer concentrations a correlation has been reported between the partition, P , of erythrocytes and their membrane ratio of poly/monounsaturated fatty acids; while in charge-sensitive phases there is some correlation between the P values and the cells' relative electrophoretic mobilities. At higher polymer concentrations red blood cells accumulate at the interface and do not partition. Under such conditions addition of the PEG–IDA–Cu (Zn is less effective) causes erythrocytes to partition into the PEG-rich phase in a non-charge-related or charge-associated sequence reminiscent of that found in the absence of chelate in non-charge-sensitive or charge-sensitive phase systems, respectively, at lower polymer concentrations. PEG–IDA–Cu may thus be useful in extending the partitioning range of Dx–PEG systems to cells having such low P values in non-charge-sensitive and/or charge-sensitive phase systems as to preclude their partitioning even when phase systems are optimized by manipulation of their components.

From the cited experiments it would appear that either the His per unit surface area of erythrocytes from different species is about the same causing the non-charge-related or charge-associated surface properties (depending on the phase system used) to determine, to a large extent, the P even in the presence of chelate or that the non-charge-related or charge-associated surface properties outweigh the differences in His content and effect the observed correlations.

In contrast to these apparently "non-specific" extractions effected by PEG–IDA–Cu, there are cases in which PEG–IDA–Cu acts as a sensitive probe for recognizing differences in cell surface properties not detected by other means.

INTRODUCTION

Partitioning in two-polymer, most commonly dextran (Dx)–poly(ethylene glycol) (PEG), aqueous phase systems is an established method

for the separation and fractionation of biomaterials including cells, membranes and organelles [1,2]. Depending on the Dx and PEG concentrations and the ionic composition and concentrations used, the phase system can either be charge-sensitive (*i.e.*, have a Donnan potential between the phases) or non-charge-sensitive [3,4]. In the case of erythrocytes from different

* Corresponding author.

species, which have been used as models, cell partitioning behavior in a charge-sensitive system with higher polymer concentrations is determined to a great extent by the cells' surface charge while in a non-charge-sensitive system with lower polymer concentrations it is lipid-related surface properties that effect the cells' partitioning behavior [3].

Affinity partitioning, utilizing the interaction between surface biomolecules and affinity ligands confined primarily to one of the phases by covalently linking them to one of the phase-forming polymers (usually PEG), has also been employed in cell separation technology. Initially, so called "general ligands", which were either charged (*e.g.*, DEAE-Dx, trimethylamino-PEG or PEG-sulfonate) or hydrophobic (*e.g.*, esters of PEG and fatty acids), were used in cell affinity partitioning [5,6]. Currently, immunoaffinity partitioning is being developed for the biospecific extraction of cell populations by use of polymer-linked antibodies [7–10].

Another approach to increase the selectivity of separation exploits the interaction of chelated transition metal ions with macromolecules [11]. This interaction depends on immobilized metal ions coordinating with electron-rich ligands on protein surfaces [12–14]. Accessible histidine residues localized in a favorable orientation on the protein surface have been reported to serve as predominant metal-binding sites [15–17]. Experiments with metal chelate-derivatized PEG in Dx-PEG and PEG-salt phase systems indicate that extraction of proteins by such ligands is histidine-mediated [18,19]. Immobilized metal ion affinity partitioning in Dx-PEG phase systems has recently been successfully applied to the extraction of cells [20].

Here we have examined the metal chelate affinity partitioning behavior of erythrocytes from different species in Dx-PEG aqueous phase systems. The influence of Cu(II) [and, in some experiments, of Zn(II)] chelated to PEG-iminodiacetate (IDA) on cell partitioning was studied in both charge-sensitive and non-charge-sensitive phase systems. Insights into factors governing the behavior of cells in affinity phase systems were obtained especially with regard to those aspects of partitioning that can be ascribed

to "specific" vs. "non-specific" extractions by an affinity ligand.

EXPERIMENTAL

Reagents

Dx T500 (lot No. 01 06905) was obtained from Pharmacia-LKB (Piscataway, NJ, USA). PEG 8000 ("Carbowax 8000") was a product of Union Carbide (Long Beach, CA, USA). Neuraminidase (*Vibrio cholerae*) was purchased from Calbiochem (San Diego, CA, USA). Monomethoxy-PEG 5000, trypsin, phenylhydrazine hydrochloride and imidazole were from Sigma (St. Louis, MO, USA). All salts used were of analytical-reagent grade.

Preparation of metal chelate-poly(ethylene glycol)

PEG-IDA was synthesized by reacting bromoacetic acid with aminomonomethoxy-poly(ethylene glycol) as previously described [18]. Charging of the chelated PEG with Cu(II) and Zn(II) was performed in 50 mM sodium acetate buffer (pH 4.0); and the product was extracted repeatedly with chloroform. The content of copper and zinc per mol of PEG-IDA was 0.64 to 0.83 and 0.80 mol, respectively.

Blood from animals and from human donors

Blood from eight different species was collected in acid-citrate-dextrose (ACD) anticoagulant solution. The ratio used was 10 ml of blood to 3 ml of ACD. Human blood was obtained by venipuncture from presumably hematologically normal individuals; dog blood was from the femoral vein; rabbit blood from the ear marginal vein; and rat blood by heart puncture. Beef blood came from Shamrock Meats (Vernon, CA, USA); while horse, pig and sheep blood were obtained from the Animal Resource Facility, University of California, Irvine. Erythrocytes were used within one week of collection in the experiments outlined below.

Neuraminidase- or trypsin-treatment of human erythrocytes

A 2-ml volume of packed human red blood cells was washed three times with 10 vols. of

phosphate-buffered saline (PBS, pH 7.0 in neuraminidase and pH 7.4 in trypsin experiments). A 0.5-ml aliquot of such washed red cells + 3.5 ml of PBS was put into a 40-ml glass centrifuge tube and incubated together with 200 μl (1 I.U./ml) of neuraminidase or with 200 μl (1 mg/ml) of trypsin at 37°C for 60 min. At the same time a similarly treated aliquot of the same cell population was incubated in the absence of enzyme. The treated cells were washed three times with PBS and used in the partition experiments described below.

Phenylhydrazine injection of rats

Some of the rats were injected subcutaneously, on each of 5 successive days, with a neutralized solution of phenylhydrazine (3 mg phenylhydrazine/100 gm rat body weight). On the eighth day these rats' red blood cell populations consisted of at least 90% reticulocytes. The cells were washed three times with PBS and used in the partition experiments described below.

Preparation of aqueous two-phase systems

A number of different aqueous two-phase systems, having different physical properties and prepared as described by Walter [3], were used. In short, stock solutions were prepared of each of the components needed to make the various phase systems [*i.e.*, a 20% (w/w) Dx T500 solution; 40% (w/w) PEG 8000 solution; 5% (w/w) PEG-IDA-Cu or PEG-IDA-Zn solution; 0.44 M sodium phosphate buffer, pH 6.8; and 0.60 M NaCl]. These solutions were weighed out in appropriate amounts to yield the required quantity of a desired phase system. The compositions of the phases used as well as their physical properties are indicated below. The shorthand employed for phase system composition is as follows: the first number given is the % Dx (w/w). This is followed by a colon and a number giving the % PEG (w/w); followed again by a colon and a number giving the % PEG-IDA-Cu (or Zn, if so indicated) (w/w). These numbers are followed by a # designating the salt composition. #1 is 0.11 M sodium phosphate buffer, pH 6.8; #2 is 0.09 M sodium phosphate buffer, pH 6.8 + 0.03 M NaCl; and #5 is 0.15 M NaCl + 0.01 M sodium phosphate buffer, pH 6.8. Thus,

a phase system given as 5:3.74:0.66 #2 contains 5% (w/w) Dx, 3.74% (w/w) PEG 8000, 0.66% (w/w) PEG-IDA-Cu, 0.09 M sodium phosphate buffer, pH 6.8 + 0.03 M NaCl.

Excess imidazole interferes with binding of the copper chelate to cell surface histidine while it does not affect the partition of cells in charge-sensitive or non-charge-sensitive phase systems devoid of PEG-IDA-Cu [20]. To establish that the partition obtained in phases containing PEG-IDA-Cu were predominantly due to the copper chelate (and not to other physical properties of the phases), partitioning was also carried out in "control" phases with imidazole (1 mM unless otherwise indicated).

Partitioning of erythrocytes in aqueous two-phase systems

The phase system which was to be used for partitioning, at 21–24°C, was mixed and poured into 50-ml centrifuge tubes. The tubes were centrifuged to speed phase separation and the top and bottom phase volumes were adjusted to be equal. The phase system was then mixed and 3-ml aliquots were delivered into 12 × 75 mm tubes. A 50- μl volume of the washed, packed erythrocytes which were to be partitioned was added to 200 μl saline. A 50- μl volume of this suspension, corresponding to between $6 \cdot 10^7$ and $1.7 \cdot 10^8$ cells, was pipetted into a mixed 3-g phase system which was mixed again. The phase systems were allowed to settle 15 min with the tubes in the vertical position. An 0.8-ml aliquot was withdrawn from the middle of the top phase. The quantity of cells in each top phase was determined by lysing the cells and measuring hemoglobin absorbance at 540 nm [21]. The quantity of cells initially added to the partition tubes was similarly determined.

Phases to be used in the neuraminidase or trypsin partition experiments, at 21–24°C, were mixed and about 12 ml was poured into partition tubes (*i.e.*, calibrated tubes, 125 mm × 16 mm). The tubes were centrifuged to speed phase separation and the top and bottom phase volumes were adjusted to be equal at 5 ml. A 30- μl aliquot of washed, packed erythrocytes was added to the mixed phases. The tubes were capped (with Parafilm), inverted a number of

times and the phases were then permitted to settle in horizontal position for 7 min. The tubes were gently raised to the vertical position (without agitating the contents) and the phases permitted to settle for one additional minute. A 1-ml aliquot of top phase was withdrawn. The quantity of cells in each top phase was determined as above.

The partition of cells is given by a P value, defined as the quantity of cells in the top phase, at the time of sampling, as a percentage of the total quantity of cells added. The distribution ratio is the quantity of cells in the top phase divided by quantity of cells at the interface plus bottom phase. In the case of phases containing PEG-IDA-Cu the P values for cells obtained both without and with imidazole are given, for purposes of discussion, in the tables; while the distribution ratios shown in the figures represent partitions of cells in phases at polymer concentrations which were so selected that the cells' partitions in the presence of imidazole are very small. Graphs were plotted using Sigma-Plot 3.0 (Jandel Scientific, Corte Madera, CA, USA). Regression lines are of single order.

RESULTS AND DISCUSSION

Basic phenomena relating to affinity partitioning using a general ligand

Partitioning of erythrocytes in Dx T500:PEG 8000 systems takes place between the top phase and the interface [3]. In non-charge-sensitive phase systems (see below), at adequately low polymer concentrations (e.g., 5% Dx:3.5% PEG), the P value of red cells is species-specific and correlates extremely well with the erythrocytes' membrane ratio of poly/monounsaturated fatty acids [22]. Red cells with high P values (e.g., those from dog) have been shown to be held more weakly at the interface than are erythrocytes with low P values (sheep, beef) [23,24]. For cell affinity partitioning with a ligand which potentially interacts with all cells albeit to a differing extent (hereafter called "general" affinity ligand, e.g., PEG-IDA-Cu), the non-charge-sensitive phase system selected should be one which has the lowest polymer concentrations at which virtually all cells are at the interface [3].

Even under these conditions it is clear that some species' red cells (e.g., dog) would, if all else were equal, be more easily pulled into the upper phase by an affinity ligand than some other species' erythrocytes (e.g., those from sheep, beef).

An analogous argument can be made with respect to charge-sensitive phase systems (see below) at higher polymer concentrations (e.g., 5:4) in which erythrocytes from different species yield P values which have some correlation with the cells' relative electrophoretic mobilities [3].

Relationship of the distribution ratios of red blood cells from different species to their surface properties in non-charge-sensitive and charge-sensitive Dx-PEG aqueous phase systems with and without PEG-IDA-Cu

Non-charge-sensitive Dx-PEG aqueous phase systems are those in which the predominant salt has ions with essentially equal affinities for the two phases (e.g., NaCl) and there is, hence, no Donnan potential between the phases [3,22]. With increasing polymer concentrations cells added to the phases tend to be increasingly adsorbed at the interface. 5:3.8 is close to the

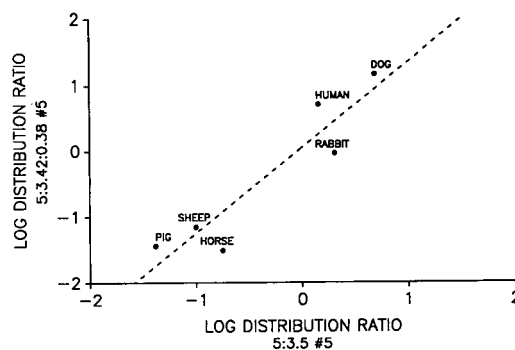


Fig. 1. The log distribution ratios of RBC from different species in a non-charge-sensitive phase system containing PEG-IDA-Cu (5% Dx:3.42% PEG:0.38% PEG-IDA-Cu, 0.15 M NaCl and 0.01 M sodium phosphate buffer, pH 6.8) plotted against those obtained in a non-charge-sensitive system with lower polymer concentration and without chelate (5% Dx:3.5% PEG, 0.15 M NaCl and 0.01 M sodium phosphate buffer, pH 6.8 [22]). A general similarity is in evidence between the groupings of extractions of RBC from different species in the two systems. Note that because of its higher polymer concentration cells do not partition in the phase system used with the PEG-IDA-Cu in its absence but remain at the interface [3]. See text for discussion.

lowest polymer concentrations at which the red blood cells of all species examined (except for rat) are almost (but not) completely adsorbed at the interface.

In Fig. 1 we depict distribution ratios of erythrocytes from a number of different species obtained in a non-charge-sensitive system with higher PEG concentrations (*i.e.*, 5:3.8 #5) in which 10% of the PEG has been replaced by PEG-IDA-Cu (ordinate). The fact that erythrocytes partition in this phase system at all reflects that the PEG-IDA-Cu, which itself partitions predominantly into the top phase [18], interacts with the cells and “pulls” cells out of the interface and into the top phase. The erythrocyte distribution ratios appear to be species-specific. For comparison we also show in this figure the previously reported partition results in a non-charge-sensitive phase system at lower polymer concentrations (5:3.5 #5) devoid of PEG-IDA-Cu (abscissa) [22]. Note a general similarity in the grouping of distribution ratios of red cells from different species in the phase systems with and without PEG-IDA-Cu (*i.e.*, dog, human, rabbit have high and horse, sheep, pig low ratios).

There is also some tendency for the distribution ratios of erythrocytes from different species, in a system containing high polymer concentrations and PEG-IDA-Cu, to increase with a larger membrane ratio of their poly/monounsaturated fatty acids (data not shown). Thus, the sequence of extraction of cells in this phase system appears to reflect a non-charge-dependence attributable to membrane lipid parameters but not to a specificity of the chelate.

Charge-sensitive Dx-PEG aqueous phase systems are those in which the predominant salt has ions which have unequal affinities for the two phases (*e.g.*, sodium phosphate) giving rise to a Donnan potential between the phases, top phase positive [3]. With increasing polymer concentrations cells added to the phases tend to be increasingly adsorbed at the interface. 5:4.4 is close to the lowest polymer concentrations at which the red blood cells of all species examined (except for rat) are almost (but not) completely adsorbed at the interface.

Fig. 2 shows the distribution ratios of erythro-

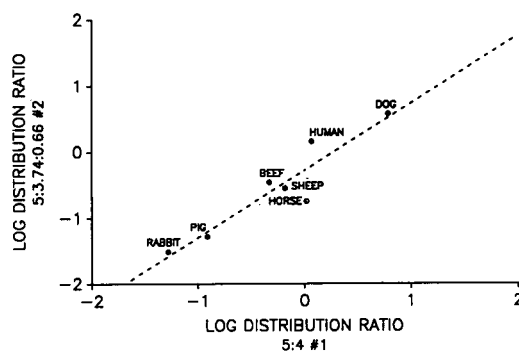


Fig. 2. The log distribution ratios of RBC from different species in a charge-sensitive phase system containing PEG-IDA-Cu (5% Dx:3.74% PEG:0.66% PEG-IDA-Cu, 0.09 M sodium phosphate buffer, pH 6.8, and 0.03 M NaCl) plotted against those obtained in a charge-sensitive phase system with lower polymer concentration and without chelate (5% Dx:4% PEG and 0.11 M sodium phosphate buffer, pH 6.8 [22]). A similarity is in evidence between the sequence of extractions of RBC from different species in the two phase systems. Beef RBC belonged to partition class I (see ref. 22 and below). Note that because of its higher polymer concentration cells do not partition in the phase system used with the PEG-IDA-Cu in its absence but remain at the interface [3]. See text for discussion.

cytes from a number of different species obtained in a charge-sensitive system with higher PEG concentrations (*i.e.*, 5:4.4 #2, ordinate) in which 15% of the PEG has been replaced by PEG-IDA-Cu. Again, PEG-IDA-Cu causes the red cells to partition into the top phase at polymer concentrations at which they would not partition in the ligand's absence. For comparison we also show in this figure the previously reported partition results in a charge-sensitive phase system at lower polymer concentrations (5:4 #1) devoid of PEG-IDA-Cu (abscissa) [3]. Note the rather good correlation between distribution ratios of red cells from different species in the phase systems with and without PEG-IDA-Cu.

The distribution ratios of erythrocytes from different species, in a system containing a high polymer concentration and PEG-IDA-Cu were also found to correlate well with the cells' relative electrophoretic mobilities (data not shown). Thus, the sequence of extraction of cells in this phase system appears to reflect a charge-dependence attributable to the Donnan potential but not to a specificity of the chelate.

The relationship between the partition ratios of red cells from different species in non-charge-sensitive and charge-sensitive phase systems with and without PEG–IDA–Cu suggests that a major effect of the PEG–IDA–Cu is the facilitation of partitioning of the cells at polymer concentrations higher than those at which they could partition without the chelate. The sequence of extraction of the cells is reminiscent of, though not identical with (see below), that observed in phases at lower polymer concentrations devoid of chelate. This implies that the histidine per unit surface area of red blood cells from different species is about the same causing the non-charge-related *or* charge-associated surface properties to determine the distribution ratios even in

the presence of chelate *or* that these properties outweigh the differences in histidine content and effect the observed correlations.

This general effect of PEG–IDA–Cu on partitioning of red blood cells (RBC) has also been corroborated by counter-current distribution studies on rat red blood cell populations of different ages (which are known, based on a combination of isotopic and partitioning experiments, to have distinct partition ratios in non-charge-sensitive phase systems without chelate [3,25]). The results indicate (data not shown) that the reticulocytes, young mature erythrocytes, middle-aged erythrocytes and old erythrocytes have relative partition ratios with respect to the total cell population that mimic those

TABLE I

THE PARTITION, P , OF RAT RED BLOOD CELLS FROM NORMAL AND FROM PHENYLHYDRAZINE-INJECTED RATS IN NON-CHARGE-SENSITIVE PHASE SYSTEMS WITH AND WITHOUT PEG–IDA–Cu

P , the partition, is defined as the quantity of cells in top phase as a percentage of total cells added. Values given are means \pm S.D. RBC (10- μ l packed cells) were partitioned in a 3-g phase system having equal top and bottom phases. Settling time was 15 min. Rats were injected with a solution containing phenylhydrazine (3 mg/100 g of body mass) on 5 successive days and were bled on the eighth day. Reticulocytes then constituted more than 90% of the total red cell population.

Rat	Phase system ^a	P			
		Percentage of PEG substituted with PEG–IDA–Cu ^a			
		0	3	5	10
Normal	5:3.9 #5	14 \pm 1	32 \pm 4	61 \pm 0	92 \pm 1
	with imidazole		26 \pm 1	53 \pm 1	75 \pm 1
	ΔP		6	8	17
Injected	5:3.9 #5	5 \pm 0	15 \pm 2	20 \pm 2	63 \pm 1
	with imidazole		7 \pm 2	7 \pm 1	18 \pm 3
	ΔP		8	13	45
Normal	5:4.0 #5	9 \pm 0	25 \pm 1	30 \pm 1	92 \pm 2
	with imidazole		9 \pm 1	10 \pm 1	20 \pm 1
	ΔP		16	20	72
Injected	5:4.0 #5	4 \pm 0	12 \pm 0	18 \pm 2	42 \pm 1
	with imidazole		4 \pm 0	7 \pm 1	8 \pm 1
	ΔP		8	11	34
Normal	5:4.2 #5	7 \pm 0	14 \pm 1	21 \pm 1	60 \pm 4
	with imidazole		9 \pm 1	12 \pm 1	9 \pm 0
	ΔP		5	9	51
Injected		n.d.	n.d.	n.d.	n.d. ^b

^a The various Dx, PEG phase systems contained 0.15 M NaCl and 0.01 M sodium phosphate buffer, pH 6.8, with the indicated percentages of PEG replaced by PEG–IDA–Cu. Control systems also contained 1 mM imidazole (see text for discussion).

^b n.d. = Not determined.

obtained in non-charge-sensitive phase systems containing lower polymer concentrations and no chelate. Again, PEG-IDA-Cu facilitates the extraction of cells into the top phase in a sequence reflecting the relative avidity of rat red cells of different ages for the interface [23,24].

Partitions of rat red blood cells from normal and from phenylhydrazine-injected rats in non-charge-sensitive phase systems containing PEG-IDA-Cu

The problems encountered in selecting an appropriate phase system for affinity partitioning using a “general” affinity ligand with cells is illustrated with the example shown in Table I. Repeated injection of rats with phenylhydrazine yields red blood cell populations composed almost entirely of reticulocytes [3]. Such cells have previously been found to have P values lower than those of erythrocytes from untreated (normal) animals [25]. In Table I we present the P values of red blood cells from normal and from injected rats in a series of non-charge-sensitive phase systems having different polymer concentrations and containing increasing quantities of PEG-IDA-Cu (*i.e.*, the latter replacing from 0 to 10% of the PEG present in the phase systems). Partitions were also carried out, as control, in phase systems containing 1 mM imidazole.

Rat red cells have a very high membrane ratio of poly/monounsaturated fatty acids which correlates with their higher P value in non-charge-sensitive phase systems, higher than that of red cells from other species [22]. Thus, the lowest polymer concentrations at which virtually all rat red cells will be at the interface has to be higher than for any other species' erythrocytes. In a 5:3.9 #5 system (Table I) the P value of rat normal RBC, in the absence of PEG-IDA-Cu, is still about 14% in the top phase. With increasing quantities of PEG-IDA-Cu this value increases to 92%. Phase systems having the same phase compositions but also containing imidazole (which interferes with the Cu chelate-cell interaction) also give an increase in the RBC P value. The latter increase illustrates the rule that substitution of a polymer of lower molecular weight (as in the case of the PEG 5000-ligand) for one of higher molecular mass (the PEG 8000 which

constitutes the bulk of the phase system) causes biomaterials (including cells) to favor the phase which contains the polymer with reduced average molecular mass [4]. High control P values obtained in the presence of imidazole should not be subtracted from P values obtained in its absence because misleading, low “net” values can result. That is because cells partitioning into the top phase in the presence of imidazole under these conditions may form part of the population that can also be extracted with PEG-IDA-Cu if a phase system with adequately high polymer concentrations were used in which the cells are retained at the interface initially (see results in 5:4 #5 and 5:4.2 #5, Table I). It follows that the P values obtained for normal rat RBC in all 5:3.9 #5 systems containing PEG-IDA-Cu do not give quantitative information on the extractability of these cells with the chelate. The same argument applies to previously published data obtained in phase systems which were close to the critical point [20].

Rat reticulocytes have lower P values than do normal mature rat RBC in non-charge-sensitive phase systems. Hence reticulocytes tend to adhere to the phase interface more strongly [23]. In a 5:3.9 #5 system with increasing quantities of PEG-IDA-Cu reticulocyte P value increases while the P values obtained in the systems containing 3 or 5% PEG-IDA-Cu and imidazole are very low. In the system containing 10% PEG-IDA-Cu and imidazole the PEG-ligand molecular mass effect on the P value (see above) is again in evidence (although less so than in the case of normal mature rat RBC).

To gauge the relative affinity of rat RBC from normal (mature RBC) from phenylhydrazine-injected (reticulocytes) animals for the copper chelate, polymer concentrations of the phase systems are increased (Table I) to the point at which inclusion of PEG-IDA-Cu (at a useful concentration) yields low P values in the presence of imidazole. Increasing the concentrations of polymers beyond this will cause cells to be held more and more firmly at the interface and result in ever-decreasing cell affinity extractions. Comparison of P values for normal RBC and for reticulocytes in phase systems having the same composition and in which both of these cell populations have low P values (*i.e.*, 10% or less)

in the presence of imidazole (e.g., 5:4 #5 with 3 or 5% PEG–IDA–Cu), indicates that normal RBC are extracted by PEG–IDA–Cu to a greater extent than reticulocytes.

Since this result is also obtained in non-charge-sensitive phase systems at lower polymer concentrations without PEG–IDA–Cu there is, again, no indication of an extraction specificity attributable to PEG–IDA–Cu.

Partitions in charge-sensitive and non-charge-sensitive phase systems with and without PEG–IDA–Cu of human normal erythrocytes (RBC) and RBC treated with neuraminidase or trypsin

It has previously been reported that when human RBC are treated with neuraminidase (thereby removing virtually all of the main charge-bearing groups on the surface of these cells) or trypsin their *P* value is markedly reduced in charge-sensitive phases (e.g.,

5:3.9 #1) and appreciably increased in non-charge-sensitive systems (e.g., 5:3.4 #5), see ref. 22 and Table II. The increase in partition of neuraminidase- or trypsin-treated cells in non-charge-sensitive phases may be a consequence of the closer interaction between the top, PEG-rich, phase and the non-charge-related surface properties possible after sialic acid or peptide and peptide-bound sialic acid removal [3,22]. In a non-charge-sensitive phase system having higher polymer concentrations and containing PEG–IDA–Cu (5:3.78:0.42 #5), selected in a manner as outlined in the previous section, the *P* value of neuraminidase-treated cells, but not of trypsin-treated cells, is also found to increase (Table II). In a charge-sensitive phase system having higher polymer concentrations and containing PEG–IDA–Cu (5:3.74:0.66 #2) the *P* value of neuraminidase-treated red cells is not only not reduced but is actually increased. This is an example of specific extraction of the treated

TABLE II

THE PARTITION, *P*, OF HUMAN NORMAL ERYTHROCYTES (RBC) AND ERYTHROCYTES TREATED WITH NEURAMINIDASE OR TRYPSIN IN CHARGE-SENSITIVE OR NON-CHARGE-SENSITIVE PHASE SYSTEMS WITH AND WITHOUT PEG–IDA–Cu

P, the partition, is defined as the quantity of cells in top phase as a percentage of total cells added. Values given are means \pm S.D. with the number of experiments in parentheses. RBC (30- μ l packed cells) were partitioned in a 10-g phase system having equal volumes of top and bottom phase. Settling time was 7 min in the horizontal position + 1 min in the vertical position.

Phase system ^a	<i>P</i>		
	Normal RBC	Neuraminidase-treated RBC	Trypsin-treated RBC
5:3.9 #1	63 \pm 3 (12)	7 \pm 3 (7)	23 \pm 1 (5)
5:3.74:0.66 #2 with imidazole	61 \pm 2 (12)	80 \pm 6 (8)	20 \pm 2 (5)
	9 \pm 2 (7)	10 \pm 0 (3)	10 \pm 1 (5)
5:3.4 #5	44 \pm 3 (12)	89 \pm 3 (7)	82 \pm 2 (5)
5:3.78:0.42 #5 with imidazole	21 \pm 2 (5)	81 \pm 1 (3)	13 \pm 1 (3)
	3 \pm 0 (5)	8 \pm 1 (3)	7 \pm 1 (3)

^a 5:3.9 #1 contained 5% Dx, 3.9% PEG, and 0.11 *M* sodium phosphate buffer, pH 6.8 (NaPB). It has a Donnan potential between the phases and is charge-sensitive. 5:3.74:0.66 #2 contained 5% Dx, 3.74% PEG, 0.66% PEG–IDA–Cu, 0.09 *M* NaPB and 0.03 *M* NaCl. The control system also contained 1 *mM* imidazole. These systems have a higher interfacial tension than 5:3.9 #1 due to the higher polymer concentrations and have a Donnan potential between the phases. They are thus charge-sensitive and contain PEG–IDA–Cu. 5:3.4 #5 contained 5% Dx, 3.4% PEG, 0.15 *M* NaCl and 0.01 *M* NaPB. It has virtually no Donnan potential between the phases and is non-charge-sensitive. 5:3.78:0.42 #5 contained 5% Dx, 3.78% PEG, 0.42% PEG–IDA–Cu, 0.15 *M* NaCl and 0.01 *M* NaPB. The control system also contained 1 *mM* imidazole. These systems have a higher interfacial tension than 5:3.4 #5 due to the higher polymer concentrations and have virtually no Donnan potential between the phases. They are thus non-charge-sensitive and contain PEG–IDA–Cu.

cells by the copper chelate [*i.e.*, an extraction that cannot be attributed to the physical (*i.e.*, charge-sensitive) properties of the phases devoid of chelate]. The removal of sialic acid may permit increased binding of PEG–IDA–Cu to the cell surface thereby raising the treated cells' *P* value. The removal of peptides and peptide-bound sialic with trypsin apparently results in diminished binding sites for the chelate as reflected by the reduced *P* value.

In other experiments (not shown) we have found that identical partitioning results are obtained over a five-fold increase in cell concentration over that used here.

Partitions of human and rabbit erythrocytes (RBC) in a non-charge-sensitive phase system with PEG–IDA–Cu or PEG–IDA–Zn

PEG–IDA–Zn is less efficient than PEG–IDA–Cu in extracting RBC in non-charge-sensitive aqueous phases. This becomes evident when PEG–IDA–Zn is substituted for PEG–IDA–Cu in a phase system of otherwise identical composition. In Table III we present, for comparison, the *P* values of human and rabbit RBC in a non-charge-sensitive phase system close to the critical point, 5:3.5 #5 [22], and in a phase system with higher polymer concentrations in

which part of the PEG has been replaced by either PEG–IDA–Cu or PEG–IDA–Zn. It is clear that the *P* value of rabbit erythrocytes is higher than that of human RBC in the non-charge-sensitive phase devoid of metal chelate, a result which fits into the general pattern correlating *P* values of erythrocytes from different species with their membrane ratio of poly/mono-unsaturated fatty acids [22]. In the presence of PEG–IDA–Cu the indicated sequence is reversed with human red cells having the higher *P* value (Table III and Fig. 1). Thus, the Cu chelate specifically extracts human erythrocytes to a greater extent than rabbit red blood cells. Furthermore, since PEG–IDA–Zn causes no reversal of the partitioning sequence of human and rabbit RBC, it appears that the interactions of these chelates with these cells' surfaces is metal-specific.

Partitioning beef red blood cells belonging to different partition classes in charge-sensitive and non-charge-sensitive phase systems containing PEG–IDA–Cu

Beef red blood cells collected from different animals have previously been found to fall into three partition classes with low (class I), intermediate (II) and high (III) *P* values in charge-sensitive phase systems [26]. These classes ap-

TABLE III

THE PARTITION, *P*, OF HUMAN AND RABBIT ERYTHROCYTES (RBC) IN A NON-CHARGE-SENSITIVE PHASE SYSTEM WITH AND WITHOUT PEG–IDA–Zn OR PEG–IDA–Cu

P, the partition, is defined as the quantity of cells in the top phase as a percentage of total cells added. Values given are means \pm S.D. with the number of experiments given in parentheses. RBC (10- μ l packed cells) were partitioned in a 3-g system having equal volumes of top and bottom phase. Settling time was 15 min.

Phase system ^a	<i>P</i>	
	Human RBC	Rabbit RBC
5:3.5 #5 ^b	59 \pm 6	67 \pm 11
5:3.42:0.38 (Cu) #5	84 \pm 6 (5)	49 \pm 6 (5)
with imidazole	4 \pm 1 (2)	4 \pm 1 (2)
5:3.42:0.38 (Zn) #5	8 \pm 2 (4)	22 \pm 3 (4)

^a 5:3.5 #5 contained 5% Dx, 3.5% PEG, 0.15 M NaCl and 0.01 M sodium phosphate buffer, pH 6.8 (NaPB). 5:3.42:0.38 (Cu) #5 contained 5% Dx, 3.42% PEG, 0.38% PEG–IDA–Cu, 0.15 M NaCl and 0.01 M NaPB. The control system also contained 1 mM imidazole. 5:3.42:0.38 (Zn) #5 contained 5% Dx, 3.42% PEG, 0.38% PEG–IDA–Zn, 0.15 M NaCl and 0.01 M NaPB.

^b Data from ref. 22.

pear to have different quantities of charge-bearing surface components (e.g., class I has far less sialic acid on its surface than does class III). Each of these classes breaks into additional and sometimes overlapping classes when partitioned in non-charge-sensitive phase systems [27].

When beef erythrocytes are partitioned in a charge-sensitive phase system with higher polymer concentrations and containing PEG-IDA-Cu no difference in partitioning behavior based on class (determined in a 5:3.9 #1 system) is in evidence (note relatively small S.D. and range of P values, Table IV). On the other hand, beef red blood cells from different animals yield a variety of P values in a non-charge-sensitive phase system at higher polymer concentrations and containing PEG-IDA-Cu (note large S.D. and range of P values, Table IV). The latter do not correlate with the class determined in the charge-sensitive phase system devoid of PEG-IDA-Cu.

Beef red blood cells belonging to classes II and

III have P values that are intermediate and high compared to other species' red cells in charge-sensitive phases while all beef erythrocytes have low P values in non-charge-sensitive phases. The uniform extraction of beef red blood cells, irrespective of class, in charge-sensitive phases containing PEG-IDA-Cu and their varied extraction in non-charge-sensitive phases containing PEG-IDA-Cu thus appears to reflect a specific extraction by the chelate.

CONCLUSIONS

PEG-IDA-Cu binds to red cells from different species and causes them to be extracted in a sequence reminiscent of *either* that obtained in charge-sensitive *or* non-charge-sensitive phase systems at lower polymer concentrations without the PEG-IDA-Cu. While the above-indicated basis for the extraction involves interaction of the affinity ligand with common binding sites on the cell surfaces and can be deemed "non-specific", PEG-IDA-Cu may prove useful in extending the partitioning range of Dx-PEG systems to cells having such low partitions (P values) in non-charge-sensitive and/or charge-sensitive phase systems as to preclude their partitioning even when phase systems are optimized by manipulation of their components.

Instances of specific extractions by PEG-IDA-Cu also occur. Examples are the increase in the P value of human neuraminidase-treated red blood cells in charge-sensitive phases containing PEG-IDA-Cu; the higher P value of human compared to rabbit erythrocytes in non-charge-sensitive phases containing the copper chelate; and the uniform extraction of beef red blood cells, belonging to different partition classes in charge-sensitive phases, in charge-sensitive phases containing PEG-IDA-Cu.

TABLE IV

THE PARTITION, P , OF BEEF ERYTHROCYTES (RBC) IN CHARGE-SENSITIVE AND NON-CHARGE-SENSITIVE PHASE SYSTEMS WITH PEG-IDA-Cu

P , the partition, is defined as the quantity of cells in the top phase as a percentage of total cells added. Values given are means \pm S.D. with the number of experiments given in parentheses. RBC (10- μ l packed cells) were partitioned in a 3-g system having equal volumes of top and bottom phase. Settling time was 15 min.

Phase system ^a	P
5:3.52:0.88 #2	26 \pm 4 ^b (15)
with imidazole	2 \pm 1 (4)
5:3.04:0.76 #5	14 \pm 13 ^c (24)
with imidazole	5 \pm 1 (5)

^a 5:3.52:0.88 #2 contained 5% Dx, 3.52% PEG, 0.88% PEG-IDA-Cu, 0.09 M sodium phosphate buffer, pH 6.8 (NaPB) and 0.03 M NaCl. The control system also contained 1 mM imidazole. 5:3.04:0.76 #5 contained 5% Dx, 3.04% PEG, 0.76% PEG-IDA-Cu, 0.15 M NaCl and 0.01 M NaPB. The control system also contained 1 mM imidazole.

^b Range: 20–31.

^c Range: 1–47.

ACKNOWLEDGEMENTS

This work was supported by the Medical Research Service of the United States Department of Veterans Affairs and by the German Ministry of Science and Technology (0319792A).

REFERENCES

- 1 H. Walter, D.E. Brooks and D. Fisher (Editors), *Partitioning in Aqueous Two-Phase Systems—Theory, Methods, Uses, and Applications to Biotechnology*, Academic Press, Orlando, FL, 1985.
- 2 H. Walter, G. Johansson and D.E. Brooks, *Anal. Biochem.*, 197 (1991) 1.
- 3 H. Walter, in H. Walter, D.E. Brooks and D. Fisher (Editors), *Partitioning in Aqueous Two-Phase Systems—Theory, Methods, Uses, and Applications to Biotechnology*, Academic Press, Orlando, FL, 1985, pp. 327–376.
- 4 D.E. Brooks, K.A. Sharp and D. Fisher, in H. Walter, D.E. Brooks and D. Fisher (Editors), *Partitioning in Aqueous Two-Phase Systems—Theory, Methods, Uses, and Applications to Biotechnology*, Academic Press, Orlando, FL, 1985, pp. 11–84.
- 5 H. Walter and F.W. Selby, *Biochim. Biophys. Acta*, 148 (1967) 517.
- 6 E. Eriksson, P.-Å. Albertsson and G. Johansson, *Mol. Cell. Biochem.*, 10 (1976) 123.
- 7 K.A. Sharp, M. Yalpani, S.J. Howard and D.E. Brooks, *Anal. Biochem.*, 154 (1986) 110.
- 8 L.J. Karr, J.M. Van Alstine, R.S. Snyder, S.G. Shafer and J.M. Harris, *J. Chromatogr.*, 442 (1988) 219.
- 9 S.J. Stocks and D.E. Brooks, *Anal. Biochem.*, 173 (1988) 86.
- 10 C. Delgado, R.J. Anderson, G.E. Francis and D. Fisher, *Anal. Biochem.*, 192 (1991) 322.
- 11 J. Porath, J. Carlsson, I. Olsson and G. Belfrage, *Nature*, 258 (1975) 598.
- 12 E. Sulkowski, *BioEssays*, 10 (1989) 169.
- 13 R.J. Sundberg and R.B. Martin, *Chem. Rev.*, 74 (1974) 471.
- 14 E. Sulkowski, *TIBTECH*, 3 (1985) 1.
- 15 E.S. Hemdan, Y.-J. Zhao, E. Sulkowski and J. Porath, *Proc. Natl. Acad. Sci. U.S.A.*, 86 (1983) 1811.
- 16 F.H. Arnold, *BioTechnology*, 9 (1991) 151.
- 17 S.-S. Suh, B.L. Haymore and F.H. Arnold, *Protein Engin.*, 4 (1991) 301.
- 18 G. Birkenmeier, M.A. Vijayalakshmi, T. Stigbrand and G. Kopperschläger, *J. Chromatogr.*, 539 (1991) 267.
- 19 S.-S. Suh and F.H. Arnold, *Biotechnol. Bioeng.*, 35 (1990) 682.
- 20 H. Goubran-Botros, G. Birkenmeier, A. Otto, G. Kopperschläger and M.A. Vijayalakshmi, *Biochim. Biophys. Acta*, 1074 (1991) 69.
- 21 H. Walter, A. Miller, E.J. Krob and G.S. Ascher, *Exp. Cell Res.*, 69 (1971) 416.
- 22 H. Walter, E.J. Krob and D.E. Brooks, *Biochemistry*, 15 (1976) 2959.
- 23 D. Fisher, F.D. Raymond and H. Walter, in D.S. Kompala and P. Todd (Editors), *Cell Separation Science and Technology*, (ACS Symposium Series, No. 464), American Chemical Society, Washington, DC, 1991, pp. 175–188.
- 24 H. Walter, F.D. Raymond and D. Fisher, *J. Chromatogr.*, 609 (1992) 219.
- 25 H. Walter and E.J. Krob, *Br. J. Haematol.*, 38 (1978) 43.
- 26 H. Walter, R. Tung, L.J. Jackson and G.V.F. Seaman, *Biochem. Biophys. Res. Commun.*, 48 (1972) 565.
- 27 H. Walter and E.J. Krob, *FEBS Lett.*, 78 (1977) 105.

Quenching in the flame photometric detector[☆]

Walter A. Aue* and Xun-yun Sun

Department of Chemistry, Dalhousie University, Halifax, Nova Scotia B3H 4J3 (Canada)

(First received October 22nd, 1992; revised manuscript received March 8th, 1993)

ABSTRACT

The conventional, roughly *quadratic* sulphur response mode in the flame photometric detector (FPD) is subject to severe quenching by co-eluting hydrocarbons. This interference is greatly reduced in a new, *linear* sulfur response mode, which tolerates an about twentyfold larger amount of quencher. Under these conditions, the response of a variety of elements is quenched to a similar extent as that of sulphur; *i.e.* the amount of quencher needed to halve response typically varies by a factor no greater than three between sulphur and any of the other five elements tested (Fe, Sn, P, Mn and Cr). It is therefore possible to speculate that linear sulfur is not quenched by a mechanism *sui generis*, but that it is simply subject to the same general quenching process(es) as other FPD analytes. The extent of quenching for all tested elements is largely *independent* of analyte concentration —provided the latter remains within linear range.

INTRODUCTION

Hydrocarbons quench the response of sulphur in the flame photometric detector (FPD) [1]. This effect is troublesome to analytical chemists, particularly those concerned with petroleum products, air pollutants, pesticide residues and food aromas. Considerable effort has therefore been expended to elucidate the quenching mechanism (ref. 2 and studies cited therein). Its most common description assumes collisional deactivation of electronically excited S₂ by CH compounds or their fragments [3].

In contrast, there exists to our knowledge no major study of quenching effects involving elements other than sulphur. This is surprising because the FPD responds to some twenty [4,5] of them: beyond sulphur, the detector is routinely used for analytes containing phosphorus or tin in many laboratories, and applications involving several more elements have been reported. In fact, the impression the reader may easily gain

from the literature is that the quenching of sulphur luminescence is unique in extent and kind. The rather sporadic nature of references to the quenching of *other* elements only serves to reinforce this impression.

Currently, quenching mechanisms for sulphur remain speculative and quenching data for other elements sparse, so that any further information should be welcome. In particular, analysts might want to predict the effects of peak overlap in *multi*-element samples. For analyzing such samples, the FPD conditions are typically chosen for optimum response of the most important element, and that is usually sulphur. Given that conditions are tailor-made for sulphur, does quenching then affect other elements? If so, to what extent?

That question arose for us during recent attempts to assess the analytical merits and demerits of a new FPD sulphur emitter (see Note added in proof), *i.e.* during a comparison of the new with the established FPD method for determining sulphur compounds. Briefly, the new mode monitors the red, the old the violet region of the visible electromagnetic spectrum; the new

* Corresponding author.

* Part of *Ph.D. Thesis* of X.-Y.S.

mode is linear in response, the old (roughly) quadratic. Response linearity strongly favors the former; sensitivity and selectivity weakly the latter [6]. Beyond these essential analytical criteria, however, it may be the *quenching* effects that could tip the balance in favor of using one or the other. Quenching data could also prove important to photometry in the absence of chromatographic resolution, as in certain types of sensors.

Experimental answers will therefore be sought in this study to a series of fairly obvious but also fairly important analytical questions: Is the response of sulphur in the linear mode *less* or *more* susceptible to quenching than in the quadratic mode? What happens to the response of *other* FPD-active elements under the quenching conditions of the linear sulphur mode? Under these conditions, does sulphur really behave *different* from other elements? What is the *extent* of quenching an analyst should expect when using the linear mode? Is it dependent on the *amount* of analyte?

EXPERIMENTAL

The instrument, an ancient Shimadzu GC-4BMPF with dual-channel flame photometric detector, and its operating conditions were essentially the same as described earlier [6] for the linear and quadratic response modes of sulphur. Briefly, the linear sulphur mode employed flows of 500 ml hydrogen and 40 ml air per minute, a 600-nm longpass filter and no quartz chimney; the quadratic (*i.e.* traditional) mode used 50 ml hydrogen and 40 ml air, a 500-nm shortpass filter and the commercial quartz chimney. Both modes were fed sulphur analyte by 26 ml/min nitrogen from a 100 × 0.3 cm I.D. borosilicate column packed with OV-101 on Chromosorb W, 100–120 mesh; and both channels were monitored by Hamamatsu R-374 photomultiplier tubes of nominal range 180 to 850 nm and maximum response at 420 nm.

Methane was added to the hydrogen supply line (which joins the column effluent in the detector before entering the flame), and its concentration or rate of introduction was calculated in parts per million (ppm, v/v) of the total

gas flow (hydrogen + air + nitrogen) for spectroscopic or mechanistic, and in microgram carbon per second for chromatographic or analytical purposes. The flow of methane was established and measured by either injecting methane into an exponential dilution flask (purged by part of the constant hydrogen stream), or by inserting a bubble flow meter with low-flow valve into the methane supply line.

(The use of an in-line bubble flow meter, though not conventional, is convenient and, judging from basic principles, reasonably precise and accurate. It eliminates the derivative role of the conventional rotameter, whose accuracy depends on that of the bubble flow meter with which it was initially calibrated. For reasons of safety as well as for ease of calculation, there must be no appreciable resistance to the hydrogen–methane flow, *i.e.* the methane pressure in the graduated tube of the bubble flow meter must be close to atmospheric. Note that the procedure introduces trace amounts of water vapor from the soap solution. However, this does not compromise the performance of an FPD. Also, the contribution of the partial pressure of water to the measurement is small enough to be neglected in the calculation.)

Chemicals were obtained from conventional commercial sources and were used as received for preparing solutions in (usually) acetone. Calibration curves, particularly in the case of sulfur, were established by injecting the *smallest* amount first. Injections were routinely performed in duplicate. As a rule, differences between corresponding peaks represented only the typical variability of syringe injection (*i.e.* the error bars from a larger number of injections would have been too short to show up to any significant extent in the graphs).

RESULTS AND DISCUSSION

Any quantitative definition of quenching effects in the new linear sulphur mode needs to include a comparison with the established quadratic mode, preferably carried out on the same instrument. Fig. 1 shows in full symbols the quenching curve (the relative fractional response) of 8 ng bis(*tert.*-butyl)disulphide against

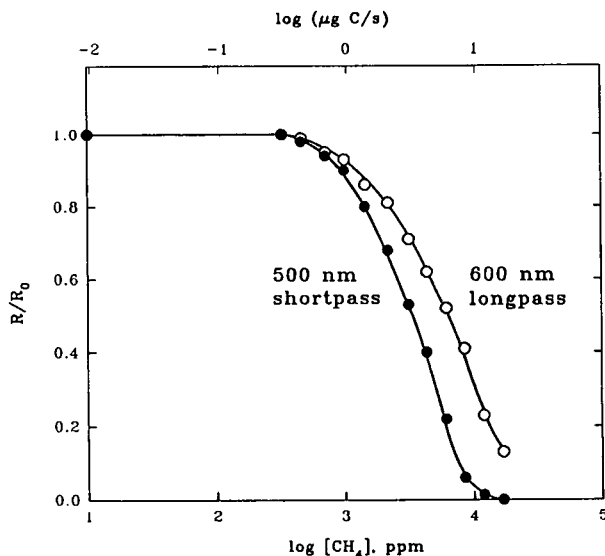


Fig. 1. Quenching of sulphur in the quadratic mode. Analyte: 8 ng of bis(*tert.*-butyl)disulphide; Quencher: methane introduced from an exponential dilution flask into the hydrogen line. R = Quenched response; R_0 = unquenched response. See Experimental for conditions of the quadratic mode.

the methane concentration at the detector flow conditions of the quadratic mode, and with almost all of the S_2 luminescence admitted by the 500-nm shortpass filter. (Essentially the same curve, though at lower sensitivity, can be obtained with the traditional 394-nm interference filter.) The approximate shape and position of this curve is well known (see Fig. 12 of ref. 7), although the *conventional* measurement uses an overlapping peak rather than, as here, a constant background of the quencher.

Given the (in a semilog plot) sigmoid shape of the curve, a measure of quenching intensity may be reasonably and conveniently taken at its halfheight, *i.e.* at the point where quenching has reduced a peak to 50% of its original size and where R/R_0 equals 1/2. This occurs in Fig. 1 for the quadratic mode at a methane concentration (calculated on the total gas flow) of about $3.7 \cdot 10^3$ ppm (v/v), or a carbon flow of $3.4 \mu\text{g/s}$. (The former unit has been chosen for comparison with the spectrochemical, the latter for comparison with the chromatographic literature. While “microgram of carbon per second” is the measure most often used in the literature to

describe FPD quenching effects, it should not be taken to imply independence of chemical structure; that is, the effect of different quenchers should not be automatically equated with the flow of carbon they introduce into the flame.) Methane has played the role of a quenching standard several times before, for instance when it was introduced *through* the column to mimic stationary phase bleed [8].

Fig. 1 also includes a measurement of the red region with a 600-nm longpass filter (empty symbols). The two curves were determined off the selfsame peaks, hence are exactly comparable. (In this and other studies, we made as much use as possible of *both* FPD channels, on the assumption that a second set of data from an optically different range would provide confirmation, serve as a back-up, and/or supply additional information—and, if it did none of these, could be easily discarded.) The 600+ nm region contains the spur of the S_2 bands plus the bands of the linear emitter, though at the flow conditions of the quadratic mode. It is nevertheless obvious that the linear emitter appears less susceptible to quenching than S_2^* . The effect is not large, about a factor of 2 at halfheight. The corresponding data for a tenfold amount of analyte—80 ng bis(*tert.*-butyl)disulphide—are very similar and, consequently, are not shown here.

(Despite the exiguity of the effect when measured by the difference in quencher concentration for equal fractional quenching, it can appear dramatic when measured by the ratio of relative peak heights for an equal—and very heavy—quencher concentration. This is demonstrated in Fig. 2—note its logarithmic ordinate!—where the ratio of two peaks changes more than a hundredfold due to the presence of the quencher. Although rare, such cases do occur in analytical practice.)

It is against this background of quenching intensity in the conventional quadratic mode, that the new linear mode has to be assessed. Peaks obtained at the conditions of the linear mode (high hydrogen, no quartz chimney) are monitored by, again, *two* photomultiplier channels. The first channel, equipped with a 600-nm longpass filter, truly represents the *linear* mode:

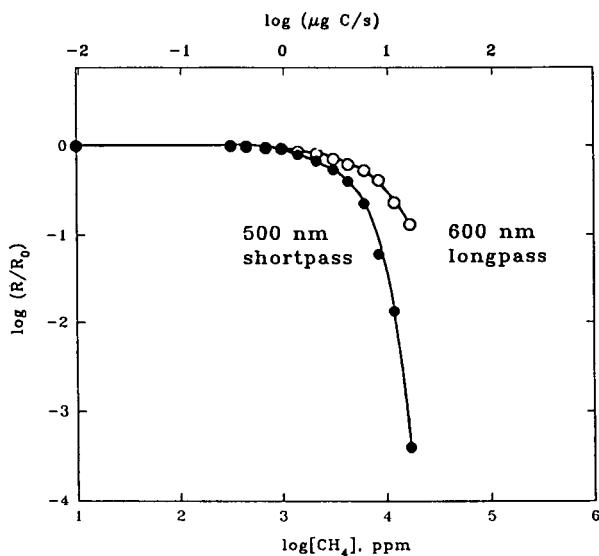


Fig. 2. Extreme quenching of sulphur in the quadratic mode. Similar to Fig. 1 but with logarithmic ordinate.

the calibration curves are purely first order. The second channel is “open” (filterless), *i.e.* it can potentially accept radiation over the full 180–850-nm range of the photomultiplier tube. Calibration curves for sulphur in this channel are approximately quadratic: though weakened by the flow conditions, the S_2 bands still dominate.

Yet, the main role of the open channel is not to pick up all the emissions of sulphur, but all the emissions of those other five elements. Those elements we consider typical of a wider variety of analytically significant FPD analytes, and we include them here to widen the experimental base for a general discussion of quenching. Nevertheless we must note that, strictly speaking, the particular numbers measured depend to some extent on the particular instrument, the particular flow conditions, and the particular combinations of analyte and quencher (as is the case in almost all studies involving flame photometric and other selective GC detectors). Still, we expect the general results and trends of this study to remain valid beyond their experimental origin, *i.e.* we expect them to apply, *mutatis mutandis*, to most GC–FPD systems.

Fig. 3 shows the quenching curves for sulphur measured under the flow conditions of the linear mode. The methane levels for peak halfheight

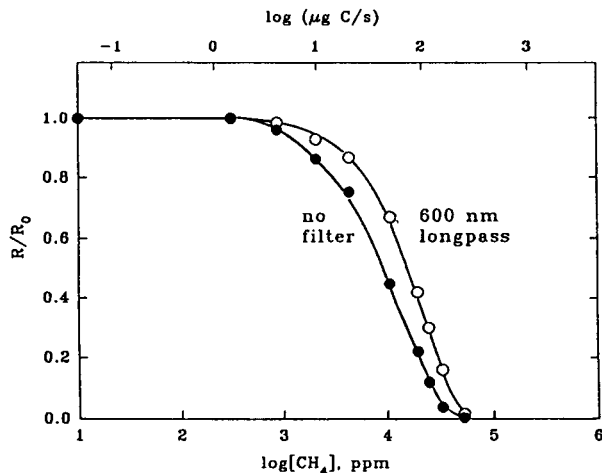


Fig. 3. Quenching of sulphur in the linear mode. Analyte: 50 ng of thianaphthene. See Experimental for conditions of the linear mode.

are about $9.6 \cdot 10^3$ ppm and $1.6 \cdot 10^4$ ppm for the open and >600-nm channels, respectively. The corresponding carbon flows are 43 and $73 \mu\text{g C/s}$. Again, the difference between the two optical channels amounts to roughly a factor of 2.

Much more important than the comparison of the two optical channels is, however, the comparison of the quadratic with the linear mode under individually optimized conditions (*i.e.* the 500-nm shortpass curve in Fig. 1 *vs.* the 600-nm longpass curve in Fig. 3). The result is quite interesting: the linear mode can tolerate a methane flow that is, in flame ppm, roughly 4.4 times and, in $\mu\text{g C/s}$, 22 times larger than in the quadratic mode (the numbers are measured at a 50% reduction in peak height, but remain fairly constant over the whole analytically interesting quenching range). The former number represents the spectrochemically and kinetically relevant one in that it addresses the flame composition; the latter, however, represents the chromatographically and analytically important one in that it predicts the relative intensity of quenching by an overlapping peak (or a heavy column bleed). That the linear mode shows an approximately twentyfold greater tolerance of quenching than the quadratic mode may prove decisive for the FPD's most common task, the

determination of sulphur compounds in complex hydrocarbon matrices.

A look at the absolute quenching intensities for sulphur reveals a surprising fact: it seems that these numbers are not all that different from the numbers that characterize the extent to which the luminescence of other elements is quenched. The literature, as mentioned before, contains some isolated descriptions of quenching beyond sulphur and, in our own work, we have occasionally measured (though never closely studied) the quenching characteristics of one or the other transition metal. To wit, the flame concentrations of methane that caused a 50% reduction of peaks containing Fe [9], Ru [10] and Mn [11], were $4.8 \cdot 10^3$, $1.6 \cdot 10^3$ and $3.5 \cdot 10^3$ ppm (v/v), respectively. That is quite close to, say, the $3.7 \cdot 10^3$ ppm measured for sulphur in the quadratic mode. However, these earlier measurements were taken at significantly different flow conditions (hydrogen range 300 to 370, air range 60 to 80, total nitrogen range 44 to 55 ml/min, *i.e.* at generally higher air flows hence higher temperatures). A direct comparison of these old data with the new ones could thus prove misleading.

What is obviously needed for a valid comparison is to examine *all* elements at approximately the *same* conditions (“approximately” because different temperatures for the chromatographic separation, hence slightly different column flows and bleed levels, as well as temporally, qualitatively, and quantitatively variable memory effects of the chromatographic system, can never be completely ruled out). The one common set of conditions that we shall apply to *all* elements of this study will obviously be that of the linear sulphur mode.

Fig. 4 shows the quenching data of the chosen five elements, plus sulphur, at the exact conditions of the linear mode. Fig. 5 takes an “open” (filter-less) look at the very same peaks. What is obvious but surprising in these figures is that all curves huddle together, with sulphur right in their middle. No curve is farther away from the sulphur curve than by a factor of two (Fig. 5) or three (Fig. 4) in quencher concentration. If all elements and both figures are combined, the strongest quenching curve turns out to be no

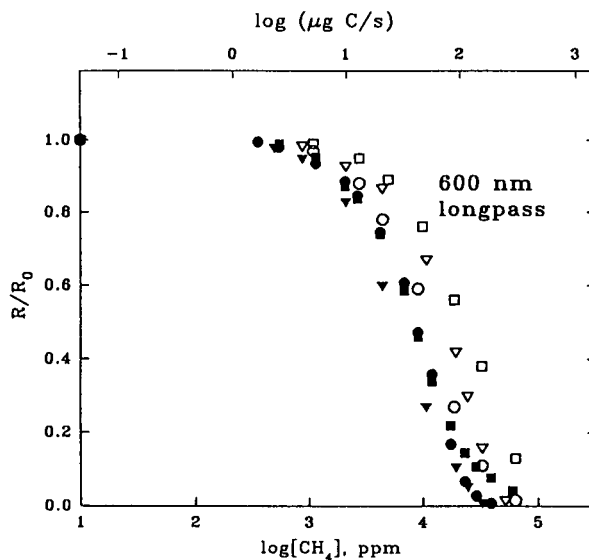


Fig. 4. Quenching of six elements in the linear-sulphur mode. Optical filter: 600 nm longpass. Curves omitted for clarity. \circ = Ferrocene; \bullet = *n*-tetrabutyltin; ∇ = thianaphthene; \blacktriangledown = triethylphosphite; \square = cyclopentadienyl manganese tricarbonyl; \blacksquare = benzene chromium tricarbonyl.

farther away from the weakest than by a factor of four. This suggests that the behavior of all elements tested in this mode is so far similar and, hence, that the behavior of *sulphur is not unique*.

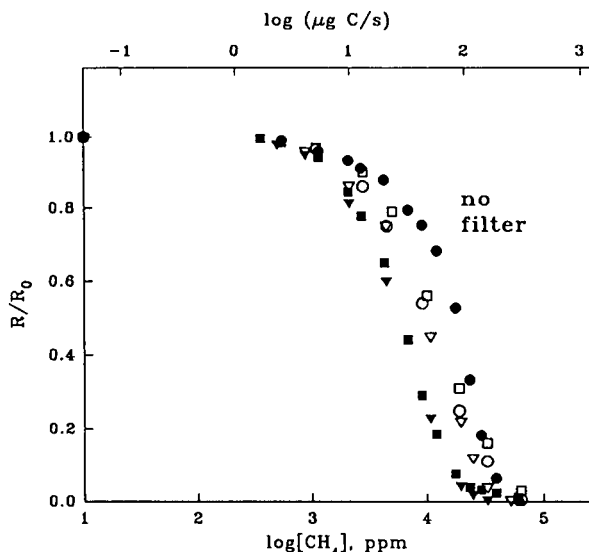


Fig. 5. Quenching of six elements in the open mode. Simultaneous measurements from the experiment shown in Fig. 4, but as seen by the second, filter-less FPD channel. Symbols as in Fig. 4.

Stark speculation may compare the narrow spread of data in Figs. 4 and 5 with—to pick an example for the sake of argument—a listing of Stern–Volmer rate constants for the quenching of singlet oxygen, which includes numbers varying over more than eight orders of magnitude [12]. Such a comparison is not to imply that collisional deactivation of the emitter can be safely excluded as the dominant quenching mechanism: one could, for instance, hypothesize that the FPD system (with similarly wide-spaced differences assumed at the molecular level) could be governed overall by a *diffusional* quenching constant. The far-flung analogy merely suggests the viability of other mechanistic scenarios. The most obvious alternative scenario: the quencher deactivates high-energy flame species that, directly or indirectly, are supplying luminescence energy. This type of mechanism, when used to rationalize the closeness of the quenching curves, also suggests that the various elements undergo common—or at least kinetically interconnected—energy-transfer processes leading to excitation. In this context it is interesting to note that the atomic emissions of several transition elements in the FPD conformed to an apparent upper limit (3.6 V) for the excited state [5]. All this suggests, oversimplified, that *hydrocarbons may quench the exciting flame rather than the excited analyte*. The concept of physical or chemical quenching of high-energy flame species has been mentioned several times before in the sulphur-FPD literature, although it is usually discounted there in favor of the direct collisional deactivation of the excited emitter [2,3,13].

In practical terms, the fact that similar quenching effects can be expected for peaks of different elements provides at least a rule-of-thumb to the analyst. Incidentally, the luminescent response of carbon is also subject to the *interference* of carbon: in fact, plain hydrocarbon peaks are somewhat stronger quenched by background methane than are peaks containing iron [9] or manganese [11].

If the extent of interference is to be estimated for analytical purposes, a crucial criterion is whether quenching does or does not depend on the amount of analyte (in the presence of a constant amount of quencher). Farwell and

Barinaga [2] have stated that, “as with nearly every aspect of the FPD sulfur response, confusion and contradiction are associated with the concept of quenching”. This applies here as well [e.g. refs. 3 and 13]; no doubt because of the very different systems and conditions that are traditionally reported under the FPD heading.

The experimental question is thus whether the calibration curve measured in the presence of a quencher is linear and, if so, whether its linear range is comparable to that of the regular calibration curve measured in the quencher's absence. Further, whether any parallelism of the two curves occurs not only through but also beyond their respective linear ranges.

Fig. 6 shows conventional log–log calibration curves for sulphur—with vs. without methane, and for the full spectrum vs. for just its linear portion. The full-spectrum runs illustrate the difficulties a quadratic emitter brings to photometric analysis: although the general shapes of the two calibration curves appear reasonably

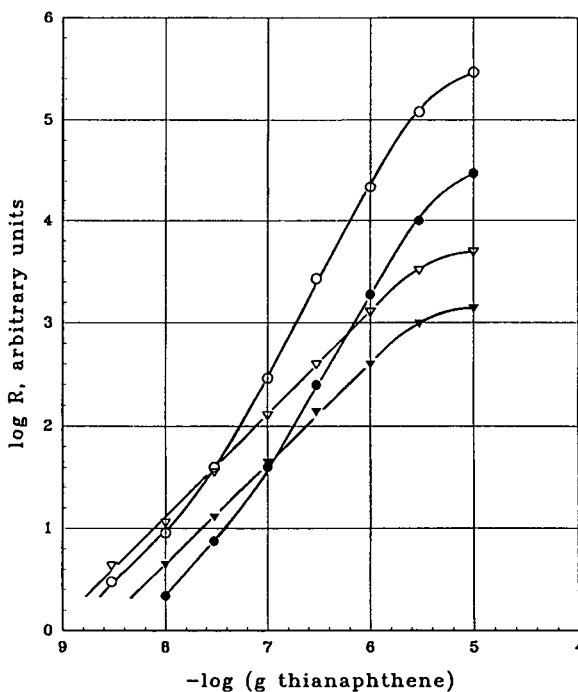


Fig. 6. Calibration curves of a sulphur compound with and without quenching in two optical modes. ○ = No filter, no CH₄; ● = no filter, with CH₄; ▽ = 600-nm longpass filter, no CH₄; ▼ = 600-nm longpass filter, with CH₄.

congruent, their response ratio fluctuates wildly. This is not surprising since (a) at least two emitters of different kinetics contribute luminescence in commensurately different proportions, and (b) the lower end of the calibration curve is, in addition, subject to the linearizing effects of contaminant background sulphur.

In contrast, the runs using the 600-nm cut-on filter, *i.e.* the quenched and unquenched calibration curves of the *linear* mode, appear nicely parallel, at least until their upper bend-off. They resemble in their linearity the quenched and unquenched calibration curves of other elements. As an example, Fig. 7 displays the corresponding set of curves for the second-most important element in the FPD, phosphorus. Again, overt differences in ratio between quenched and unquenched calibration occur only when the linear range is about to end.

Yet, conventional calibration curves still appear too tolerant of small differences in ratio. Also, several more elements need to be brought into the picture. Therefore we have plotted the ratio of the calibration curves (the fractional quenching) *versus* the flow of the FPD-active element X in $\log[\text{mol X/s}]$; and we have also

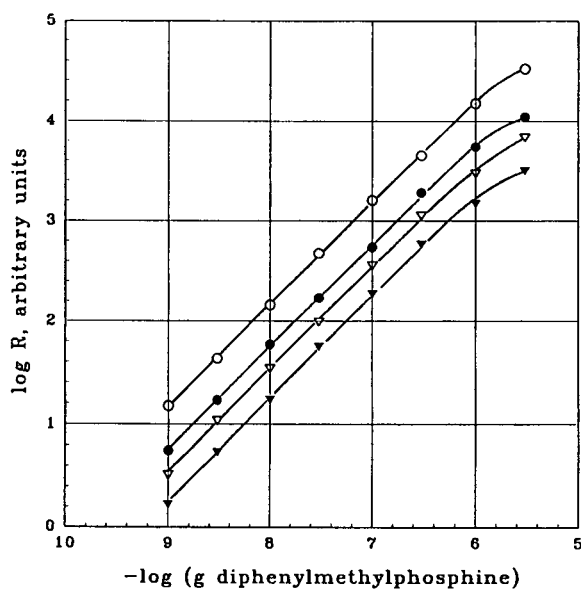


Fig. 7. Calibration curves of a phosphorus compound with and without quenching in two optical modes. The conditions are those characteristic of the linear-sulphur mode as used in Fig. 6. Symbols as in Fig. 6.

included arrows to point to the upper (-10%) end of the linear (or, in two cases involving sulphur, quadratic) response range of the unquenched curves. Fig. 8 shows this for the 600-nm longpass filter (*i.e.* the linear sulfur mode), Fig. 9 for the corresponding filter-less operation. The choice of the individual quenching level of methane was arbitrary for each analyte; however, we aimed for a general range of 40 to 70% peak reduction so that any change in the relative quenching intensity would show up clearly in the figures for later analytical and mechanistic interpretation. The analytical interpretation, for one, turned out to be pleasantly unambiguous.

Fig. 8 establishes that *fractional quenching is generally independent of analyte concentration* over most of the linear range (of the unquenched calibration curves). Even beyond the linear range, however, most deviations from this rule are relatively minor. Linear sulphur is certainly well-behaved in this regard. The only major deviation is that of iron, perhaps because of multiple emitters [9]. No experimental effort was made to extend the horizontal lines all the way back to the detection limit, but then, no devia-

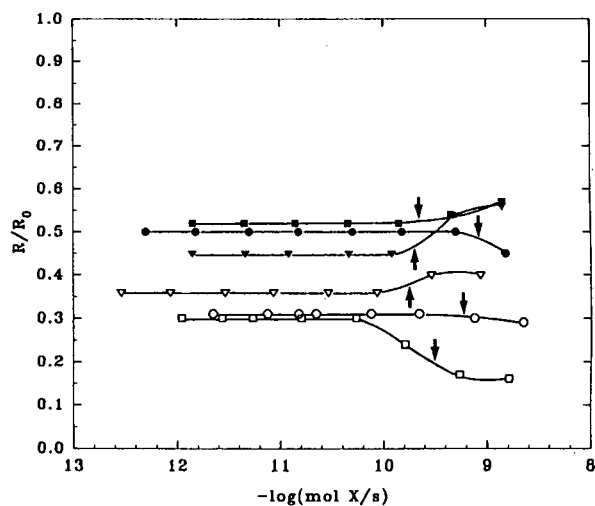


Fig. 8. Fractional response of six elements under constant quenching conditions in the linear-sulphur mode. X = FPD-active element. The arrows mark the upper end of the linear range (10% deviation) as taken from the unquenched calibration curve. \circ = Thianaphthene; \square = ferrocene; ∇ = tetrabutyltin; \bullet = diphenylmethylphosphine; \blacksquare = chromium hexacarbonyl; \blacktriangledown = methylcyclopentadienyl manganese tricarbonyl. 600-nm longpass filter.

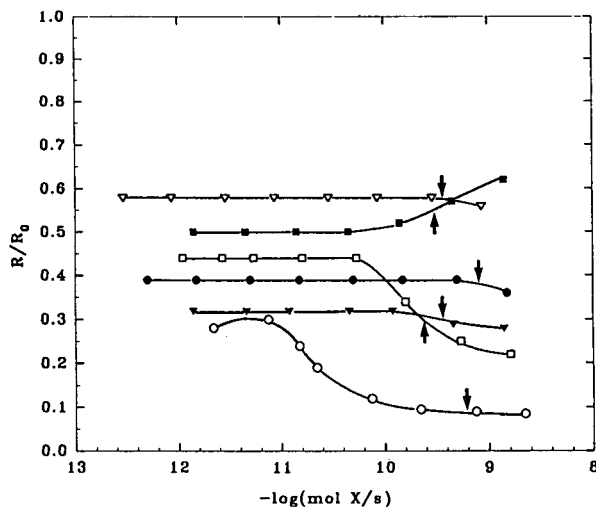


Fig. 9. Fractional response of six elements under constant quenching conditions in the open mode. Simultaneous measurements of the experiment shown in Fig. 8, but as monitored by the second, filter-less FPD channel. Symbols as in Fig. 8.

tions from a constant R/R_0 ratio would be expected to occur at low concentrations, either. That quenching can be considered independent of the amount of analyte (a fact familiar to many analysts working with sulphur, but one that needed confirmation in regard to the *linear* sulphur mode and in regard to other elements) should prove helpful in analytical practice.

Presumably, the assumption of quenching being constant would be more severely tested in a wider optical range. In open mode, more emitters will be seen: tin will emit via SnOH, SnH and the blue surface emission on quartz [14]; some transition metals will radiate via atomic lines, molecular bands and continua [5], etc. It could be argued that this should make no difference as long as all simultaneous emissions, though being affected to different degrees by quenching, do obey first-order kinetics. However, different emitters (of the same element), quenched to different degrees, will likely have different endpoints of linearity. Thus it is to be expected that multiple-emitter systems will exhibit variations of the R/R_0 ratio when the optical conditions are changed, or when the analyte amount exceeds one or more of the different linear ranges. Generally speaking, the extent of deviation from the ideal, *i.e.* constant

R/R_0 ratio should therefore depend on the position and width of the optical window.

This may indeed have been the case for some elements in the optically open configuration of Fig. 9; although no deviation is excessive and, for a case like tin, turns out to be even smaller than in the 600–850-nm region. (Such a case may, for instance, occur if the spectrally open mode would allow the strongest emitter to dominate, while a spectrally more limited mode would curtail its dominance and hence allow another emitter to be noticed as well.) The only roguish curve is that of sulphur—but, as can be ascertained from Fig. 6, that is mostly due to a quadratic joining in with a linear emitter. It would therefore seem that the rule of constant relative quenching could be extended even to very *wide* spectral regions (provided that all monitored emitters respond in linear fashion and remain in linear range).

NOTE ADDED IN PROOF

A prescient comment on “linear sulfur emission” and the “linear sulfur mode” has just appeared in print [15], and we would like to draw the attention of the reader to it. Also, in our earlier reports [6,16,17] we had characterized the linear sulfur emitter—which is of importance in the context of this manuscript—as “unknown”. At the time we were, however, unaware of a particular spectrum that had been obtained some time ago by Schurath *et al.* [18]. The luminescence in question emanated from the system $O_2/O + H_2S + O_3/O_2$ (total pressure 1.3 torr) + 50 mtorr water vapor, and was assigned to the (vibrationally cooled) $^2A' - ^2A''$ electronic transition of HSO [18]. This cited spectrum is remarkably similar to the spectrum of the linear sulfur emitter [6]. In particular, the HSO 0,1 band shows up clearly at 749 nm, as do the (incompletely resolved) 0,0 and 1,1 bands at 696 and 711 nm. The 2,0, 1,0 and 0,2 bands at 634, 663 and 809 nm appear to be present as well [6]. While we cannot exclude the presence of the “infra-red and far red” systems of S_2 —note, for instance, that 0,0 bandheads of the latter are listed at 751 and 710 nm [19]—the resemblance of the recorded spectra and the linearity of the

emission (*i.e.* the linear calibration curve for sulfur analytes) argue strongly against the (presumably second-order) emitter S_2 and for the (presumably first-order) emitter HSO.

ACKNOWLEDGEMENT

This study was supported by NSERC operating grant A-9604.

REFERENCES

- 1 M. Dressler, *Selective Gas Chromatographic Detectors (Journal of Chromatography Library, Vol 36)*, Elsevier, Amsterdam, 1986, pp. 152–156.
- 2 S.O. Farwell and C.J. Barinaga, *J. Chromatogr. Sci.*, 24 (1986) 483.
- 3 T. Sugiyama, Y. Suzuki and T. Takeuchi, *J. Chromatogr.*, 80 (1973) 61.
- 4 W.A. Aue, X.-Y. Sun and B. Millier, *J. Chromatogr.*, 606 (1992) 73.
- 5 X.-Y. Sun, B. Millier and W.A. Aue, *Can. J. Chem.*, 70 (1992) 1129.
- 6 W.A. Aue and X.-Y. Sun, *J. Chromatogr.*, 633 (1993) 151.
- 7 M. Maruyama and M. Kakemoto, *J. Chromatogr. Sci.*, 16 (1978) 1.
- 8 M. Dressler, *J. Chromatogr.*, 270 (1973) 145.
- 9 X.-Y. Sun and W.A. Aue, *J. Chromatogr.*, 467 (1989) 75.
- 10 X.-Y. Sun and W.A. Aue, *Can. J. Chem.*, 67 (1989) 897.
- 11 W.A. Aue, B. Millier and X.-Y. Sun, *Anal. Chem.*, 62 (1990) 2453.
- 12 N.J. Turro, *Modern Molecular Photochemistry*, Benjamin/Cummings, Menlo Park, CA, 1978, p. 593.
- 13 S.V. Olesik, L.A. Pekay and E.A. Paliwoda, *Anal. Chem.*, 61 (1989) 58.
- 14 C.G. Flinn and W.A. Aue, *Can. J. Spectr.*, 25 (1980) 141.
- 15 S. Cheskis, E. Atar and A. Amirav, *Anal. Chem.*, 65 (1993) 539; p. 546, Fig. 8.
- 16 B. Millier, X.-Y. Sun and W.A. Aue, presented at the 75th CIC Conference, Edmonton, Alberta, June 1992.
- 17 X.-Y. Sun and W.A. Aue, *Anal. Chem.*, July 1992, submitted for publication.
- 18 U. Schurath, M. Weber and K.H. Becker, *J. Chem. Phys.*, 67 (1977) 110; p. 112, Fig. 2b.
- 19 R.W.B. Pearse and A.G. Gaydon, *The Identification of Molecular Spectra*, Chapman & Hall, London, 4th ed., 1976.

Thermodynamic study of polystyrene–*n*-alkane systems by inverse gas chromatography

Luisa Bonifaci* and Gian Paolo Ravanetti

ENICHEM, Mantua Research Centre, Via G. Taliercio, 14, 46100 Mantova (Italy)

(Received January 26th, 1993)

ABSTRACT

Phase diagrams of systems containing high-carbon-number *n*-alkanes (up to *n*-pentatriacontane) and polystyrene were studied in the temperature range from 190 to 250°C. Experimental data obtained for low-carbon-number alkanes by inverse gas chromatography were extrapolated taking advantage of the linear relationships between $\ln V_g^0$ (specific retention volume at 0°C) and the inverse of the temperature and between $\ln V_g^0$ and the number of carbon atoms for homologous series. The resulting activity coefficients and interaction parameters were typical of systems with a poor compatibility. The Gibbs free energy of mixing (ΔG_m) for polystyrene–alkane systems was calculated, with the Flory–Huggins χ parameter assumed to be independent of the composition. The ΔG_m vs. alkane volume fraction curves exhibited a shape corresponding to solution instability at low concentrations of both components. On this basis the phase diagram of the system polystyrene–alkanes was calculated.

INTRODUCTION

A description of the phase behaviour of binary polymer–solvent systems is useful for optimal equipment design in the polymer industry. Polymer devolatilization, purification and plastification are examples of manufacturing operations in which knowledge of the solubility relations is one of the key requirements.

In the present work the solubility limits of high-carbon-number *n*-alkanes in polystyrene at elevated temperatures were studied. Owing to the physical characteristics of these alkanes (high melting point, very low vapour pressure), it was impossible to find a method for the direct measure of the polystyrene–solute phase diagram. Therefore, the thermodynamic characterization of these systems was obtained by extrapolating experimental data from low- to higher-carbon-number alkanes.

Polymer–solute interactions in highly concen-

trated polymeric solutions were measured by inverse gas chromatography, thus obtaining the mass fraction infinite dilution activity coefficient (Ω^∞) of nine alkanes from hexane (C₆) to tricosane (C₂₃) at temperatures ranging from 150 to 210°C. Thermodynamic data of alkanes up to 35 carbon atoms at temperatures up to 250°C were obtained by extrapolating the chromatographic data.

Finally, Flory polymer–solvent interaction parameters at infinite dilution (χ^∞) were calculated, and phase diagrams were drawn following the Flory–Huggins theory, assuming that the χ^∞ parameter depends on the temperature, but not on the concentration.

EXPERIMENTAL

Materials

Polystyrene (Edistir N1280) was supplied by Enichem Polimeri (Mantova, Italy). Its mass-average molecular mass and its glass transition temperature (T_g) were 300 000 and 98°C, respectively.

* Corresponding author.

TABLE I

EXPERIMENTAL MASS FRACTION ACTIVITY COEFFICIENTS AND FLORY-HUGGINS χ PARAMETERS AT INFINITE DILUTION FOR POLYSTYRENE-*n*-ALKANE SYSTEMS AT TEMPERATURES RANGING FROM 150°C TO 210°C

	$T = 150^\circ\text{C}$		$T = 170^\circ\text{C}$		$T = 190^\circ\text{C}$		$T = 210^\circ\text{C}$	
	Ω^∞	χ^∞	Ω^∞	χ^∞	Ω^∞	χ^∞	Ω^∞	χ^∞
C_6	12.51	0.88	11.80	0.78	11.58	0.69	9.95	0.45
C_7	12.37	0.92	11.35	0.80	10.73	0.71	10.03	0.59
C_{10}	11.98	1.03	11.06	0.94	10.36	0.85	9.95	0.79
C_{12}	12.16	1.09	11.25	1.00	10.50	0.92	9.96	0.85
C_{14}	12.65	1.16	11.59	1.06	10.71	0.97	10.17	0.91
C_{15}	12.70	1.17	11.77	1.09	10.87	1.00	10.31	0.94
C_{16}			12.09	1.12	11.13	1.03	10.46	0.96
C_{18}					10.82	1.02	10.13	0.95
C_{23}							11.79	1.13

Hexane (C_6), heptane (C_7), decane (C_{10}), dodecane (C_{12}), tetradecane (C_{14}), pentadecane (C_{15}), hexadecane (C_{16}), octadecane (C_{18}) and tricosane (C_{23}) were supplied by Carlo Erba (Italy) and were used without further purification.

Column preparation

Polystyrene was coated on the inert support (Chromosorb W DMCS 80–100 mesh, Carlo Erba) by evaporation from its chloroform solution.

The coated support was dried to constant weight in a vacuum oven at 50°C, then it was packed in a stainless-steel column (130 cm \times 4 mm I.D. \times 6 mm O.D.). The amount of column loading was measured by thermal gravimetric analysis using the appropriate blank correction. The final coverage ratio was 15.17%.

Equipment

Chromatographic analyses were carried out on a Carlo Erba HRGC 5300 Mega Series gas chromatograph, equipped with a flame ionization detector. Helium was used as carrier gas. Flow-rates ranging from 12 to 30 ml/min were chosen, and were measured with a soap bubble flow meter at the detector outlet.

Three different flow-rates were tested for each sample and temperature, in order to check the influence of flow-rate on the specific retention

volume. The pressure drop in the column was measured with a mercury manometer. To keep the sample size as small as possible, the probes were usually injected in the vapour form. Tricosane and octadecane were dissolved in hexane

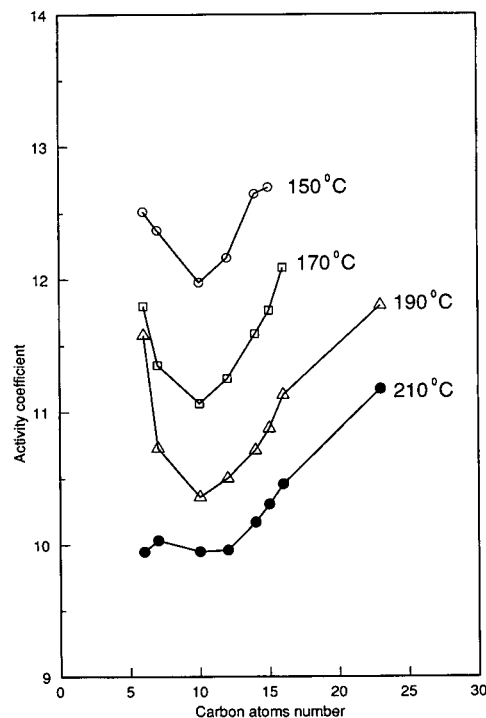


Fig. 1. Experimental mass fraction activity coefficients at infinite dilution as a function of carbon atom number at the indicated temperatures.

and the obtained solutions were injected using a 1- μ l Hamilton syringe.

RESULTS AND DISCUSSION

Chromatographic data reduction

The elution behaviour of volatiles in gas chromatographic columns can be described by the specific retention volume, usually referred to a column temperature of 0°C [1]:

$$V_g^0 = \frac{J \cdot 273.15 \cdot (t_p - t_m) \cdot F}{T_{\text{room}} \cdot W} \quad (1)$$

where V_g^0 is the specific retention volume at 0°C, J is the James–Martin pressure correction term, t_p is the probe retention time, t_m is the marker retention term, F is the flow-rate of the carrier gas, measured at room temperature (T_{room}), and W is the mass of stationary phase in the column.

The mass fraction activity coefficient of the solute probe at infinite dilution (Ω^∞) can be

calculated from the equation:

$$\ln \Omega^\infty = \ln \left(\frac{273.15 \cdot R}{V_g^0 \cdot p_1^0 \cdot M_1} \right) - \frac{p_1^0 \cdot (B_{11} - V_1)}{R \cdot T} \quad (2)$$

where R is the universal gas constant, p_1^0 is the vapour pressure, M_1 is the molecular mass, B_{11} is the second virial coefficient and V_1 is the molar volume of the solute.

The infinite dilution Flory–Huggins interaction parameter (χ^∞) can be determined from experimental inverse gas chromatographic data by the relation:

$$\chi^\infty = \ln \Omega^\infty + \frac{V_1}{M_n \cdot v_2} - \ln \frac{v_1}{v_2} - 1 \quad (3)$$

where v_1 and v_2 are solute- and polymer-specific volume, respectively, and M_n is the number-average molecular mass of the polymer.

Experimental Ω^∞ and χ^∞ of nine alkanes were calculated by eqns. 1–3, for temperatures ranging from 150 to 210°C. The solute vapour pres-

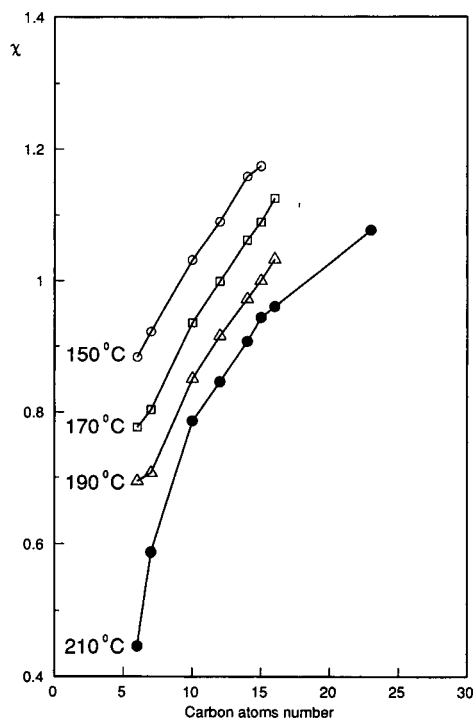


Fig. 2. Experimental Flory–Huggins χ parameters at infinite dilution as a function of carbon atom number at the indicated temperatures.

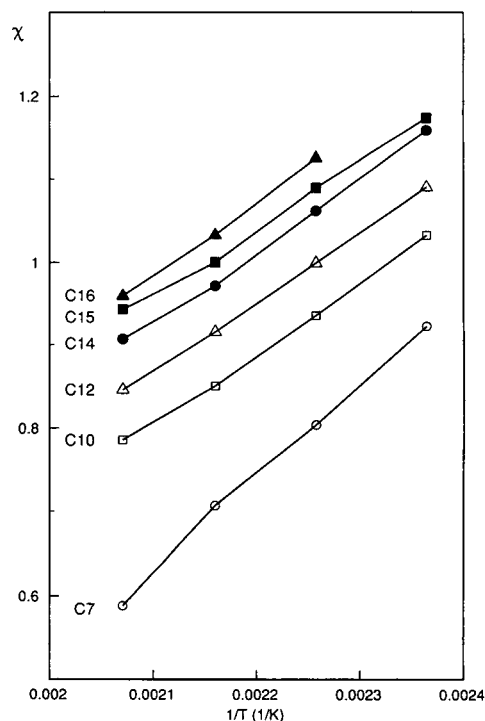


Fig. 3. Experimental Flory–Huggins χ parameters at infinite dilution as a function of $1/T$.

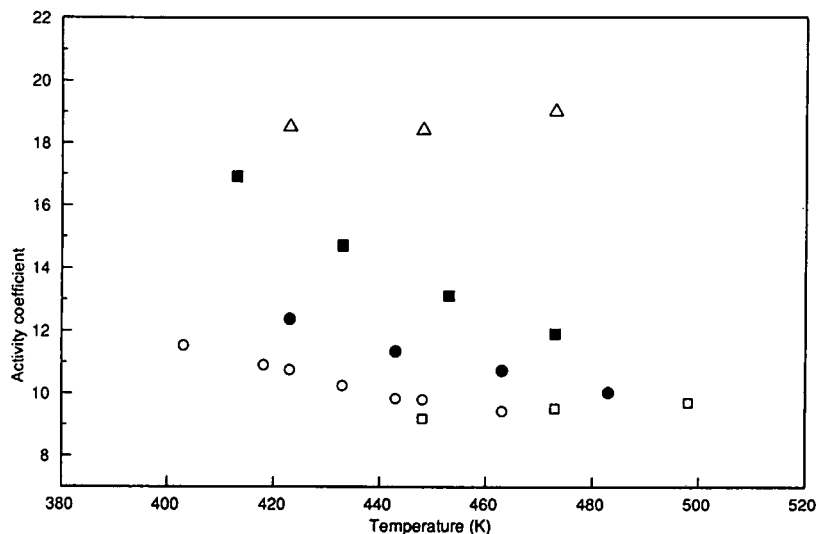


Fig. 4. Comparison of experimental mass fraction activity coefficients obtained by several authors by inverse gas chromatography. ○ = Ref. 9; □ = ref. 7; △ = ref. 6; ● = this work; ■ = ref. 8.

sure p_1^0 was obtained by the Antoine equation, using the constants taken from literature sources [2,3], the second virial coefficients (B_{11}) were calculated by the method of Hayden and O'Connell [4] and the saturated liquid density by the method of Yen and Woods [5]. Critical constants of alkanes were taken from ref. 2.

Table I summarizes our experimental results. Figs. 1 and 2 show the relationship between Ω^∞ , χ^∞ and the number of carbon atoms of alkanes. The elevated values of Ω^∞ and χ^∞ are typical of systems with a poor compatibility; the increasing value of Ω^∞ with the number of carbon atoms indicates a reduction in the affinity with polystyrene increasing the chain length. A minimum can be observed between heptane and decane, as already observed by other authors [6]. In Fig. 3, the temperature dependence of χ^∞ of heptane, decane, dodecane, tetradecane, pentadecane, hexadecane is shown. A remarkable linearity between χ^∞ and $1/T$ can be noted. Moreover, the lower the temperature, the lower is the affinity of alkanes with polystyrene.

Inverse gas chromatography has been used by several authors [6–9] in order to obtain thermodynamic data in polystyrene–alkane systems. In Fig. 4 infinite dilution activity coefficients of heptane in polystyrene reported in literature are compared with those obtained in this study. Our data are lower than those reported by Lipatov

and Nesterov [6] and Galin and Rupprecht [8], and higher than those reported by Stiel and Harnish [7] and Schuster *et al.* [9]. A significant disagreement exists between the results obtained

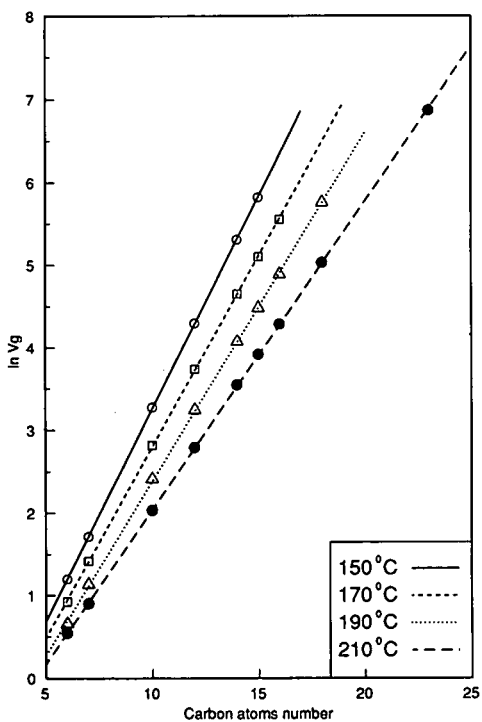


Fig. 5. Plot of $\ln V_g^0$ as a function of carbon atom number.

by different authors, particularly at low temperatures.

Chromatographic data extrapolation

In order to obtain χ^∞ for alkanes with a carbon atom number between 23 and 35 at elevated temperatures, the experimental specific retention volumes were extrapolated taking advantage of the linear relationships between $\ln V_g^0$ and $1/T$ and between $\ln V_g^0$ and the number of carbon atoms for homologous series [1].

From Fig. 5 it is evident that a remarkable correlation exists between our experimental $\ln V_g^0$ data and the carbon atom number for all the tested temperatures. Moreover, Fig. 6 shows the linearity of experimental $\ln V_g^0$ versus $1/T$. The results of the double extrapolation, up to 35 carbon atoms and 250°C, are shown in Fig. 7.

With V_g^0 available, Ω^∞ and χ^∞ were easily obtained using eqns. 2 and 3. In this case the second term on the right-hand side of eqn. 2 was neglected, owing to the very low vapour pressure of alkanes with more than 20 carbon atoms. The saturated vapour pressures of the long-chain

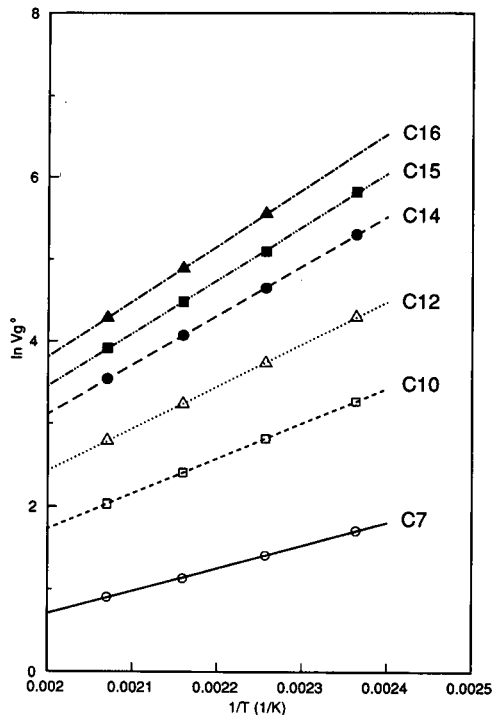


Fig. 6. Retention plot for several *n*-alkanes in polystyrene.

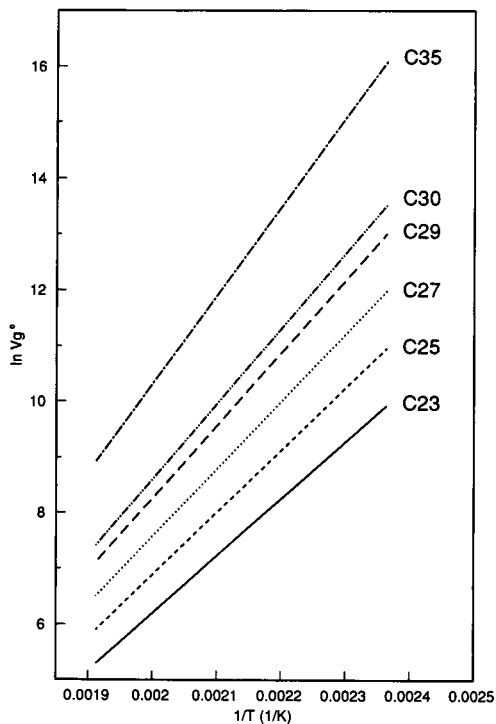


Fig. 7. Specific retention volumes obtained from a two-step extrapolation of experimental data (see text).

alkanes were calculated by the Kudchadker–Zwolinski correlation [3]. The densities were calculated by the method of Elbro *et al.* [10], instead of the method of Yen and Woods [5], as the critical constants were not available.

As an example, Fig. 8 shows Ω^∞ for the homologous series with number of carbon atoms ranging from 6 to 35, whereas Fig. 9 shows the relationship between χ^∞ and the inverse of the temperature.

Phase diagram

Flory–Huggins χ parameter can be used to predict the equilibrium behaviour of two liquid phases containing a polymer and a solvent. Following the classical Flory–Huggins theory [11], with χ parameter and density available, it is possible to calculate the Gibbs free energy of mixing (ΔG_m) as a function of the solute volume fraction:

$$\Delta G_m = RT \left(\frac{\varphi_1}{r_1} \ln \varphi_1 + \frac{\varphi_2}{r_2} \ln \varphi_2 + \chi \varphi_1 \varphi_2 \right) \quad (4)$$

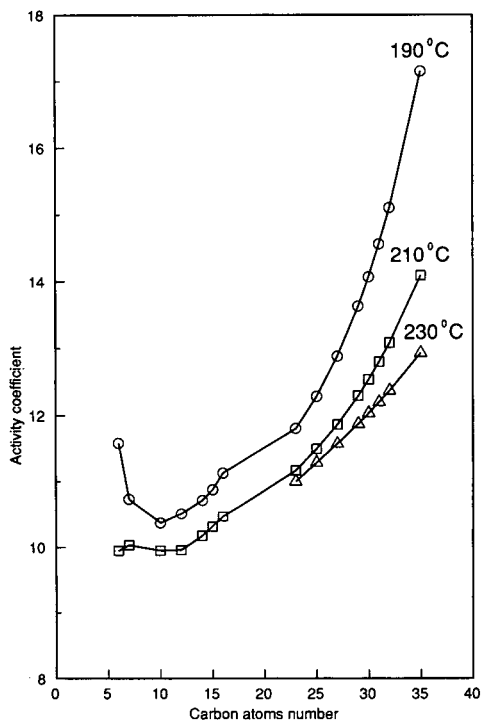


Fig. 8. Plot of mass fraction activity coefficients for the examined homologous series showing experimental (C_6 - C_{23}) and calculated (C_{25} - C_{35}) data.

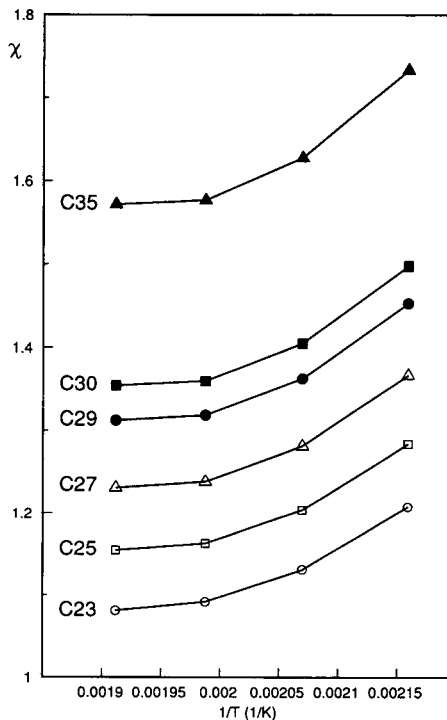


Fig. 9. Calculated Flory-Huggins χ parameters at infinite dilution as a function of $1/T$ for some high-carbon-number alkanes.

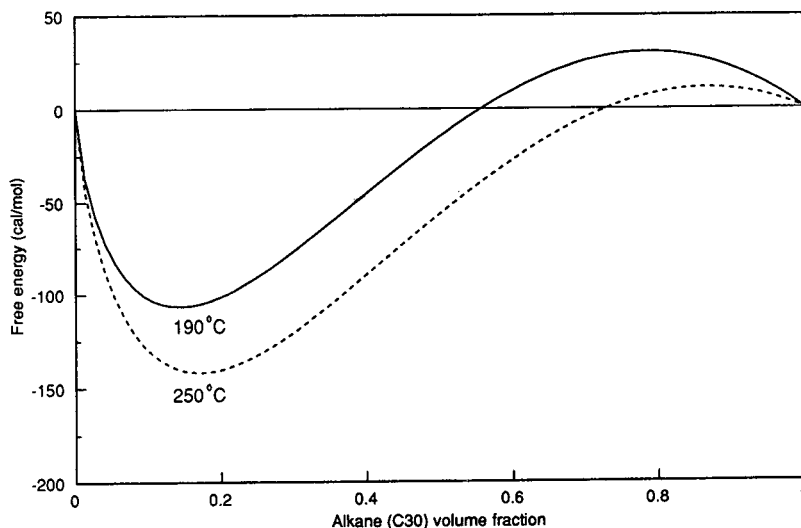


Fig. 10. Example of relationship between Gibbs free energy and alkane volume fraction for *n*-triacontane (C_{30}) at two different temperatures. 1 cal = 4.14 J.

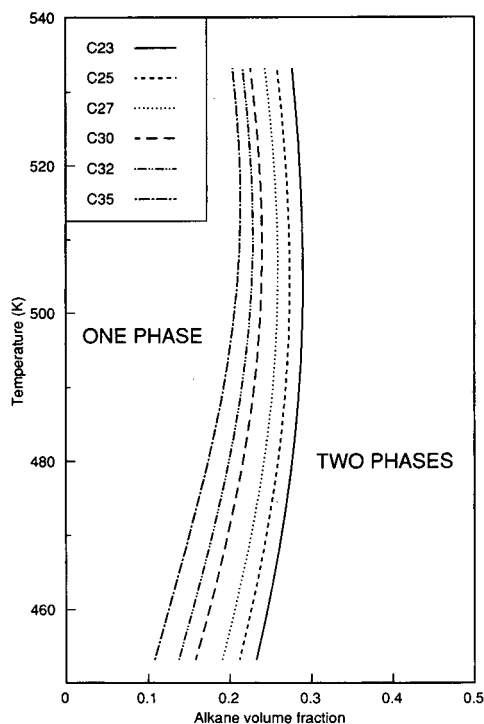


Fig. 11. Phase diagram for the system polystyrene–long-chain alkanes (x -axis is reduced for clarity).

where φ_1 and φ_2 are volume fractions and r_1 and r_2 are the number of segments of the molecules calculated with respect to a reference volume which, in this case, is the solvent molar volume.

Complete miscibility occurs when ΔG_m is less than the Gibbs energy of the components, and the solution maintains its homogeneity only as long as ΔG_m remains less than the Gibbs free energy of any two possible coexisting phases. As an example in Fig. 10 ΔG_m is plotted *versus* the volume fraction for the system polystyrene–C₃₀ calculated by eqn. 4 at two different temperatures (190 and 250°C). The free energy–compo-

sition curve has a shape that clearly shows how two liquid phases coexist; one of them is the pure solvent. Such a behaviour has already been observed for the system acetone–polystyrene [12].

The analogous curves and the solubility limits for the long-chain alkanes were calculated at temperatures ranging from 190 to 250°C, using the extrapolated interaction parameter, assumed to be independent of the composition, and a molecular mass of 300 000 for polystyrene.

The results of these calculations are collected in Fig. 11: the solubility limits range between 10 and 25% volume for temperatures between 180°C and 260°C, and the conjugated phase is always the pure alkane.

REFERENCES

- 1 J.R. Conder and C.L. Young, *Physicochemical Measurements by Gas Chromatography*, Wiley, Chichester, 1979.
- 2 T.E. Daubert and R.P. Danner, *Physical and Thermodynamic Properties of Pure Chemicals—Data Compilation*, Hemisphere, Washington, DC, 1989.
- 3 A.P. Kudchadker and B.J. Zwolinski, *J. Chem. Eng. Data*, 11 (1966) 253.
- 4 J.G. Hayden and J. O'Connell, *Ind. Eng. Chem. Proc. Des. Dev.*, 14 (1975) 209.
- 5 L.C. Yen and S.S. Woods, *AIChE J.*, 12 (1966) 95.
- 6 Y.S. Lipatov and A.E. Nesterov, *Macromolecules*, 8 (1975) 889.
- 7 L.I. Stiel and D.F. Harnish, *AIChE J.*, 22 (1976) 117.
- 8 M. Galin and M.C. Rupprecht, *Polymer*, 19 (1978) 506.
- 9 R.H. Schuster, H. Grater and H.J. Cantow, *Macromolecules*, 17 (1984) 619.
- 10 H.S. Elbro, A. Fredenslund and P. Rasmussen, *Ind. Eng. Chem. Res.*, 30 (1991) 2576.
- 11 P.J. Flory, *Principles of Polymer Chemistry*, Cornell University Press, Ithaca, NY and London, 1953.
- 12 A.A. Patwardhan and L.A. Belfiore, *J. Polym. Sci.: Polym. Phys.*, 24 (1986) 2473.

High-resolution gas chromatographic–mass spectrometric determination of neutral chlorinated aromatic sulphur compounds in stack gas samples

S. Sinkkonen*, E. Kolehmainen, J. Koistinen and M. Lahtiperä

Department of Chemistry, University of Jyväskylä, P.O. Box 35, SF-40 351 Jyväskylä (Finland)

(First received January 8th, 1993; revised manuscript received March 25th, 1993)

ABSTRACT

Four stack gas samples from waste incineration were analysed by high-resolution GC–MS for neutral chlorinated aromatic sulphur compounds such as polychlorinated dibenzothiophenes, thianthrenes and diphenyl sulphides. Samples were analysed tentatively also for some methylated derivatives of these compounds. The stack gas samples had earlier been found to contain some tri- and tetrachlorodiphenyl sulphides. Two of the stack gas samples contained tetra- and pentachlorodibenzothiophenes. One sample was strongly suspected to contain some tri- and tetrachlorothianthrenes in low concentrations. No methylated derivatives of these compounds could be found. Polychlorothianthrenes, some polychlorodibenzothiophenes and some methylated model compounds were prepared; some of the model compounds used in the analysis had been prepared previously. The model compounds were purified by reversed-phase HPLC and their structures were determined by GC–MS and ¹H NMR spectroscopy.

INTRODUCTION

Polychlorinated dibenzothiophenes (PCDBTs) have attracted interest along owing to the availability of model compounds and the discovery of these compounds in incineration gases, bleached pulp mill effluents and some aquatic organisms [1–4]. In the combustion of chlorine-containing materials many kinds of persistent chlorinated aromatic compounds, such as polychlorinated dibenzo-*p*-dioxins, dibenzofurans, diphenyl ethers and chlorophenols [5,6] are formed. Sulphur compounds are generally found in raw materials and chemicals and during the combustion process can react with chlorinated materials in the waste or fuels used in combustion. Hence it is possible that many kinds of chlorinated

sulphur-containing compounds are formed. PCDBTs, polychlorinated thianthrenes (PCTAs) and polychlorinated diphenyl sulphides (PCDPSs) are three groups of compounds which in theory can possibly be formed in this way.

Reference materials and model compounds for the high-resolution gas chromatography–mass spectrometry (HRGC–HRMS) determination of PCDBTs and PCDPSs have been prepared previously [7–10]. In this study, mixtures of chlorinated derivatives were prepared by direct chlorination of the parent compounds dibenzothiophene (DBT) and thianthrene (TA) with sulphuryl chloride and some methylated derivatives from polychloropolymethylbenzenes and sulphur using AlCl₃ as catalyst. Pure isomers were obtained by RP-HPLC fractionation of the chlorination mixtures.

Four stack gas samples from waste incineration were analysed by HRGC–HRMS with a resolution of 20 000 for the occurrence of these compounds. Tetra (Te)- to hexa (He)CDBTs, tri

* Corresponding author.

(Tri)- to penta (Pe)CTAs and Tri- to HeCDPSs were analysed by GC–selected ion monitoring (SIM) MS using the exact values of the M^+ and $(M + 2)^+$ ions. However, a resolution of near 40 000 is needed for the unique separation of some of these compounds and the fragments of these based exclusively on MS. Additionally, some methylated derivatives of these compounds were tentatively screened in a similar way.

Several Te- and PeCDBTs and Tri- and TeCDPSs were found in the samples. One stack gas sample which was not found to contain any Te- and PeCDBTs was strongly suspected to contain Tri- and TeCTAs in low concentrations. The detailed analyses of these samples for PCDPs have been reported previously [10]. Methylated derivatives of these compounds were not found.

EXPERIMENTAL

Model compounds

Preparation and purification. Model compound mixtures were prepared by direct chlorination of the parent compounds DBT, TA and DPS. Sulphuryl chloride was used as the chlorination agent in a mixture of *o*- and *p*-chlorotoluene (50:50). Buckholtz *et al.* [11] have used this mixture in the chlorination of thianthrene. Sulphuryl chloride was added stepwise during 4 h at 60°C until the GC–photoionization detection (PID) analysis showed that no parent compound was present any longer and that the degree of chlorination was three to four.

The chlorination of TA produced one TriCTA and one TeCTA as the main products. Additionally, two TriCTAs, four TeCTAs and some PeCTAs were observed in minor concentrations. Fig. 1 shows the SIM chromatograms of the chlorination mixture with exact m/z values of $(M + 2)^+$ ions of (a) TriCTAs (m/z 319.8869), (b) TeCTAs (m/z 353.8479) and (c) PeCTAs (m/z 387.8089).

The chlorination mixture was fractionated by reversed-phase HPLC with an Elscico C₈ column. Acetonitrile–water (65:35) at a flow-rate of 1 ml/min was used as the eluent. UV detection at 254 nm was applied. The fractions obtained from HPLC were analysed by GC–MS and their

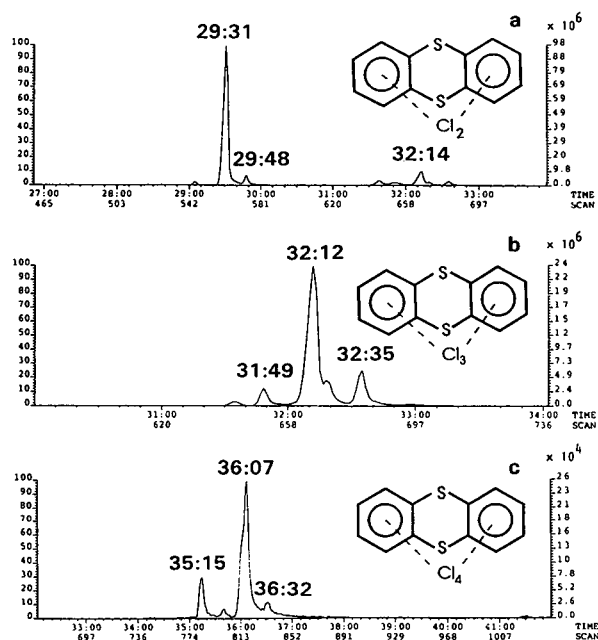


Fig. 1. SIM chromatograms of the chlorination mixture of TA with exact m/z values of $(M + 2)^+$ ions of (a) TriCTAs (m/z 319.8869), (b) TeCTAs (m/z 353.8479) and (c) PeCTAs (m/z 387.8089). Time in min.

structures were determined by ¹H NMR spectroscopy. The main TriCTA isomer was obtained in >90% purity and ¹H NMR analysis showed it to be 2,3,7-TriCTA; the ¹H NMR spectrum of 2,3,7-TriCTA and its interpretation are given in

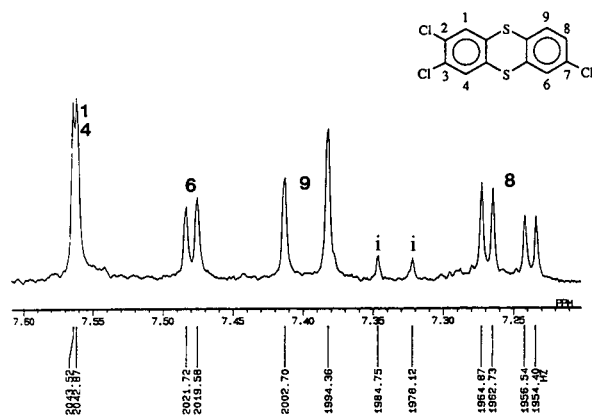


Fig. 2. ¹H NMR spectrum of 2,3,7-trichlorothianthrene and its interpretation. Chemical shifts, δ (ppm): 7.57 and 7.56 (H-1 and H-4, assignment is ambiguous), 7.48 (H-6), 7.40 (H-9), 7.26 (H-8). Coupling constants (Hz): 2.14, 4J (H-6, H-8); 8.34, 3J (H-8, H-9). Impurity signals are denoted by i.

Fig. 2. The purification of the main component of TeCTAs partially failed; the fraction obtained was calculated to consist of about 80% of this TeCTA isomer. The ^1H NMR spectrum of this TeCTA contained only one peak at δ 7.57 ppm (from TMS), which is very close to the values of protons 1 and 4 at δ 7.56 and 7.57 (assignment is ambiguous) of 2,3,7-TriCTA (see Fig. 2). Therefore, it can be concluded that the tetrachloro isomer obtained is 2,3,7,8-TeCTA (thio analogue of 2,3,7,8-TCDD). This finding is in agreement with the general knowledge of the *ortho*- and *para*-directing properties of sulphur in electrophilic aromatic substitution reactions.

The mixture of PCDBTs obtained from the chlorination of DBT with sulphuryl chloride in similar way to that of TA was more complex,

containing at least 20–30 different chlorinated compounds. The GC–MS total ion chromatogram (m/z 50–500) of the chlorination mixture of DBT and electron impact (EI) mass spectra of one Di-, one Tri- and one TeCDBT isomer are presented in Fig. 3.

When DPS was chlorinated in similar way, 2,4,4'-TriCDPS and 2,2',4,4'-TeCDPS were the main products obtained, as was expected from the *ortho*- and *para*-directing properties of sulphur. Additionally, three DiCDPSs and five PeCDPSs in small concentrations were formed [10]. Fig. 4 presents the SIM chromatograms of the chlorination mixture of DPS with the exact m/z values of the $(M+2)^+$ ions of (a) DiCDPSs (m/z 253.9724), (b) TriCDPSs (m/z 289.9305), (c) TeCDPSs (m/z 323.8915) and (d) PeCDPSs

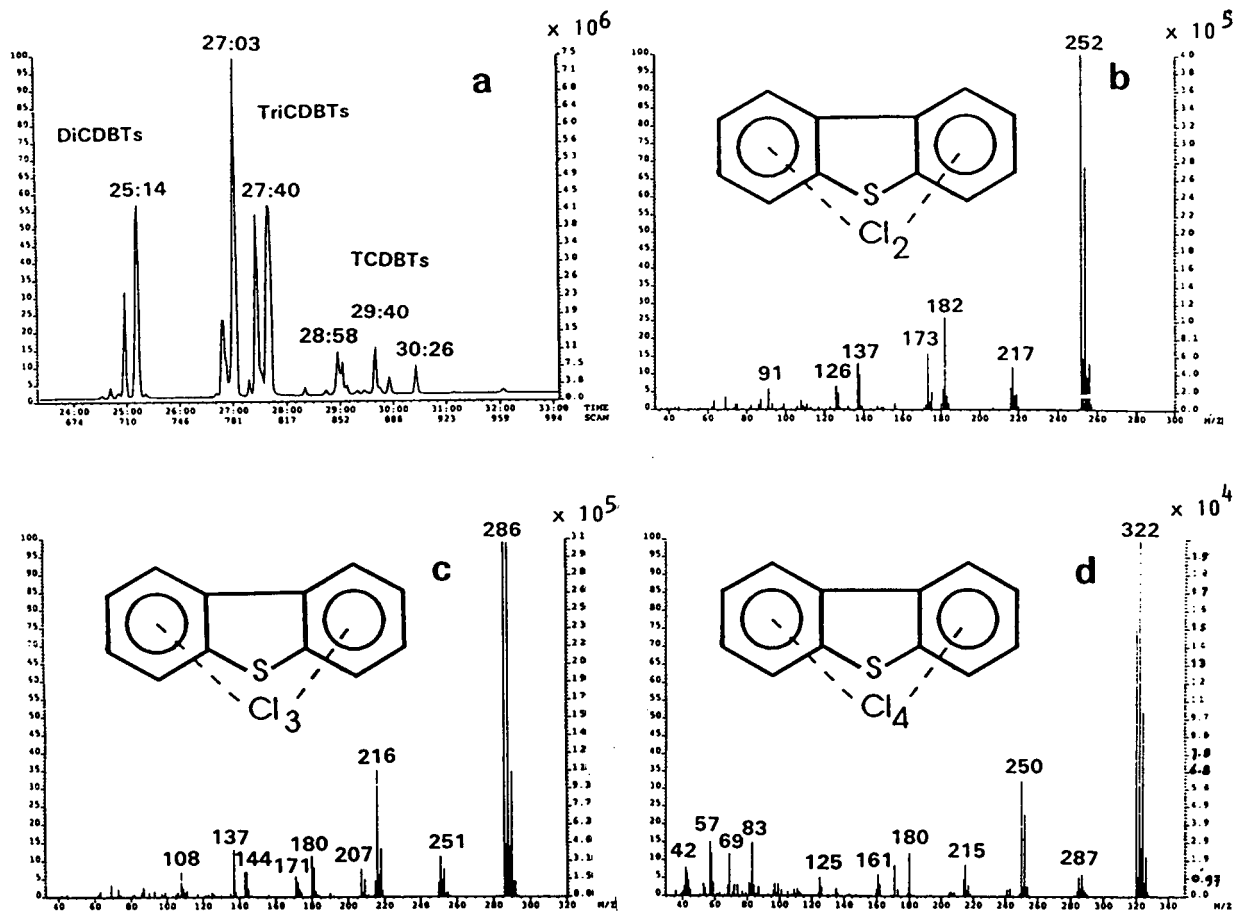


Fig. 3. (a) GC–MS total ion chromatogram (m/z 50–500) of the chlorination mixture of DBT, and EI mass spectra of (b) one DiCDBT, (c) one TriCDBT and (d) one TeCDBT isomer.

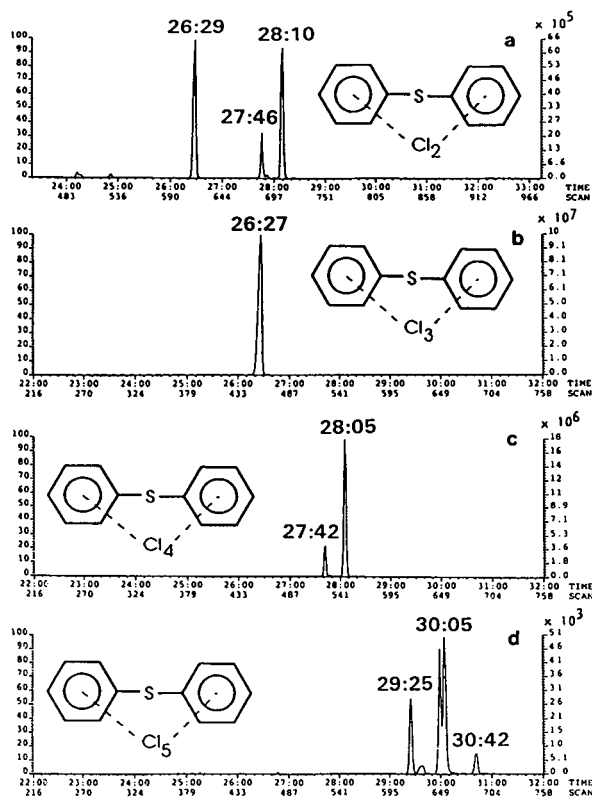


Fig. 4. SIM chromatograms of the chlorination mixture of DPS with the exact m/z values of the $(M+2)^+$ ions of (a) DiCDPSs (m/z 253.9724), (b) TriCDPSs (m/z 289.9305), (c) TeCDPSs (m/z 323.8915) and (d) PeCDPSs (m/z 357.8525).

(m/z 357.8525). The scales of the ion intensities in the chromatograms are different so the concentrations of the compounds cannot be directly compared using the heights or areas of the peaks.

PCDBTs have also been prepared by reactions of PCBs with sulphur [7–9]. Some PCDPSs have been prepared from chlorobenzenes and sulphur with $AlCl_3$ as catalyst [10]. Some dichlorodimethyldiphenyl sulphides have been prepared similarly from chlorotoluenes. For example, 2-chlorotoluene produced a mixture containing four dichlorodimethyldiphenyl sulphides as the main products and two dichlorodimethyldiphenylsulphides as minor products. Several dichloromethyl sulphides were also found to be formed in small amounts. Additionally, relatively large amounts of some dichlorodimethylthianthrenes and dichlorodimethyldiphenyl disul-

phides were formed. Fig. 5 presents (a) the total ion chromatogram of the synthesis mixture, and EI mass spectra of (b) a dichlorodimethyl diphenylsulfide, (c) a dichlorodimethyldiphenyl disulfide and (d) a dichlorodimethylthianthrene isomer. The mixture could not be fractionated by RP-HPLC with Elsico or Spherisorb columns and acetonitrile–water eluents.

GC-MS. A VG AutoSpec high-resolution mass spectrometer connected to an HP 5890 Series II gas chromatograph was used for GC–full-scan (m/z 50–500) EI–MS of the model compounds. The column was 25 m \times 0.2 mm I.D. HP-5 (0.11 μ m). Helium was used as carrier gas. The temperature program was 100°C (held for 1 min), increased at 20°C/min to 180°C then at 5°C/min to 280°C (held for 15 min). The temperatures were injector 260°C, transfer line 280°C and ion source 260°C. The EI potential was 36 eV.

The EI mass spectra of PCDBTs, PCTAs and PCDPSs all have an intense molecular ion (M^+). The molecular ion and the fragment ions show the typical expected clustering due to chlorine isotopes. The EI mass spectra of PCDBTs show a relatively small $M^+ - 2Cl$ fragment and a smaller $M^+ - Cl$ fragment. Tri- and TeCTAs show strong fragments due to the formation of $M^+ - Cl$ and $M^+ - 2Cl$ ions. PCDPSs show a very strong fragment due to $M^+ - 2Cl$ and a small fragment due to $M^+ - Cl$.

NMR spectroscopy. High-resolution 1H NMR spectroscopy combined with HRMS provides an excellent tool for isomer-specific structure elucidation of substituted aromatics such as DPSS, DBTs and TA [8–10]. Using these methods, three isomeric TriCDPSs, 2,2',4-TriCDPS, 2,4,4'-TriCDPS and 2,4',6-TriCDPS, and two isomeric TeCDPSs, bis(2,4-dichlorophenyl) and bis(3,4-dichlorophenyl) sulphide, have been determined [10]. Further, two isomeric DBTs, 2,3,7,8- and 2,3,6,7-tetramethyl derivatives, and three PCDBTs, 3-chloro-, 1,3-dichloro- and 1,3,4-trichloro derivatives, have been verified in the reaction mixtures. The existence of a thio analogue of the highly toxic 2,3,7,8-tetrachlorodibenzodioxin (TCDD), *viz.*, 2,3,7,8-TeCTA, has also been proposed.

A disadvantage of 1H and even more of ^{13}C

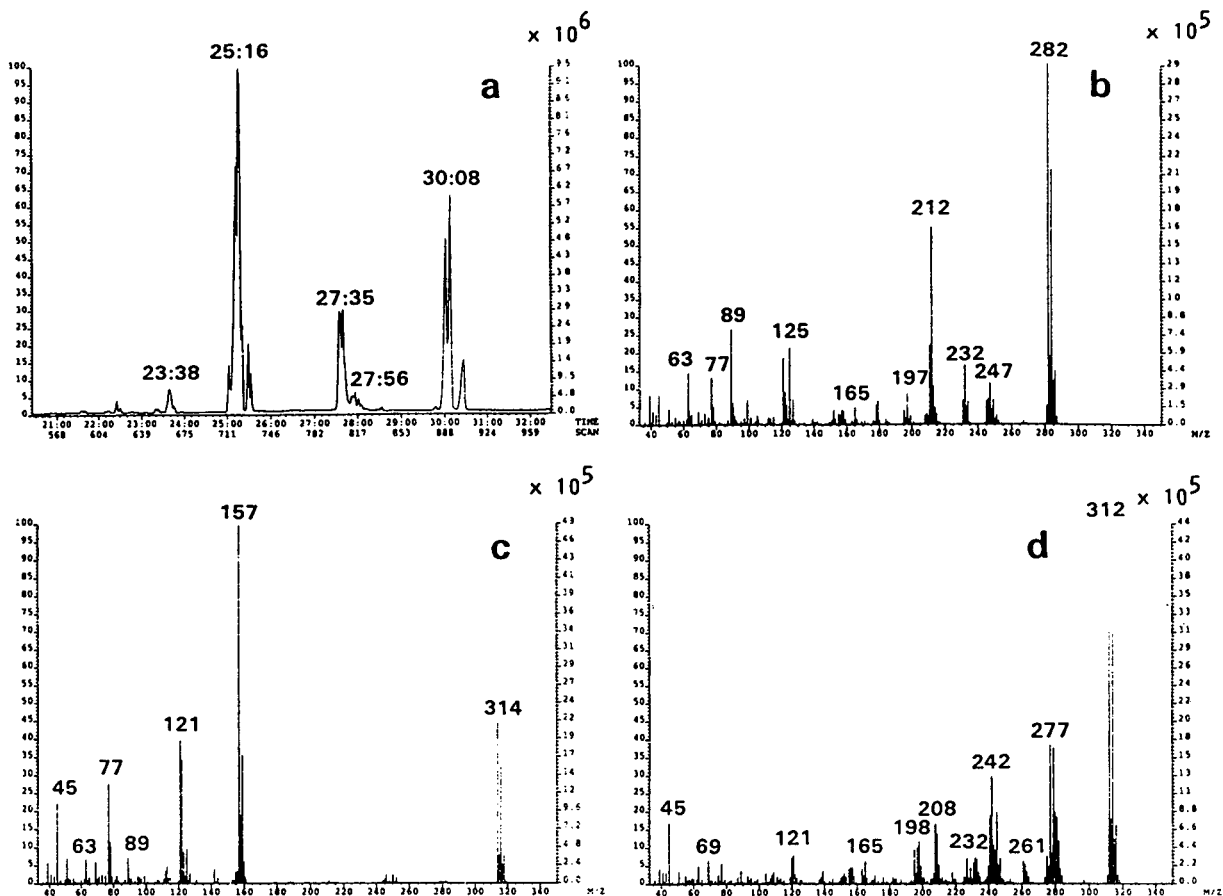


Fig. 5. (a) Total ion chromatogram of the synthesis mixture, and EI mass spectra of (b) a dichlorodimethyldiphenyl sulfide, (c) a dichlorodimethyldiphenyl disulfide and (d) a dichlorodimethylthianthrene isomer.

NMR spectroscopy is their insensitivity in comparison with, *e.g.*, MS or FT-IR spectroscopic methods. This insensitivity can be problematic, because the synthetic scale and concentrations of these potentially harmful compounds should be maintained as low as possible. In addition, interferences to NMR resonances from solvent and/or impurity signals may strongly disturb the reliable detection and analysis of the NMR spectra. Therefore, the selection of the measuring conditions and especially choosing a suitable solvent and minimizing its amount are of extreme importance.

The method developed for terpenoid type off-flavour compounds [12] was used. By this means, a ^1H NMR spectrum of *ca.* 5 μg of mono-terpenoid compound collected directly in the NMR solvent by preparative GC could be mea-

sured reliably. In order to decrease the solvent volume from 700 μl (a recommended amount in a standard 5 mm O.D. NMR tube) to 100 μl , a thick-wall (5 mm O.D., 2 mm I.D.) sample tube was selected for these measurements. By using special spherically shaped ampoules the volume of the solvent can be further decreased. A special ^1H high-sensitivity probe head available for the JEOL GSX-270 FT-NMR spectrometer was used. In some instances subtraction of the solvent signal also gave good results.

For the aromatic sulphur compounds studied, $\text{C}_2\text{H}_2\text{Cl}_2$ was found to be a suitable medium, because its ^1H NMR signal is located at 5.30 ppm from tetramethylsilane (TMS). Consequently, it does not overlap with either the ^1H NMR lines of aromatic protons, which resonate characteristically at δ 6.9–8.9 ppm [1–3], or with

the aryl-bound methyl signals, which resonate at δ 2.3–2.5 ppm [2] from TMS. Similarly, $C^{2}H_2Cl_2$ can be used in ^{13}C NMR spectroscopy, hence its resonance pattern does not interfere with the signals of aromatic carbons and aryl-bound methyls under any conditions or in any neutral derivative concerned.

1H NMR spectral assignment was mainly based on the synthetic procedure used, symmetry considerations of possible products and characteristic intra-aromatic couplings. The 1H NMR parameters refined by computer-assisted iterations [13]. In ^{13}C NMR spectral assignment, the substituent chemical shifts were generally utilized.

Preparation of stack gas samples

The four stack gas samples from waste incineration were originally prepared for the determination of polychlorinated dibenzo-*p*-dioxins and dibenzofurans at the Institute for Environmental Research in Jyväskylä and were kindly given to us for the determination of the chlorinated sulphur compounds. These compounds have been found to enter the dioxin fraction in the analysis process [3,4,10].

Two of the samples contained gas phase and particles (samples 2 and 4) and two only particles (samples 1 and 3). The volume of the gas phase was 3.5 N m³ (0°C, 101.3 kPa). The particle phase was extracted with toluene for 48 h and treated with sulphuric acid and the dioxin fraction was isolated by column chromatography with basic alumina and activated carbon [14]. $^{13}C_{12}$ -labelled 2,3,7,8-TeCDD (12.5 ng/per sample), which was used as an internal standard in the dioxin analysis, was added to all samples before extraction.

HRGC–HRMS of the samples

The same VG AutoSpec high resolution mass spectrometer that was used to measure full-scan EI mass spectra was used in the HRGC–HRMS analysis of the stack gas samples. The same GC and MS conditions were utilized.

Because of the complexity of the fractions analysed, the resolution was normally kept at 20 000 (5% valley) to eliminate interfering com-

TABLE I
EXACT m/z VALUES OF M^+ AND $(M+2)^+$ IONS USED IN THE HRGC–SIM–HRMS ANALYSIS

Compound	Formula	M^+	$(M+2)^+$
TeCDD	$C_{12}H_4O_2Cl_4$	319.8965	321.8937
PeCDD	$C_{12}H_3O_2Cl_5$	353.8576	355.8547
TriCDBT	$C_{12}H_5S_2Cl_3$	285.9178	287.9148
TeCDBT	$C_{12}H_4S_2Cl_4$	319.8788	321.8758
PeCDBT	$C_{12}H_3S_2Cl_5$	353.8398	355.8369
TriCTA	$C_{12}H_5S_2Cl_3$	317.8898	319.8869
TeCTA	$C_{12}H_4S_2Cl_4$	351.8509	353.8479
PeCTA	$C_{12}H_3S_2Cl_5$	385.8119	387.8089
TriCDPS	$C_{12}H_7S_2Cl_3$	287.9334	289.9305
TeCDPS	$C_{12}H_6S_2Cl_4$	321.8944	323.8915
PeCDPS	$C_{12}H_5S_2Cl_5$	355.8555	357.8525

pounds or fragments of compounds with higher molecular mass. For example, the exact mass of the $(M+2)^+$ ion of TeCTA is 353.8479 and that of the M^+ ion of pentachlorodioxin 353.8398, so a resolution near 44 000 is needed for the separation of these two ions. The TeCTAs and PeCDDs had close retention times under the GC–MS conditions used.

Selected ion monitoring was done with the m/z values of M^+ and $(M+2)^+$ ions for TeCDDs, PeCDDs, TeCDBTs, PeCDBTs, TriCTAs, TeCTAs, PeCTAs, TriCDPSs, TeDPSs and PeCDPSs. The exact values for the M^+ and $(M+2)^+$ ions of tri-, tetra- and pentachlorinated compounds used in the HRGC–SIM–HRMS analysis were calculated by the Opus Version I.6 isotope program of the Fisons Instruments V6 Analytical Autospec mass spectrometer. The values are given in Table I.

RESULTS AND DISCUSSION

The results from the HRGC–SIM–HRMS analyses are given in Table II. Rough quantitative estimations were made by comparing the peak heights of the compounds under investigation with that of the $^{13}C_{12}$ -labelled 2,3,7,8-TeCDD. The knowledge of the MS fragmentation of PCDDs and PCTAs was applied in their quantification.

TABLE II

RESULTS OF DETERMINATION OF THE COMPOUNDS IN THE SAMPLES

Concentrations of individual isomers (ng per sample) with number of isomers in parentheses.

Compound	Sample 1	Sample 2	Sample 3	Sample 4
TeCDBT	14 (1)	7–69 (10–15)	n.d. ^a	5–63 (15–20)
PeCDBT	n.d.	1–5 (10–15)	n.d.	1–5 (15–20)
TriCDPS	0.1–0.3 (3)		n.d.	n.d.
TeCDPS	1.6, 0.5 (2)		n.d.	n.d.
TriCTA	n.d.	n.d.	2.1, 0.9 (2)	n.d.
TeCTA	n.d.	n.d.	1.8, 1.5 (2)	n.d.

^a n.d. = Not detected.

Samples 2 and 4 were found to contain TeCDBTs in relatively high concentrations. The isomer profiles of the TeCDBTs in these two samples were identical. About twenty resolved isomers could be seen. The real number of isomers in the samples may be greater owing to unresolved peaks. The number of possible TeCDBT isomers is 38. The total concentration of all TeCDBTs seems to be nearly equal to the total concentration of all TeCDDs, even though the concentrations of individual TeCDBT isomers is about one tenth of the concentration of the most abundant TeCDD isomer.

Fig. 6 shows the SIM chromatograms of sample 2 with the values for the $(M+2)^+$ ions of (a) TeCDBTs (321.8758) and (b) TeCDDs (321.8937).

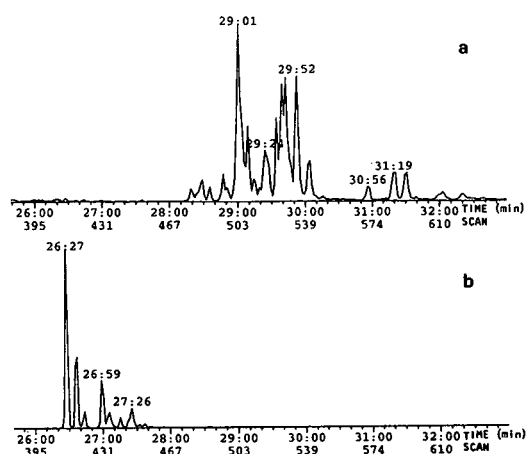


Fig. 6. SIM chromatograms of sample 2 with the values for $(M+2)^+$ ions of (a) TeCDBTs (321.8758) and (b) TeCDDs (321.8937).

(321.8937). With the ions used to analyse PeCDBTs there were many interfering peaks in sample 2. There were some peaks with the correct $M^+/(M+2)^+$ peak ratios in the retention window of the PeCDBTs, but these peaks could not be unambiguously ascertained to be pure PeCDBT isomers. The situation was the same with HeCDBTs. Sample 1 contained one TeCDBT isomer but no PeCDBTs. Neither TeCDDs nor PeCDDs could be found this sample. Sample 3 did not contain any TeCDBTs or PeCDBTs. TeCDDs could be found in very low concentrations, but no PeCDDs were detected.

The PCDPs have been determined previously in the same stack gas samples [10]. Some Tri- and TeCDPSs were found.

With the m/z values of 317.8898 and 319.8869 for TriCTAs, 351.8509 and 353.8479 for TeCTAs and 385.8119 and 387.8089 for PeCTAs, the interpretation of the chromatograms was difficult because of many interfering peaks in the same retention time range as for the compounds studied. Relatively large interfering peaks with these ions appeared in the retention time range 30–36 min. The origin of these peaks could not be elucidated. It is possible that they originate as fragment ions from some kind of larger chlorinated compounds. For example, when samples, that contain PCDBTs are analysed it must be taken into account that for the separation of the $(M+2)^+$ ion for TriCTA (319.8869) from the M^+ ion for TeCDBT (319.8788) a resolution near 40 000 (39 500) in MS is needed. Some isomers of the TriCTAs and TeCDBTs were

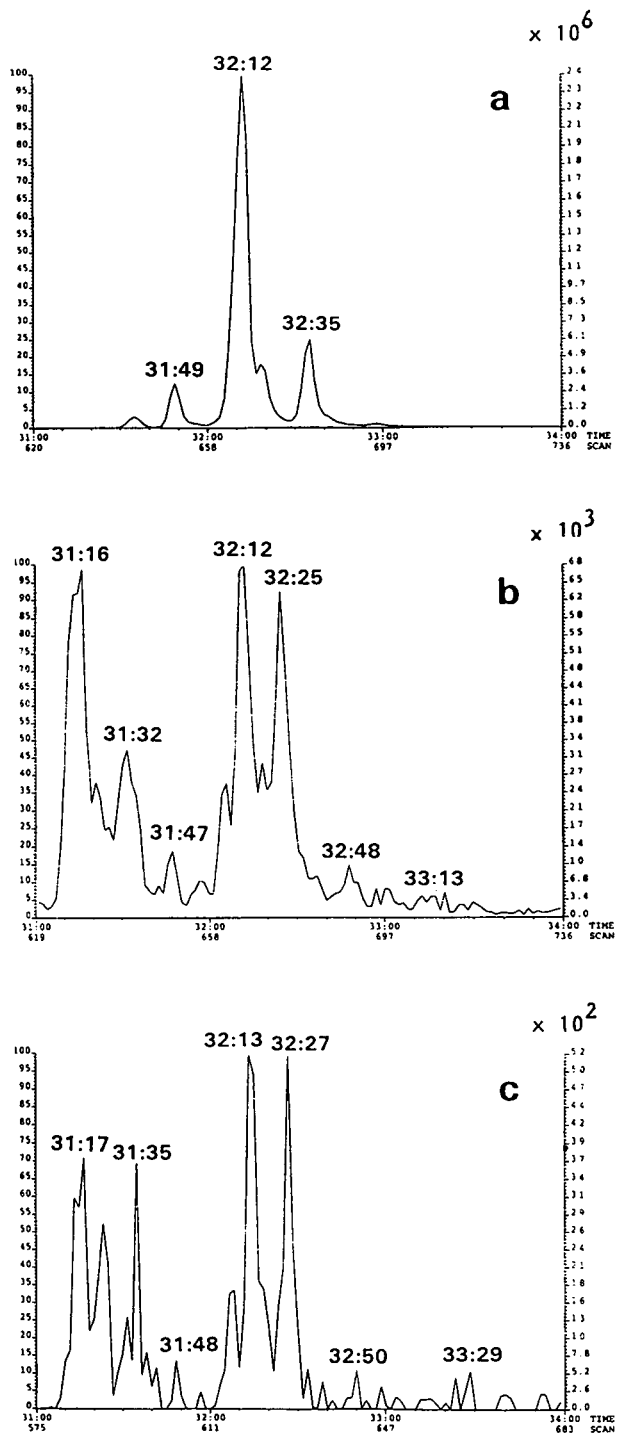


Fig. 7. SIM chromatograms of (a) the chlorination mixture of TA, (b) sample 4 with the value of the $(M+2)^+$ ion of TeCTAs (353.8479) and (c) sample 4 with the value of the M^+ ion of PeCDBTs (353.8398).

eluted simultaneously in GC under these conditions. The situation was the same with PeCDBTs and TeCTAs and probably also with the corresponding higher chlorinated isomers. Fig. 7 presents the SIM chromatograms of (a) the chlorination mixture of TA, (b) sample 4 with the value of the $(M+2)^+$ ion of TeCTAs (353.8479) and (c) sample 4 with the value of the M^+ ion of PeCDBTs (353.8398). This makes it impossible to use the ratios $M^+/(M+2)^+$ for the unambiguous identification of these compounds. However, the $M^+/(M+2)^+$ ratios for the TeCDBTs and PeCDBTs were so close to the theoretically correct values that it can be concluded that if there are any Tri-, Te- or PeCTAs in the samples their concentrations are very low compared with the concentrations of the PCDBTs. However, sample 3, which did not contain any TeCDBTs or PeCDBTs, is suspected to contain at least two TriCTA isomers with the correct retention times and the correct $M^+/(M+2)^+$ ratio for trichlorinated compounds. In sample 3 there could also be seen small peaks with the m/z values of the M^+ and $(M+2)^+$ ions of TeCTAs with a retention time very close to that of 2,3,7,8-TeCTA. The $M^+/(M+2)^+$ ratio was also typical for tetrachlorinated compounds. For a more reliable analysis of PCTAs from this kind of sample, however, more purification is needed even if an MS resolution of more than 20 000 is used.

REFERENCES

- 1 H.-R. Buser and C. Rappe, *Anal. Chem.*, 63 (1991) 1210–1217.
- 2 H.-R. Buser, I.S. Dolezar, M. Wolfensberger and C. Rappe, *Environ. Sci. Technol.*, 25 (1991) 1637–1643.
- 3 S. Sinkkonen, J. Paasivirta, J. Koistinen and J. Tarhanen, *Chemosphere*, 23 (1991) 583–587.
- 4 S. Sinkkonen, J. Paasivirta, J. Koistinen, M. Lahtiperä and R. Lammi, *Chemosphere*, 24 (1992) 1755–1763.
- 5 B. Ahling and A. Lindskog, in O. Hutzinger, R.W. Frei, E. Merian and F. Pocchiari (Editors), *Chlorinated Dioxins and Related Compounds*, Pergamon Press, New York, 1982, 215–225.
- 6 K. Olie, P.L. Vermeulen and O. Hutzinger, *Chemosphere*, 6 (1977) 455–459.
- 7 S. Sinkkonen and J. Koistinen, *Chemosphere*, 21 (1990) 1161–1171.
- 8 S. Sinkkonen, E. Kolehmainen and J. Koistinen, *Int. J. Environ. Anal. Chem.*, 47 (1992) 7–20.

- 9 S. Sinkkonen, E. Kolehmainen, K. Laihia and J. Koistinen, *Int. J. Environ. Anal. Chem.* in press.
- 10 S. Sinkkonen, E. Kolehmainen, K. Laihia, J. Koistinen and T. Rantio, *Environ. Sci. Technol.*, in press.
- 11 H.E. Buckholtz, *U.S. Pat.*, 3 989 715 (1976).
- 12 A. Veijanen, E. Kolehmainen, R. Kauppinen, M. Lahtiperä and J. Paasivirta, *Water Sci. Technol.*, 25 (1992) 165–170.
- 13 R. Laatikainen, *J. Magn. Reson.*, 27 (1977) 169–180.
- 14 J. Tarhanen, J. Koistinen, J. Paasivirta, P.J. Vuorinen, J. Koivusaari, I. Nuuja, N. Kannan and R. Tatsukawa, *Chemosphere*, 18 (1989) 1067–1077.

Capillary gas chromatography of acidic non-steroidal antiinflammatory drugs as *tert.*-butyldimethylsilyl derivatives

Kyoung-Rae Kim*, Wean-Hee Shim and You-Jin Shin

College of Pharmacy, Sungkyunkwan University, Suwon 440-746 (South Korea)

Jongsei Park, Seoungwon Myung and Jongki Hong

Doping Control Centre, Korea Institute of Science and Technology, P.O. Box 131, Cheongryang, Seoul (South Korea)

(First received September 29th, 1992; revised manuscript received March 15th, 1993)

ABSTRACT

The quantitative conversion of 26 acidic non-steroidal anti-inflammatory drugs (NSAIDs) simultaneously to their corresponding *tert.*-butyldimethylsilyl (TBDMS) derivatives in a single step was examined. The NSAIDs dissolved in triethylamine were silylated with *N*-methyl-*N*-(*tert.*-butyldimethylsilyl)trifluoroacetamide in isooctane at room temperature for 30 min and subsequently analysed by capillary gas chromatography and gas chromatography–mass spectrometry. The TBDMS derivatives were eluted as untailed sharp peaks and the characteristic $[M - 57]^{+}$ ions in the mass spectra permitted their rapid confirmation. The temperature-programmed retention index (*I*) sets measured on a DB-5 and DB-17 dual-capillary column system were characteristic of each NSAID to be used for the rapid identification by computer *I* matching. The derivatization yields of the NSAIDs studied were linear in the range 10–120 μ g with high overall precisions. The method provided simultaneous screening and accurate confirmation of each drug when applied to serum samples spiked with NSAIDs.

INTRODUCTION

The many acidic non-steroidal anti-inflammatory drugs (NSAIDs), which are monocarboxylic aromatic acids, constitute the principal class of agents for controlling the pain and inflammation of rheumatic diseases. The carboxylated NSAIDs include salicylates, acetic acids, propionic acids and fenamates.

The simultaneous detection and identification of these NSAIDs is a commonly encountered problem for the systematic screening especially in general unknown cases [1–6]. In the literature, high-performance liquid chromatography

(HPLC) [1,3,4,6] has been extensively employed with a few gas chromatographic (GC) methods [2,5,6] for this purpose. However, it is well known that GC is more suitable for qualitative and quantitative multi-component analyses because of its inherent high resolution, sensitivity and precision compared with HPLC. In the analyses of essential oils, drugs and organic acids, GC peaks are routinely identified by comparing their characteristic retention index (*I*) sets with reference values measured on columns of different polarity [7–11].

GC analyses of the carboxylated NSAIDs require an appropriate derivatization procedure and mainly methylation with hazardous diazomethane has been used to convert the carboxyl functions into the corresponding methyl

* Corresponding author.

esters [2,5]. In recent years, *tert.*-butyldimethylsilyl (TBDMS) derivatization of carboxyl functions has been widely used [10–16], principally because of the high hydrolytic stability and superior GC and mass spectrometric (MS) properties of the TBDMS derivatives [12,17]. However, no report on the application of TBDMS derivatization to the NSAIDs has been published. Previously, we reported the simultaneous TBDMS derivatization of volatile and non-volatile organic acids [16].

If systematic screening for NSAIDs is to be used routinely in forensic and clinical chemistry laboratories, a simple and rapid GC profiling method that can identify the most commonly used NSAIDs in a single analysis must be developed.

As the first step towards that goal, this study was undertaken to investigate the optimum conditions for converting 26 carboxylated NSAID mixture simultaneously into their corresponding TBDMS derivatives in a single step, rapidly and quantitatively. The structures of the TBDMS derivatives which are new to the literature were confirmed by GC–MS.

EXPERIMENTAL

Materials

Standards of the NSAIDs studied were obtained from Sigma (St. Louis, MO, USA) and various pharmaceutical companies. The silylating reagent, *N*-methyl-*N*-(*tert.*-butyldimethylsilyl)trifluoroacetamide (MTBSTFA) was obtained from Pierce (Rockford, IL, USA), triethylamine (TEA) from Aldrich (Milwaukee, WI, USA) and *n*-alkane standards (C₁₆–C₃₆, even numbers only) from Polyscience (Niles, IL, USA). All other chemicals were of analytical-reagent grade and used as received.

NSAID solutions and internal standard solutions

NSAID solutions containing NSAIDs in their free acid forms, 10 µg/µl in methanol or acetone, were used as stock solutions. *n*-Hexacosane or *n*-octacosane used as the internal standard (I.S.) was dissolved in isooctane at a concentration of 1 µg/µl.

tert.-Butyldimethylsilylation

An NSAID mixed solution containing 20 µg of each NSAID was evaporated to dryness under a gentle stream of nitrogen at 50°C after adding 10 µl of I.S. solution. To the residue were added 10 µl of TEA, 10 µl of MTBSTFA and 30 µl of isooctane, and the mixture was vortex mixed to form TBDMS derivatives. The reaction mixture was directly examined by GC and GC–MS. The effects of TEA addition and heating at 60°C on the derivative yields were investigated. The derivative yield curves were prepared by plotting the heating time against the peak-area ratio of NSAID to the internal standard. The standard samples for constructing the calibration graphs were prepared with four NSAID standard solutions containing 10, 20, 60 and 120 µg of each NSAID and 40 µg of internal standard.

TABLE I
ACIDIC NON-STEROIDAL ANTI-INFLAMMATORY DRUGS STUDIED

Group	NSAID (abbreviation)
Salicylates	Acetylsalicylic acid (ASA) Diflunisal (DFN) Salicylic acid (SCA)
Acetic acids	Alclofenac (ACF) Diclofenac (DCF) Fenclofenac (FCF) Fentiazac (FTZ) Indomethacin (IMC) Lonazolac (LNZ) Sulindac (SLD) Tolmetin (TMT) Zomepirac (ZPR)
Propionic acids	Fenoprofen (FPE) Flurbiprofen (FBF) Ibuprofen (IBF) Indoprofen (IPF) Ketoprofen (KPF) Naproxen (NPX) Pirprofen (PPF) Suprofen (SPF) Tiaprofenic acid (TPA)
Fenamates	Flufenamic acid (FFA) Flunixin (FNX) Mefenamic acid (MFA) Niflumic acid (NFA) Tolfenamic acid (TFA)

Sample preparation

A 200- μ l volume of serum spiked with NSAIDs at 100 ppm was acidified to pH 1.0 with sulphuric acid and saturated with sodium chloride. It was then extracted with diethyl ether (4 \times 1 ml). The collected ether layers were evaporated to dryness at 50°C under a stream of nitrogen. The residue was subjected to derivatization, as described above.

Gas chromatography

GC analyses were conducted with a Pye Unicam (Cambridge, UK) GCV gas chromatograph equipped with a flame ionization detector and interfaced to a Shimadzu (Kyoto, Japan) C-R 2AX data processor. A DB-1 (J & W Scientific, Rancho Cordova, CA, USA) fused-silica capillary column (13 m \times 0.25 mm I.D.; 0.25 μ m film thickness) was used. Nitrogen at a flow-rate of

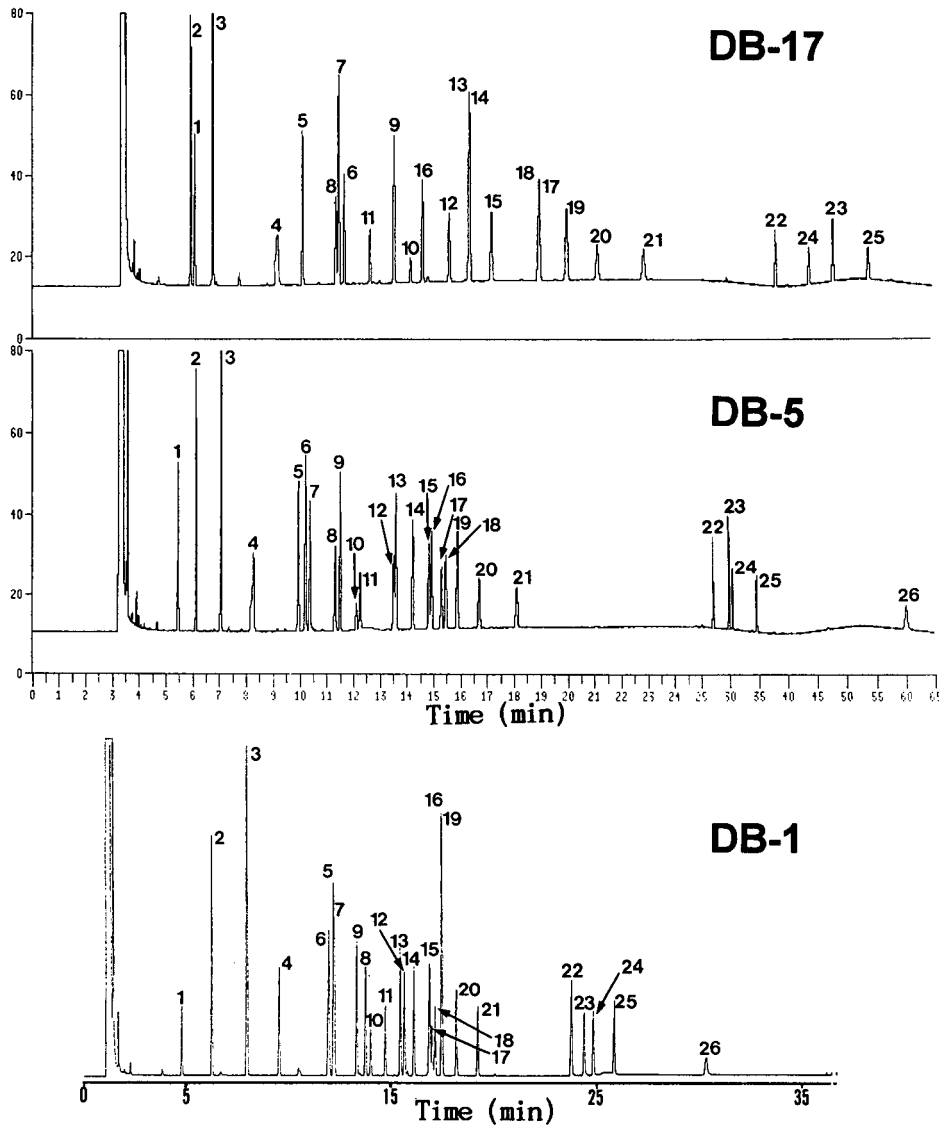


Fig. 1. Chromatograms of the mixture of 26 NSAIDs as their TBDMS derivatives separated on DB-1 (13 m \times 0.25 mm I.D.), DB-5 (30 m \times 0.25 mm I.D.) and DB-17 (30 m \times 0.25 mm I.D.) fused-silica capillary columns. Peak numbers correspond to the numbers in Table II. GC conditions are given in the text.

0.7 ml/min was used as the carrier gas, and 0.5- μ l aliquots of samples were injected with a splitting ratio of 10:1. After an initial hold time of 3 min at 170°C, the oven temperature was programmed to 280°C at a rate 5°C/min. The injector and detector temperatures were 280 and 300°C, respectively.

GC analyses for the retention index (*I*) measurements and dual-capillary profiling analysis were performed with a Hewlett-Packard HP 5890A gas chromatograph, equipped with a split/

splitless inlet system, two flame ionization detectors, and an HP 3392A integrator and interfaced to an HP 5895A GC ChemStation (Hewlett-Packard, Avondale, PA, USA) on dual DB-5 (30 m \times 0.25 mm I.D.; 0.25 μ m film thickness) and DB-17 (30 m \times 0.25 mm I.D.; 0.25 μ m film thickness) fused-silica capillary columns (J & W Scientific). After an initial hold time of 2 min at 230°C, the oven temperature was programmed to 280°C at a rate of 4°C/min. A standard solution of *n*-alkanes (C₁₆–C₃₆, even numbers only) in

TABLE II

GAS CHROMATOGRAPHIC AND MASS SPECTRAL DATA FOR TBDMS DERIVATIVES OF NSAIDS

No.	NSAID	GC <i>I</i> ^a data set		Mass spectral data set ^b						
		DB-5	DB-17	[M] ⁺	[M – 57] ⁺	[M – 15] ⁺	[M – 131] ⁺	[M – 159] ⁺	Other ions	
1	ASP	1790.8	2058.6	294(0)	237(44)	279(1)	163(2)	135(17)	195(100)	121(8)
2	IBU	1876.5	2039.8	320(0)	263(100)	305(2)	189(0)	161(2)	75(11)	73(7)
3	SCA	1993.5	2149.1	366(0)	309(100)	351(6)	235(1)	207(0)	195(5)	73(21)
4	ACF	2103.0	2388.1	340(0)	283(100)	325(1)	209(0)	181(1)	75(21)	242(12)
5	FFA	2258.4	2587.4	395(35)	338(100)	380(3)	264(23)	236(1)	244(27)	222(16)
6	FPF	2239.9	2466.7	356(0)	299(100)	341(1)	225(0)	197(2)	75(24)	73(10)
7	FBF	2269.2	2571.0	358(0)	301(100)	343(1)	227(0)	199(2)	75(9)	179(8)
8	NFA	2335.6	2571.0	396(19)	339(100)	381(4)	265(7)	237(1)	245(30)	218(5)
9	NPX	2349.4	2717.3	344(10)	287(100)	329(1)	213(1)	185(11)	75(7)	73(7)
10	PPF	2392.1	2759.3	365(30)	308(100)	350(2)	234(3)	206(36)	306(58)	75(14)
11	FNX	2400.0	2655.4	410(41)	353(73)	395(100)	279(9)	251(8)	239(31)	263(19)
12	MFA	2485.3	2890.1	355(59)	298(100)	340(4)	224(42)	196(1)	223(12)	209(8)
13	KPF	2479.8	2847.9	368(0)	311(100)	353(2)	237(0)	209(0)	295(19)	75(7)
14	FCF	2523.9	2890.1	410(0)	353(100)	395(2)	279(1)	251(1)	75(9)	215(7)
15	TFA	2561.4	2936.1	375(32)	318(100)	360(3)	244(29)	216(1)	209(7)	208(7)
16	DFN	2567.9	2789.7	478(0)	421(100)	463(3)	347(1)	319(0)	73(24)	307(7)
17	TPA	2590.7	3027.5	374(0)	317(100)	359(3)	243(1)	215(2)	73(11)	105(7)
18	DCF	2600.0	3026.4	409(19)	352(100)	394(2)	278(2)	250(1)	75(30)	214(23)
19	SPF	2621.5	3069.1	374(0)	317(100)	359(1)	243(0)	215(1)	75(11)	111(7)
20	TMT	2661.4	3116.2	371(25)	314(92)	356(5)	240(1)	212(31)	119(100)	73(29)
21	ZPR	2729.1	3187.1	405(40)	348(100)	390(3)	274(3)	246(36)	139(43)	73(20)
22	LNZ	3045.1	3559.1	426(4)	369(100)	411(2)	295(5)	267(6)	75(8)	73(5)
23	IPF	3110.3	>3600.0	395(1)	338(100)	380(2)	264(1)	236(15)	73(6)	75(4)
24	FTZ	3123.9	>3600.0	443(7)	386(100)	428(1)	312(4)	284(5)	73(33)	239(13)
25	IMC	3212.0	>3600.0	471(31)	414(38)	456(3)	340(1)	312(21)	139(100)	111(21)
26	SLD	3532.0	nd ^c	470(7)	413(72)	455(20)	339(1)	311(2)	397(100)	73(61)

^a Retention index (*I*) values on DB-5 and DB-17 (30 m \times 0.25 mm I.D., 0.25 μ m film thickness) capillary columns programmed from 230°C (held for 2 min) to 280°C at 4°C/min. Relative standard deviations ranged from 0.01 to 0.05% for three measurements.

^b *m/z* Values with relative abundances of ions (%) in parentheses.

^c Not detected.

isooctane was co-injected with the samples in the split mode (30:1). All samples were analysed in triplicate.

Gas chromatography–mass spectrometry

A Hewlett-Packard HP 5890A gas chromatograph, interfaced to an HP 5970B mass-selective detector (70 eV, EI mode) which was coupled

on-line to a HP 59940A MS ChemStation system, was used with an HP-1 cross-linked capillary column (12 m × 0.20 mm I.D.; 0.33 μm film thickness) to obtain mass spectra. Samples were introduced in the split injection mode (30:1) at 260°C, and the oven temperature was initially 180°C and then programmed to 280°C at 20°C/min. The interface and ion source temperatures were 300 and *ca.* 250°C, respectively. The

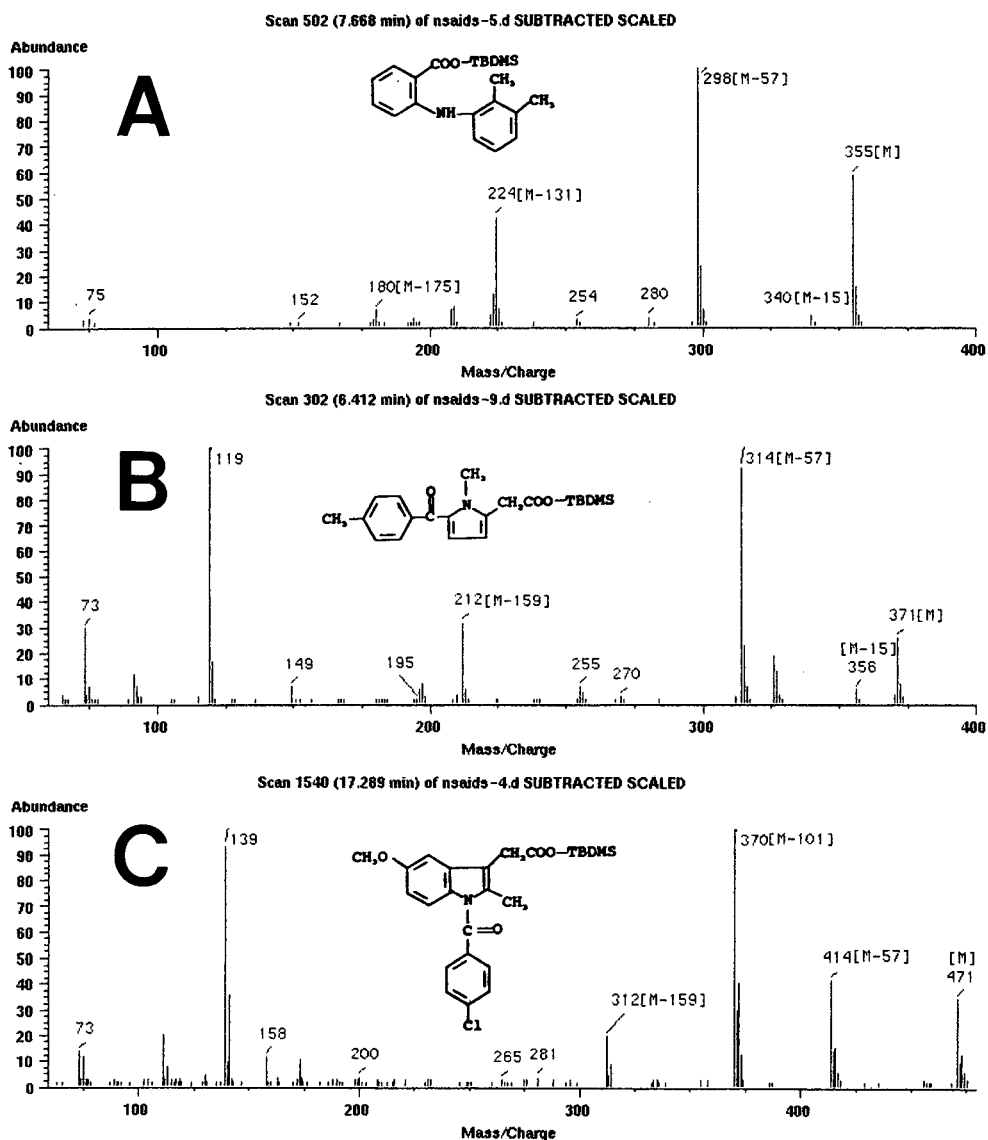


Fig. 2. Electron impact mass spectra of TBDMS derivatives of (A) mefenamic acid, (B) tolmetin and (C) indomethacin.

mass range scanned was from 60 to 500 u at a rate of 1.29 scans/s.

RESULTS AND DISCUSSION

The TBDMS derivatization of the NSAIDs and their metabolites offer advantages over methylation, as the carboxyl groups and any protic polar groups if present are all converted into TBDMS derivatives which generate diagnostically useful $[M-57]^+$ ions in their mass

spectra. The 26 NSAIDs examined in this study are listed in Table I.

On reaction with the silylating reagent, MTBSTFA, in isoctane, all the compounds converted into single TBDMS derivatives. The separation of the 26 NSAIDs as TBDMS derivatives on three different fused-silica capillary columns is presented in Fig. 1. Each NSAID derivative displayed a single symmetrical peak. On the short non-polar DB-1 column, no resolutions were achieved between flufenamic acid

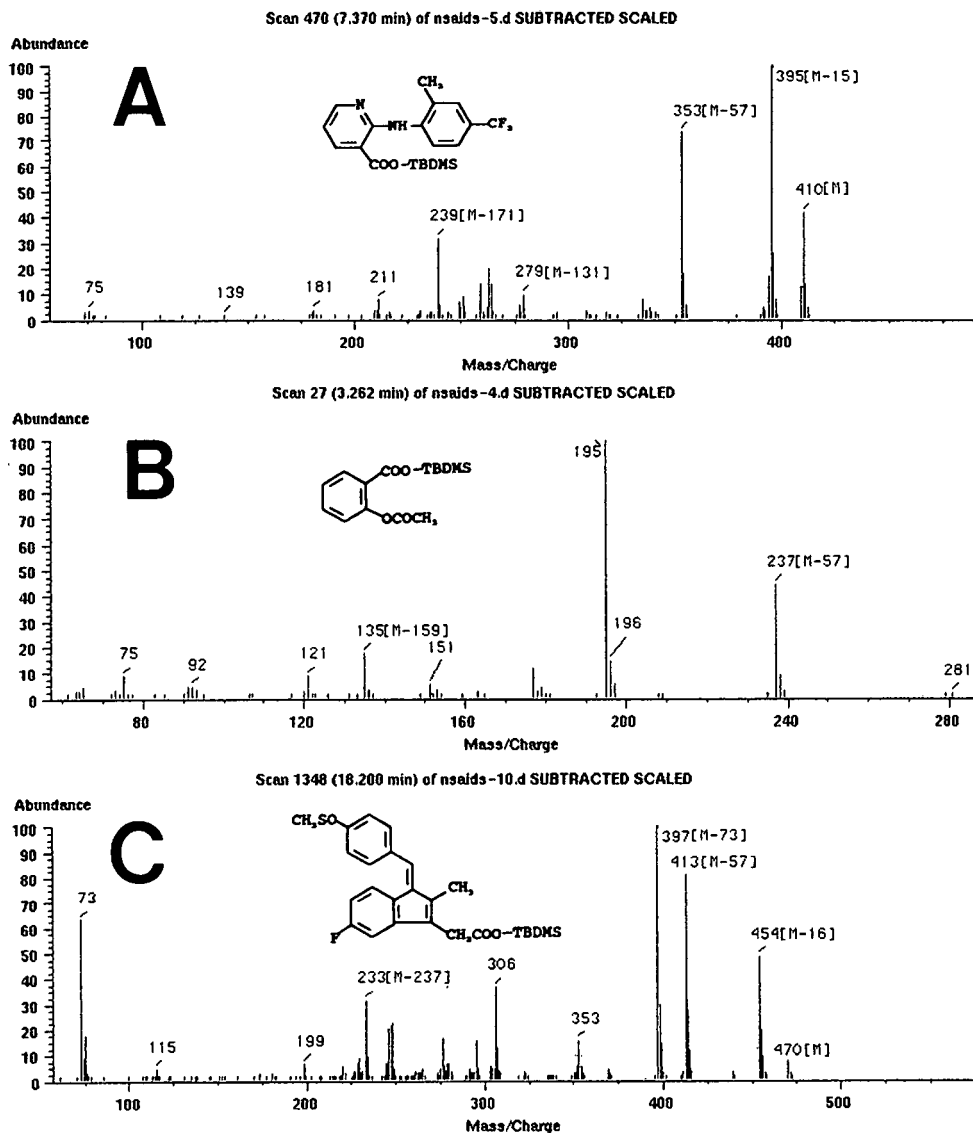


Fig. 3. Electron impact mass spectra of TBDMS derivatives of (A) flunixin, (B) aspirin and (C) sulindac.

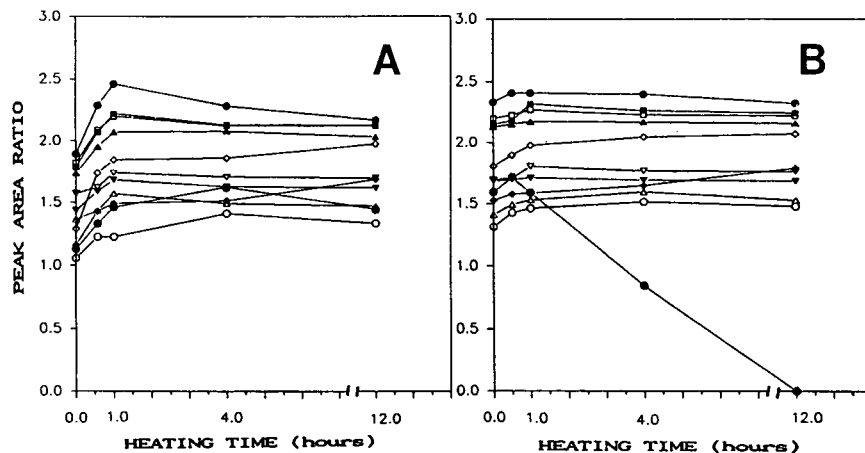


Fig. 4. Effect of heating at 60°C (A) without and (B) with addition of triethylamine on the derivative yields for (●) ibuprofen, (▽) alclofenac, (▼) fenoprofen, (□) flubiprofen, (■) naproxen, (△) niflumic acid, (▲) ketoprofen, (◇) mefenamic acid, (◆) lonazolac, (○) indomethacin and (*) tiaprofenic acid. The peak-area ratio of each NSAID to the internal standard is plotted against heating time.

and flurbiprofen, between diflunisal and suprofen or between tolfenamic acid, tiaprofenic acid and diclofenac, whereas they were well resolved on the longer DB-5 column. On the non-polar DB-5 column, no resolutions between mefenamic acid and ketoprofen or between tolfenamic acid and diflunisal were observed, but they were well separated on the medium-polarity DB-17 column. Ketoprofen and tiaprofenic acid co-eluted with fenclofenac and diclofenac, respectively, on DB-17, but were well resolved on the DB-5 column. Sulindac was not eluted from the DB-17 column.

Temperature-programmed retention index (I) sets for each derivative measured on both columns are given in Table II. The I sets were characteristic of each NSAID, thus being useful for the rapid identification by the computer I library matching as described in our organic acid profiling work [10].

The derivatives were subjected to GC-MS for the confirmation of their structures, which are new to the literature. All the monocarboxylic NSAIDs were converted into monoTBDMS derivatives with the exception of salicylic acid and diflunisal, which possess one phenolic hydroxyl group and formed bisTBDMS derivatives. The electron-impact MS data are summarized in Table II.

As is characteristic of the TBDMS derivatives [12–17], the intense $[M - 57]^+$ ions formed by the loss of the labile *tert.*-butyl function, together with weak $[M - 15]^+$, $[M - 131]^+$ and $[M - 159]^+$ ions generated by the losses of CH_3 , OTBDMS and COOTBDMS from the molecular ions, respectively, were useful for the structural confirmation of each NSAID.

$[M - 57]^+$ ions constitute the base peaks for most NSAIDs and the molecular ions are intense for the NSAIDs having two aromatic rings with a few exceptions, as exemplified by the mass spectrum of mefenamic acid (Fig. 2A). The base peaks at m/z 119 of tolmetin (Fig. 2B) and at m/z 139 of indomethacin (Fig. 2C) are formed by the preferential cleavage of the bond between CO and the pyrrole ring and the bond between CO and the indole ring, respectively.

For flunixin the ion at m/z 395 formed by the loss CH_3 from the molecular ion constitutes the base peak while the base peaks at m/z 195 of aspirin and at m/z 397 of sulindac appear to represent the losses of CH_2CO and CH_4 from the $[M - 57]^+$ ions, respectively, as shown in Fig. 3.

In a previous study [16], we established that the addition of triethylamine (TEA) improves the overall precision of the simultaneous TBDMS derivatization of volatile and non-vol-

TABLE III
LINEAR REGRESSION ANALYSIS FOR THE
CALIBRATION GRAPHS OF NSAIDS AS THEIR
TBDMS DERIVATIVES

NSAID	Regression line ^a		Correlation coefficient, <i>r</i>
	<i>m</i>	<i>b</i>	
ASA	0.009	-0.020	0.9999
IBU	0.035	0.048	0.9997
ACF	0.026	-0.051	0.9995
FPF	0.024	0.030	0.9999
FFA	0.030	-0.060	0.9993
FBF	0.029	0.018	0.9999
NPX	0.034	-0.065	0.9994
NFA	0.020	0.004	0.9999
PPF	0.026	-0.057	0.9993
FNX	0.013	0.009	0.9999
KPF	0.034	-0.054	0.9996
MFA	0.028	0.009	0.9998
FCF	0.027	-0.042	0.9997
DCF	0.022	-0.045	0.9992
SPF	0.029	-0.061	0.9995
TFA	0.024	0.022	0.9998
IPF	0.024	-0.002	0.9999
DFN	0.028	0.014	0.9999
ZPR	0.015	0.012	0.9999
LNZ	0.020	0.028	0.9993
IMC	0.016	0.028	0.9996
TPA	0.028	0.008	0.9999
TMT	0.026	-0.019	0.9999
FTZ	0.024	0.018	0.9998
SLD	0.016	-0.010	0.9999

^a *m* = Slope = relative mass response = mean peak-area ratio of NSAID × mass of I.S./mass of NSAID; *b* = *y*-intercept.

atile organic acids. When the effects of TEA and heating at 60°C on the silylation of NSAIDs were tested, similar trends were obtained as shown by the derivative yield curves for eleven NSAIDs in Fig. 4.

Without TEA addition, the derivatization of most NSAIDs went to completion on heating for 4 or 12 h (Fig. 4A). For ibuprofen, its response began to reduce when heated over 1 h. When TEA was added (Fig. 4B), the reaction was nearly complete (>95%) on mixing at room temperature, with the exception of NSAIDs containing carboxyl functions which are sterically hindered or near to an electron-withdrawing heterocyclic ring, such as mefenamic acid, niflumic acid, lonazolac and indomethacin. They

required heating for more than 1 h to obtain the higher derivative yields. Tiaprofenic acid, however, started to give an abruptly reduced response when heated for longer than 30 min.

When reacted at room temperature for 30 min without heating in the presence of TEA, the overall derivative yields were satisfactory. Under this condition, the TBDMS derivatization of the 26 NSAID mixtures was examined for the precision and linearity of the calibration graphs. Linear responses in the range 10–20 µg were obtained with correlation coefficients varying from 0.9992 to 0.9999 (Table III). The relative standard deviations (*n* = 3) ranged from 0.1 to 10.0%, but in most instances they were lower than 5%, except for the inherently unstable aspirin. The overall reproducibility appears to be satisfactory for the quantification of NSAIDs. The TBDMS derivatives were stable for at least 2 months when stored at 4°C, with the exception of aspirin, which was gradually converted into stable salicylic acid.

We added the data sets of the NSAIDs listed in the Table II to our own TBDMS reference libraries [10] built in the GC and MS ChemStations for the rapid peak identification of unknown NSAIDs in screening work, and the libraries will continue to be expanded to include the major metabolites and other acidic NSAIDs.

The present derivatization and dual-capillary profiling analysis were applied to serum samples spiked with various NSAIDs. Simultaneous screening and accurate confirmation of the 26 NSAIDs could be achieved, as exemplified in Fig. 5.

CONCLUSIONS

A significant advantage of the present silylation with MTBSTFA in isooctane after TEA addition over methylation is that the carboxylated NSAIDs are simultaneously converted in a single step into the corresponding stable TBDMS derivatives, which generate diagnostically useful $[M - 57]^+$ ions in their mass spectra. The rapid derivatization process will make this method suitable for routine NSAID screening work. For the selective isolation of trace NSAIDs from biological samples prior to TBDMS derivatiza-

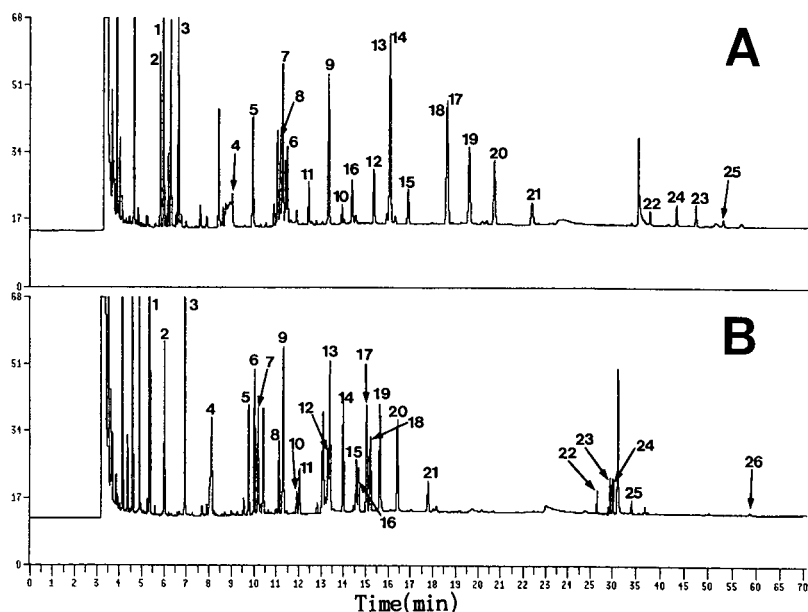


Fig. 5. (A) DB-17 and (B) DB-5 dual-capillary profiling analysis of serum spiked with 26 NSAIDs at 100 ppm. Peak numbers correspond to the numbers in Table II. GC conditions are given in the text.

tion, further investigation of efficient solid-phase extraction is in progress. The extension of the present method to the rapid profiling and screening of NSAIDs at the low concentrations present in biological samples is under way.

ACKNOWLEDGEMENTS

This paper was supported in part by the Korea Science and Engineering Foundation (1988, project number 881-0304-005-2) and in part by the Non-directed Research Fund, Korea Research Foundation, 1992.

REFERENCES

- G.E. Hardee, J.W. Lai and J.H. Morre, *J. Liq. Chromatogr.*, 5 (1982) 1991.
- C. Giachetti, S. Canali and G. Zanolò, *J. Chromatogr.*, 279 (1983) 387.
- H.J. Battista, G. Wehiger and R. Henn, *J. Chromatogr.*, 345 (1985) 77.
- F. Lapique, P. Netter, B. Bannwarth, P. Trechot, P. Gillet, H. Lambert and R.J. Royer, *J. Chromatogr.*, 496 (1989) 301.
- C. Giachetti, G. Zanolò, P. Poletti and F. Perovanni, *J. High Resolut. Chromatogr.*, 13 (1990) 789.
- A.K. Singh, Y. Jang, U. Mishra and K. Granley, *J. Chromatogr.*, 568 (1991) 351.
- B. Newton and R.F. Forey, *J. Anal. Toxicol.*, 8 (1984) 129.
- C. Wurth, A. Kumps and Y. Mardens, *J. Chromatogr.*, 491 (1989) 186.
- N.W. Davies, *J. Chromatogr.*, 503 (1990) 1.
- K.R. Kim, J.H. Kim, H.K. Park and C.H. Oh, *Bull. Korean Chem. Soc.*, 12 (1991) 87.
- K.R. Kim, J.H. Kim, C.H. Oh and T.J. Mabry, *J. Chromatogr.*, 605 (1992) 241.
- A.P.J.M. de Jong, J. Elema and B.J.T. van de Berg, *Biomed. Mass Spectrom.*, 7 (1980) 359.
- T. Cronholm and C. Norsten, *J. Chromatogr.*, 344 (1985) 1.
- D.L. Schooley, F.M. Kubiak and J.V. Evans, *J. Chromatogr.*, 23 (1985) 385.
- T.P. Mawhinney, R.S.R. Robinet, A. Atalay and M.A. Madson, *J. Chromatogr.*, 361 (1986) 117.
- K.R. Kim, M.K. Hahn, A. Zlatis, E.C. Horning and B.S. Middleditch, *J. Chromatogr.*, 468 (1989) 289.
- T.P. Mawhinney and M.A. Madson, *J. Org. Chem.*, 47 (1982) 3336.

Thermodynamic pitfalls in chromatography revisited: supercritical fluid chromatography

Michal Roth

Institute of Analytical Chemistry, Academy of Sciences of the Czech Republic, 61142 Brno (Czech Republic)

(Received January 18th, 1993)

ABSTRACT

Relationships between solute retention in supercritical fluid chromatography and thermodynamic properties of solute transfer from the mobile to the stationary phase are reviewed and illustrated with statistical thermodynamic calculations on a model system. Attention is paid to the effect of sorption of the mobile phase fluid into the stationary phase. The nearly linear plots of $\ln k'$ vs. $1/T$ at a constant density of the mobile phase fluid ("Van 't Hoff plots") are shown to be of little use in themselves for determining the solute transfer properties. Apparent linearity of these plots results from cancellation of thermodynamic anomalies near the critical point of the mobile phase fluid.

INTRODUCTION

The connection between chromatographic retention and standard thermodynamic properties of sorption was discussed by James *et al.* in a classical but topical paper [1] entitled "Thermodynamic pitfalls in gas chromatography", to which the title of the present contribution makes a deliberate reference. James *et al.* emphasized that, in the equation for the standard molar Gibbs energy of sorption,

$$\Delta G_{sp}^0 = -RT \ln K \quad (1)$$

where R is the molar gas constant and T is the absolute temperature, K is the thermodynamic equilibrium constant given by the ratio of solute activities in the stationary and the mobile phase. The choice of standard states in expressing the activities [2] then determines the physical meaning of ΔG_{sp}^0 and of the derived properties (ΔH_{sp}^0 , ΔS_{sp}^0 , etc.). A clear explanation of this topic has been given by Meyer in two papers concerned

with gas–liquid [3] and gas–solid [4] chromatography.

Chromatographers often yield to temptation to replace the equilibrium constant in eqn. 1 with the chromatographic partition coefficient given by the ratio of solute concentrations in the stationary and the mobile phase. However, such a substitution deprives ΔG_{sp}^0 and the derived properties of their exact meaning because it is then no longer clear what the states of the solute are in both phases to which the sorption properties refer.

In supercritical fluid chromatography (SFC), the standard thermodynamic properties of sorption have not been much used, possibly because the actual physical states of a non-volatile solute in a supercritical mobile phase and in a swollen stationary phase cannot be conveniently related to any sensible choice of standard states for the solute. Instead, thermodynamics of solute retention in SFC have been treated in terms of transfer properties, *i.e.*, the property changes

associated with the transfer of the solute from its actual state in the mobile phase to its actual state in the stationary phase. Similarly as with the standard properties of sorption, the relationships between the transfer properties and the various retention parameters have sometimes been misinterpreted; an example is provided by what is called “Van ’t Hoff plots” (see ref. 5 and the citations therein).

The purpose of this contribution is to present a consistent picture of the connections between the thermodynamic properties of solute transfer and the variations of solute retention with temperature and pressure. The discussion will be limited to partition chromatography at infinite dilution of the solute, and it will be illustrated by statistical thermodynamic calculations on a model system typical of open-tubular capillary column SFC. The transfer properties discussed will only be those at the level of the first derivatives of Gibbs energy with respect to temperature and pressure. Determination of higher order transfer properties (*e.g.*, the heat capacity of transfer) from experimental SFC retention data is precluded by insufficient precision of the data and by theoretical problems such as the effects of pressure- or temperature-induced changes in volume and composition of the stationary phase (“swelling”).

THEORY

Transfer properties of the solute

Provided that the solute is infinitely diluted by both phases, a transfer property ΔZ_t per mol of the solute may be written as

$$\Delta Z_t = \bar{z}_{1s}^\infty - \bar{z}_{1m}^\infty \quad (2)$$

where \bar{z}_{1s}^∞ and \bar{z}_{1m}^∞ are the respective partial molar thermodynamic properties of the solute (1) at infinite dilution in the stationary (s) and the mobile (m) phases. The definition of ΔZ_t by eqn. 2 does not invoke any standard states.

According to eqn. 2, the Gibbs energy of transfer, ΔG_t , is equal to the difference between the infinite-dilution chemical potentials (= infinite-dilution partial molar Gibbs energies) of

the solute in the stationary and the mobile phases. However, the temperature and pressure in the two phases are the same and, in the centre of a chromatographic band, distribution of the solute between the two phases reflects the thermodynamic equilibrium. Consequently, the two chemical potentials must be the same, and

$$\Delta G_t = 0 \quad (3)$$

As $\Delta G_t = \Delta H_t - T \Delta S_t$, where ΔH_t and ΔS_t are the enthalpy and entropy of transfer, respectively, it follows from eqn. 3 that

$$\Delta S_t = \Delta H_t / T \quad (4)$$

It is useful to concentrate on the enthalpy of transfer and on the volume of transfer, ΔV_t , because these two quantities make important contributions to the temperature and pressure changes in solute retention, respectively. In accordance with eqn. 2,

$$\Delta V_t = \bar{v}_{1s}^\infty - \bar{v}_{1m}^\infty \quad (5)$$

and

$$\Delta H_t = \bar{h}_{1s}^\infty - \bar{h}_{1m}^\infty \quad (6)$$

The infinite-dilution partial molar volume, \bar{v}_{1m}^∞ , and the infinite-dilution partial molar enthalpy, \bar{h}_{1m}^∞ , of the solute in the mobile phase are known to diverge as the temperature and pressure approach the critical point of the mobile phase fluid [6,7]. Near the critical point, \bar{v}_{1m}^∞ is proportional to the isothermal compressibility of the mobile phase fluid, β_{mT} [8–11] and \bar{h}_{1m}^∞ is proportional to the isobaric expansivity of the mobile phase fluid, α_{mP} [11]. The quantities α_{mP} and β_{mT} are defined by

$$\alpha_{mP} = (1/v_3)(\partial v_3 / \partial T)_P \quad (7)$$

and

$$\beta_{mT} = -(1/v_3)(\partial v_3 / \partial P)_T \quad (8)$$

where P is the pressure and v_3 is the molar volume of the pure mobile phase fluid. At the critical point, $\alpha_{mP} \rightarrow +\infty$ and $\beta_{mT} \rightarrow +\infty$. According to the classification presented by DeBenedetti and co-workers [12,13], in the solute–mobile phase systems encountered in SFC, $\bar{v}_{1m}^\infty \rightarrow -\infty$ and $\bar{h}_{1m}^\infty \rightarrow -\infty$ at the critical point of the mobile

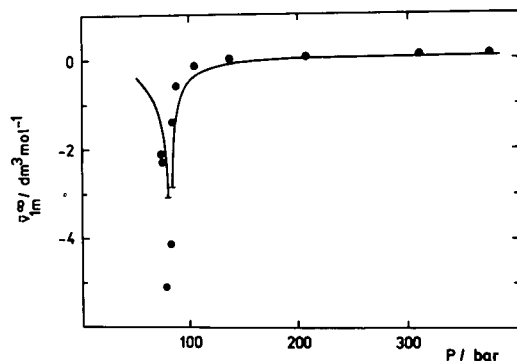


Fig. 1. Infinite-dilution partial molar volume of naphthalene in carbon dioxide at 35.23°C as a function of pressure. Experimental data are from ref. 14.

phase fluid. Large negative values of \bar{v}_{1m}^{∞} and \bar{h}_{1m}^{∞} persist at certain combinations of temperature and pressure in the supercritical region.

Fig. 1 shows the pressure dependence of \bar{v}_{1m}^{∞} for naphthalene in carbon dioxide at 35.23°C. The experimental values were obtained [14] from density measurements of high accuracy. The curve was calculated from a statistical thermodynamic treatment based on the mean-field lattice model designed by Panayiotou and Vera [15]. The details and parameterization of the treatment have been described elsewhere [16,17]. The break in the calculated curve near the minimum in \bar{v}_{1m}^{∞} results from decreased performance of mean-field models near the critical point. Nevertheless, the treatment correctly reproduces the essential features of the pressure course of \bar{v}_{1m}^{∞} .

The behaviour of \bar{h}_{1m}^{∞} in the supercritical region (Fig. 2) is similar to that of \bar{v}_{1m}^{∞} . As the

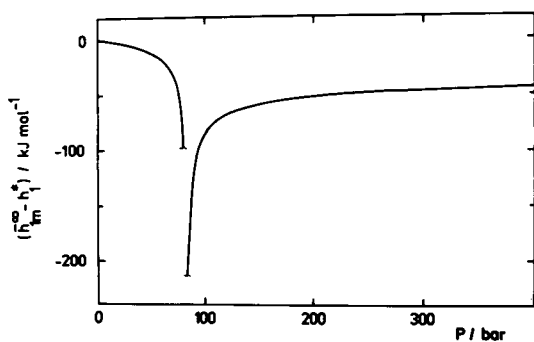


Fig. 2. Difference $(\bar{h}_{1m}^{\infty} - h_1^*)$ for naphthalene in carbon dioxide as a function of pressure at 35°C.

statistical thermodynamic model employed cannot yield \bar{h}_{1m}^{∞} directly, the quantity plotted in Fig. 2 is $\bar{h}_{1m}^{\infty} - h_1^*$, where h_1^* is the molar enthalpy of pure naphthalene in an ideal-gas state at 35°C (h_1^* is independent of pressure).

Now let us return to the transfer properties ΔV_t and ΔH_t (eqns. 5 and 6) to consider how these quantities are affected by the large negative values of \bar{v}_{1m}^{∞} and \bar{h}_{1m}^{∞} near the mobile-phase critical point. Under the SFC conditions, an appreciable amount of the mobile phase fluid is sorbed in (or on) the stationary phase (see refs. 18 and 19 for reviews). Nevertheless, the arrangement of molecules in the stationary phase is still largely determined by the principal component of the stationary phase, *e.g.*, by the alkyl chains bonded to the surface of a silica particle in packed-column SFC or by a cross-linked siloxane polymer in open-tubular capillary SFC. Therefore, in the stationary phase there is no divergence in the range of molecular correlations as the temperature and pressure approach the mobile-phase critical point and, thereby, there is no physical reason for the quantities \bar{v}_{1s}^{∞} and \bar{h}_{1s}^{∞} to diverge. Consequently, eqns. 5 and 6 translate the large *negative* values of \bar{v}_{1m}^{∞} and \bar{h}_{1m}^{∞} near the critical point into large *positive* values of ΔV_t and ΔH_t . To illustrate this, Fig. 3 shows the pressure

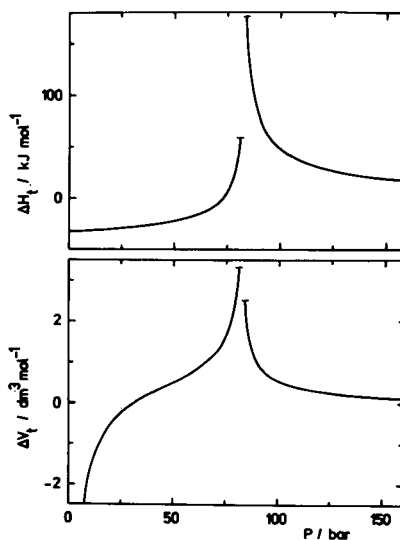


Fig. 3. Enthalpy of transfer and volume of transfer for naphthalene in the PDMS-carbon dioxide system at 35°C as functions of pressure.

courses at 35°C of ΔV_t and ΔH_t for naphthalene in the poly(dimethylsiloxane) (PDMS)–carbon dioxide system calculated with the mean-field lattice model mentioned above. The model takes the “swelling” of the stationary phase into account, and it predicts some variations of \bar{v}_{1s}^∞ and \bar{h}_{1s}^∞ with changing temperature or pressure. Near the critical point of the mobile phase, however, the variations in \bar{v}_{1s}^∞ and \bar{h}_{1s}^∞ are much less significant than those in \bar{v}_{1m}^∞ and \bar{h}_{1m}^∞ , respectively.

Transfer properties versus the effects of pressure and temperature on solute retention

In this section, the title relationships will be illustrated by computer calculations performed for the naphthalene (1)–PDMS (2)–carbon dioxide (3) system. The calculations are based on the statistical thermodynamic treatment mentioned above. It is assumed that a single mechanism of retention is operative, namely partitioning of the solute between the bulk mobile phase and the bulk stationary phase. As the treatment accounts for an appreciable swelling of PDMS by supercritical carbon dioxide [20,21], a reference value of the phase ratio is needed; it is assumed that, at 25°C and zero pressure (*i.e.*, no swelling), the phase ratio V_s/V_m is 0.04, which corresponds to a 50 μm I.D. capillary column containing a 0.5- μm thick film of PDMS. Further, it is assumed that the equilibrium concentration of carbon dioxide in PDMS at a given temperature and pressure is not disturbed by the presence of a trace amount of naphthalene (infinite dilution). The calculations also assume that there is a zero pressure drop along the column, but this assumption does not affect the discussion below. Solute retention will be expressed through the solute capacity factor, k' .

(i) *Pressure dependence of $\ln k'$ at a constant temperature.* Fig. 4 displays three calculated isotherms for $\ln k'$ of naphthalene in the present system. At a subcritical temperature (20°C), the calculated curve shows a discontinuity caused by liquefaction of carbon dioxide. The step decrease in $\ln k'$ reflects a sudden switch from gas chromatography (GC) to liquid chromatography (LC) as the pressure increases. At a temperature (40°C) not far above the critical temperature of

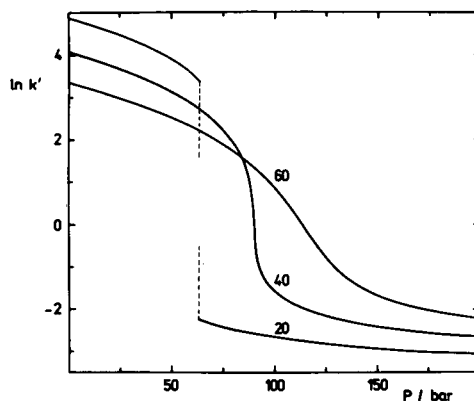


Fig. 4. Pressure dependence of $\ln k'$ for naphthalene in the PDMS–carbon dioxide system. Phase ratio at 20°C and zero pressure: $V_s/V_m = 0.04$. Numbers on the curves indicate the temperature (°C).

carbon dioxide, the discontinuity is replaced by a steep but continuous decrease in $\ln k'$. As the temperature increases, the S-shaped pattern in the isotherms becomes less apparent (60°C).

The slope of a tangent to an isotherm shown in Fig. 4 is given by [22–24]

$$\left(\frac{\partial \ln k'}{\partial P}\right)_T = -\Delta V_t / (RT) - \beta_{mT} - (V_s/V_m)\beta_{sT} - [1/(RT)](\partial \mu_{1s}^\infty / \partial w_{3s})_{T,P}(\partial w_{3s} / \partial P)_{T,\sigma} \quad (9)$$

where V_m and V_s are the volumes of the mobile and the stationary phase in the column, respectively, β_{sT} is the isothermal compressibility of the stationary phase, μ_{1s}^∞ is the infinite-dilution chemical potential of the solute in the stationary phase, w_{3s} is the mass fraction of the mobile phase fluid in the stationary phase and subscript σ denotes saturation of the stationary phase with the mobile phase fluid. The “unpleasant” last term on the right-hand side of eqn. 9 results from the effect of swelling; calculations indicate [17] that this term makes a positive contribution to $(\partial \ln k' / \partial P)_T$ in the present system. Generally, at a given temperature, the relative contribution to $(\partial \ln k' / \partial P)_T$ of the last term in eqn. 9 is minimum at the pressure where β_{mT} is maximum for the given temperature [17]. The term $(V_s/V_m)\beta_{sT}$ is negligible under most conditions.

Therefore, the large negative values of the slope $(\partial \ln k'/\partial P)_T$ near the mobile-phase critical point result from large positive values of β_{mT} and ΔV_t . Hypothetically, at the critical point itself, $(\partial \ln k'/\partial P)_T \rightarrow -\infty$ because $\beta_{mT} \rightarrow +\infty$ and $\Delta V_t \rightarrow +\infty$.

Eqn. 9 may serve as a basis for the determination of ΔV_t and \bar{v}_{1m}^∞ from the pressure course of solute retention at a constant temperature. The most recent applications of SFC for this purpose are those of Shim and Johnston [21,25]. In applying eqn. 9, allowance should be made for the pressure drop along the column [26–28].

Chimowitz and Kelley [22] and Shim and Johnston [25] pointed out that, to avoid the difficult fitting of the $\ln k'$ vs. P curve near the critical point, it is convenient to plot the experimental data as $\ln k'$ vs. $\ln \rho_m$, where ρ_m is the density of the mobile phase fluid. Unlike $(\partial \ln k'/\partial P)_T$, the derivative $(\partial \ln k'/\partial \ln \rho_m)_T$ does not diverge in the near-critical region. From eqn. 9 it follows that

$$\begin{aligned} (\partial \ln k'/\partial \ln \rho_m)_T &= -\Delta V_t/(RT\beta_{mT}) - 1 \\ &- (V_s/V_m)\beta_{sT}/\beta_{mT} - [1/(RT\beta_{mT})] \\ &\times (\partial \mu_{1s}^\infty/\partial w_{3s})_{T,P}(\partial w_{3s}/\partial P)_{T,\sigma} \end{aligned} \quad (10)$$

As the temperature and pressure approach the critical point, β_{mT} and ΔV_t increase and the relative contributions of the β_{sT} - and μ_{1s}^∞ -containing terms in eqn. 10 to $(\partial \ln k'/\partial \ln \rho_m)_T$ decrease [17]. Hypothetically, at the critical point itself, the derivative $(\partial \ln k'/\partial \ln \rho_m)_T$ would be equal to $-\Delta V_t/(RT\beta_{mT}) - 1$. The plot of $\ln k'$ vs. $\ln \rho_m$ is nearly linear, primarily because the ratio $\bar{v}_{1m}^\infty/\beta_{mT}$ is relatively constant in the near-critical region [8–11,14,22].

(ii) *Temperature dependence of $\ln k'$ at a constant pressure.* Fig. 5 shows several calculated isobars for $\ln k'$ of naphthalene in the present system. The break in the 70-bar curve results from vaporization of carbon dioxide which is accompanied by discontinuous decreases in density and solvating power. The break reflects a sudden switch from LC to GC as the temperature increases. In the LC domain, k' increases with increasing temperature at a constant pressure because of a decrease in the

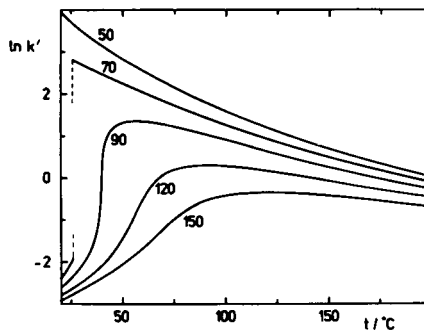


Fig. 5. Temperature dependence of $\ln k'$ for naphthalene in the PDMS-carbon dioxide system. Phase ratio at 20°C and zero pressure: $V_s/V_m = 0.04$. Numbers on the curves indicate the pressure (bar).

solvating power of carbon dioxide. In the GC domain, k' decreases with increasing temperature because of increasing volatility of naphthalene [29]. At supercritical pressures, the isobars become continuous and display maxima [30] that shift to higher temperatures at the pressure increases.

The slope of a tangent to an isobar in Fig. 5 may be written as [23,24]

$$\begin{aligned} (\partial \ln k'/\partial T)_P &= \Delta H_t/(RT^2) + \alpha_{mP} + (V_s/V_m)\alpha_{sP} \\ &- [1/(RT)](\partial \mu_{1s}^\infty/\partial w_{3s})_{T,P}(\partial w_{3s}/\partial T)_{P,\sigma} \end{aligned} \quad (11)$$

where α_{sP} is the isobaric expansivity of the stationary phase. The last term on the right-hand side of eqn. 11 results from the effect of swelling and it makes a negative contribution to $(\partial \ln k'/\partial T)_P$ in the present system. Generally, at a given pressure, the relative contribution to $(\partial \ln k'/\partial T)_P$ of the last term in eqn. 11 is minimum at the temperature where α_{mP} is maximum for the given pressure [17]. Except for the region near the isobar maximum, $\Delta H_t/(RT^2)$ is the major term on the right-hand side of eqn. 11 and the sign of $(\partial \ln k'/\partial T)_P$ is that of ΔH_t . The large positive values of the slope $(\partial \ln k'/\partial T)_P$ near the mobile-phase critical point result from large positive values of α_{mP} and ΔH_t . Hypothetically, at the critical point itself, $(\partial \ln k'/\partial T)_P \rightarrow +\infty$ because $\alpha_{mP} \rightarrow +\infty$ and $\Delta H_t \rightarrow +\infty$.

Eqn. 11 provides a way to determine ΔH_t and \bar{h}_{1m}^∞ from the temperature course of solute retention at a constant pressure. The most recent applications of SFC to this purpose are those of

Shim and Johnston [21,25], who also suggested a convenient mathematical transformation to avoid the difficulties imposed by the divergence of $(\partial \ln k'/\partial T)_p$ near the mobile-phase critical point, namely

$$(\partial \ln k'/\partial T)_p = \alpha_{mP}(\partial \ln k'/\partial \ln \rho_m)_T - T^2[\partial \ln k'/\partial(1/T)]_{\rho_m} \quad (12)$$

The slopes $(\partial \ln k'/\partial \ln \rho_m)_T$ (see above) and $[\partial \ln k'/\partial(1/T)]_{\rho_m}$ (see below) do not diverge near the critical point. In the near-critical region, therefore, the value of $(\partial \ln k'/\partial T)_p$ may be obtained from the experimental data on the “well behaved” quantities $(\partial \ln k'/\partial \ln \rho_m)_T$ and $[\partial \ln k'/\partial(1/T)]_{\rho_m}$ and from α_{mP} calculated from an accurate equation of state for the mobile phase concerned.

(iii) *Temperature dependence of $\ln k'$ at a constant density.* Fig. 6 shows $\ln k'$ for naphthalene calculated as a function of the reciprocal of absolute temperature at a constant density of carbon dioxide. The plots are nearly linear provided that suitable scales have been chosen for both axes. Lauer *et al.* [31] postulated a proportionality between ΔH_t and the slope of a constant-density plot. Thermodynamic analysis [5,17] yields a different expression for the slope, namely

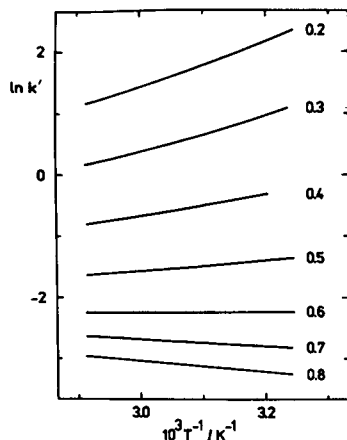


Fig. 6. Dependence of $\ln k'$ for naphthalene in the PDMS–carbon dioxide system on the reciprocal of absolute temperature. Phase ratio at 20°C and zero pressure: $V_s/V_m = 0.04$. Numbers adjacent to the lines indicate the density of carbon dioxide (g/cm^3).

$$\begin{aligned} [\partial \ln k'/\partial(1/T)]_{\rho_m} = & -(\Delta H_t - T\gamma_{mV} \Delta V_t)/R \\ & + T^2(V_s/V_m)(\beta_{sT}\gamma_{mV} - \alpha_{sP}) \\ & + (T/R)(\partial \mu_{1s}^\infty/\partial w_{3s})_{T,P}[(\partial w_{3s}/\partial T)_{P,\sigma} \\ & + \gamma_{mV}(\partial w_{3s}/\partial P)_{T,\sigma}] \end{aligned} \quad (13)$$

where $\gamma_{mV} = \alpha_{mP}/\beta_{mT}$ is the thermal pressure coefficient of the mobile phase fluid. Linearity of the constant-density plots has been interpreted by Martire and Boehm [32] in terms of the unified molecular theory of chromatography, *i.e.*, at a microscopic level. Eqn. 13 supports an alternative, model-independent interpretation at a macroscopic level. It reflects the different nature of constant-density plots compared with those labelling sections (i) and (ii) above. First, the quantities α_{mP} and β_{mT} that diverge at the mobile-phase critical point are absent from eqn. 13 (compare eqns. 9 and 11). Second, it has been shown [8–11] that, although both \bar{v}_{1m}^∞ and \bar{h}_{1m}^∞ diverge at the mobile-phase critical point, the difference $\bar{h}_{1m}^\infty - T\gamma_{mV}\bar{v}_{1m}^\infty$ always remains finite. This particular difference appears in eqn. 11 (see eqns. 5 and 6). In other words, unlike the plots labelling sections (i) and (ii) above, the constant-density plots are *not* sensitive to the near-critical anomalies in \bar{v}_{1m}^∞ and \bar{h}_{1m}^∞ because the anomalies cancel in eqn. 13. The other terms in eqn. 13 do not diverge near the critical point [17]. Therefore, the slope given by eqn. 13 remains relatively constant within narrow temperature intervals and the plot appears to be nearly linear. These considerations also imply that, contrary to popular belief, the constant-density plots themselves are of little use for determination of solute transfer properties.

CONCLUSIONS

Relationships between solute retention in partition chromatography and thermodynamic properties of solute transfer from the mobile to the stationary phase have been reviewed and illustrated by using a statistical thermodynamic model. The model of transfer, ΔV_t , may be obtained from the pressure derivative of $\ln k'$ at a constant temperature, and the enthalpy of transfer, ΔH_t , from the temperature derivative of

In k' at a constant pressure. Near the mobile-phase critical point where the two derivatives diverge, it is convenient to employ the transformations suggested by Chimowitz and Kelley [22] and by Shim and Johnston [25]. The entropy of transfer, ΔS_t , equals $\Delta H_t/T$ because the Gibbs energy of transfer is zero. In reducing the chromatographic data to thermodynamic properties, allowance should be made for the effects of swelling and for the pressure drop along the column. One should also bear in mind that the relationships given above assume infinite dilution of the solute in both phases and the absence of interfacial adsorption of both the solute and the mobile phase fluid. The nearly linear plots of $\ln k'$ vs. $1/T$ at a constant density of the mobile phase fluid ("Van 't Hoff plots") are of little use in themselves for determining the solute transfer properties. The apparent linearity of these plots arises from cancellation of near-critical anomalies in \bar{v}_{1m}^∞ and \bar{h}_{1m}^∞ .

ACKNOWLEDGEMENT

This contribution is based on work supported by the Grant Agency of the Czechoslovak Academy of Sciences under Grant No. 43154, which the author gratefully acknowledges.

REFERENCES

- M.R. James, J.C. Giddings and R.A. Keller, *J. Gas Chromatogr.*, 3 (1965) 57.
- J.M. Prausnitz, *Molecular Thermodynamics of Fluid-Phase Equilibria*, Prentice-Hall, Englewood Cliffs, NJ, 1969, Ch. 6.
- E.F. Meyer, *J. Chem. Educ.*, 50 (1973) 191.
- E.F. Meyer, *J. Chem. Educ.*, 57 (1980) 120.
- M. Roth, *J. Chromatogr.*, 543 (1991) 262.
- I.R. Krichevskii, *Zh. Fiz. Khim.*, 41 (1967) 2458.
- A.M. Rozen, *Zh. Fiz. Khim.*, 50 (1976) 1381.
- J.C. Wheeler, *Ber. Bunsenges. Phys. Chem.*, 76 (1972) 308.
- R.F. Chang and J.M.H. Levelt Sengers, *J. Phys. Chem.*, 90 (1986) 5921.
- P.G. Debenedetti and S.K. Kumar, *AIChE J.*, 34 (1988) 645.
- J.M.H. Levelt Sengers, *J. Supercrit. Fluids*, 4 (1991) 215.
- P.G. Debenedetti and R.S. Mohamed, *J. Chem. Phys.*, 90 (1989) 4528.
- P.G. Debenedetti, I.B. Petsche and R.S. Mohamed, *Fluid Phase Equilib.*, 52 (1989) 347.
- C.A. Eckert, D.H. Ziger, K.P. Johnston and S. Kim, *J. Phys. Chem.*, 90 (1986) 2738.
- C. Panayiotou and J.H. Vera, *Polym. J.*, 14 (1982) 681.
- M. Roth, *J. Phys. Chem.*, 96 (1992) 8548.
- M. Roth, *J. Phys. Chem.*, 96 (1992) 8552.
- C.R. Yonker and R.D. Smith, *J. Chromatogr.*, 550 (1991) 775.
- M. Roth, *J. Microcol. Sep.*, 3 (1991) 173.
- J.-J. Shim and K.P. Johnston, *AIChE J.*, 35 (1989) 1097.
- J.-J. Shim and K.P. Johnston, *AIChE J.*, 37 (1991) 607.
- E.H. Chimowitz and F.D. Kelley, *J. Supercrit. Fluids*, 2 (1989) 106.
- F.D. Kelley and E.H. Chimowitz, *AIChE J.*, 36 (1990) 1163.
- M. Roth, *J. Phys. Chem.*, 94 (1990) 4309.
- J.-J. Shim and K.P. Johnston, *J. Phys. Chem.*, 95 (1991) 353.
- D.E. Martire, *J. Chromatogr.*, 461 (1989) 165.
- K.D. Bartle, T. Boddington, A.A. Clifford and G.F. Shilstone, *J. Chromatogr.*, 471 (1989) 347.
- D.E. Martire, R.L. Riester, T.J. Bruno, A. Hussam and D.P. Poe, *J. Chromatogr.*, 545 (1991) 135.
- T.L. Chester and D.P. Innis, *J. High Resolut. Chromatogr. Chromatogr. Commun.*, 8 (1985) 561.
- S.T. Sie and G.W.A. Rijnders, *Sep. Sci.*, 2 (1967) 755.
- H.H. Lauer, D. McManigill and R.D. Board, *Anal. Chem.*, 55 (1983) 1370.
- D.E. Martire and R.E. Boehm, *J. Phys. Chem.*, 91 (1987) 2433.

Comparison of flame ionization and inductively coupled plasma mass spectrometry for the detection of organometallics separated by capillary supercritical fluid chromatography[☆]

Nohora P. Vela and Joseph A. Caruso*

Department of Chemistry, University of Cincinnati, Cincinnati, OH 45221-0172 (USA)

(First received December 1st, 1992; revised manuscript received February 24th, 1993)

ABSTRACT

Organotin compounds are separated by capillary supercritical fluid chromatography (SFC) and a comparison of the detection by flame ionization (FID) and inductively coupled plasma mass spectrometry (ICP-MS) is presented. Resolution, detection limits, linear dynamic range and reproducibility are the parameters compared between SFC-FID and SFC-ICP-MS, for the detection of tri- and tetraorganotin compounds. The resolution obtained in the SFC-FID system is not always observed in SFC-ICP-MS. Degradation in resolution is due to fluctuations in transfer line temperature. Baseline resolution for the organotins considered is achieved in both systems by using a longer column. Detection limits (DLs) are calculated as $3\sigma/S$, where σ is the standard deviation of the blank signal and S is the slope of the calibration curve. Detection limits of 10.3, 12.5, 12.0 and 9.0 pg are obtained for tetrabutyltin, tributyltin chloride, triphenyltin chloride and tetraphenyltin, respectively, using SFC-FID. An improvement in detection limits of one order of magnitude is achieved by SFC-ICP-MS for the same organotins (0.26, 0.80, 0.57 and 0.20 pg, respectively). The relative standard deviations using SFC-FID for five 50-nl injections, containing 0.5 ng Sn, ranged from 3.2 to 6.4%. Using SFC-ICP-MS, five replicate injections of 0.05 ng Sn give R.S.D.s from 1.3 to 3.4%.

INTRODUCTION

Supercritical fluid chromatography (SFC) spans the gap between liquid chromatography (HPLC) and gas chromatography (GC), making it possible to separate non-volatile, thermally labile and high-molecular-mass compounds in short analysis time [1–5]. This approach is due to the liquid-like property (density) and gas-like characteristics (viscosity and diffusion coefficients) of the supercritical fluids. Another advantage of SFC is its compatibility with the existing detectors for HPLC and GC. Liquid-phase and

gas-phase detectors are suitable for SFC, since detection can be performed before or after the decompression zone of the mobile phase [1–7]. Ultraviolet-visible (UV-Vis) detection was first used in SFC and is still the most common detector for packed-column SFC [4–7]. Fluorescence, light scattering and chemiluminescence are among other optical detection methods used for SFC [1,5,7].

Performance of GC detectors coupled to SFC has been the topic of several publications [4,5,8–14]. Flame ionization detection (FID) is a universal detector and is easy to interface to SFC [4,5,8–11]. Selective detection systems used in GC, such as flame photometric (FPD) [8–11], electron-capture (ECD) [8–12] and thermionic ionization (TID) [8,13,14] have been evaluated for SFC. A variety of papers have been pub-

* Corresponding author.

* This work was presented in part at the *Pittsburgh Conference, New Orleans, March 1992* (paper 084).

lished concerning the interface of SFC with detectors that provide structural information, such as Fourier transform infrared spectroscopy [5,6,15] and mass spectrometry [5,6,16–18]. SFC with detection based on atomic emission has been used as an element-selective detector for organometallics and halogenated compounds [19–25].

High-molecular-mass organotin compounds are good candidates for SFC, since they are not easily amenable to GC or HPLC separation. In general, organotin compounds are used as biocides and as antifouling agents in marine paints. These applications are the main source for the continuous release and accumulation of organotins in water, sediments and aquatic organisms [26,27]. Studies demonstrate that tetra and triorganotin compounds are the most toxic, while a decrease in the number of organic substituents linked to the tin atom is related to lower toxicity. The chemical form of the organic group also determines toxicity, resulting in the need for speciation information [26,27].

Organotin compounds with butyl and phenyl substituents are the most frequently used and a variety of papers have been published concerning their determination [24–41]. Speciation is obtained by GC, HPLC or SFC separation coupled to a universal or selective detector [24–42]. Most of the papers that describe the separation of organotins by GC involve the preparation of volatile derivatives (hydrides or pentyl derivatives) prior to the injection into the GC system [27–37]. Different techniques have been coupled to detect the chromatographic effluent, including ECD [28–29], FPD [30–34], FPD using quartz surface induced luminescence [35], atomic absorption (AAS) [36], quartz furnace atomic absorption [37], direct current plasma (DCP) [34] and microwave induced plasma detection (MIP) [38]. Dual detection by FPD–DCP has also been suggested [34].

Detection of organotins after HPLC has been obtained by several techniques including graphite furnace–atomic absorption spectroscopy (GF-AAS) [39], flame-laser excited atomic fluorescence spectroscopy (LEAFS) [40], inductively coupled plasma atomic emission spectroscopy (ICP-AES) and inductively coupled plasma mass

spectrometry (ICP-MS) [20,41,42]. The applicability of SFC for the speciation of tetra- and triorganotin compounds with ICP-MS detection has also been demonstrated [24,25]. In this study, capillary SFC with FID and ICP-MS detection is used for the speciation and detection of organotin compounds. Comparison of resolution, detection limits, linear dynamic range and reproducibility for tributyltin chloride, tetra-butyltin, triphenyltin chloride and tetraphenyltin using SFC–FID and SFC–ICP-MS is presented.

EXPERIMENTAL

Instrumentation

A description of the SFC–ICP-MS system used for the experiments was presented in a previous publication [24]. Fig. 1 illustrates the SFC–ICP-MS interface and detailed information was presented elsewhere [24]. Operating conditions for ICP-MS are: forward power: 1.35 kW; reflected power: < 5 W; argon coolant flow: 15 l/min; argon auxiliary flow: 1.5 l/min and make-up gas flow: 0.65 l/min. Carbon dioxide, SFC-grade (Scott Specialty Gases, Plumsteadville, PA, USA) was used as a mobile phase. An SB-Biphenyl-30 capillary column (0.25 μm film thickness, 50 μm I.D., 375 μm O.D.) with different lengths of 2.5 and 4 m were purchased from Lee Scientific (Salt Lake City, UT, USA). Frit restrictors (50 μm I.D.) with a linear velocity of 1.5 cm/s were also obtained from Lee Scientific. Calibration of the time split injector indicates that a duration of 0.075 s injection time corresponds to 50 nl injection volume.

A conventional flame ionization detector, obtained from Hewlett-Packard (Avondale, PA,

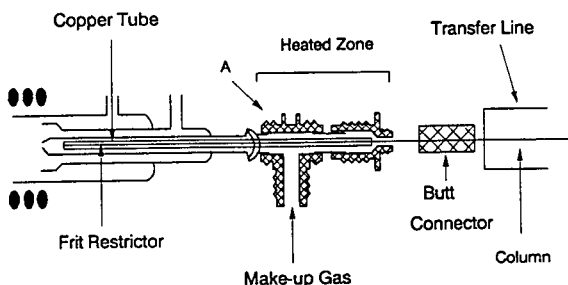


Fig. 1. SFC–ICP-MS interface.

USA) was installed in the gas chromatograph oven (Hewlett-Packard Model 5890). A jet tip (0.011 in. I.D.; 1 in. = 2.54 cm) that accommodates capillary columns was used for the detector. No additional modifications were required to convert the GC system into the SFC mode. The flow of the gases used with FID were: hydrogen: 45 ml/min; air: 400 ml/min and nitrogen (detector make-up gas): 32 ml/min. The temperature of the FID system was 300°C.

Reagents

The organometallic compounds, tetrabutyltin (TBT, 97% purity), tetraphenyltin (TPT, unknown purity), tetraphenyllead (TPL, 98% purity), tributyltin chloride (TrBT-Cl, 95% purity in metal basis) and triphenyltin chloride (TrPT-Cl, 95% purity), were obtained from Alfa Products (Danvers, MA, USA). They were used without further purification. Stock solutions of 1000 ppm (w/w) Sn corrected to the purity of the compounds, were prepared in HPLC grade methylene chloride (Aldrich, Milwaukee, WI, USA). Fresh working solutions were prepared daily by serial dilution with methylene chloride.

RESULTS AND DISCUSSION

The comparison between FID and ICP-MS for the detection of organometallics after SFC, is based on three aspects. The first is the effect of the detector temperature (SFC-FID) or interface temperature (SFC-ICP-MS) in the signal response, for organotin with different molecular weight and volatility. The second aspect investigated is with certain chromatographic conditions (pressure program and temperature) there are any variations in the resolution as a function of the detector used. Finally, analytical figures of merit are compared using SFC-FID and SFC-ICP-MS in the speciation of organotin.

A mixture of 50 ng of each TBT and TPT, 100 ng of TrBT-Cl and 150 ng of TrPT-Cl is injected to obtain SFC-FID chromatograms. A lower concentration, consisting of a mixture of 5 ng each of TBT, TrBT-Cl, TrPT-Cl and TPT is used during SFC-ICP-MS experiments.

Effect of interface temperature

Fig. 2 shows the variation in % normalized peak area for several organotin, as a function of the interface temperature, using SFC coupled to FID and ICP-MS. This figure indicates only minor variations in the organotin peak areas for FID temperatures ranging from 215 to 350°C. Variations are within the R.S.D. (1.1–5.5%) calculated for several injections at a constant FID temperature. On the other hand, the response obtained with SFC-ICP-MS is highly dependent on interface temperature. Interface temperature affects not only peak area, but also retention time and peak shape, mostly for the less volatile organotin that are TrPT-Cl and TPT, as it has been demonstrated in a previous study [25]. Variations in the results obtained between SFC-FID and SFC-ICP-MS, are explained by the different efficiency in which the heat is transferred to the restrictor tip. In the

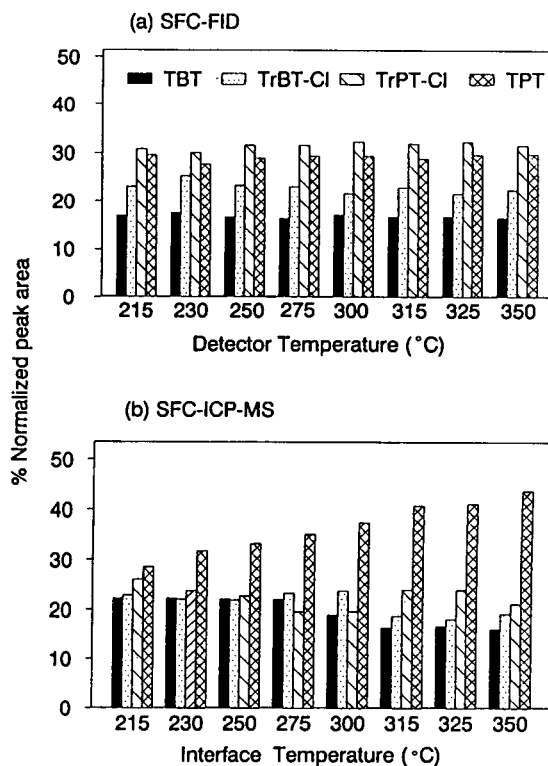


Fig. 2. Variation in peak area for several organotin as a function of (a) SFC-FID detector temperature and (b) SFC-ICP-MS interface temperature.

case of the FID, the proximity of the restrictor to the heating block allows an efficient heat transfer. For ICP-MS detection, heat to the frit is supplied by a preheated gas (see Fig. 1) that continuously flows along the restrictor. The temperature of the interface is taken at point A of the preheated zone. Results indicate that there is some temperature difference between point A and the tip of the restrictor in the ICP-MS interface. Nevertheless, chromatograms obtained for an SFC-ICP-MS interface temperature of 300°C are comparable to those obtained by SFC-FID [25].

Resolution as a function of chromatographic conditions

A pressure program, usually required to resolve a mixture, generally involves at least two steps. First, the pressure is maintained constant during enough time to allow solvent elution and second a pressure ramp is applied to resolve the components of the mixture. Fig. 3 indicates no significant variation in capacity factors for organotin compounds using SFC-FID, when the pressure (70

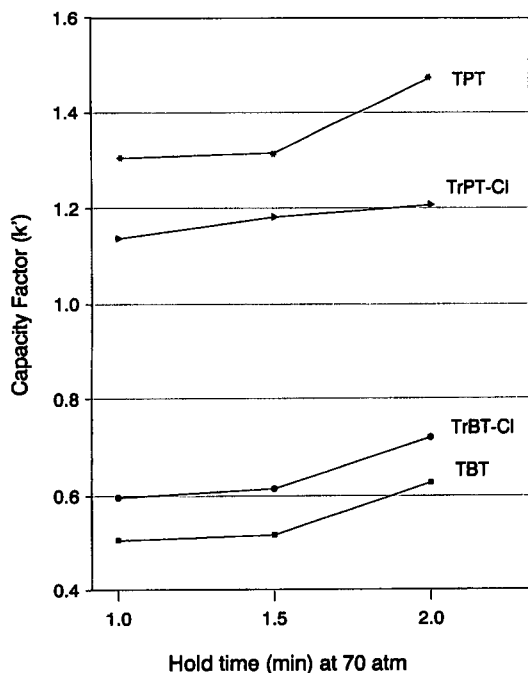


Fig. 3. Variation of capacity factor (k') for organotin compounds with different hold times in the pressure program.

atm; 1 atm = 101 325 Pa) is held constant for 1 and 1.5 min. Capacity factors as well as resolution are slightly increased by having a constant pressure of 70 atm for 2 min before the pressure ramp. Fig. 4 shows the chromatograms obtained at an oven temperature of 75°C for different hold times and for all of them baseline resolution is observed. An initial pressure of 70 atm held for 1 min, followed by a variable pressure ramp, is used for the next SFC-FID experiments.

An important difference between flame ionization and plasma detection is that the second detector is transparent to the solvent and to mobile phases that give response with FID [22,23,25] because ICP-MS is an element-selective detector. ICP-MS has a m/z resolution of better than 1 u, so a single-ion scan mode can be selected to detect a certain mass. Fig. 5 presents

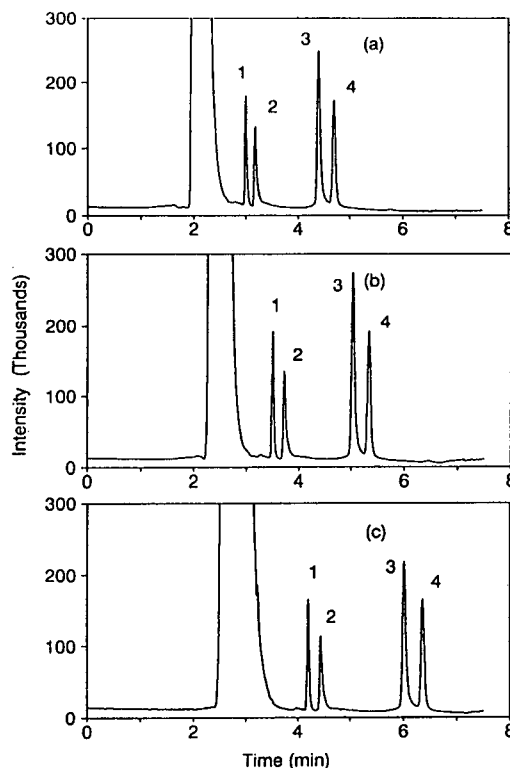


Fig. 4. Effect of hold time at an initial pressure of 70 atm. Pressure ramp: 60 atm/min; final pressure: 300 atm; oven temperature: 75°C. FID temperature: 300°C. Hold time: (a) 1 min, (b) 1.5 min and (c) 2 min. Peaks: 1 = TBT; 2 = TrBT-Cl; 3 = TrPT-Cl; 4 = TPT.

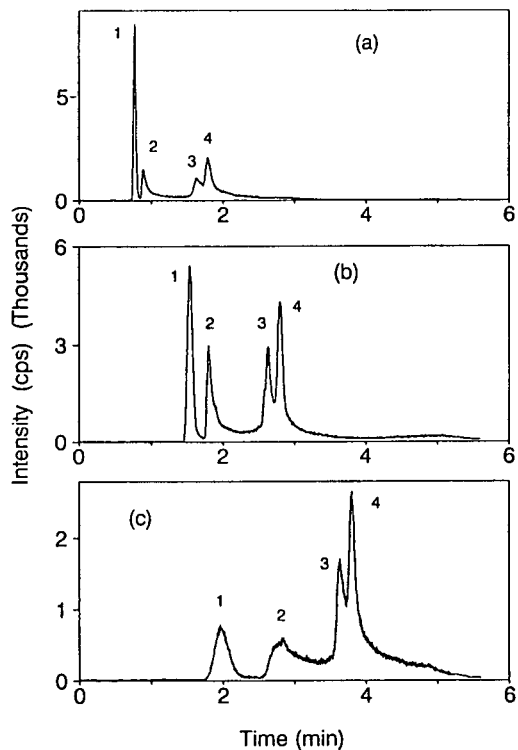


Fig. 5. Effect of hold time at an initial pressure of 70 atm. Pressure ramp: 60 atm/min; final pressure: 300 atm; oven temperature: 75°C. ICP-MS interface temperature: 300°C. Hold time: (a) no hold time, (b) 1 min and (c) 2 min. Peaks: 1 = TBT; 2 = TrBT-Cl; 3 = TrPT-Cl; 4 = TPT.

the chromatograms obtained for a 5-ng injection using SFC-ICP-MS and having different hold times at an initial pressure of 70 atm. The ICP-MS feature of detecting compounds that coelute with the solvent is illustrated in Fig. 5a. However, conditions are not always recommended

where one of the compounds coelute with the solvent, since sensitivity and reproducibility are affected. Chromatograms presented in Fig. 5 demonstrate that retention time, peak shape and relative peak height, especially for TBT and TrBT-Cl are affected by the length of the hold time. As with SFC-FID, for the next SFC-ICP-MS experiments, the pressure was started at 70 atm and was held constant for 1 min before the pressure ramp was initiated.

Table I shows the effect of pressure ramp in the resolution of organotin compounds using ICP-MS and FID, at a fixed temperature of 50°C. The general trend observed is a decrease in resolution with the increase in pressure ramp. Comparing resolution between TBT and TrBT-Cl, better values are obtained with ICP-MS detection. As it was pointed out earlier, ICP-MS is transparent to the solvent and with FID, TBT and TrBT-Cl elute in the tail of the solvent peak, at a column temperature of 50°C (see Fig. 6). TrBT-Cl and TrPT-Cl are baseline resolved using both detectors, at pressure ramps between 20 and 60 atm/min. Table I also shows that better resolution between TrPT-Cl and TPT is observed with FID. Loss in resolution in SFC-ICP-MS is due to peak broadening attributed to fluctuations in transfer line temperature.

Variation in resolution for the same pressure program, as a function of the temperature is presented in Table II. Using FID, better resolution is obtained at 100°C, although baseline resolution is also observed at 75°C. Resolution between TBT and TrBT-Cl with ICP-MS detection is slightly affected by variation in column

TABLE I

EFFECT OF THE PRESSURE RAMP IN THE RESOLUTION OF ORGANOTIN COMPOUNDS USING SFC COUPLED TO ICP-MS AND FID

Pressure program: 70 atm held for 1 min; variable pressure ramp up to 320 atm. Column temperature: 50°C.

Ramp (atm/min)	TBT and TrBT-Cl		TrBT-Cl and TrPT-Cl		TrPT-Cl and TPT	
	ICP-MS	FID	ICP-MS	FID	ICP-MS	FID
20	1.105	1.428	3.702	7.330	0.908	2.000
40	1.200	0.833	3.417	4.555	0.867	1.300
60	0.933	0.571	3.200	4.133	0.692	1.125

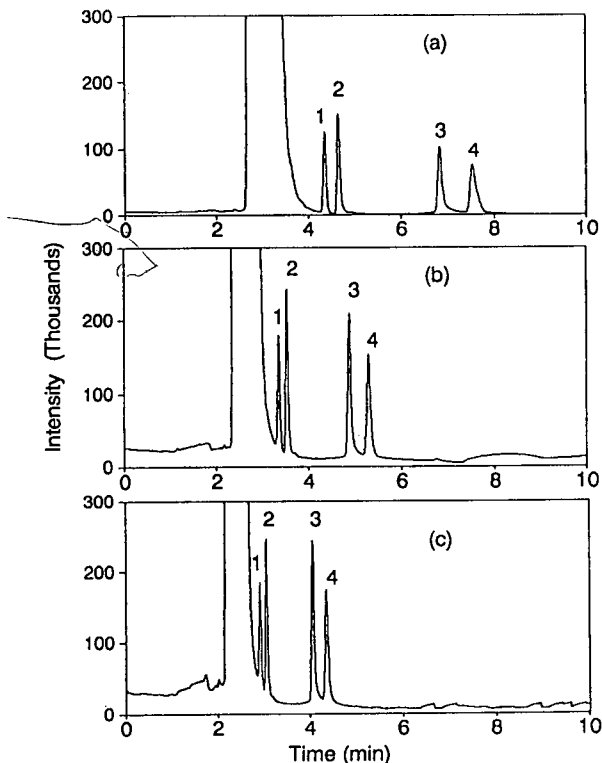


Fig. 6. Effect of pressure ramps at an oven temperature of 50°C: (a) 20 atm/min, (b) 40 atm/min and (c) 60 atm/min. FID temperature: 300°C. Initial pressure: 70 atm held for 1 min; final pressure: 350 atm. Peaks: 1 = TBT; 2 = TrBT-Cl; 3 = TrPT-Cl; 4 = TPT.

temperatures, however, better peak shape is obtained at 50°C. The same tendency is observed for the resolution between TrPT-Cl and TPT using SFC-ICP-MS. Another factor involved in peak broadening for ICP-MS detection is related to interface design and operation. The distance

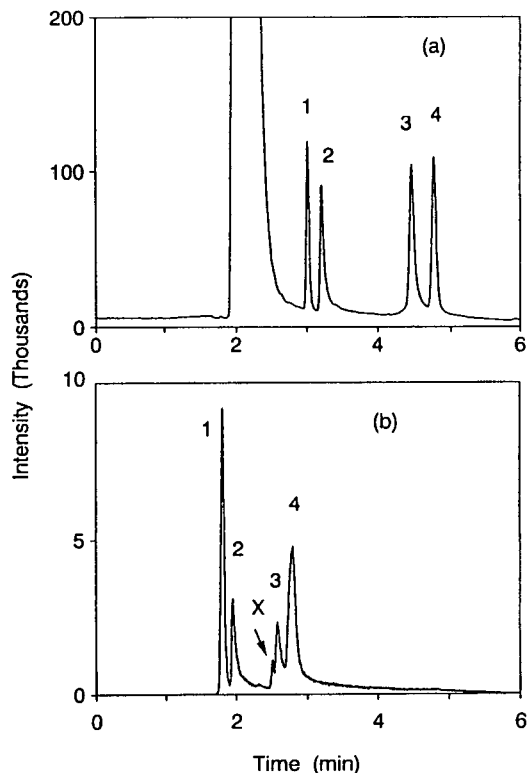


Fig. 7. (a) SFC-FID using the following conditions: Oven temperature: 75°C; initial pressure 70 atm held for 1 min, pressure ramp: 60 atm/min, final pressure: 360 atm. (b) SFC-ICP-MS chromatogram using an oven temperature of 50°C and the same pressure program described for (a). Peaks: 1 = TBT; 2 = TrBT-Cl; 3 = TrPT-Cl; 4 = TPT.

between the tip of the restrictor and the detection zone is longer in ICP-MS than in FID. The lower temperature at the tip of the restrictor for SFC-ICP-MS causes a slow release of the analyte and as a consequence, peak broadening

TABLE II

EFFECT OF TEMPERATURE IN THE RESOLUTION OF ORGANOTIN COMPOUNDS USING SFC INTERFACED TO ICP-MS AND FID

Pressure program: 70 atm held for 1 min; ramp: 60 atm/min to 320 atm.

Oven temperature (°C)	TBT and TrBT-Cl		TrBT-Cl and TrPT-Cl		TrPT-Cl and TPT	
	ICP-MS	FID	ICP-MS	FID	ICP-MS	FID
50	0.933	0.571	3.200	4.133	0.692	1.125
75	1.067	1.002	2.355	5.250	0.540	1.455
100	1.071	1.263	1.654	5.308	0.513	1.467

and decrease in resolution are observed. Fig. 7 presents the best chromatograms obtained using a 2.5-m capillary column for the separation of organotin using SFC coupled to FID and ICP-MS. Variations in the temperatures of the oven, of the transfer line and of the restrictor tip affect mobile phase density and mobile phase velocity. As a consequence, there are changes in retention times and peak widths as well as in resolution comparing the two systems (SFC-FID and SFC-ICP-MS). A comparison of the chromatograms obtained using a longer column (4 m) is presented in Fig. 8. Baseline resolution between TrPT-Cl and TPT is now possible for the SFC-ICP-MS system (see Fig. 8b). Also, the impurity detected in the standard solutions and labeled as X in Fig. 7b is resolved into two peaks when a 4-m column is used. These impurities correspond

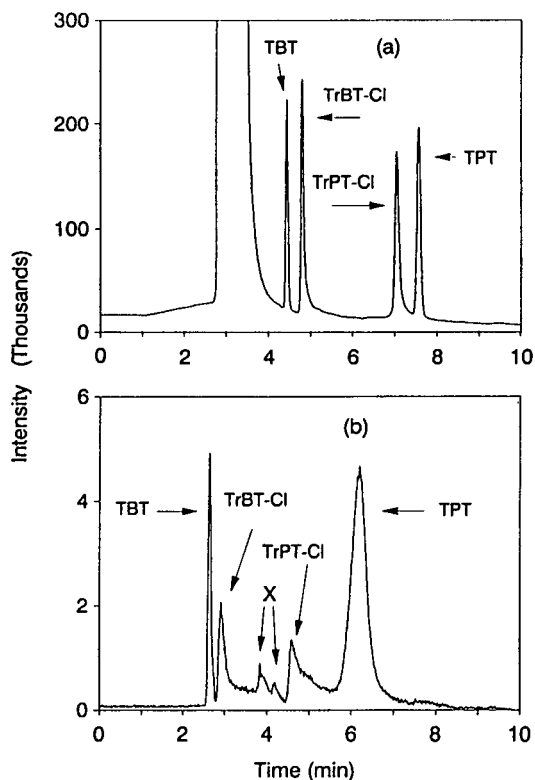


Fig. 8. Separation of organotin using a 4-m SB-Biphenyl-30 column: (a) SFC-ICP-MS and (b) SFC-FID. Initial pressure: 80 atm held for 2.5 min, followed by a pressure ramp of (a) 150 atm/min for ICP-MS and (b) 60 atm/min for SFC-FID; final pressure: 400 atm held for 5 min.

to compounds containing tin and they were not detected by SFC-FID, most likely because of the difference in sensitivity of the detectors.

FID vs. ICP-MS: sensitivity and selectivity

Analytical figures of merit for tri- and tetraorganotin using SFC-FID and SFC-ICP-MS are presented in Table III. Five 50-nl injections containing 0.5 ng Sn gives a reproducibility range from 3.2 to 6.4% R.S.D. in the SFC-FID experiments. Using the same number of injections, but samples containing 0.05 ng Sn, reproducibility varies from 1.3 to 3.4% R.S.D. with the SFC-ICP-MS system. Detection limits are calculated as three times the standard deviation

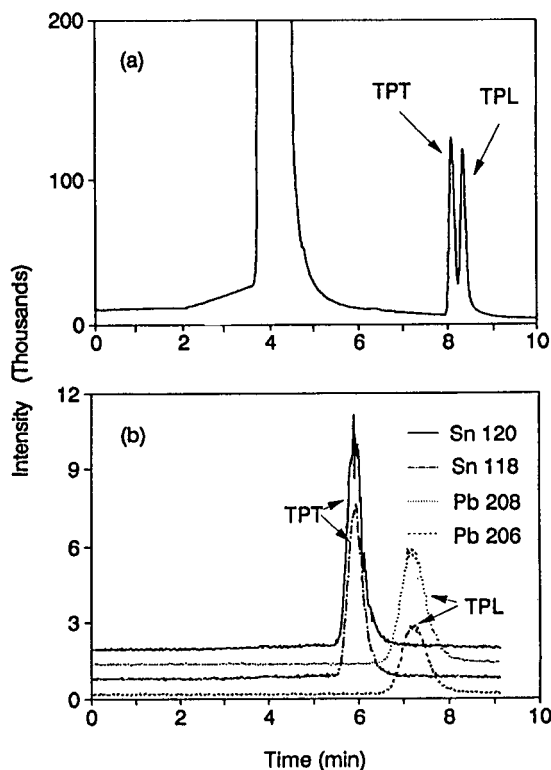


Fig. 9. Chromatograms for a mixture of tetraphenyltin (TPT) and tetraphenyllead (TPL). Column: SB-Biphenyl-30, 4 m length. Oven temperature: 75°C. (a) SFC-FID. Conditions: initial pressure: 70 atm held for 2 min followed by a pressure ramp of 40 atm/min up to 320 atm; detector temperature: 350°C. (b) SFC-ICP-MS. Conditions: initial pressure 80 atm held for 2 min followed by a pressure ramp of 150 atm/min up to 400 atm (held for 4 min); interface temperature: 350°C.

TABLE III

COMPARISON OF ANALYTICAL FIGURES OF MERIT FOR ORGANOTIN COMPOUNDS USING SFC-FID AND SFC-ICP-MS

		TBT	TrBT-Cl	TrPT-Cl	TPT
Reproducibility (%) ^a	SFC-FID	4.64	4.92	6.43	3.20
	SFC-ICP-MS	1.29	1.52	1.67	3.42
Absolute detection limit (pg), 50-nl injection	SFC-FID	10.3	12.5	12.0	9.0
	SFC-ICP-MS	0.26	0.80	0.57	0.20
Linear range ^b	SFC-FID	3	3	3	3
	SFC-ICP-MS	3	3	3	3
Slope (log-log)	SFC-FID	1.0006	0.9736	1.0130	0.9816
	SFC-ICP-MS	0.9647	1.1749	1.0980	1.0310
R ² (correlation coefficient)	SFC-FID	0.9990	0.9981	0.9969	0.9991
	SFC-ICP-MS	0.9936	0.9960	0.9870	0.9803

^a Reproducibility in peak area; 5 and 0.5 ng injection for SFC-FID and SFC-ICP-MS, respectively.

^b Linear range between 0.5 and 50 ng for SFC-FID and between 0.05 and 5 ng using SFC-ICP-MS.

(σ) of the blank signal divided by the slope of the calibration curve. Absolute detection limits (50 nl injection volume) for organotins with SFC-FID range from 9.0 to 12.5 pg. An improvement of one order of magnitude in sensitivity is found for SFC-ICP-MS detection (absolute detection limits range from 0.2 to 0.8 pg). Linearity over three orders of magnitude is presented for both SFC-FID and SFC-ICP-MS in the detection of organotins.

Differences in mobile phase velocity, comparing SFC-FID and SFC-ICP-MS have some advantages. This is the case of the baseline resolution obtained using SFC-ICP-MS for the separation of TPT and TPL (see Fig. 9b). Different chromatographic conditions were evaluated in SFC-FID to resolve TPT and TPL, but no baseline resolution was possible and the best chromatogram is shown in Fig. 9a. Another relevant advantage of ICP-MS over FID is the element-selective capability of the former detector. Non-baseline resolution and coelution of compounds with a different central atom can be resolved using the time-resolved acquisition software of the VG PlasmaQuad, that allows monitoring several m/z positions by moving rapidly between them. Fig. 9b also demonstrates the ICP-MS capability to detect selected isotopes

and the potential to obtain multielement chromatograms.

CONCLUSIONS

Control of the temperature for the SFC-ICP-MS interface is vitally important, while variations for the detector temperature for SFC-FID, in the same range of temperatures (215 to 350°C), do not affect the results. Fluctuations in the transfer line temperature for the SFC-ICP-MS system is the main source of peak broadening. Better resolution among organotins is obtained in SFC-FID at a column temperature of 75°C; while in SFC-ICP-MS the best results (but non-baseline resolution between TrPT-Cl and TPT) is obtained at 50°C. The use of a 4-m column improves separation, and baseline resolution is obtained among tri- and tetraorganotins in both SFC-FID and SFC-ICP-MS. The major advantages of FID are low cost and ease of operation, while ICP-MS as a detector for SFC is more sensitive and selective than FID. In addition ICP-MS allows the use of modifiers. Application of the technique for the analysis of real samples, will yield more interferences by SFC-FID than by SFC-ICP-MS since FID is an universal detector and ICP-MS is an element-

selective detector. Thus a cleaner and more conclusive chromatogram will be obtained by using SFC–ICP–MS.

ACKNOWLEDGEMENTS

The authors are grateful to the National Institute of Environmental Health Science for support through research grants ES-03221 and ES-04908. We also acknowledge the NIH-BRS Shared Instruments Grants program for providing the VG PlasmaQuad through grant number S10 RR02714. VG Elemental and Lee Scientific are credited for providing partial instrument support. Special thanks to Uma Kumar and Jeff Giglio for helping with the manuscript.

REFERENCES

- J.C. Fjeldsted and M.L. Lee, *Anal. Chem.*, 56 (1984) 619A.
- C.M. White and R.K. Houck, *J. High Resolut. Chromatogr. Chromatogr. Commun.*, 9 (1986) 4.
- P.J. Schoenmakers and F.C.C.J.C. Verhoeven, *Trends Anal. Chem.*, 6 (1987) 10.
- R.D. Smith, B.W. Wright and C.R. Yonker, *Anal. Chem.*, 60 (1988) 1323A.
- M.L. Lee and K.E. Markides (Editors), *Analytical Supercritical Fluid Chromatography and Extraction*, Chromatography Conferences, Provo, UT, 1990.
- D.W. Later, D.J. Bornhop, E.D. Lee, J.D. Henion and R.C. Wieboldt, *LC · GC*, 5 (1987) 804.
- D.J. Bornhop and J.G. Wangsgaard, *J. Chromatogr. Sci.*, 27 (1989) 293.
- B.E. Richter, D.J. Bornhop, J.T. Swanson, J.G. Wangsgaard and M.R. Andersen, *J. Chromatogr. Sci.*, 27 (1989) 303.
- J.C. Fjeldsted, R.C. Kong and M.L. Lee, *J. Chromatogr.*, 279 (1983) 449.
- M.A. Morrissey and H.H. Hill, Jr., *J. High Resolut. Chromatogr. Chromatogr. Commun.*, 11 (1988) 375.
- L.A. Pekay and S.V. Olesik, *Anal. Chem.*, 61 (1989) 2616.
- H-C.K. Chang and L.T. Taylor, *J. Chromatogr. Sci.*, 28 (1990) 29.
- W.R. West and M.L. Lee, *J. High Resolut. Chromatogr. Chromatogr. Commun.*, 9 (1986) 161.
- E.R. Campbell and B.E. Richter, *LC · GC*, 10 (1992) 40.
- K.D. Bartle, M.W. Raynor, A.A. Clifford, I.L. Davies, J.P. Kithinji, G.F. Shilstone, J.M. Chalmers and B.W. Cook, *J. Chromatogr. Sci.*, 27 (1989) 283.
- P.J. Arpino, J. Cousin and J. Higgins, *Trends Anal. Chem.*, 6 (1987) 69.
- A.J. Berry, D.E. Games, I.C. Mylchreest, J.R. Perkins and S. Pleasance, *J. High Resolut. Chromatogr. Chromatogr. Commun.*, 11 (1988) 61.
- J.D. Pinkston, G.D. Owens, L.J. Burkes, T.E. Delaney, D.S. Millington and D.A. Maltby, *Anal. Chem.*, 60 (1988) 962.
- R.J. Skelton, Jr., P.B. Farnsworth, K.E. Markides and M.L. Lee, *Anal. Chem.*, 61 (1989) 1815.
- P.C. Uden (Editor), *Element-Specific Chromatographic Detection by Atomic Emission Spectroscopy (ACS Symposium Series, No. 479)*, American Chemical Society, Washington, DC, 1992, p. 19.
- C.B. Motley, M. Ashraf-Khorassani and G.L. Long, *Appl. Spectrosc.*, 43 (1989) 737.
- M. Ashraf-Khorassani, J.W. Hellgeth and L.T. Taylor, *Anal. Chem.*, 59 (1987) 2077.
- C. Fujimoto, H. Yoshida and K. Jinno, *J. Microcol. Sep.*, 1 (1989) 19.
- W.L. Shen, N.P. Vela, B.S. Sheppard and J.A. Caruso, *Anal. Chem.*, 63 (1991) 1491.
- N.P. Vela and J.A. Caruso, *J. Anal. At. Spectrom.*, 7 (1992) 971.
- P.G. Harrison, in P.G. Harrison (Editor), *Chemistry of Tin*, Chapman & Hall, New York, 1989, p. 358.
- R.M. Harrison and S. Rapsomanikis, in R.M. Harrison and S. Rapsomanikis (Editors), *Environmental Analysis using Chromatography Interfaced with Atomic Spectroscopy*, Wiley, New York, 1989, p. 189.
- O. Evans, B.J. Jacobs and A.I. Cohen, *Analyst*, 116 (1991) 15.
- T. Tsuda, H. Nakaniski, S. Aoki and J. Takebayashi, *J. Chromatogr.*, 387 (1987) 361.
- J.J. Sullivan, J.D. Torkelson, M.M. Wekell, T.A. Hollingworth, W.L. Saxton and G.A. Miller, *Anal. Chem.*, 60 (1988) 626.
- S. Ohhira and H. Matsui, *J. Chromatogr.*, 525 (1990) 105.
- K.W.M. Siu, P.S. Maxwell and S.S. Berman, *J. Chromatogr.*, 475 (1989) 373.
- M.O. Stallard, S.Y. Cola and C.A. Dooley, *J. Organomet. Chem.*, 3 (1989) 105.
- I.S. Krull, K.W. Panaro, J. Noonan and D. Erickson, *J. Organomet. Chem.*, 3 (1989) 295.
- G.B. Jiang, P.S. Maxwell, K.W.M. Siu, X.T. Loung and S.S. Berman, *Anal. Chem.*, 63 (1991) 1506.
- Y.K. Chau, P.T.S. Wong, G.A. Bengert and J. Yaromich, *Chem. Speciation Bioavailability*, 1 (1989) 151.
- V. Desauziers, F. Leguille, M. Astruc and R. Pinel, *J. Organomet. Chem.*, 3 (1989) 469.
- H. Suyani, J. Creed and J.A. Caruso, *J. Anal. At. Spectrom.*, 4 (1989) 777.
- E.J. Parks, F.E. Brinckman, K.L. Jewett, W.R. Blair and C.S. Weiss, *Appl. Organomet. Chem.*, 2 (1988) 441.
- A.P. Walton, G.T. Wei, Z. Liang, R. Michel and J.B. Morris, *Anal. Chem.*, 63 (1991) 232.
- H. Suyani, J. Creed, T. Davidson and J.A. Caruso, *J. Chromatogr. Sci.*, 27 (1989) 139.
- H. Suyani, D. Heitkemper, J. Creed and J.A. Caruso, *Appl. Spectrosc.*, 43 (1989) 962.

Characterization of fuels by multi-dimensional supercritical fluid chromatography and supercritical fluid chromatography–mass spectrometry

P.E. Andersson, M. Demirbüker and L.G. Blomberg*

Department of Analytical Chemistry, Arrhenius Laboratories for Natural Sciences, Stockholm University, S-106 91 Stockholm (Sweden)

(First received December 24th, 1992; revised manuscript received March 23rd, 1993)

ABSTRACT

A multi-dimensional supercritical fluid chromatographic (SFC) system was evaluated for the determination of saturated compounds, alkenes, mono-, di- and triaromatics and polar compounds in diesel fuel distillates. The system consisted of three packed microcolumns, which were packed with cyano-modified silica, silica and *in situ* silver ion-impregnated cation exchanger. Further, an interface for SFC–electron impact MS was constructed. The application of direct fluid introduction was possible when packed microcolumns of 50 μm I.D. were employed. The different groups of organic compounds were readily separated, with the exception of alkanes/alkenes and monoaromatics. This separation became increasingly incomplete as the boiling range of the distillates was increased. Using SFC–MS, it was found that the lack of baseline separation depended solely on the tailing of the alkane/alkene peak. However, for most diesel distillates, only a minor part of the alkane/alkene peak co-eluted with the monoaromatics. In addition, examination by SFC–MS provided data for the proper selection of integration limits. The determination of aromatics was in good agreement with the results obtained using the HPLC method IP 391/90.

INTRODUCTION

It has been demonstrated that there may be a strong correlation between the composition of a fuel and the exhaust that is formed on combustion [1]. In this context, chemical characterization of fuels has become of increasing importance. Several methods have been used for such characterizations [2]; however, the most promising results in recent years have been achieved by supercritical fluid chromatography (SFC) [3–13].

In general, the chromatographic analysis concerns the contents of some different groups of hydrocarbons, *e.g.*, alkanes, alkenes, mono-, di- and triaromatics and polar compounds. For such a group separation, SFC in a multi-column

mode is very suitable [2–4,6,7,10,12]. Further, quantification in such systems is facilitated by the use of flame ionization detection (FID).

The objective of this work was to evaluate and improve the performance of a multi-dimensional SFC system for the analysis of diesel fuels. A satisfactory separation of alkanes/alkenes from monoaromatics was, in most instances, achieved on columns packed with silica of pore size 60 Å and particle size 4 μm . For distillates having a broad boiling range, the separation became less complete. In this work, the composition of the co-eluting section of the chromatogram and the separation of the different classes of aromatics was studied by SFC–MS. This study was intended to serve as a basis for the selection of proper switching times in the multi-dimensional system and to establish the appropriate integration limits for quantitative analysis. Further, the

* Corresponding author.

occurrence in diesel fuels of some other types of compounds, *e.g.*, biphenyls and dibenzothiophenes, was examined by SFC–MS.

EXPERIMENTAL

Instrumentation and columns

The analytical system consisted of a Lee Scientific (Salt Lake City, UT, USA) 600 Series SFC instrument, connected to an ELDS (Kungshög, Sweden) data system. Three different columns were used, the first being packed with Deltabond-SFC, cyano-bonded, 5 μm (Keystone Scientific, Bellefonte, PA, USA), length 25 mm, the second with Superspher Si 60, 4 μm (Merck, Darmstadt, Germany), length 290 mm, and the third with Nucleosil 5 SA (Macherey–Nagel, Düren, Germany), impregnated *in situ* with AgNO_3 , length 100 mm. All these columns had an I.D. of 250 μm . The columns were connected to the injector, two Valco (Houston, TX, USA) N6W six-port switching valves and the flame ionization detector by means of fused-silica capillary tubing, of 22 μm I.D. (Polymicro Technology, Phoenix, AZ, USA). A frit restrictor (Lee Scientific) (50 μm I.D.), adjusted to give a linear flow-rate of 5.5 mm/s, was used. Carbon dioxide of SFC grade (Scott Specialty Gases, Plumsteadville, PA, USA) was used as the mobile phase. Samples were introduced without dilution using a 60-nl internal sample loop valve (Valco). A splitting ratio of 1:1 and a timed split of 0.2 s were used.

Column preparation

Columns were prepared from fused-silica capillary tubing, 250 μm I.D. and 430 μm O.D. or 50 μm I.D. and 375 μm O.D. (Polymicro Technology). The columns were packed using a slurry packing technique, the packing material being suspended in a solvent [toluene–cyclohexanol (4:5, v/v)] for the cation exchanger and acetonitrile for CN-silica and silica; generally, 0.25 g of packing material was slurried in 2.5 ml of solvent. The slurry was transferred to a packing reservoir that could be magnetically stirred, thus applying an approach suggested by Kennedy and Jorgenson [14]. The reservoir was pressurized with acetonitrile to 350 atm (1 atm =

101 325 Pa); packing was performed downwards using a Varian (Walnut Creek, CA, USA) Model 8500 syringe pump. During packing, the bed was supported by a glass-fibre filter, which in turn was supported by a piece of fused-silica capillary (20 mm \times 100 μm I.D.). The supporting capillary was attached to the column by MVSU/004 and MDGF/005 graphite ferrule mini-unions (SGE, Ringwood, Victoria, Australia). Polyimide ferrules (FS.25; Valco) could also be used, but graphite ferrules are less expensive and they can be used three or four times. After packing, a glass-fibre filter was applied to the capillary on top of the packing. The filter was kept firmly attached to the packed bed by the injector transfer line, which was attached by mini-unions (SGE). Similarly, the detector transfer line was attached to the column outlet. The cation exchanger was modified with AgNO_3 as described previously [15]. Finally, the columns were dried in the chromatograph under carbon dioxide at 275 atm and 115°C.

The preparation of columns of I.D. 50 μm was done in the same way, except that the glass-fibre filter at the column end was secured between the column and a butt-connected capillary. Further, as the packed bed was physically very stable, it was unnecessary to use a filter on the injector side.

In columns packed with silica, the bed had to be compacted in order to achieve sufficient physical stability. This was accomplished by treatment with carbon dioxide at 65°C and 300 atm. After the treatment, depressurization was carried out very gently, to avoid disturbing the bed. The pressure was thus released overnight through the split. Compaction of the bed in columns packed with cation exchanger was achieved by water treatment. If necessary, the columns were shortened after compaction.

Samples

A series of diesel distillates obtained from BP International (Sunbury-on-Thames, UK) were analysed.

Conditions

Separations were performed at 375 atm and 75°C (0.81 g/ml). Injection of the sample was on

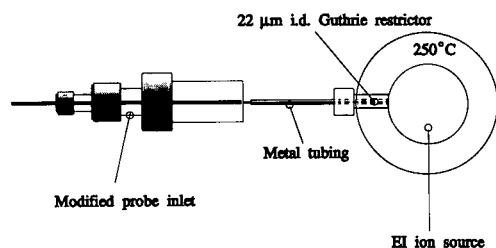


Fig. 1. Schematic diagram of SFC-MS interface.

the cyano-bonded column, where polar compounds were retained; aromatics were retained on the silica column, while alkanes and alkenes were retained on the silver-impregnated column. The last column was then switched out of the system and the aromatics were eluted from the silica column to the detector. Next, the polar compounds were back-flushed from the cyano-bonded column, after which the saturates were eluted from the silver-impregnated column. Finally, the alkenes were back-flushed from the silver-impregnated column. Peak areas (%) were used for quantification.

SFC-MS

SFC-MS was performed on a Lee Scientific 600 Series instrument connected to a Jeol JMS-D 300 magnetic sector instrument. A simple interface via the probe inlet was used for the connection (Fig. 1). The rod of the interface was heated by the ion source heater. Capillaries (350 mm \times 50 μ m I.D.) packed with Superspher Si 60, 4 μ m (Merck), were used for the separation. The restrictor was of the Guthrie type [16], prepared from a piece of fused-silica capillary of 22 μ m I.D. The conditions were 50°C and 220 atm (0.81 g/ml). Injection was by timed split (0.07 s) and a split of 1:20 was applied. Electron impact (EI) ionization at 70 eV was used, and the ion source temperature was 250°C. Masses were scanned over the m/z range 52–400, scanning time 1 s.

RESULTS AND DISCUSSION

Packed bed stability

Back-flushing is a precondition for the successful performance of the present multi-column system. Difficulties have been reported concern-

ing the use of packed microcolumns in the back-flush mode. Skaar *et al.* [10] reported that their packed capillary columns did not withstand alternating flow directions, and Hirata [17] proposed that back-flushing should be avoided for packed capillary columns. Compaction of the bed when the column is being used is a major reason for poor bed stability. This effect can be eliminated by proper column conditioning. After such a conditioning, the bed should be secured by a suitable end fitting. Compaction of the bed by means of water treatment has been described by Konishi *et al.* [18].

The physical stability of the packed bed is considerably increased when the ratio of column and particle diameters is decreased. Capillary columns having an I.D. of 50 μ m and which are packed with 4- or 5- μ m particles can thus be attached to the injector in the same fashion as 50- μ m open-tubular columns. However, as the first section of the column would then be situated outside the oven on the Lee Scientific instrument, we preferred to use a transfer capillary also in this instance.

Chromatographic system

A column packed with cyano-modified silica was incorporated in the system. This column protects the silica column from analytes that would be irreversibly adsorbed. Further, this column facilitates the elution of polar compounds by back-flushing. This has been demonstrated previously by Greibrokk and co-workers [4,6,10].

If true baseline separation is not achieved, analytes will be entrained in the transfer capillary. In the present system, this will happen after the first switch (Fig. 2). The loop which is closed in position B will contain sample components. Before applying position C, the system is switched to position A for 4 s, and the sample contained in the transfer capillary will thereby be transferred into the silver-impregnated column. Such a double switch results in two small switch peaks (Fig. 3). Narrow-bore transfer capillaries of 22 μ m I.D. were employed in order to diminish the dead volumes. As a consequence of the extra time in position A, the length of the silver-impregnated column had to be increased

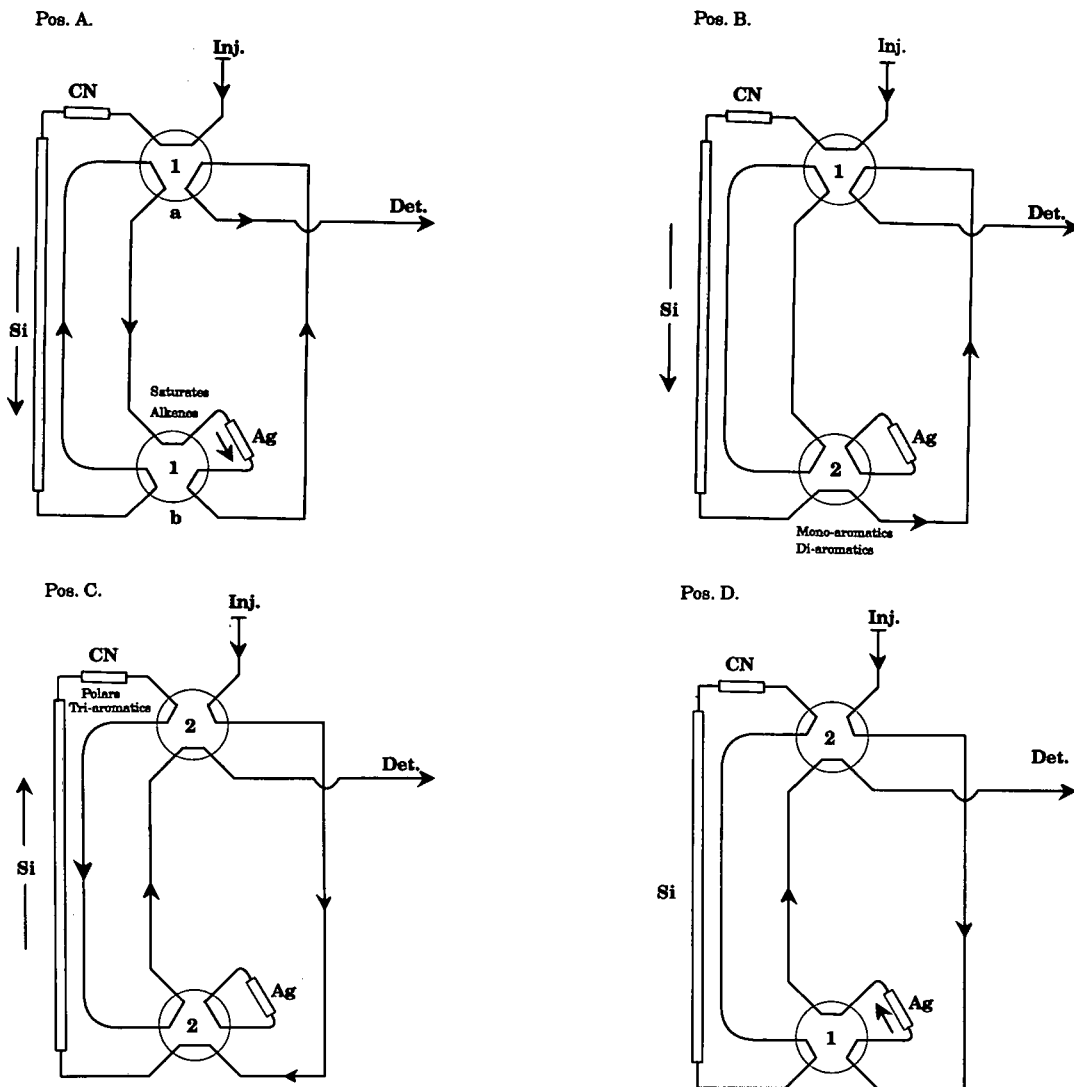


Fig. 2. Schematic diagram of the column-switching system. (A) Separation on the CN and Si columns, polar compounds retained on the CN column, saturates and alkenes transferred to the Ag column; (B) aromatics transferred from Si column to flame ionization detector; (C) polar compounds back-flushed from the CN column; (A) saturates eluted from the Ag column; (D) alkenes back-flushed from the Ag column.

to prevent elution of alkanes at this time. As a result, it was necessary to increase the column temperature in order to ensure the proper elution of the alkenes from the silver-impregnated column. The temperature was thus increased to 75°C, and to maintain the density at 0.81 g/ml the pressure was increased to 375 atm.

When switching from position C to A, both valves had to be switched. In order to prevent back-flushing of the silver-impregnated column,

valve a was switched just before valve b, resulting in double switch peaks (Fig. 3). Finally, switching to position D led to a small elevation of the baseline (Fig. 3). This can be explained by the decrease in pressure drop over the system.

Mass spectrometry

The separation achieved on the column packed with silica was studied by EI-MS. The purpose was to obtain a basis for column switch-

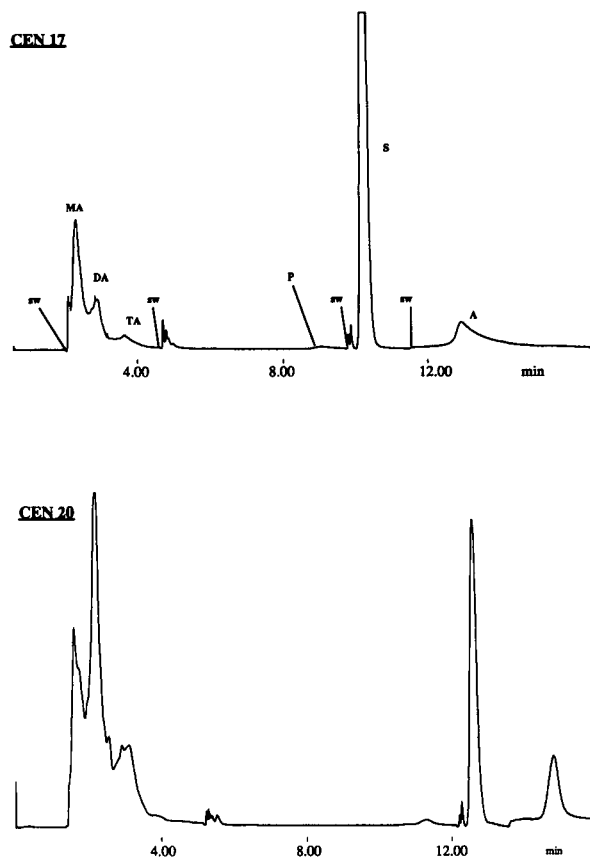


Fig. 3. Supercritical fluid chromatogram (FID) of two diesel fuels, CEN 17 and 20, obtained with the coupled system. Columns: fused silica (25 mm \times 0.25 mm I.D.), packed with Deltabond-SFC, cyano-bonded, 5 μ m; fused silica (290 mm \times 0.25 mm I.D.), packed with Superspher Si 60, 4 μ m; fused silica (100 mm \times 0.250 mm I.D.), packed with Nucleosil 5 SA and impregnated *in situ* with AgNO₃. Mobile phase, carbon dioxide at 75°C and 375 atm. Peaks: MA = monoaromatics; DA = diaromatics; TA = triaromatics; P = polar compounds; S = saturated compounds; A = alkenes. Switching points are indicated by sw.

ing and selection of integration limits. Further, it was of interest to demonstrate the presence of some different types of aromatics in the fuels.

Polycyclic aromatic compounds have been extensively studied by GC-MS [19] and SFC-MS has been applied to some extent [8,20,21]. For our purposes, it was necessary to design a system for SFC-MS that would give EI mass spectra. For the connection of open-tubular SFC with MS, it has been reported that the ion source pressure will become too high at elevated column pressures [22]. As a consequence, the

sensitivity was much decreased, and chemical ionization (CI) took place in addition to EI, thus leading to mixed EI and mass CI spectra. Some different attempts have been made to solve this problem. Lower mobile phase flow-rates have thus been applied [23], a split between the column and the mass spectrometer has been used [23–25], the MS pumping has been improved [26] or a moving belt technique has been applied [27]. The approach taken in this work was to apply packed narrow-bore separation columns that would give extremely low flow-rates. The columns used here give a flow-rate of expanded carbon dioxide of *ca.* 50 μ l/min (at atmospheric pressure). With such low flow-rates, the heating of the restrictor can be performed in a very simple way. Further, the ion source pressure was, without instrument modifications, kept at $1.8 \cdot 10^{-5}$ Torr (1 Torr = 133.322 Pa), thus providing EI conditions. The exit of the restrictor was placed about 2 mm from the ion source. When the restrictor protruded into the ion source, CO₂ clustering was observed. The heating was obviously unsatisfactory in this instance.

Selection of switching points

As alkanes/alkenes and monoaromatics are not fully separated, the selection of the switching point may be critical. In diesel distillates, having a broad range of boiling points, highly substituted monoaromatics and long-chain alkanes will co-elute. The broader the boiling range, the poorer the separation will be.

In order to investigate the nature of the overlapping compounds, the separation on a column packed with silica was studied by SFC-MS. It was found that, for broad distillates, alkanes/alkenes were, to a small extent, eluted after the valley between the peaks, and no part of the monoaromatics tended to be eluted before that valley (Fig. 4). For this type of distillate, switching in the valley would therefore, in quantitative analysis, lead to too high values of the content of monoaromatics. It should be noted, however, that the alkane/alkene peak in Fig. 4 is high and the degree of overlap, when using the present stationary phase, is relatively small. The switching has to be made on the basis of time only. A UV detector could be installed after the column, although when the detector responds to

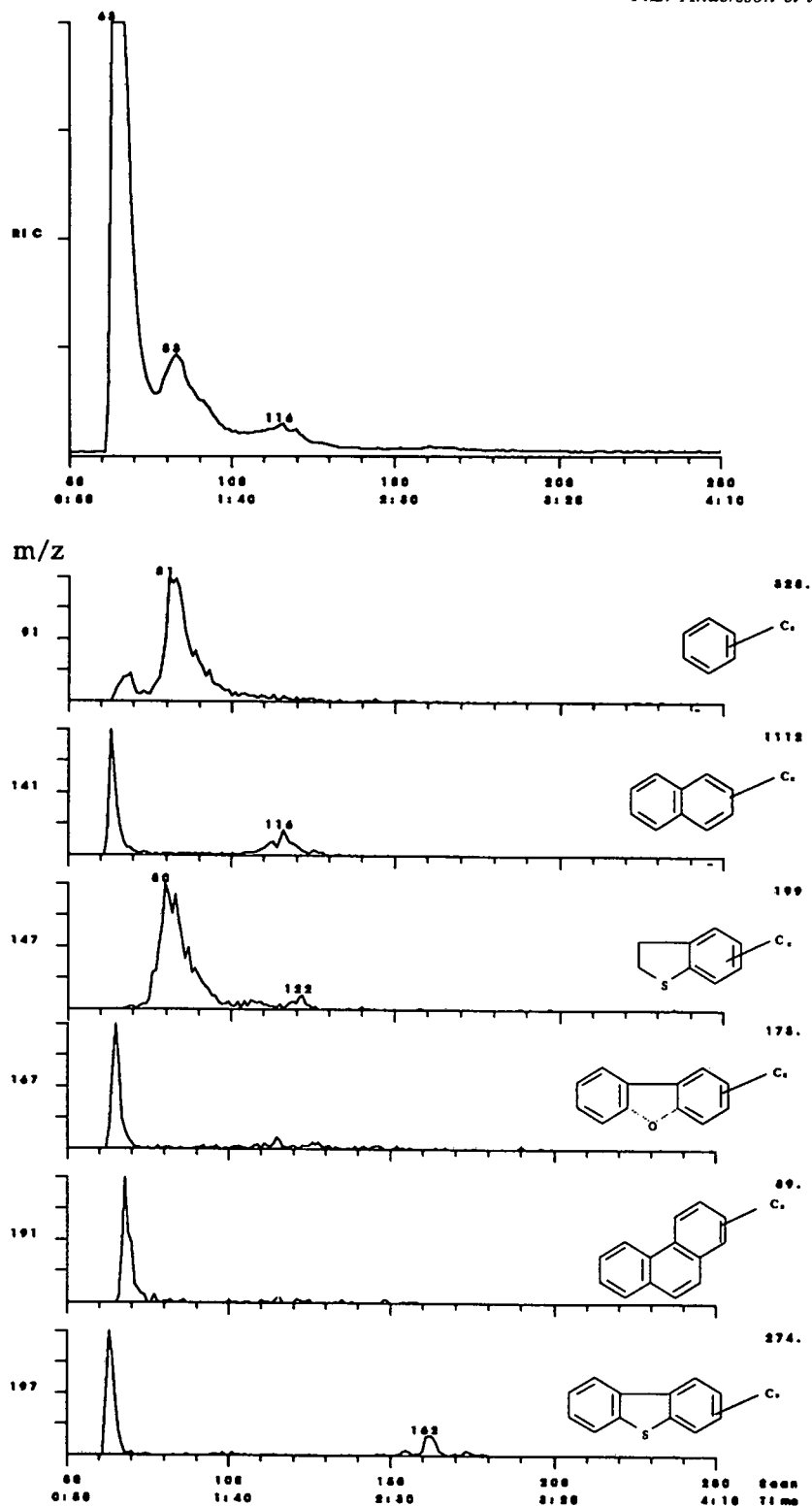


Fig. 4. Total ionization chromatogram and mass chromatograms of a diesel fuel (CEN 17) obtained by SFC-MS. Column, fused silica (350 mm \times 50 μ m I.D.) packed with Superspher Si 60, 4 μ m. Mobile phase, carbon dioxide at 50°C and 220 atm. Electron impact ionization at 70 eV; ion source temperature, 250°C. Time in min:s.

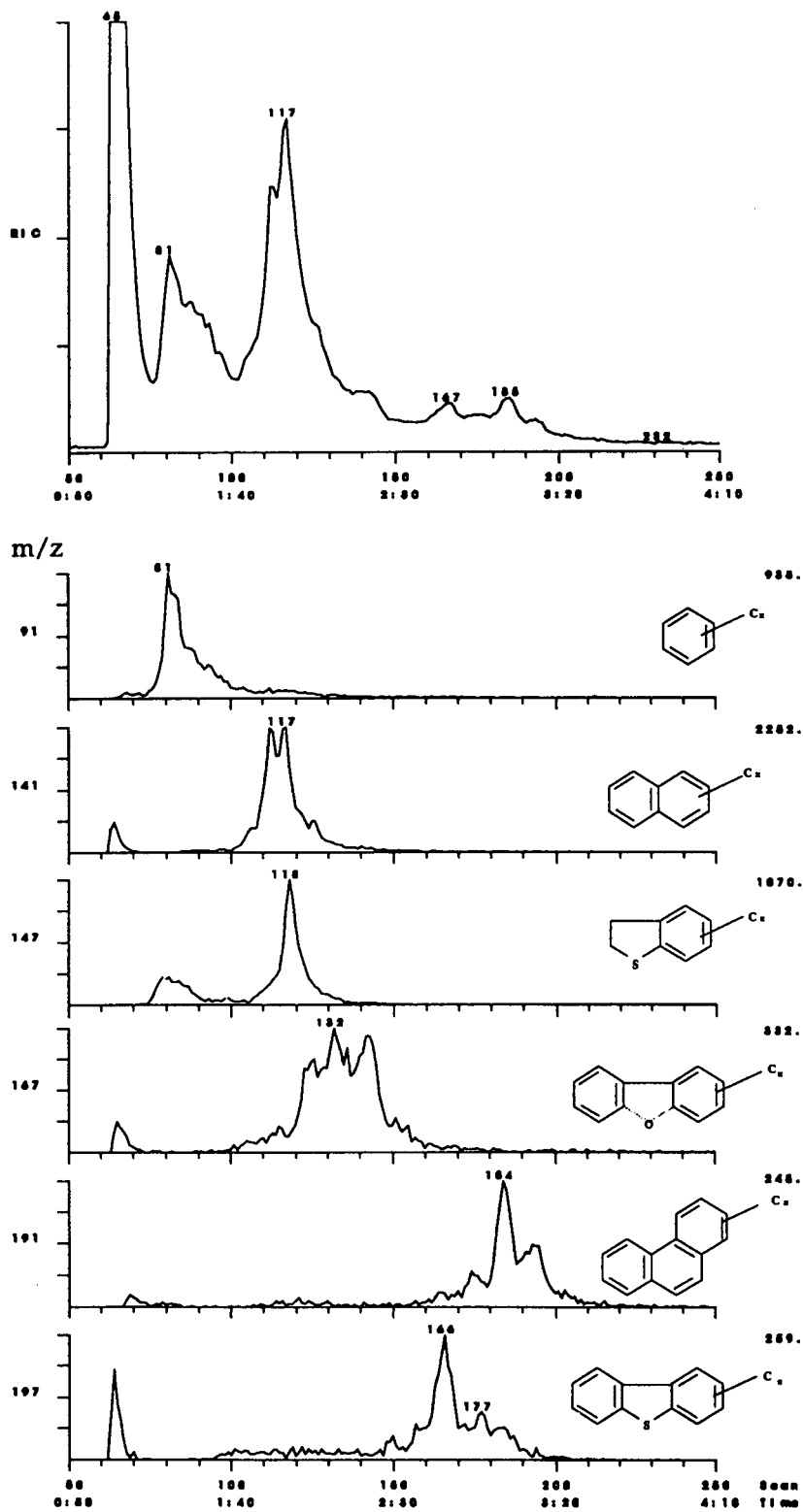


Fig. 5. Total ionization chromatogram and mass chromatograms of a diesel fuel (CEN 20) obtained by SFC-MS. Column and conditions as in Fig. 4.

the first aromatics it is already too late for switching.

Selection of integration limits for quantitative analysis

In order to establish proper integration limits for the determination of aromatics, the separation was studied by SFC–MS (Fig. 5). There was almost no overlap between mono- and diaromatics. For practical reasons, the same conditions could not be applied with SFC–MS as

with SFC–FID. However, the conditions applied with SFC–FID resulted in the most complete separations. In samples containing relatively large amounts of high-boiling substances, several minor peaks could be discerned after the main peak emanating from diaromatics (Fig. 5). Mass spectrometric examination at m/z 147, 167 and 197 indicated the presence of several sub-groups of aromatics. These mass numbers are not totally selective [19], hence several peaks were observed in the mass chromatograms. Substances such as

TABLE I
COMPOSITIONS OF SOME GAS OILS OF THE DIESEL FUEL BOILING RANGE

Fuel	Components	HPLC (vol. %)	SFC–FID (mass%)
CEN 17	Monoaromatics	15.7	16.0
	Diaromatics	8.7	8.0
	Triaromatics	2.1	2.3
	Polar compounds		0.6
	Saturated compounds		65.8
	Alkenes		7.2
CEN 18	Monoaromatics	17.5	17.2
	Diaromatics	11.6	11.6
	Triaromatics	5.9	7.8 ^a
	Polar compounds		0.7
	Saturated compounds		55.4
	Alkenes		7.2
CEN 19	Monoaromatics	27.4	28.7
	Diaromatics	12.5	14.3
	Triaromatics	4.0	6.1
	Polar compounds		0.4
	Saturated compounds		46.6
	Alkenes		3.8
CEN 20	Monoaromatics	20.6	19.0
	Diaromatics	33.7	37.8 ^b
	Triaromatics	11.9	16.2 ^c
	Polar compounds		0.5
	Saturated compounds		19.6
	Alkenes		6.8
CEN 21	Monoaromatics	28.8	27.9
	Diaromatics	5.9	6.4
	Triaromatics	0.9	1.1
	Polar compounds		–
	Saturated compounds		56.8
	Alkenes		7.7

^a Gives a response at m/z 198, dibenzothiophenes and naphthothiophenes.

^b The value includes peaks, corresponding to 6.4 mass%, giving a response at m/z 167, biphenyls, acenaphthenes and dibenzofurans.

^c The value includes peaks, corresponding to 6.2 mass%, giving a response at m/z 198.

biphenyls, benzothiophenes and dibenzothiophenes were thus detected. When the retention of these compounds is known, their occurrence will be accounted for separately (Table I).

Comparison of methods

A series of samples of gas oils of the diesel fuel boiling range were analysed and the results were compared with those of aromatic-type (vol.%) analyses by HPLC (IP 391/90) [28]. Although our data are given in mass%, good agreement was found (Table I). The repeatability of the analysis by SFC was in the same range as reported previously [2]. The determination of compounds present at high and moderate concentrations thus gave a relative standard deviation (R.S.D.) of 1.5–2.4%, whereas minor components, typically polar compounds, gave R.S.D. \approx 11%. The precision of the HPLC method was poorer [28]. Further, SFC gives, as discussed earlier, shorter analysis times than HPLC [2]. The main drawback of HPLC in fuel analysis, however, is the lack of universal detectors. A refractive index detector is used in method 391/90, but the response of such a detector will vary greatly with the nature of the solutes. The merit of FID is that it provides a relatively uniform response for the organic compounds present in the fuels.

In this work, packed microcolumns were used. Using such columns, the costs of the stationary and mobile phases will be low. It seems that the main expense in the application of the present method will concern instrumentation.

ACKNOWLEDGEMENTS

This work was financially supported by Neste (Porvoo, Finland). Samples were kindly provided by Dr. I. Roberts (BP Research, Sunbury-on-Thames, UK). S. Hoffmann, S. Smith and A. Christensen are acknowledged for their contributions in the initial stages of the development of the SFC–MS interface.

REFERENCES

- 1 R. Westerholm and K-E. Egeback, *Impact of Fuels on Diesel Exhaust Emissions*, Report 3968, Swedish Environmental Protection Agency, Solna, 1991.

- 2 P.E. Andersson, M. Demirbükler and L.G. Blomberg, *J. Chromatogr.*, 595 (1992) 301.
- 3 T.A. Norris and M.G. Rawdon, *Anal. Chem.*, 56 (1984) 1767.
- 4 E. Lundanes and T. Greibrokk, *J. Chromatogr.*, 349 (1985) 439.
- 5 H.E. Schwartz and R.G. Brownlee, *J. Chromatogr.*, 353 (1986) 77.
- 6 E. Lundanes, B. Iversen and T. Greibrokk, *J. Chromatogr.*, 366 (1986) 391.
- 7 R.M. Campbell, N.M. Djordjevic, K.E. Markides and M.L. Lee, *Anal. Chem.*, 60 (1988) 356.
- 8 B.W. Wright, H.R. Udseth, E.K. Chess and R.D. Smith, *J. Chromatogr. Sci.*, 26 (1988) 228.
- 9 S.W. Lee, B.J. Fuhr, L.R. Holloway and C. Reichert, *Energy Fuels*, 3 (1989) 80.
- 10 H. Skaar, H.R. Norli, E. Lundanes and T. Greibrokk, *J. Microcol. Sep.*, 2 (1990) 222.
- 11 F.P. Di Sanzo and R.E. Yoder, *J. Chromatogr. Sci.*, 29 (1991) 4.
- 12 B.J. Fuhr, L.L. Klein, C. Reichert and S.W. Lee, *LC·GC Int.*, 4 No. 1 (1991) 36.
- 13 M. Ashraf-Khorassani, J.M. Levy and L.A. Dolata, *Am. Lab.*, 24 No. 8 (1992) 29.
- 14 R.T. Kennedy and J.W. Jorgenson, *Anal. Chem.*, 61 (1989) 1128.
- 15 M. Demirbükler and L.G. Blomberg, *J. Chromatogr.*, 550 (1991) 765.
- 16 E.J. Guthrie and H.E. Schwartz, *J. Chromatogr. Sci.*, 24 (1986) 236.
- 17 Y. Hirata, *J. Microcol. Sep.*, 2 (1990) 214.
- 18 M. Konishi, Y. Mori and T. Amano, *Anal. Chem.*, 57 (1985) 2235.
- 19 M.L. Lee, M.V. Novotny and K.D. Bartle, *Analytical Chemistry of Polycyclic Aromatic Compounds*, Academic Press, New York, 1981, pp. 242–289.
- 20 M.L. Lee and K.E. Markides (Editors), *Analytical Supercritical Fluid Chromatography and Extraction*, Chromatography Conferences, Provo, UT, 1990.
- 21 B.W. Wright, H.R. Udseth, R.D. Smith and R.N. Hazlett, *J. Chromatogr.*, 314 (1984) 253.
- 22 E.C. Huang, B.J. Jackson, K.E. Markides and M.L. Lee, *Chromatographia*, 25 (1988) 51.
- 23 H.C. Chung, J.C. Aldridge and D.S. Moore, *Anal. Instrum.*, 19, Nos. 2 and 3 (1990) 99.
- 24 G. Holzer, S. Deluca and K.J. Voorhes, *J. High Resolut. Chromatogr. Chromatogr. Commun.*, 8 (1985) 528.
- 25 M. Takeuchi and T. Saito, in K. Jinno (Editor), *Hyphenated Techniques in Supercritical Fluid Chromatography and Extraction (Journal of Chromatography Library, Vol. 53)*, Elsevier, Amsterdam 1992, pp. 47–63.
- 26 S.D. Zaugg, S.J. Deluca, G.U. Holzer and K.J. Voorhes, *J. High Resolut. Chromatogr. Chromatogr. Commun.*, 10 (1987) 100.
- 27 A.J. Berry, D.E. Games and J.R. Perkins, *J. Chromatogr.*, 363 (1986) 147.
- 28 *IP Standard Methods for Analysis and Testing of Petroleum Products*, Designation IP 391/90, Institute of Petroleum, London, 1990.

High-speed supercritical fluid extraction method for routine measurement of polycyclic aromatic hydrocarbons in environmental soils with dichloromethane as a static modifier

J. Dankers, M. Groenenboom, L.H.A. Scholtis and C. van der Heiden*

BCO Centrum voor Onderzoek BV, Bergschot 71, P.O. Box 2176, 4800 CD Breda (Netherlands)

(First received December 18th, 1992; revised manuscript received March 22nd, 1993)

ABSTRACT

Supercritical fluid extraction (SFE) modified for the high-speed and efficient extraction of polycyclic aromatic hydrocarbons (PAHs) from polluted soil samples was evaluated and shown to be usable in a routine setting. On starting SFE, a small amount of dichloromethane is added to a chemically dried and cryogenic-ground soil sample. The SFE extract is collected within 15–20 min and the PAHs are determined by HPLC equipped with fluorescence and UV detectors. Within-day and day-to-day reproducibilities were comparable to those obtained after a 4-h sample preparation including liquid–liquid extraction. A good correlation was found between the PAH concentrations measured after modified SFE and liquid–liquid extraction. Recoveries of samples spiked with PAHs were of the order of 100%. In two samples used in a quality control programme, PAH concentrations were similar to those obtained by eleven other laboratories. The modified SFE procedure fulfils the requirements of rapidity, high extraction efficiency and simple performance.

INTRODUCTION

Much progress has been made in the last 10 years in instrumental chromatographic techniques. However, extractions of organic compounds from solids are still performed in traditional ways (liquid–liquid partitioning, Soxhlet extraction, etc.). These extraction techniques are time consuming (5–6 h) for routine applications, require the use of large volumes of mostly toxic organic solvents, and produce substantial amounts of waste solvents, and loss of volatile compounds may occur during evaporation.

Supercritical fluids have physical properties, such as low viscosity, high solute diffusive power

and density-linked solvent strength, that make extraction selectivity and automation feasible. Therefore, supercritical fluid extraction (SFE) offers a promising alternative to traditional extraction techniques. Quantitative SFE procedures have already been reported for the extraction of various analytes from different matrices that are difficult to process [1–4]. SFE has been applied to the extraction of soil samples with and without a clean-up procedure [5], to sand samples spiked with nitroaromatic compounds, halo ethers and organochlorine pesticides, and to standard reference soils [6].

Attempts have been made to improve the extraction recoveries of the sixteen polycyclic aromatic hydrocarbons (PAHs) defined according to the US Environmental Protection Agency (EPA) from random samples of different types of

* Corresponding author.

environmental soils by combining SFE with mostly dynamic modifiers or alternative extraction fluids [6–9]. Nevertheless, time-consuming and exhaustive extraction procedures are required to achieve an extraction efficiency of 90% [10].

This paper describes the application of SFE in daily routine practice for the extraction of PAHs from environmental soils. The results demonstrate that the addition of small amounts of a “static” modifier, dichloromethane, to the cryogenic-ground sample immediately before SFE extraction is begun is essential to achieve quantitative results. Dichloromethane has the power to penetrate the soil particles and render PAHs soluble in order to obtain quantitative extraction even of high-molecular-mass analytes from soil matrices.

EXPERIMENTAL

Supercritical fluid extraction (SFE)

SFE was performed using special SFE-grade carbon dioxide (Scott Speciality Gases, Breda, Netherlands) on an ISCO (Lincoln, NE, USA) modular SFE Series 2000 system. This consists of a dual solvent-pumping system (Model 260D) for programmable modifier addition or constant solvent delivery and two dual-chamber extraction systems (Model SFX 2-10), operated in the constant-pressure mode. Rapid and efficient SFE of PAHs was obtained with settings of density 0.76 g/ml, pressure 350 atm and temperature 90°C. Flow-rates were controlled by *ca.* 30-cm capillary restrictors (fused-silica tubing of 50 μ m I.D.; Chrompack, Middelburg, Netherlands), resulting in pump flow-rates between 2 and 6 ml/min. SFE of PAHs was completed within 15–20 min. The capillary outlet was protected from blockage due to freezing of the extracted water by thermostating the collection vessel at 20°C. Extracted analytes were collected in a 15-ml conical vial (150 \times 15 mm) containing 2–5 ml of dichloromethane (organic residue grade).

Liquid–liquid extraction

PAHs were also isolated by means of liquid–liquid partition. Cryogenic-homogenized samples were extracted twice with 100 ml of light pet-

roleum (b.p. 30–60°C), evaporated with a Kuderna Danish apparatus and analysed under the same conditions according to the national standard procedure NEN 5731 [11].

Sample preparation

In order to obtain a representative sample, the sample material was cryogenic-ground and homogenized analogously to the national standard procedure NVN 5730 [11]. A minimum of 100 g of soil sample was chemically dried by adding dry sodium sulphate, chilled under liquid nitrogen, ground and sieved to less than 1-mm particles. Of this homogenate, 5 g were placed in a standard 10-ml sample cartridge. Immediately before SFE was started, 2 ml of dichloromethane was added to the homogenate.

HPLC analyses

HPLC analyses were performed on a Kratos Spectroflow 450 gradient system with serial fluorescence (HP 1046A) and UV detection (Kratos Spectroflow 757) under the following conditions: detection wavelength, fluorescence, 0–9 min, excitation at 275 nm, emission at 348 nm; 9–40 min, excitation at 254 nm, emission, 320 nm cut-off filter; UV absorbance, 230 nm.

The column used was Chromspher 5 PAH, stainless steel (150 \times 4.6 mm I.D.), thermostated at 30°C. The column was eluted with an acetonitrile–water gradient at a flow-rate of 1.5 ml/min. The gradient was started with 50% acetonitrile (HPLC reagent grade) for the first 6 min, subsequently linearly programmed to 73% acetonitrile at a rate of 1.4%/min (6–22 min), increased to 100% acetonitrile at a rate of 2.2%/min (22–35 min) and finally held at 100% acetonitrile for the last 5 min.

Blank sample material

Blank sample material was prepared by heating soil originating from a non-contaminated land area at 600°C.

Quality control samples (QC samples)

Samples from interlaboratory quality control programmes were obtained from Wageningen Agricultural University (Netherlands) and used to test the efficiency of the extraction method.

Reference material

A standard reference material solution, SRM 1647B (National Institute of Standards and Technology, Gaithersburg, MD, USA) containing the sixteen EPA chosen priority PAH pollutants at certified concentrations, was diluted to appropriate concentrations in acetonitrile for calibration and spiking purposes. Retene purified by HPLC (ICN Biomedicals, Zoetermeer, Netherlands) was added to all extracts as an internal standard for peak identification (relative retention times).

RESULTS

Parameter settings for SFE such as density, as a consequence of pressure and temperature choice, and carbon dioxide volume (extraction time and flow-rate) were investigated to achieve a high extraction output. The efficiency of SFE in extracting the sixteen PAHs must at least equal that of liquid-liquid extraction. The percentage ratios of the PAHs isolated from actual soil samples by SFE and by liquid-liquid extraction are presented in Fig. 1. The SFE recoveries are poor (ca. 30%) for PAHs with molecular masses greater than that of pyrene. The SFE

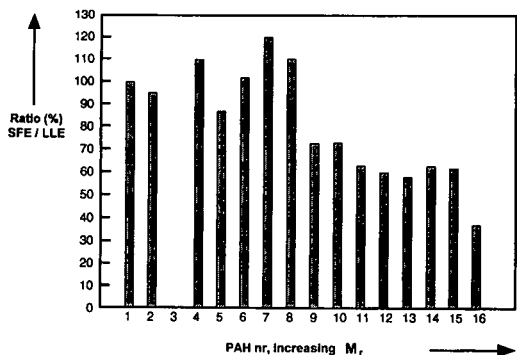


Fig. 1. Percentage ratios of sixteen individual PAHs from actual soil samples ($n = 6$) numbered according to increasing molecular mass (M_r) isolated by means of SFE and liquid-liquid extraction (LLE). 1 = Naphthalene; 2 = acenaphthylene; 3 = acenaphthene; 4 = fluorene; 5 = phenanthrene; 6 = anthracene; 7 = fluoranthene; 8 = pyrene; 9 = benzo[a]anthracene; 10 = chrysene; 11 = benzo[b]fluoranthene; 12 = benzo[k]fluoranthene; 13 = benzo[a]pyrene; 14 = dibenz[a,h]anthracene; 15 = benzo[ghi]perylene and 16 = indeno[1,2,3-cd]pyrene. SFE conditions: carbon dioxide, density 0.77 g/ml; pressure, 270 atm; temperature, 70°C; time, 30 min.

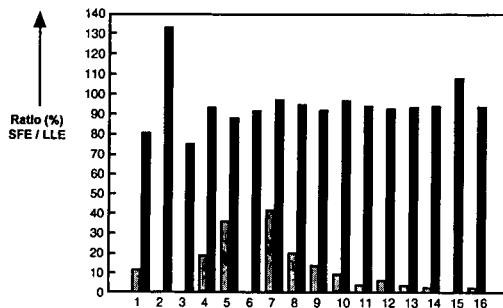


Fig. 2. Percentage ratios of sixteen PAHs determined in a random soil sample by means of HPLC after SFE with (black bars) and without (hatched bars) addition of the static modifier dichloromethane to the pretreated sample. SFE conditions: carbon dioxide, density 0.76 g/ml; pressure, 350 atm; temperature, 90°C; time, 15 min. Compounds as in Fig. 1.

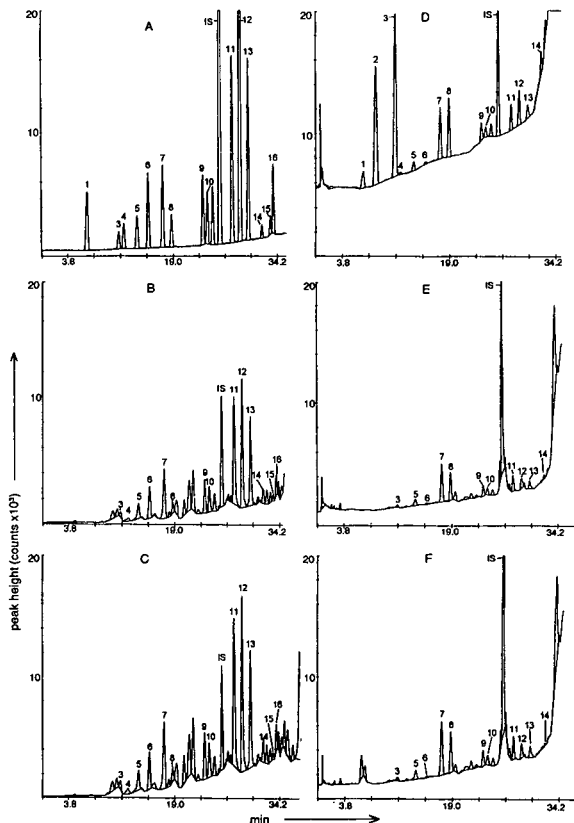


Fig. 3. Chromatograms of PAHs monitored with fluorescence detection from (A) an EPA standard sample, (B) a random soil sample obtained after SFE and (C) after liquid-liquid extraction with (D, E, F) their corresponding UV-monitored chromatograms.

parameter settings were set to values of carbon dioxide density 0.76 g/ml, pressure 350 atm and temperature 90°C. In the SFE procedure the dynamic modifier methanol was added. The results did not show a sufficient improvement, so a static modifier was tested. Dichloromethane was added to the cryogenic-ground sample immediately before SFE was started. Dichloromethane was also introduced as collecting solvent because of its higher solubility capacity than solvents such as acetonitrile or methanol. The SFE procedure could be ended after 15–20 min. Fig. 2 shows the percentage ratios of the 16 PAHs determined by HPLC after SFE with and without addition of dichloromethane as static modifier.

Chromatograms of the PAHs extracted from the EPA standard solution and from a random polluted soil sample are shown in Fig. 3. A good separation of the main PAHs in soil is obtained. The chromatographic patterns obtained after SFE and liquid–liquid extraction are fully comparable. Components isolated by means of SFE and interfering chromatographically with one or more of the individual PAHs are not observed.

Blank soil samples were spiked with PAHs at a level of 0.1 mg/kg. Recoveries of the individual PAHs ranged from 88 to 100% with a relative standard deviation of 2–15%.

The within-day and day-to-day reproducibilities were examined to establish the ruggedness of the SFE extraction procedure. In Table I, the results of the within-day and the day-to-day reproducibilities of PAHs determinations in two random samples are presented. With the exception of the three highest molecular mass PAHs with a low relative chromatographic response, the relative standard deviations of all other components are below 20%.

The PAHs were isolated from five random soil samples by SFE and by liquid–liquid extraction and analysed by HPLC. The PAH concentrations expressed in mg/kg dry mass were correlated. A good correlation was found ($n = 68$; regression coefficient = 0.914, y -axis intercept = 0.094 mg/kg dry mass, correlation coefficient = 0.959).

Two quality control samples from an inter-laboratory quality control programme contained PAHs at concentrations of 4 and 10 mg/kg dry mass. The PAHs were isolated from these sam-

TABLE I

WITHIN-DAY AND DAY-TO-DAY REPRODUCIBILITIES OF PAH COMPOUNDS, EXPRESSED IN mg/kg DRY MATERIAL, ESTABLISHED IN TWO RANDOM SAMPLES

Compound	Within-day						Day-to-day					
	Sample I ($n = 5$)			Sample II ($n = 5$)			Sample III ($n = 8$)			Sample IV ($n = 9$)		
	x	S.D.	R.S.D. (%)	x	S.D.	R.S.D. (%)	x	S.D.	R.S.D. (%)	x	S.D.	R.S.D. (%)
Naphthalene	0.32	0.06	20	9.2	1.6	17	0.18	0.04	20	7.6	1.5	20
Acenaphthylene	–	–	–	–	–	–	–	–	–	–	–	–
Acenaphthene	–	–	–	–	–	–	–	–	–	–	–	–
Fluorene	0.27	0.06	23	8.2	0.5	6	0.19	0.04	22	10.0	1.9	19
Phenanthrene	0.86	0.16	18	32.8	2.7	8	0.58	0.11	19	34.2	4.9	14
Anthracene	0.22	0.04	16	10.6	0.7	7	0.15	0.02	15	11.0	1.7	15
Fluoranthene	1.44	0.24	17	36.2	3.1	8	1.00	0.16	16	38.1	5.6	15
Pyrene	2.02	0.33	17	33.1	2.3	7	1.16	0.32	28	30.1	5.1	17
Benzo[<i>a</i>]anthracene	0.72	0.11	15	13.3	1.3	10	0.47	0.08	17	13.8	2.2	16
Chrysene	0.71	0.11	16	12.6	1.4	11	0.45	0.07	16	12.9	2.4	19
Benzo[<i>b</i>]fluoranthene	0.70	0.03	4	14.4	1.9	13	0.58	0.08	15	14.2	2.6	18
Benzo[<i>k</i>]fluoranthene	0.21	0.01	6	4.8	0.6	13	0.19	0.03	14	5.0	0.9	27
Benzo[<i>a</i>]pyrene	0.55	0.07	14	8.0	1.1	14	0.40	0.10	24	8.7	2.0	23
Dibenzo[<i>ah</i>]anthracene	1.05	0.17	16	23.1	3.5	15	0.56	0.18	33	19.5	5.2	27
Benzo[<i>ghi</i>]perylene	0.85	0.11	13	10.9	1.5	14	0.39	0.14	36	9.4	3.2	34
Indeno[1,2,3- <i>cd</i>]pyrene	0.23	0.03	14	2.9	0.4	15	0.24	0.04	16	4.1	1.3	33

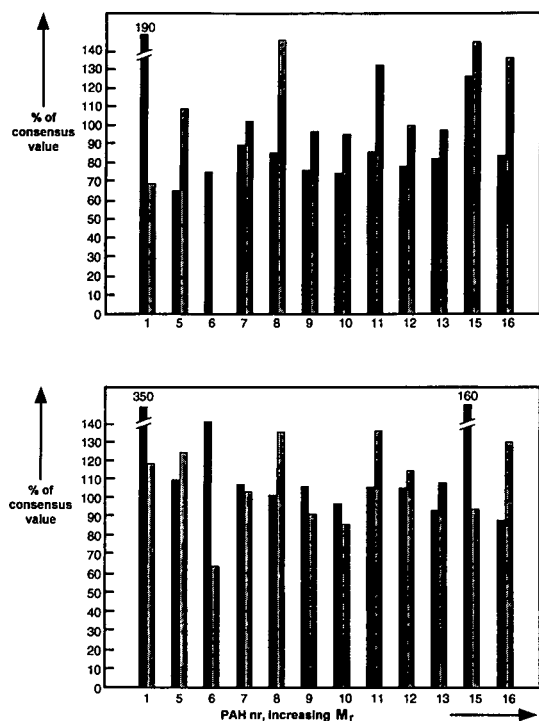


Fig. 4. Individual PAHs isolated from two quality control samples (top: 4 mg/kg dry mass; bottom: 10 mg/kg dry mass) by means of SFE (black bars) and liquid-liquid extraction (hatched bars) and expressed as percentages of the consensus value established by eleven independent laboratories. Compounds as in Fig. 1.

ples by SFE and liquid-liquid extraction. The PAHs were expressed as percentages of the consensus value of the concentrations established by the eleven participating laboratories (Fig. 4). The PAH concentrations measured after isolation by the modified SFE method in the extract are fully comparable with those obtained after a traditional extraction. Naphthalene is extracted even more efficiently by the modified SFE than by liquid-liquid extraction. It is known that loss of naphthalene may occur during evaporation after liquid-liquid extraction.

DISCUSSION

Soil clearance programmes demand new and modern adaptations of laboratory technology. PAH determinations should be capable of being performed rapidly in a routine setting with a low

error level. These requirements can only be fulfilled if robust methods for extraction and instrumental measurement (*e.g.*, HPLC) of PAHs are available. HPLC is widely accepted for the determination of individual PAHs. Although highly efficient, the extraction of PAHs still takes many hours and is consequently the rate-limiting step in PAH analyses.

High speed and efficiency in a routine setting might be feasible when SFE is performed under well defined conditions. These conditions include pretreatment of the sample, optimum settings of SFE and the addition and mode of application of a modifier.

Wet sample material can be successfully extracted by SFE provided that it is granular and the water content is less than 40%. However, cryogenic grinding of a soil sample chemically dried with sodium sulphate is recommended. Pretreatment of samples minimizes the matrix effects caused by differences in water content.

The selection of the density and carbon dioxide volume and the choice of the modifier and collection solvent together with the mode of application of the modifier are important factors in the successful isolation of PAHs by SFE. Flow-rates and cell geometry have negligible effects on the extraction efficiency. Inappropriate solvent trapping conditions may result in losses which are wrongly attributed to poor SFE efficiency [12].

In our experiments all sixteen individual EPA PAHs show comparable recoveries, even within the extraction time of 15–20 min. Obtaining a rapid extraction and high recoveries that are independent of the PAH molecular mass is the main problem in all SFE experiments. The extraction of benzo[*a*]pyrene, a high-molecular mass PAH, has been reported to require 2 h of exhaustive extraction (density 0.76 g/l, 350 atm, 90°C) to achieve an extraction recovery of 90% [10]. Also, the matrix may influence the recovery. Actual environmental soils appeared to show interaction forces between analytes and their matrices [7,8], *e.g.*, in diesel fuel contamination of clay-like material [13]. Many modifiers and modes of application have been tried to achieve acceptable recoveries of PAHs over the whole range of molecular masses. Under vari-

able experimental conditions, Lopez-Avila *et al.* [6] used toluene as a modifier. Nevertheless, they found a wide range of recoveries, especially of the high-molecular-mass PAHs.

Addition of methanol to the carbon dioxide improves the recoveries of some PAHs. However, the larger compounds are only partially extracted [14]. The extraction recovery of the high-molecular-mass PAHs can be improved by extending the extraction time, but this is not acceptable when a high-speed extraction is desirable. Owing to its polar character, the dynamic modifier methanol has been shown to extract the drying reagent, sodium sulphate, from the chemically dried samples, causing clogging problems in the capillary restrictor. Hence the use of methanol is very impracticable.

The less polar dichloromethane, added as a static modifier in very small volumes (2 ml), has been shown to give nearly 100% recoveries of the PAHs that are independent of their molecular mass, and within a very short extraction time (15–20 min).

The static modifier dichloromethane has the power to penetrate the soil particles and to render the soil aggregates soluble. In this way, contact between the particles and the extractant is strongly increased. A similar process might occur in the liquid–liquid extraction. This penetration of particles is probably also the explanation for the difference between the extraction yields of PAHs from spiked and actual samples (14). Consequently, in the extraction procedure presented here, hardly any difference was found between the PAH concentrations determined with the two extraction procedures.

SFE also has the advantage of reducing considerably the large volumes of organic extraction fluids needed in liquid–liquid extraction.

Finally, it may be concluded that the modified SFE procedure presented here fulfils all the requirements for use in daily routine practice,

viz., simplicity, rapid performance and a high extraction efficiency.

ACKNOWLEDGEMENTS

The authors thank Mrs. A.Ch.M. Cantrijn and Mr. M.J.H. Zodenkamp for their help in preparing the manuscript.

REFERENCES

- 1 C.A. Thomson and D.J. Chesney, *Anal. Chem.*, 64 (1992) 848.
- 2 R.M. Smith and M.D. Burford, *J. Chromatogr.*, 600 (1992) 175.
- 3 W.H. Griest, R.S. Ramsey, C.-H. Ho and W.M. Caldwell, *J. Chromatogr.*, 600 (1992) 273.
- 4 H.-B. Lee, T.E. Peart and R.L. Hong-You, *J. Chromatogr.*, 605 (1992) 109.
- 5 B. Wencławiak, C. Rathmann and A. Tenbie, *Fresenius' J. Anal. Chem.*, 344 (1992) 497.
- 6 V. Lopez-Avila and W.F. Beckert, in F.V. Bright and M.E.P. McNally (Editors), *Supercritical Fluid Technology—Theoretical and Applied Approaches to Analytical Chemistry (ACS Symposium Series, No. 488)*, American Chemical Society, Washington, D.C., 1992, Ch. 14, pp. 179–205.
- 7 J.W. Hills and H.H. Hill, *J. Chromatogr. Sci.*, 31 (1993) 6.
- 8 S.B. Hawthorne, J.J. Langenfeld, D.J. Miller and M.D. Burford, *Anal. Chem.*, 64 (1992) 1614.
- 9 T. Paschke, S.B. Hawthorne, D.J. Miller and B. Wencławiak, *J. Chromatogr.*, 609 (1992) 333.
- 10 L.J.D. Myer, J.H. Damian, P.B. Liescheski and J. Tehrani, in F.V. Bright and M.E.P. McNally (Editors), *Supercritical Fluid Technology—Theoretical and Applied Approaches to Analytical Chemistry (ACS Symposium Series, No. 488)*, American Chemical Society, Washington, D.C., 1992, Ch. 16, pp. 221–236.
- 11 *NNI Catalogus, Deel 1*, Nederlands Normalisatie Instituut (NNI), Delft, 1992, p. 376.
- 12 J.J. Langenfeld, M.D. Burford, S.B. Hawthorne and D.J. Miller, *J. Chromatogr.*, 594 (1992) 297.
- 13 A.P. Emery, S.N. Chesler and W.A. MacCrehan, *J. Chromatogr.*, 606 (1992) 221.
- 14 S.B. Hawthorne and D.J. Miller, *Anal. Chem.*, 57 (1987) 1705.

Isotachopheresis superimposed on capillary zone electrophoresis

J.L. Beckers

Laboratory of Instrumental Analysis, Eindhoven University of Technology, P.O. Box 513, 5600 MB Eindhoven (Netherlands)

(First received November 25th, 1992; revised manuscript received March 8th, 1993)

ABSTRACT

Applying isotachopheresis (ITP) superimposed on capillary zone electrophoresis (CZE), which will be denoted the ITP/CZE mode, components migrate in an ITP way on top of a background electrolyte. In such an ITP/CZE system the leading electrolyte consists of a mixture of an ionic species L_1 with a high mobility (the leading ion of the ITP system), an ionic species L_2 with low mobility (the co-ions of the ZE system) and buffering counter ions, whereas the terminating solution contains only the ionic species L_2 and the buffering counter ions. The zones of the components migrating in the ITP/CZE mode are very sharp owing to the self-correcting effect and the concentrations of the components are adapted to the concentration of the L_1 ions of the system. Calculated mobility windows are given, indicating which components can migrate in the ITP/CZE mode and features and possibilities of ITP/CZE are discussed on the basis of several electropherograms.

INTRODUCTION

Although capillary zone electrophoresis (CZE) [1,2] has been developed into a worthwhile analytical separation method with a remarkable separation power, useful in a variety of application fields, a severe drawback is the high detection limits. Especially for components present in a sample at low concentrations, large sample volumes have to be injected in order to introduce detectable amounts of components and therefore the sample components have to be concentrated to obtain high plate numbers and a good resolution. For this purpose, field amplification [3,4] or sample stacking [5,6] is often applied. These techniques can result, however, in a disastrous decrease in separation power [7], especially for large sample volumes.

Isotachopheresis (ITP) can also be used as preconcentration technique. A separate ITP system can be coupled to a separate CE system [8–10], through which compounds can be selected from the sample in the ITP system and introduced into the CZE system. Another way is

to convert an ITP system into a CZE system by filling the capillary partially with different electrolytes through which all the sample components move first in an ITP system and after some time in a CZE system [11]. In the conversion of an ITP system into a CZE system the choice of the electrolytes is limited, whereas components present in excess in a sample and concentrated at high concentrations in the ITP system can disturb the CZE system. Further, the narrow bands formed in the ITP mode at a high concentration broaden very quickly in the CZE mode owing to diffusion and electrodispersion and extra peak broadening [3] can occur owing to a mismatch in the electroosmotic flow (EOF) if the capillary is filled with different electrolytes. For these reasons, on-line preconcentration in ITP often gives scarcely better results than a simple sample stacking whereby the sample is introduced at a lower ionic strength than that of the background electrolyte. For components present at a low concentration in a complex matrix a concentration procedure often fails owing to the presence of a large excess of other components.

The fundamental aspect in applying the foregoing injection techniques is always how a trace component can be separated and concentrated from a complex matrix at high ionic strength. In some instances this problem can probably be solved by combining ITP and CZE in another way, which has not yet received attention, *viz.*, the principle of ITP superimposed on CZE, which will be denoted ITP/CZE to distinguish it from several other combinations of ITP and CZE, such as on-column transient and coupled-column ITP preconcentration in CZE [12] and the use of discontinuous buffer systems in CZE [13]. The basis of ITP/CZE can be found in ITP with two leading ions (a so-called 2L-ITP system) [14], whereby some components of a sample migrate in the ITP mode and others in the CZE mode, depending on the concentrations of the leading ions and the mobilities of the concerning ionic species.

In this work, the conditions under which ITP/CZE is possible were studied and some features and possibilities of ITP/CZE are discussed on the basis of several electropherograms.

THEORY

In CZE, the whole system is filled with a background electrolyte and sample components migrate in order of decreasing effective mobilities. In Fig. 1A, a schematic representation is given of the concentration profiles of the cationic species X, Y and Z migrating in a zone electrophoretic way in the separation compartment filled with the background electrolyte AB. Peaks will be diffuse owing to several peak-broadening effects such as electrodispersion and diffusion [15]. Especially when injecting long sampling zones, the sample components have to be concentrated in order to obtain a good separation and high plate numbers.

In a standard ITP electrolyte system [16], a leading ion L is chosen with an effective mobility higher than those of the sample components, whereas that of the terminating ion T must be lower than the latter. Components with an effective mobility higher than that of the leading ion or lower than that of the terminating ion will migrate in a zone electrophoretic way in the

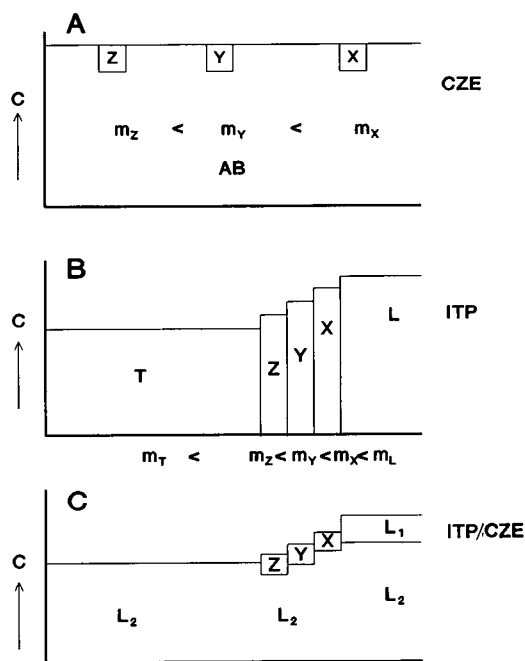


Fig. 1. Schematic representation of different modes in capillary electrophoresis. (A) In the CZE mode the whole system is filled with a background electrolyte AB and the cations X, Y and Z migrate in a zone electrophoretic way (from the left to the right-hand side) in order of decreasing mobilities. (B) In an ITP system the cations X, Y and Z migrate in consecutive zones between the leading ions L and terminating ions T. (C) In a 2L-ITP system the leading electrolyte contains two leading ions L_1 and L_2 . The ion with the lowest ionic mobility, L_2 , forms the terminating zone. The cations X, Y and Z migrate in consecutive zones in the ITP mode superimposed on a background electrolyte of L_2 and the counter ions in the so-called ITP/CZE mode.

leading or terminating electrolyte, respectively. All other components migrate in an ITP way between leading and terminating ions. The zone boundaries are sharp owing to the self-correction of the zones. The concentrations of all components migrating in the ITP more are adapted to that of the leading electrolyte. In Fig. 1B the concentration profiles of the different zones are schematically represented.

In an ITP system with two leading ions (a so-called 2L-ITP system), components behave in a similar way, on the understanding that not only the effective mobilities of the leading and terminating ions, but also the concentrations of the

two leading ions regulate the migration behaviour. In the model of a 2L-ITP system a leading electrolyte is used with two leading ions whereas the terminating electrolyte contains only that with the lowest effective mobility. The leading ion with the lowest effective mobility, L_2 , remains partially behind the leading ion with the highest mobility, L_1 , and creates a terminating L_2 zone with a fixed E gradient and specific zone resistance (SZR) [17], characterized by a specific R_E value [18]. Beckers and Everaerts [14] have already described a mathematical model for 2L-ITP systems and with this model it can be calculated whether components migrate in the ITP or the ZE mode.

Sample ions migrate in the ITP mode if the calculated value of the SZR or R_E values of the S/L_2 zone (the sample ions S always migrate in a mixed zone with L_2 ions) are smaller than those of the terminating zone L_2 (see Fig. 1C for the concentration profiles). In fact, an ITP system is created superimposed on a zone electrophoretic system of the L_2 ions and the counter ions, the so-called ITP/CZE mode.

Mobility windows in 2L-ITP systems

With the model of 2L-ITP [14], the R_E values of the terminating L_2 zone and sample zones can be calculated and the sample components migrate in the ITP/CZE mode if their R_E values are smaller than that of the L_2 zone. To demonstrate the features of a 2L-ITP system for negative ions, the calculated R_E values for the terminating L_2 zones are given (dashed lines) in Fig. 2 (right-hand scale) of (A) a leading electrolyte consisting of 0.01 M chloride as L_1 ions and varying concentrations of 2-(*N*-morpholino)ethanesulphonate (MES) as L_2 ions and (B) a leading electrolyte consisting of 0.01 M MES as L_2 ions and varying concentrations of chloride as L_1 ions. As terminating electrolyte 0.02 M MES was used. All electrolytes were adjusted to pH 6 by adding histidine. In Table I the pK values and mobilities at infinite dilution are given for the ionic species used in the calculations and experiments.

Further, we calculated with the mathematical model for 2L-ITP systems the mobilities (at infinite dilution) of components, with assumed

pK values of 3, which migrate in the ITP mode in these 2L-ITP systems. In Fig. 2A and B, the mobility windows for the components migrating in the ITP mode are indicated by the hatched areas (left-hand scale). The upper limit of the mobility window is always the mobility of the leading ion L_1 with the highest mobility (in this instance chloride), whereas the lower limit is determined by both the mobilities and the concentrations of L_1 and L_2 in the leading zone. This in contrast with standard ITP, where only the mobilities of the terminating ions are of importance. Beyond the lower and upper limits of the mobility window, ITP changes into CZE. The dashed lines labelled B give the R_E values for benzoic acid in the different systems. Because the R_E values of benzoic acid in Fig. 2A are always smaller than the R_E values of the terminating L_2 zone, it migrates in the ITP/CZE mode. This can also be concluded from its mobility of $-33.6 \cdot 10^{-5} \text{ cm}^2/\text{V} \cdot \text{s}$ that is covered by the mobility window. In all systems in Fig. 2B the R_E values of benzoic acid are larger than that of the terminating L_2 zone and it always migrates in the CZE mode.

The mobility window is reduced with decreasing values of the concentration of L_1 and increasing values of the concentration of L_2 and has a maximum width in the pure ITP mode (left-hand side of Fig. 2A with $[L_2] = 0 \text{ M}$ and $[L_1] = 0.01 \text{ M}$) and a minimum width in the pure CZE mode (right-hand side of Fig. 2B with $[L_2] = 0.01 \text{ M}$ and $[L_1] = 0 \text{ M}$). In fact, this mobility window indicates which components can migrate in an ITP system with leading ions L_1 superimposed on a background electrolyte consisting of L_2 and the counter ions. In the combined plot of calculated mobility windows (left-hand scale) and calculated R_E values (right-hand scale) of 2L-ITP systems the mobilities and R_E values are not linearly related.

For a further illustration of the features of ITP/CZE systems, the same parameters as in Fig. 2A and B are given in Fig. 2C and D for 2L-ITP systems consisting of various concentrations of an ionic species L_1 with a mobility of $-40 \cdot 10^{-5} \text{ cm}^2/\text{V} \cdot \text{s}$ and of L_2 with a mobility of $-20 \cdot 10^{-5} \text{ cm}^2/\text{V} \cdot \text{s}$ at a pH of 6 by adding histidine (assumed pK values of the sample

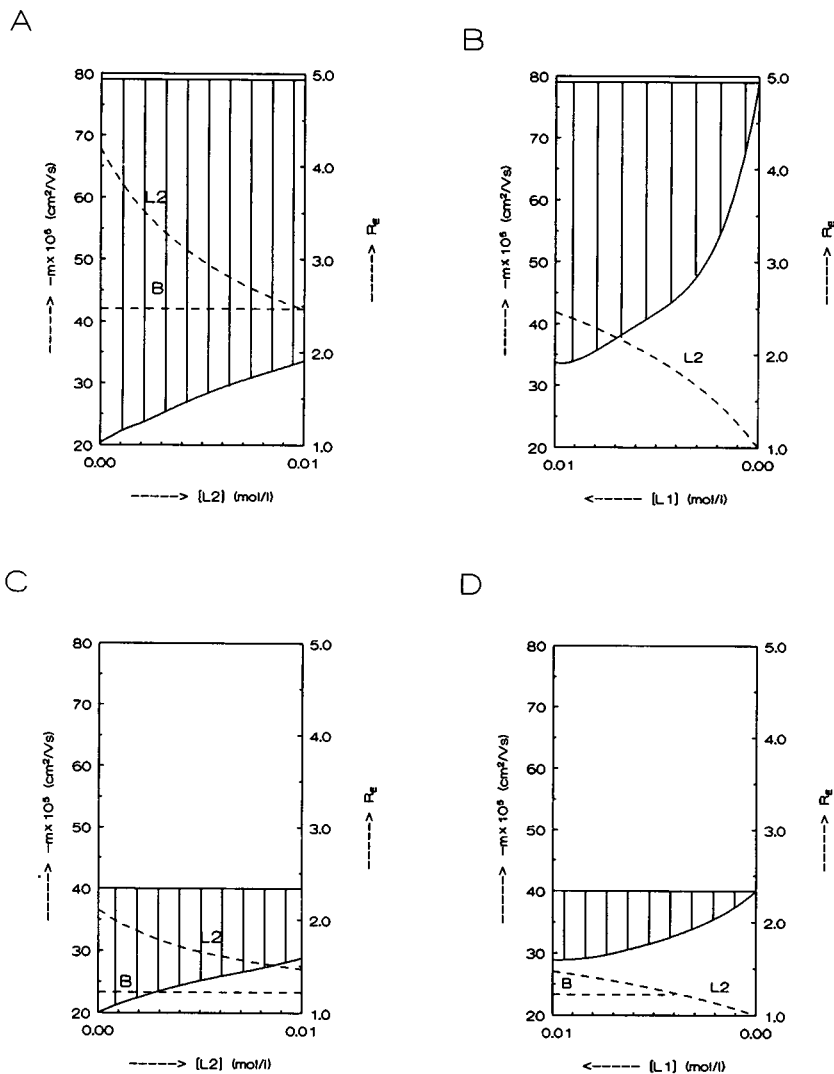


Fig. 2. Combined plot of mobility windows (left-hand scale) and R_E values (right-hand scale) for several 2L-ITP systems. The calculated mobility windows (hatched areas) indicate which negative components migrate in the ITP mode in 2L-ITP systems for varying concentrations of the leading ions (A, B) chloride and MES and (C, D) leading ions with mobilities of $-40 \cdot 10^{-5}$ and $-20 \cdot 10^{-5} \text{ cm}^2/\text{V}\cdot\text{s}$, respectively. The dashed lines labelled L2 show the R_E values of the terminating L₂ zone and those labelled B show those of the component benzoic acid. From (C) and (D) it can be concluded that the mobility window width is reduced if the mobilities of L₁ and L₂ approach each other. The mobility window width is maximum for a pure ITP system [left-hand side of (A) and (C)] and minimum for a pure CZE system [right-hand side of (B) and (D)]. For further details, see text.

components are 3). It is clear from Fig. 2 that the mobility window can be reduced if the mobilities of L₁ and L₂ approach each other and with decreasing concentrations of the L₁ ions. In Fig. 2C benzoic acid always migrates in the ITP/CZE mode because the R_E values are always smaller than that of the terminating L₂ zone and from Fig. 2D it can be concluded that benzoic acid migrates in the CZE mode in a background

electrolyte consisting of a mixture of 0.01 M L₁ and a concentration of L₂ lower than about 0.004 M.

Concentrations in ITP/CZE systems

As already indicated, components can migrate in an ITP system superimposed on a background electrolyte. In such an ITP/CZE system the concentrations of the sample components, mi-

TABLE I

IONIC MOBILITIES AT INFINITE DILUTION, m (10^{-5} $\text{cm}^2/\text{V}\cdot\text{s}$), AND pK VALUES FOR IONIC SPECIES USED IN THE CALCULATIONS AND EXPERIMENTS

Ionic species ^a	m	pK
Acetic acid	-42.4	4.76
BALA	36.7	3.552
Benzoic acid	-33.6	4.203
Histidine	29.7	6.03
Hydrochloric acid	-79.1	-2.0
Imidazole	48.7	6.953
MES	-28.0	6.095
Potassium	76.2	-
Salicylic acid	-35.4	3.107
Sodium	51.9	-
Sulphosalicylic acid	-54.5	-
Tris	29.5	8.1

^a BALA = β -Alanine; MES = 2-(N-morpholino)ethanesulphonic acid; Tris = tris(hydroxymethyl)aminomethane.

grating in the ITP mode, are adapted to that of the leading ion with the highest mobility, L_1 . In Fig. 3, the calculated total concentrations of components are given as a function of their mobility at infinite dilution, assuming pK values of 3, in a pure ITP system (dashed line) for a leading electrolyte of 0.01 M HCl adjusted to pH 6 by adding histidine and for an ITP/CZE system

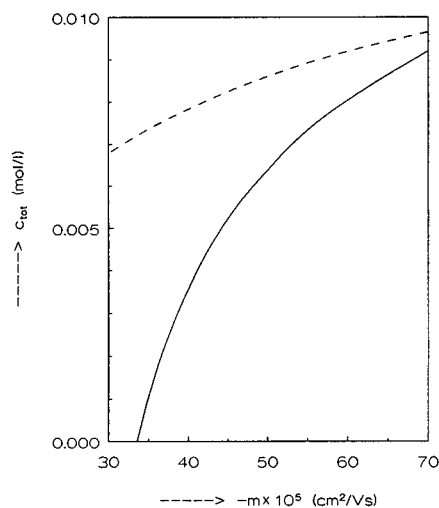


Fig. 3. Total concentrations of components as a function of their mobilities for an ITP system (dashed line) and for an ITP/CZE system. For components with low mobilities, where the ITP/CZE mode is converted into the CZE mode, the concentration decreases. For further details, see text.

with a leading electrolyte consisting of a mixture of 0.01 M HCl (L_1) and 0.01 M MES (L_2) at pH 6 adjusted by adding histidine. From Fig. 3 it can be concluded that the sample concentrations in ITP/CZE system decrease strongly at mobilities where ITP changes into CZE. The mobility window for the corresponding 2L-ITP system (see Fig. 2A) covers anionic mobilities of the sample components from $79.1 \cdot 10^5$ to $ca. 34 \cdot 10^5$ $\text{cm}^2/\text{V}\cdot\text{s}$. In Fig. 4 the calculated total concentrations of components with anionic mobilities of $70 \cdot 10^5$, $60 \cdot 10^5$ and $50 \cdot 10^5$ $\text{cm}^2/\text{V}\cdot\text{s}$ are given for 2L-ITP systems consisting of a mixture of 0.01 M MES (L_2) and various concentrations of chloride (L_1) at a pH of 6 adjusted by adding histidine. An interesting point is that the concentrations of the sample components migrating in the ITP mode in a 2L-ITP system are adapted to the concentration of the L_1 ion. Calculations for cations gave analogous results.

Optimization of mobility windows

It has been shown that ITP/CZE systems can be applied and by an appropriate choice of the electrolyte system it can be managed that a specific component of a complex sample with a specific mobility migrates in the ITP/CZE mode,

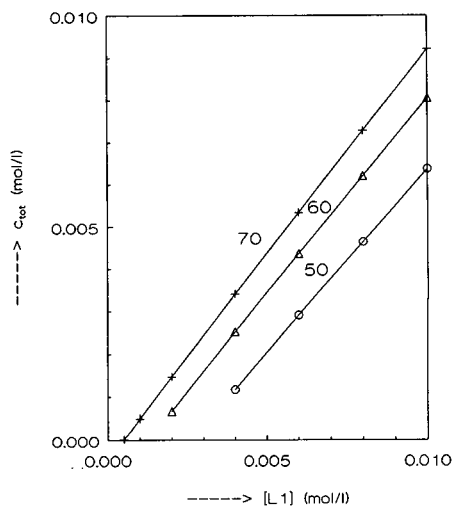


Fig. 4. Relationship between total concentrations of components migrating in the ITP/CZE mode and the concentration of L_1 . The concentrations of the components are adapted to that of L_1 . The numbers refer to the anionic mobilities of the components in 10^{-5} $\text{cm}^2/\text{V}\cdot\text{s}$. For further details, see text.

with a concentration that can be regulated by the choice of the concentration of the leading L_1 ions and with the advantage of self-correcting zone boundaries. The difference from the normal ITP mode applying the same concentration of a leading ion L_1 is that in the ITP/CZE mode the loadability of the system can be expected to be larger owing to the presence of the large concen-

tration of background electrolyte. The question now is how to choose an optimum electrolyte system.

We shall answer this question on the basis of the determination of imidazole in a mixture of cations and try to find a system with a small mobility window at a low L_1 concentration. Imidazole is a cation with a pK value of 6.953

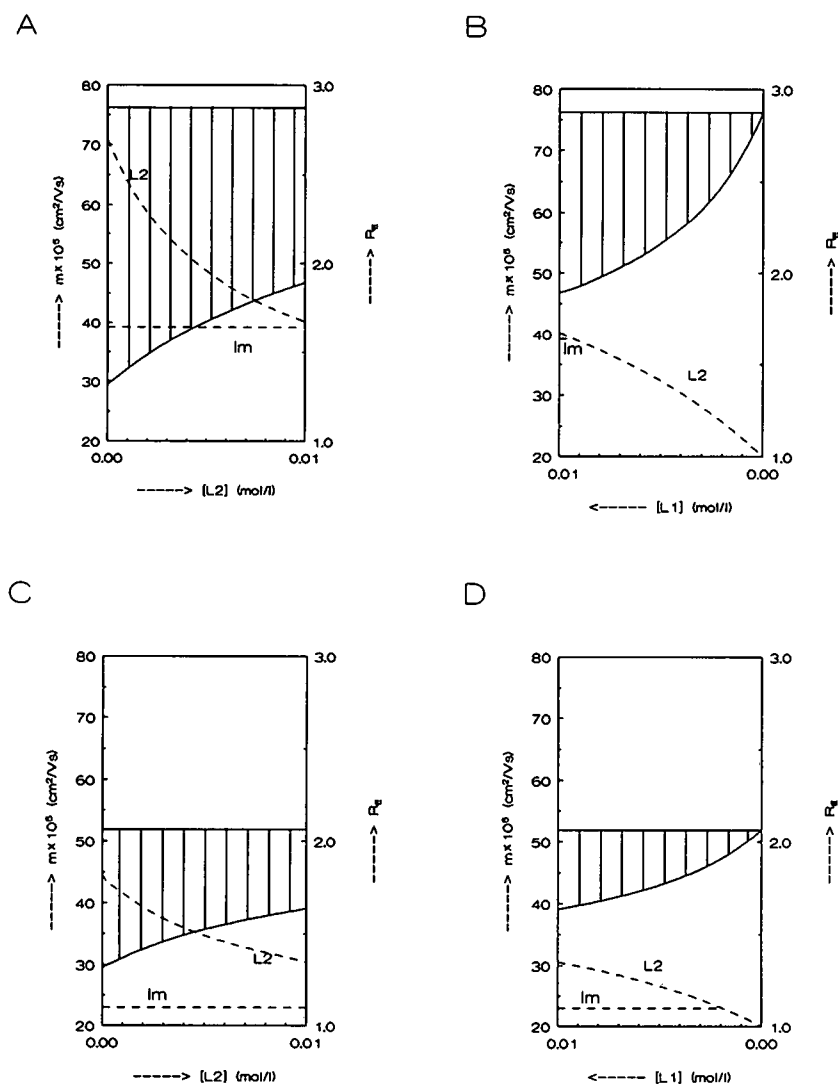


Fig. 5. Combined plot of mobility windows (left-hand scale) and R_E values (right-hand scale) for several 2L-ITP systems. The mobility windows (hatched areas) indicate which positive components migrate in the ITP mode in 2L-ITP systems for varying concentrations of the leading ions (A, B) potassium and Tris and (C, D) sodium and Tris. The dashed lines labelled L2 show the R_E values of the terminating L_2 zone and those labelled Im show those of the component imidazole. From (C) and (D) it can be concluded that the mobility window width is reduced if the mobilities of L_1 and L_2 approach each other. The mobility window width is maximum for a pure ITP system [left-hand side of (A) and (C)] and minimum for a pure CZE system [right-hand side of (B) and (D)]. For further details, see text.

and a mobility of $48.7 \cdot 10^{-5} \text{ cm}^2/\text{V}\cdot\text{s}$. This mobility is determined by ITP measurements according to a procedure described previously [17,19], applying a leading electrolyte of 0.01 M NaOH adjusted to pH 4.75 by adding acetic acid and a terminator of 0.01 M LiCl. For a first impression, the mobility windows and the R_E values of the terminating L_2 zone and imidazole zone were calculated for a system with various concentrations of potassium (L_1) and Tris (L_2). In Fig. 5 the mobility windows (hatched areas) and R_E values (dashed lines) of the terminating L_2 zone and of imidazole are given for (A) varying L_2 concentrations at a concentration of L_1 of 0.01 M and (B) varying L_1 concentrations at a concentration of L_2 of 0.01 M, and it can be seen that in (A) imidazole always migrates in the ITP mode and in (B) it migrates in the ITP mode above a concentration of *ca.* 0.009 M of L_1 ($R_{E,Im} < R_{E,L_2}$). In these systems the widths of the mobility windows are too large and the necessary concentration of the L_1 ions is high, in order that imidazole migrates in the ITP/CZE mode. In Fig. 5C and D the same parameters are given for electrolytes with various concentrations of sodium (L_1) and Tris (L_2). The effective mobility of sodium is slightly higher than that of imidazole. The width of the mobility window is much smaller and the lowest concentration of L_1 , whereby imidazole migrates in the ITP mode, is now *ca.* 0.002 M. For a further minimization of the mobility window, the mobility windows were calculated for several systems with L_2 ions with a mobility close to that of sodium. Although the mobility windows were narrower, the L_1 concentration could not be lowered further.

From the above calculations, it can be concluded that an optimum ITP/CZE system can be obtained by choosing an L_1 ion with a mobility just slightly higher than that of the sample component and the width of the mobility window can be diminished by choosing an L_2 ion with mobility close to that of L_1 .

EXPERIMENTAL

Instrumentation

For all CZE experiments a P/ACE System 2000 HPCE (Beckman, Palo Alto, CA, USA)

was used. All experiments were carried out with Beckman eCAP capillary tubing (75 μm I.D.) with a total length 46.70 cm and a distance between injection and detection of 40.00 cm. The wavelength of the UV detector was set at 214 nm. All experiments were carried out in the cationic mode applying a constant voltage of 10 kV, unless stated otherwise, and the operating temperature was 25°C. Sample introduction was performed by applying pressure injection, where a 1-s pressure injection represents an injected amount of *ca.* 6 nl and an injected length of 0.136 cm. Data analysis was performed using the laboratory-written data analysis program CAESAR.

Chemicals

All chemicals were of analytical-reagent grade. Deionized water was used for the preparation of all buffer and sample solutions. The cationic surfactant FC 135 [20] was donated by 3M (Zoeterwoude, Netherlands).

RESULTS AND DISCUSSION

In 2L-ITP systems, components with mobilities covered by the previously described mobility windows migrate in the ITP/CZE mode whereas the other components migrate in the CZE mode. Components migrating in the ITP/CZE mode are concentrated to a concentration determined by that of the L_1 ions. In order to study this concentration effect, other concentration effects must be eliminated. This means that (1) the sample components may not be dissolved in water or dilute buffer to avoid sample stacking, (2) the sample components may not be injected after a plug of water or of diluted background electrolyte to avoid field amplification, (3) the sample may not contain an excess of ionic species with high mobility to avoid the concentration effect of a 2L-ITP system and (4) the sample solution may not contain a large excess of sample ions with low mobility in order to avoid the concentration effect due to the presence of a terminator. For all experiments the sample components were dissolved in background electrolyte.

To visualize the concentration effect of ITP/

CZE systems, in Fig. 6 the electropherograms are given for a sample solution of 0.0001 M imidazole and 0.0001 M histidine dissolved in 0.01 M Tris acetate at pH 5.5 for leading electrolytes of (A) 0.01 M Tris, (B) a mixture of 0.01 M Tris and 0.003 M sodium hydroxide, (C) a mixture of 0.01 M Tris and 0.004 M NaOH and (D) a mixture of 0.01 M Tris and 0.01 M NaOH. All electrolytes were adjusted to pH 5.5 by adding acetic acid. In all experiments (cationic mode) the anode compartment was filled with the terminating electrolyte, 0.01 M Tris acetate at pH 5.5. The sample solutions were introduced by pressure injection for 10 s. The very sharp concentration effect in the ITP/CZE systems with 0.004 M and 0.01 M sodium (L_1) ions compared with the CZE system can be clearly seen (Fig. 6A). In fact, the sharpening effect was expected at a lower concentration of sodium (see Fig. 5D). It must be remembered,

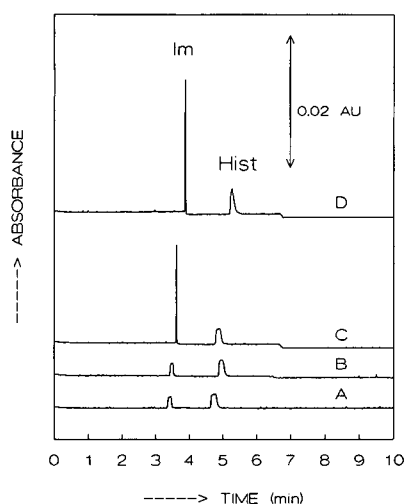


Fig. 6. Electropherograms for the separation of 0.0001 M imidazole (Im) and 0.0001 M histidine (Hist) dissolved in Tris acetate (pH 5.5), applying 2L-ITP systems consisting of 0.01 M Tris (L_2 ions) and (A) 0, (B) 0.003, (C) 0.004 and (D) 0.01 M sodium ions as L_1 ions. All electrolytes were adjusted to pH 5.5 by adding acetic acid. All experiments were carried out in the cationic mode, applying 10 kV with pressure injection for 10 s. The anode compartment (at the inlet) was always filled with 0.01 M Tris acetate (pH 5.5) as terminating electrolyte. It can be clearly seen that from a concentration of 0.004 M sodium ions, imidazole migrates in the ITP/CZE mode resulting in very sharp peaks.

however, that at low concentrations of the L_1 ions the differences between the R_E values of leading, terminating and sample zones are very small, hence the separation force is small.

In order to determine the imidazole concentration in ITP/CZE systems with various sodium concentrations the following experiments were carried out. First, the UV absorbances were measured of known concentrations of imidazole dissolved in 0.01 M Tris adjusted to pH 5.5 by adding acetic acid. The UV detector was set to zero by applying a solution of 0.01 M Tris acetate (pH 5.5). In Fig. 7 the relationship between UV absorbance and imidazole concentration is given (solid line). Then the maximum UV absorbances, with injection of increasing amounts, of the imidazole peaks were determined in ITP/CZE systems with several sodium concentrations. Using the relationship between UV absorbance and the imidazole concentration in Fig. 7 (solid line), the concentration of imidazole in the ITP/CZE systems can be determined. In an ITP/CZE system with, e.g., a concentration of Na^+ of 0.01 M, the concentration of IM^+ seems to be ca. 0.008 M. In Table II, the concentrations of imidazole calculated with the 2L-ITP model and measured concentrations in ITP/CZE systems are given, showing good agreement.

Applying ITP/CZE systems, a gain in detection limits can be expected. In Fig. 8 the electropherograms are given for CZE separations with a background electrolyte of 0.01 M NaOH and 0.01 M Tris adjusted to pH 5.5 by adding acetic acid for sample solutions of imidazole and histidine dissolved in 0.01 M Tris acetate (pH 5.5) at concentrations of (A) $1 \cdot 10^{-5}$ M and (B) $1 \cdot 10^{-4}$ M (5-s pressure injection) and separations with an ITP/CZE system with a leading electrolyte of 0.01 M NaOH and 0.01 M Tris (pH 5.5) and a terminator solution of 0.01 M Tris acetate (pH 5.5) for sample solutions of imidazole and histidine at concentrations of (C) $1 \cdot 10^{-5}$ M and (D) $1 \cdot 10^{-4}$ M (5-s pressure injection). From Fig. 8 a gain in detection limit of about a factor of ten can be concluded.

Calibration graphs were also constructed for several systems. Although the experiments were carried out in the fast rise mode of the UV

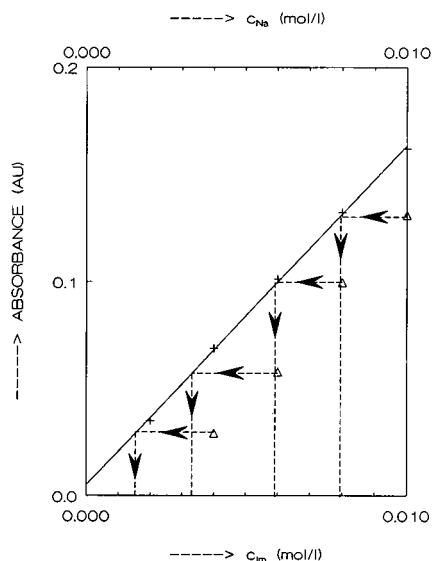


Fig. 7. Relationship between measured UV absorbances and concentrations of standard solutions of imidazole (C_{1m}) dissolved in 0.01 M Tris acetate at pH 5.5 (solid line). From (Δ) measured UV absorbances of the imidazole peaks in ITP/CZE systems with leading electrolytes consisting of 0.01 M Tris (L_2) and several concentrations of sodium (L_1), the concentration of the imidazole zone migrating in the ITP/CZE mode can be deduced.

detector and a data rate of 10 Hz (highest value of the apparatus), bad calibration graphs were obtained on injecting small sample amounts because often peak widths of 0.1–0.2 s were obtained. Applying ITP/CZE systems high demands are made on the detector electronics and the data system concerning handling of extremely sharp peaks.

To visualize the concentration effects in ITP/

TABLE II

CALCULATED, c_{calc} , AND MEASURED, c_{meas} , VALUES OF THE CONCENTRATION OF IMIDAZOLE IN ITP/CZE SYSTEMS WITH LEADING ELECTROLYTES CONSISTING OF 0.01 M TRIS (L_2) AND VARIOUS CONCENTRATIONS OF SODIUM (L_1)

c_{Na} in 2L-ITP system (M)	c_{calc} (M)	c_{meas} (M)
0.010	0.0079	0.0079
0.008	0.0060	0.0059
0.006	0.0039	0.0033
0.004	0.0021	0.0015

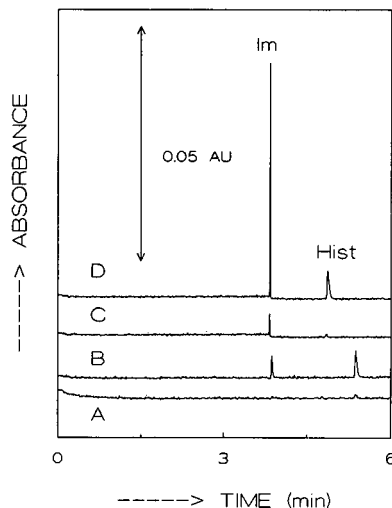


Fig. 8. Electropherograms for the separation of imidazole (Im) and histidine (Hist) dissolved in 0.01 M Tris acetate (pH 5.5) at concentrations of (B, D) $1 \cdot 10^{-4}$ M and (A, C) $1 \cdot 10^{-5}$ M in (A, B) CZE systems with a background electrolyte of 0.01 M NaOH and 0.01 M Tris adjusted to pH 5.5 by adding acetic acid and (C, D) applying ITP/CZE with a leading electrolyte of 0.01 M NaOH and 0.01 M Tris (pH 5.5) and a terminating electrolyte of 0.01 M Tris acetate (pH 5.5). Pressure injection time, 5 s. In the ITP/CZE systems a gain in detection limit of a factor of ca. ten can be obtained.

CZE for negative ionic species, experiments were carried out in the anionic mode with reversed EOF by adding the cationic surfactant FC 135 ($5 \mu\text{g/ml}$) to the background solution. In Fig. 9 the electropherograms are given for a mixture of 0.0001 M sulphosalicylic acid and 0.0001 M salicylic acid dissolved in 0.01 M MES–histidine (pH 6) for leading electrolytes consisting of 0.01 M MES (as L_2 ions) with (A) 0, (B) 0.003, (C) 0.005 and (D) 0.009 M HCl as L_1 ions. All electrolytes were adjusted to pH 6 by adding histidine. The experiments were carried out in the anionic mode (anode placed at the outlet), the cathode compartment being filled with 0.01 M MES adjusted to pH 6 by adding histidine. In Fig. 9E the isotachopherogram obtained by applying a leading electrolyte of 0.01 M HCl and a terminating electrolyte of 0.01 M MES, both adjusted to pH 6 by adding histidine, is shown. All sample solutions were introduced by pressure injection for 10 s. From Fig. 9 it can be concluded that the concentration effect due to the ITP/CZE mode for sulphosalicylic acid acts

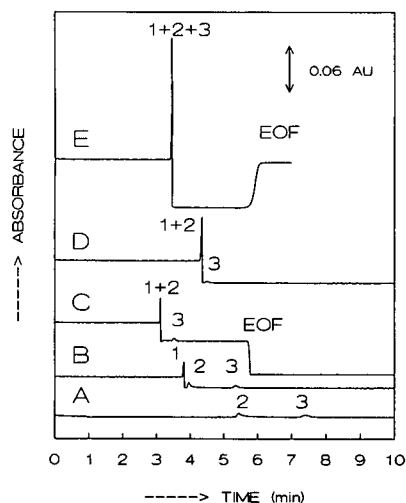


Fig. 9. Electropherograms for the separation of (2) 0.0001 *M* sulphosalicylic acid and (3) 0.0001 *M* salicylic acid in 0.01 *M* MES adjusted to pH 6 by adding histidine for 2L-ITP systems consisting of 0.01 *M* MES as L_2 ions and (A) 0, (B) 0.003, (C) 0.005 and (D) 0.009 *M* chloride as L_1 ions. All electrolytes were adjusted to pH 6 by adding histidine. Pressure injection time, 10 s. The experiments were carried out in the anionic mode whereby the EOF was reversed by addition of FC 135 (5 $\mu\text{g}/\text{ml}$) and the cathode compartment (at the inlet site) was filled with a solution of 0.01 *M* MES adjusted to pH 6 by adding histidine. In (E) the separation was carried out in a pure ITP system with leading electrolyte 0.01 *M* HCl and terminating electrolyte 0.01 *M* MES, both adjusted to pH 6 by adding histidine. In (C) and (D) sulphosalicylic acid migrates in the ITP/CZE mode. (1) System peak, possibly due to the presence of iodide ions in FC 135, always migrating in the ITP/CZE mode.

at a concentration of about 0.004 *M* chloride in the background electrolyte, whereas salicylic acid migrates in the CZE mode (see Fig. 9A–D). In a pure ITP system it migrates in the ITP mode. In the systems in Fig. 9B–E an extra system peak (1) was always present, possibly owing to the presence of iodide ions in FC 135 [20]. In all systems, however, the increase in this peak due to the presence of peak 2 (Fig. 9C and D) or peaks 2 and 3 (Fig. 9E) was carefully checked. To demonstrate that in an ITP system sulphosalicylic acid and salicylic acid migrate in the ITP mode, in Fig. 10 the isotachopherogram obtained under the same conditions as in Fig. 9E for a sample composition of 0.005 *M* sulphosalicylic acid and 0.005 *M* salicylic acid in

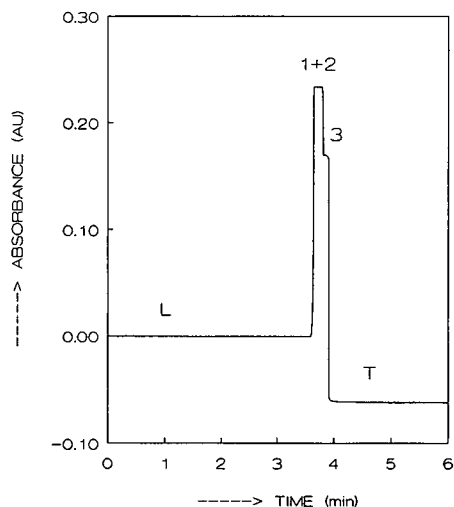


Fig. 10. Isotachopherogram for the separation of (1) system peak, (2) 0.005 *M* sulphosalicylic acid and (3) 0.005 *M* salicylic acid with (L) leading electrolyte 0.01 *M* histidine chloride at pH 6 and (T) terminator 0.01 *M* MES–histidine at pH 6. Pressure injection time, 5 s.

water is given. The separate steps can be clearly seen.

CONCLUSIONS

By applying a leading electrolyte consisting of two ionic species, components can migrate in an ITP system superimposed on CZE, the so-called ITP/CZE mode, whereby the leading ions L_1 with the highest mobility act as the leading ions in the ITP system and the leading ions L_2 with the lowest mobility create the terminating zone and act as co-ions of the CZE system. With the mathematical model of 2L-ITP, mobility windows can be calculated, indicating which components migrate in the ITP/CZE mode, and these components migrate at a concentration determined by the concentration of the L_1 ions. By choosing a suitable leading electrolyte in ITP/CZE systems, one can select which components migrate in the ITP mode and at what concentration. Components migrating in the ITP mode in such an ITP/CZE system show sharp peaks owing to the self-correcting property of the zones. By this means a gain in detection limit of a factor of *ca.* ten could be established. Great

demands, however, are made on the detection system and data acquisition in order to handle the very sharp peaks in a proper quantitative way. Experimental work is in progress to investigate the applicability and ruggedness of ITP/CZE systems.

REFERENCES

- 1 F.E.P. Mikkers, F.M. Everaerts and Th.P.E.M. Verheggen, *J. Chromatogr.*, 169 (1979) 1.
- 2 J.W. Jorgenson and K.D. Lukacs, *Anal. Chem.*, 53 (1981) 1298.
- 3 R.L. Chien and J.C. Helmer, *Anal. Chem.*, 63 (1991) 1354.
- 4 R.L. Chien and D.S. Burgi, *J. Chromatogr.*, 559 (1991) 141.
- 5 D.S. Burgi and R.L. Chien, *Anal. Chem.*, 63 (1991) 2042.
- 6 R.L. Chien and D.S. Burgi, *Anal. Chem.*, 64 (1992) 1046.
- 7 J.L. Beckers and M.T. Ackermans, *J. Chromatogr.*, 629 (1993) 371.
- 8 D. Kaniansky and J. Marák, *J. Chromatogr.*, 498 (1990) 191.
- 9 F. Foret, V. Šustáček and P. Boček, *J. Microcol. Sep.*, 2 (1990) 229.
- 10 D.S. Stegehuis, H. Irth, U.R. Tjaden and J. van der Greef, *J. Chromatogr.*, 538 (1991) 393.
- 11 V. Dolnik, K.A. Cobb and M. Novotny, *J. Microcol. Sep.*, 2 (1990) 127.
- 12 F. Foret, E. Szoko and B.L. Karger, *J. Chromatogr.*, 608 (1992) 3.
- 13 C. Schwer and F. Lottspeich, *J. Chromatogr.*, 623 (1992) 345.
- 14 J.L. Beckers and F.M. Everaerts, *J. Chromatogr.*, 508 (1990) 3.
- 15 F. Foret, M. Deml and P. Boček, *J. Chromatogr.*, 452 (1988) 601.
- 16 F.M. Everaerts, J.L. Beckers and Th.P.E.M. Verheggen, *Isotachopheresis—Theory, Instrumentation and Applications*, Elsevier, Amsterdam, 1976.
- 17 J.L. Beckers and F.M. Everaerts, *J. Chromatogr.*, 470 (1989) 277.
- 18 T. Hirokawa, M. Nishino, N. Aoki, Y. Kiso, Y. Sawamoto, T. Yagi and J. Akiyama, *J. Chromatogr.*, 271 (1983) D1-D106.
- 19 J.L. Beckers, *J. Chromatogr.*, 320 (1985) 147.
- 20 A. Emmer, M. Janssen and J. Roeraade, *J. Chromatogr.*, 547 (1991) 544.

Capillary electrophoresis with on-line sample pretreatment for the analysis of biological samples with direct injection

Ikue Morita^{*,☆}

Institute of Pharmaceutical Sciences, Hiroshima University School of Medicine, 1-2-3 Kasumi, Minami-ku, Hiroshima 734 (Japan) and Division of Biochemistry and Immunochemistry, National Institute of Hygienic Sciences, 1-18-1 Kamiyoga, Setagaya-ku, Tokyo 158 (Japan)

Jun-ichi Sawada

Division of Biochemistry and Immunochemistry, National Institute of Hygienic Sciences, 1-18-1 Kamiyoga, Setagaya-ku, Tokyo 158 (Japan)

(First received September 8th, 1992; revised manuscript received March 16th, 1993)

ABSTRACT

A method of capillary electrophoresis (CE) using on-line sample pretreatment was developed. The system utilized on-line solid-phase extraction and capillary column switching. To explore the advantages of the method, propranolol in serum was determined by direct injection. The pretreatment part of the system consisted of an injection capillary including a small bed of protein-coated ODS. The protein-coated ODS concentrated the analyte by hydrophobic interactions, and the serum proteins were allowed to flow into a drain capillary. As samples up to ca. 1 μ l could be loaded without a decrease in resolution, the detection limit was improved by two orders of magnitude (0.15 μ g/ml). Propranolol was detected in a separation capillary by UV absorbance measurement without any interfering peaks. A linear response was obtained between 100 fg and 2 ng per injection. This method provides novel possibilities for extending the application of capillary electrophoresis.

INTRODUCTION

Capillary electrophoresis (CE) techniques that use electrical force to drive separations in capillary tubes have been applied in many areas of analysis [1–3]. Compared with high-performance liquid chromatography (HPLC), the practical

use of CE has been focused on the analysis of highly purified samples (ranging from small molecules to macromolecules), and few papers have described the application of CE to substances in a mixture of complex matrices. Often the analyte of interest is present at a low concentration in a complex matrix, which may cause problems owing to the presence of proteins that may adhere to the wall of the capillary [4].

There are various approaches by which these difficulties may be overcome. One way is to use traditional sample pretreatment such as liquid-liquid or solid-phase extraction prior to analysis by capillary zone electrophoresis (CZE), which

* Corresponding author. Address for correspondence: Division of Biochemistry and Immunochemistry, National Institute of Hygienic Sciences, 1-18-1 Kamiyoga, Setagaya-ku, Tokyo 158, Japan.

☆ National Institute Postdoctoral Fellow.

has become one of the high-performance separation techniques for the analysis of complex mixtures because of its very high resolution [5,6]. The traditional sample pretreatments serve for clean-up (deproteinization) and preconcentration of analytes. However, the methods are not combined “on-line” with the CZE analysis.

Compared with ordinary HPLC, CZE requires much smaller volumes of samples. However, the detection of analytes at lower concentrations is difficult. Some instrumental devices have been reported for performing on-capillary peak concentration to enhance the detectability in CZE, *e.g.*, the use of multiple capillaries arranged in bundles and combined into a single capillary through a glass connector [7] or coupling of isotachopheresis and CZE [8]. These techniques contributed to improved detection limits by increasing the amounts of sample loaded into the capillary.

Micellar electrokinetic chromatography (MEKC), which was introduced by Terabe and co-workers in 1984 [24], is performed with the same instrument as in CZE and uses an ionic surfactant solution at a concentration above the critical micellar concentration (CMC). MEKC has many attractive advantages in addition to the capability of electrophoretic separation of electrically neutral substances. In its application to pharmaceutical analysis, plasma samples were injected directly without any sample pretreatment prior to analysis [9,10]. In the MEKC with sodium dodecyl sulphate (SDS), plasma proteins were probably solubilized by the anionic SDS micelles, and it eliminated the adsorption of plasma proteins on the capillary wall. Consequently, similarly to micellar HPLC, MEKC permitted direct plasma sample injection without any sample pretreatment such as deproteinization or extraction.

In HPLC, various approaches have been developed to streamline sample pretreatment [11,12], including the use of column switching, specially designed HPLC columns or a micellar mobile phase with conventional reversed-phase HPLC. Morita and co-workers have reported HPLC methods for the analysis of biological samples with direct injection [13–19]. The development of protein-coated ODS, which was

designed to partition small molecules but to elute proteins in one peak with high recovery, allowed the direct injection of plasma samples without sample pretreatment such as protein precipitation, and the determination of drugs (procainamide, propranolol, doxorubicin, etc.) or endogenous components (tryptophan and its metabolites) in biological fluids using a precolumn packed with protein-coated ODS has been reported. These techniques have contributed the automation of analyses with high precision.

The aim of this paper is to present a new concept of CE with the advantages of both liquid chromatography and electrophoresis. This modified CE method, which was designed to include on-line sample pretreatment and column-switching techniques, provides possibilities for introducing multi-separation fields with a single injection of sample by using different separation modes coupled with solid-phase extraction. This paper reports the development of CE with sample pretreatment for the determination of drugs in biological fluids with direct injection and demonstrates some of its features with the separation of propranolol in serum.

EXPERIMENTAL

Reagents and samples

Propranolol (Nacalai Tesque, Kyoto, Japan) was used as a model compound. Human serum was purchased from Sigma (St. Louis, MO, USA). A stock solution of propranolol (0.01 M, 2.9 mg/ml as hydrochloride salt) was prepared with distilled water and stored at -20°C . Addi-

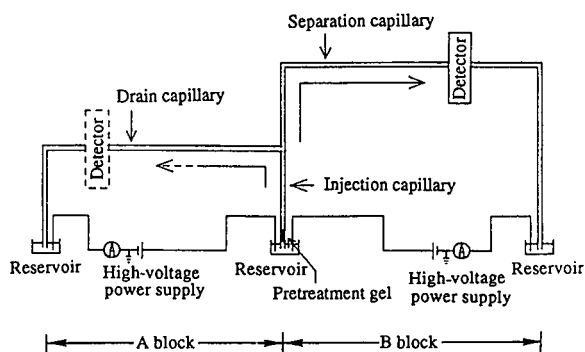


Fig. 1. Schematic diagram of the apparatus.

tional sample solutions were prepared by appropriate dilution of the standard propranolol solution in human serum (serum sample) or in phosphate buffer (buffer sample). The electrophoretic separation was performed using phosphate buffer (sodium salt); 50 mM phosphate buffer (pH 7.0) was used as the running buffer and acetonitrile–20 mM phosphate buffer (pH 7.0) (75:25) was used as the elution buffer. The buffers were passed through a 0.45- μm membrane filter and degassed by ultrasonication before use. Acetone (1%) was used as a neutral marker solute (no electrophoretic mobility) to obtain the electroosmotic flow-rate (V_{eo}). All chemicals were of analytical-reagent grade.

Apparatus

A schematic illustration of the system used in this study is shown in Fig. 1 [20]. A Model 890-CE high-voltage power supply was obtained from Jasco (Tokyo, Japan). Detection of separated solutes was monitored by on-column measurement of UV absorption at 290 nm using a Model 875-CE instrument (Jasco). A Chromatopac C-R6A (Shimadzu, Kyoto, Japan) was used for data processing. Untreated fused-silica capillary tubes were obtained from GL Sciences (Tokyo, Japan), and various lengths were used.

The system consisted of three pieces of capillary tubing connected to each other through a T-type connector; one was an injection capillary (5 cm \times 50 μm I.D.). The injection capillary

was tipped with a short capillary that contained a small bed of gel (protein-coated ODS). The fabrication of the injection capillary with gel was carried out as follows. The polyimide coating outside the capillary at the inlet side of the capillary (50 μm I.D. and 370 μm O.D.) was removed by burning, then the capillary was inserted into a capillary of 350 μm I.D. and 470 μm O.D., inside which a small bed of protein-coated ODS gel (particle size 20–32 μm , prepared as described [15,21]) was held by two porous glass frits. The other two capillaries were drain and separation capillaries (50 μm I.D., 35 and 60 cm long, respectively). The drain and separation capillaries were connected with the injection capillary using a T-type connector.

The system was operated by applying a high voltage between two capillaries (the injection capillary was placed in the anodic reservoir and the drain or the separation capillary was placed in the cathodic reservoir; A or B block in Fig. 1) alternately to produce an electric field as a driving force.

Procedures

Typical working procedures are given in Table I. The injection capillary (capillary with gel) was first conditioned by passing 100% organic solvent (acetonitrile). All three pieces of capillary tubes were filled with phosphate buffer (pH 7.0, 50 mM) by using a 50- μl microsyringe and the ends of the capillaries were dipped into the phosphate

TABLE I
PROCEDURES FOR DIRECT INJECTION ANALYSIS OF DRUG

Injection capillary with protein-coated ODS, 5 cm \times 50 μm I.D. Drain capillary, 50 μm I.D. \times 35 cm long (effective length 17 cm). Separation capillary, 50 μm I.D. \times 60 cm long (effective length 40 cm).

Step	Operation	Procedure		Electric field	Conditions		
		Pretreatment	Separation		Anodic reservoir	Voltage (kV)	Time
1	Sample injection	Concentration	–	A block	Sample	15	2.5–50 s
2	Clean-up	Deproteinization	–	A block	Running buffer ^a	15	10 min
3	Elution	–	–	B block	Elution buffer ^b	10	15 s
4	Separation	–	+	B block	Running buffer ^a	15	10 min

^a Running buffer: 50 mM phosphate buffer (pH 7.0).

^b Elution buffer: acetonitrile–20 mM phosphate buffer (pH 7.0) (75:25).

buffer (running buffer) solutions whose surfaces were kept at the same level. The anodic reservoir at the injection capillary side was changed according to the procedures. Samples were electrokinetically injected into the injection capillary for 2.5–50 s at 15 kV using the A block (step 1). After injection, a high voltage (+15 kV at the sample introduction side and 0 V at the end of the drain capillary, A block) was applied (step 2). Sample pretreatment included the retention of the analyte on the protein-coated ODS packed in the injection capillary and the drawing of serum proteins and others into the drain capillary. The analyte was eluted from the protein-coated ODS with the elution buffer [acetonitrile–20 mM phosphate buffer (pH 7.0) (75:25)] by applying a high voltage (10 kV at the end of the injection capillary and 0 V at the end of separation capillary, B block) for 15 s (step 3). By applying a high voltage (15 kV) to B block, the electric field was changed from A block to B block, and the analyte could be separated in the field of the separation capillary with the phosphate buffer (step 4).

For CZE, a Model CE-800 capillary electrophoresis system (Jasco) was used in the CZE mode. It was equipped with a 50 μm I.D. fused-silica capillary. Sample solution was electrokinetically injected into the anodic end of the capillary and CZE was performed with on-column measurement of the UV absorption at 290 nm. A longer capillary with gel (50 cm) was

used to investigate the loading capacity of the injection capillary and in that case an elution step (at 10 kV for 15 s with elution buffer) was introduced before the CZE analysis.

RESULTS AND DISCUSSION

The system is based on the combination of packed-column capillary electrochromatography (CEK) [22,23] and CZE. These techniques differ from microcolumn HPLC in that the flow of effluent is driven by an electric field rather than pressure. Throughout this experiment, electroosmotic flows were used as a driving force in addition to electromigration of ionic substances.

Use of protein-coated ODS gel as an analyte concentrator

It is expected that the capillary containing ODS gel will have the advantage of a higher loading capacity than open-tubular capillaries. Prior to analysis, the loading capacity of the gel (protein-coated ODS) within the injection capillary was investigated by increasing the injection volume of aqueous propranolol (Fig. 2). Plots of peak height (area) *versus* volume injected were linear up to 500 s at 15 kV (1200 nl) in the CZE system using the capillary with the gel. The injected volume was found to increase linearly with time at the rate of 2.4 nl/s. In a capillary without gel (open-tubular capillary as reference), the plot of peak height *versus* volume injected

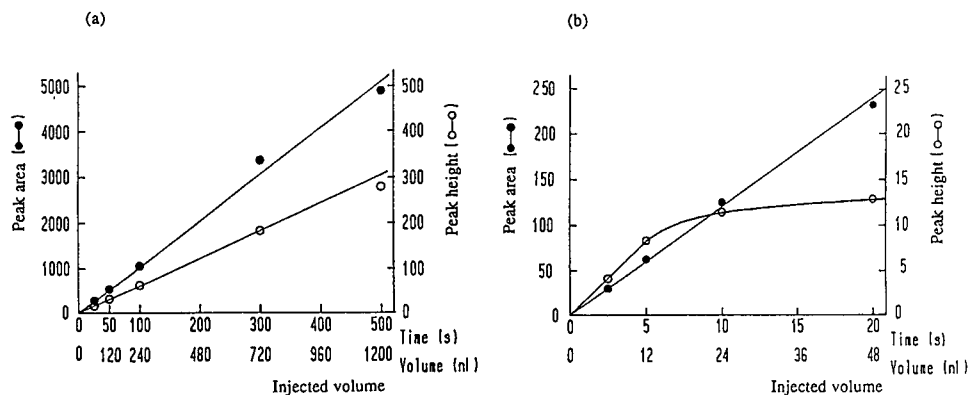


Fig. 2. Plots of (○) peak height and (●) peak area as a function of volume injected in the CZE mode using (a) a capillary containing gel and (b) a capillary without gel. Test compound, propranolol ($5 \cdot 10^{-5}$ M) in phosphate buffer (50 mM, pH 7.0). Capillary size, 50 μm I.D., 50 cm long (30 cm effective length). Injection was made electrokinetically at 15 kV for several seconds and electromigration was performed at 15 kV with the running buffer. For other conditions, see Experimental.

did not increase linearly over 5 s at 15 kV (12 nl). The capillary with the gel permitted concentration of propranolol, being based on solid-phase extraction, and the sensitivity with respect to sample concentration was increased by two orders of magnitude by permitting loading of larger sample volumes (detection limit $0.5 \mu\text{M}$, $0.15 \mu\text{g/ml}$).

Electropherograms of an aqueous propranolol sample obtained by CZE using a capillary with or without gel are shown in Fig. 3. As the $\text{p}K_a$ of propranolol is 9.45, under the neutral conditions employed in this analysis the analyte migrates towards the cathode faster than the electroosmotic flow. In Fig. 3a, a negative peak shows the migration position of a neutral compound (organic solvent used in the elution buffer). Compared with the capillary without gel, a slight decrease in electroosmotic flow-rate ($V_{\text{eo}} = 0.85 \text{ mm/s}$) was observed in CZE using the capillary with gel (ca. 10%). This might be due to the suppression of electroosmotic flow by the change in the electrical double layer in the area of the packed gel in the capillary. The theoretical plate number of propranolol in CZE analysis using the capillary with gel was ca. 88 000/m, showing a similar chromatographic performance to the corresponding CZE analysis using an open-tubular capillary (reference capillary, ca. 91 000 plates/

m). This means that it is possible to perform concentration of propranolol without a great decrease in plate number. The decrease in the theoretical plate number often encountered, although usually less than 10%, seemed to be due to the band broadening caused by the connection of the capillaries. Therefore, the manufacture of analyte concentrators is critical for optimum performance.

Analysis of biological samples with direct injection

The protein-coated ODS columns were specially designed to partition small molecules and elute proteins in one peak with a high recovery for the analysis of biological samples with direct injection. It had characteristics of reversed-phase packings for small molecules owing to the presence of ODS on the internal surfaces of small pores, but had no longer affinity for plasma proteins [21]. Plasma proteins could not be adsorbed on the external surface of the protein-coated ODS gel, and deproteinization in the protein-coated ODS column was accompanied by size exclusion due to the small pores of the packing.

The pretreatment part of the CZE system consisted of a capillary with protein-coated ODS gel which extracted propranolol dynamically from directly injected samples and allowed serum proteins to flow out under electroosmotic flow in CZE, similarly to HPLC. However, even with the use of the protein-coated ODS gel-packed capillary, the problem would still remain that serum proteins might adhere to capillary wall and therefore cause a slower migration in the following run in CZE.

Column switching was used to avoid the problems caused by proteins. By changing the electrical force between the two blocks alternately, two separation fields were produced, one to drain out proteins and the other for the separation of an analyte. The operational procedures used are given in Table I. Fig. 4 shows typical electropherograms for propranolol. As acetone could not be retained on the protein-coated ODS, acetone was drawn into the drain capillary during the clean-up step under an electroosmotic flow, while propranolol was retained on the

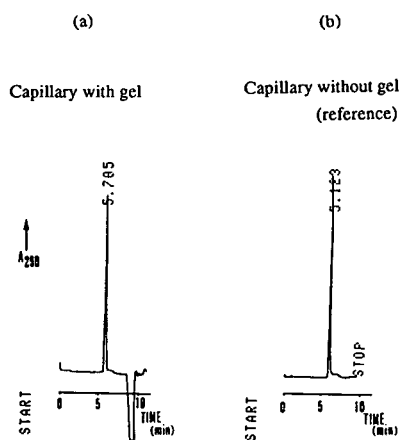


Fig. 3. Electropherograms of propranolol in CZE analysis using (a) a capillary containing gel and (b) a capillary without gel. Propranolol in phosphate buffer ($5 \cdot 10^{-4} \text{ M}$) was injected electrokinetically at 15 kV for 5 s. Other conditions as in Fig. 2.

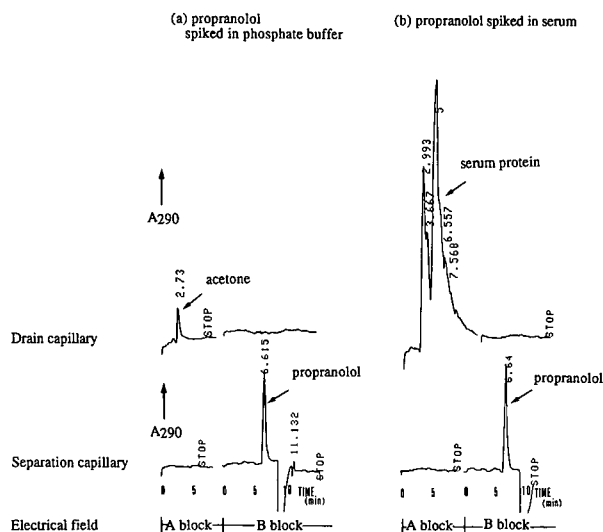


Fig. 4. Electropherograms of propranolol ($5 \cdot 10^{-4} M$) added to (a) phosphate buffer (50 mM, pH 7.0) and (b) serum. For details, see Experimental.

protein-coated ODS in the injection capillary. The propranolol was then eluted from the protein-coated ODS by passage of a solution containing a high concentration of organic solvent (elution buffer) and electrophoresed in the field of the separation capillary. UV monitoring of the drain capillary in addition to the separation capillary proved that there was no leakage of the samples in the non-electrical field. The direct injection assay was validated for concentrations ranging from 15 to 300 $\mu\text{g/ml}$ ($5 \cdot 10^{-5}$ to $1 \cdot 10^{-3} M$) of propranolol in human serum by electrokinetic injection of samples (15 kV, 5 s) (Fig. 5). The calibration graph for propranolol in human plasma was linear.

As a reference, Fig. 6 shows the separation profiles of serum spiked with propranolol obtained by CZE with direct injection. Propranolol migrated toward the cathode, eluting before serum proteins, but the elution position was close to that of serum proteins. With the proposed system, serum proteins were drawn into the drain capillary and easily separated from propranolol. Hence propranolol was detected as a single peak without any interfering peaks of biological components in the separation capillary tube.

As a preliminary study, the recovery of pro-

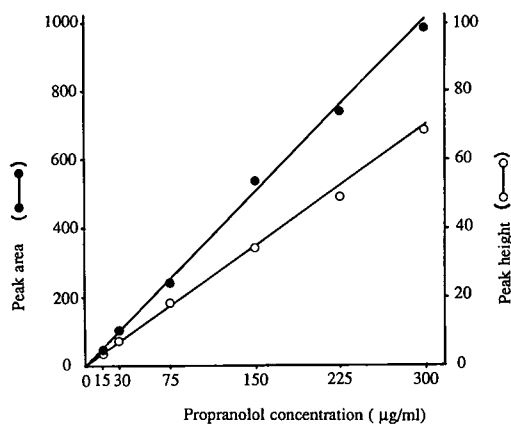


Fig. 5. Plots of (●) peak area and (○) peak height vs. propranolol concentration obtained from analysis of samples containing various amounts of propranolol added to normal human serum. Experimental conditions as in Fig. 4.

pranolol was determined by comparing the peak height of propranolol in serum with that of a standard sample. In CZE with direct injection, the average recovery of propranolol added to serum (150 $\mu\text{g/ml}$, $5 \cdot 10^{-4} M$) was ca. 70% ($n = 5$). To decrease the protein content, serum was diluted 1:10 with phosphate buffer, and the

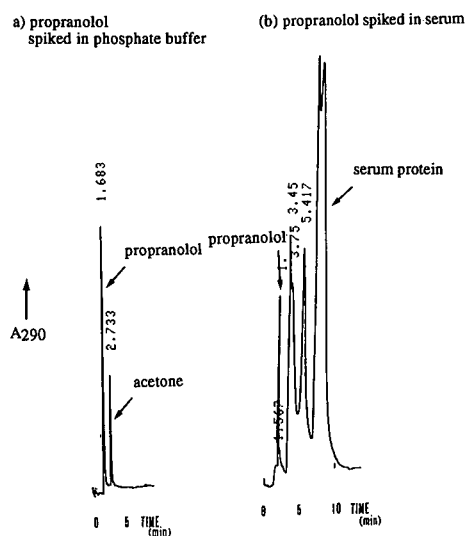


Fig. 6. Typical separation profiles in the CZE of propranolol ($5 \cdot 10^{-4} M$) added to (a) phosphate buffer (50 mM, pH 7.0) and (b) serum. Injection was made electrokinetically at 15 kV for 5 s and electromigration was performed at 15 kV with the running buffer. Capillary size, 50 μm I.D., 45 cm long (18 cm effective length).

recovery in serum (1:10 dilution) was ca. 90% ($n = 5$). These results suggest that a higher protein binding of propranolol caused a slower release of propranolol from the proteins, which resulted in a decrease in recovery. With the modified system with direct injection, an almost quantitative recovery (100%) was obtained in both serum and diluted serum (1:10 dilution) samples ($n = 3$). Therefore, the total amount of both bound and unbound propranolol could be determined.

CONCLUSIONS

A modified method of CE including a sample pretreatment system and a capillary column-switching system has been developed. A capillary with protein-coated ODS gel at the inlet side served as an analyte concentrator to achieve an increased injection volume. Direct injection of serum samples without any sample pretreatment was applied to determine propranolol in serum. The sample pretreatment part of the system retained the analyte on the protein-coated ODS within the injection capillary while drawing serum proteins into the drain capillary. Therefore, an analyte separated from serum proteins could be detected as a single peak without any interfering peaks in the separation capillary. The protein-bound drug was released in a free form by partitioning to the hydrophobic phase on the protein-coated ODS. Hence it is assumed (but not proved) that the concentration of total drug could be determined. This method presents novel possibilities for extending the application of CE.

ACKNOWLEDGEMENTS

The authors express their thanks to Dr. E. Otaka, Hiroshima University, for assistance and encouragement. The help of Dr. K. Suzuki is also greatly appreciated. This work was supported in part by Grant-in-Aid 03857316 from the Ministry of Education, Science and Culture,

and by the Science and Technology Agency, Japan.

REFERENCES

- 1 J.W. Jorgenson and K.D. Lukacs, *Anal. Chem.*, 53 (1981) 1298.
- 2 A.G. Ewing, R.A. Walling and T.M. Olefirowicz, *Anal. Chem.*, 58 (1986) 743A.
- 3 B.L. Karger, A.S. Cohen and A. Guttman, *J. Chromatogr.*, 492 (1989) 585.
- 4 S. Hjerten, *J. Chromatogr.*, 347 (1985) 191.
- 5 S. Fujiwara and S. Honda, *Anal. Chem.*, 58 (1986) 1811.
- 6 M.C. Roach, P. Gozeland and R.N. Zare, *J. Chromatogr.*, 426 (1988) 129.
- 7 N.A. Guzman, M.A. Trebilcock and J.P. Advis, *J. Liq. Chromatogr.*, 14 (1991) 997.
- 8 F. Foret, V. Sustacek and P. Bocek, *J. Microcol. Sep.*, 2 (1990) 229.
- 9 T. Nakagawa, Y. Oda, A. Shibukawa, H. Fukuda and H. Tanaka, *Chem. Pharm. Bull.*, 37 (1989) 707.
- 10 N. Nishi, T. Fukuyama and M. Matsuo, *J. Chromatogr.*, 515 (1990) 245.
- 11 F.W. Willmott, I. Mackenzie and R. Dorphin, *J. Chromatogr.*, 167 (1978) 31.
- 12 T.C. Pinkerton, *J. Chromatogr.*, 544 (1991) 13.
- 13 H. Yoshida, I. Morita, T. Masujima and H. Imai, *Chem. Pharm. Bull.*, 30 (1982) 2287.
- 14 H. Yoshida, I. Morita, T. Masujima and H. Imai, *Chem. Pharm. Bull.*, 30 (1982) 3827.
- 15 H. Yoshida, K. Takano, I. Morita, T. Masujima and H. Imai, *Jpn. J. Clin. Chem.*, 12 (1983) 312.
- 16 G. Tamai, I. Morita, T. Masujima, H. Yoshida and H. Imai, *J. Pharm. Sci.*, 73 (1984) 1825.
- 17 I. Morita, T. Masujima, H. Yoshida and H. Imai, *Anal. Biochem.*, 151 (1985) 358.
- 18 I. Morita, M. Kawamoto, M. Hattori, K. Eguchi, K. Sekiba and H. Yoshida, *J. Chromatogr.*, 526 (1990) 367.
- 19 I. Morita, M. Kawamoto and H. Yoshida, *J. Chromatogr.*, 576 (1992) 334.
- 20 I. Morita, *Jpn. Pat. Appl.* (1991); presented at the 112th Annual Meeting of Pharmaceutical Sciences, Fukuoka, March 1992.
- 21 H. Yoshida, I. Morita, G. Tamai, T. Masujima, T. Tsuru, N. Takai and H. Imai, *Chromatographia*, 19 (1985) 466.
- 22 J.W. Jorgenson and K.D. Lukacs, *J. Chromatogr.*, 218 (1981) 209.
- 23 J.H. Knox and I.H. Grant, *Chromatographia*, 24 (1987) 135.
- 24 S. Terabe, K. Otsuka, K. Ichikawa, A. Tsuchiya and T. Ando, *Anal. Chem.*, 56 (1984) 111.

Characterization of each isoform of a F(ab')₂ by capillary electrophoresis

Renaud Vincentelli and Nicolas Bihoreau*

T.M. Innovation (Centre National de Transfusion Sanguine, Institut Merieux), 3 Avenue des Tropiques, BP 100, 91943 Les Ulis (France)

(First received January 21st, 1993; revised manuscript received March 29th, 1993)

ABSTRACT

Free solution capillary electrophoresis was investigated for the characterization of an M_r 100 000 purified F(ab')₂. Optimization of the experimental conditions allowed the identification of five separated peaks, suggesting the presence of isoforms which differed by only 0.2 pH unit. This heterogeneity was still detectable with 80 amol of protein. After a preparative separation by chromatofocusing, identification of each form was performed for the first time by capillary electrophoresis. A quantitative and qualitative correlation with isoelectric focusing showed that free solution capillary electrophoresis represents a sensitive method for revealing subtle differences in charge, even for large proteins.

INTRODUCTION

Wenisch *et al.* [1] described different forms of a purified immunoglobulin using isoelectric focusing (IEF). This heterogeneity was explained by the binding to carrier ampholytes or by the presence of different immunoglobulin G (IgG) complexes [2]. In contrast, Moellering *et al.* [3] attributed this physico-chemical difference to a deamidation of the monoclonal antibody studied. Before entering a protein product in clinical trials, it is important to develop different techniques to identify such heterogeneity as far as possible.

An alternative method, rapidly becoming the separation technique of choice for the analysis of polypeptides, is capillary electrophoresis. Lauer and McManigill [4] separated two small peptides of 162 amino acids for which the pI values differed by 0.1 pH unit, indicating that the large apparent number of theoretical plates allowed

discrimination between small differences in charge densities. Nevertheless, most publications on capillary electrophoresis have been concerned with oligonucleotides, amino acids or low-molecular-mass products [5,6], and only a few data have been presented on proteins [7,8].

Among the different methods, free solution capillary electrophoresis (FSCE) is well suited for analytical studies on proteins in their native state and allows an increased separation efficiency by a limited zone broadening effect [9]. However, Grossman *et al.* [10] have shown that, as the electrophoretic mobility of a peptide is related to its charge/size ratio, serious adsorption problems can alter the mobility of large proteins and prohibit proper separations by FSCE. One option for avoiding wall adsorption of proteins in solution is to operate at a pH that is near or below the point of zero charge for the fused silica (*ca.* pH 2) [11]. Unfortunately, this is a pH at which most proteins are not in their native conformation. An alternative procedure that can be used to eliminate the effect of solute-wall interactions is to operate at a pH

* Corresponding author.

above the *pI* of the protein, resulting in a repulsion between the capillary wall and the molecule [4]. Further, as FSCE is a method strongly dependent on charge differences between proteins, one can manipulate the selectivity of a separation by modifying the pH of the running buffer [12]. Recently, FSCE has been used to characterize isoforms of recombinant erythropoietin [13], tissue plasminogen activator [14] and a monoclonal antibody [15].

This paper describes capillary electrophoresis as an alternative technique to isoelectric focusing for the identification and determination of isoforms of a purified $F(ab')_2$. The effects of separation variables such as pH, voltage and buffer type on the resolution and sensitivity of the method were determined. Further, to ascertain that this $F(ab')_2$ heterogeneity was not due to the presence of residual unproteolysed IgG, a kinetic analysis of pepsination of the antibody was also followed by FSCE. As the different forms have the same molecular mass of 100 000, they should differ essentially in their charge. Thus, a comparative analysis of the product was performed using classical isoelectric focusing. Another limitation of this technique is the identification of the different peaks observed on the electropherograms. Separation of the different forms of the $F(ab')_2$ by preparative chromatofocusing [16] led to the first identification by capillary electrophoresis of each $F(ab')_2$ isoform.

EXPERIMENTAL

Kinetics of pepsination

The IgG1 anti Fc γ RI [17] was obtained and purified as already described [18], then buffer-exchanged into phosphate-buffered saline (PBS) (pH 7.2). The antibody was incubated at 37°C in 1.5 M sodium citrate (pH 3.5) with pepsin (specific activity 4770 U/mg) (Sigma) in a ratio 20:1 (w/w). Hydrolysis was stopped increasing the pH to 7.2 (with 2 M K_2HPO_4). The samples were then dialysed against 20 mM phosphate buffer (pH 6.8).

Sodium dodecyl sulphate–polyacrylamide gel electrophoresis (SDS-PAGE)

SDS-PAGE was carried out according to Laemmli [19]. Aliquots were diluted in sample

buffer [3% (v/v) glycerol–0.125 M Tris–HCl–5% (w/v) SDS–0.1% (w/v) bromophenol blue] and heated for 5 min at 95°C under non-reducing conditions. Samples were placed on a 3% (w/v) stacking gel and 7.5% (w/v) separating gel using a Phast-System (Method 110.1; Pharmacia, Uppsala, Sweden), then silver stained (Method 210.2). A mixture of high-molecular-mass proteins (Bio-Rad Labs.) was used as markers. Quantification was achieved by densitometric scanning of the gels (Preference, Sebia, France).

High-performance size-exclusion chromatography (HPSEC)

The IgG and the fragments were resolved by HPSEC (Waters Model 810 liquid chromatographic system) on a 5- μ m TSK G3000 SWXL column (300 \times 7.5 mm I.D.) equilibrated with 20 mM phosphate buffer containing 0.2 M NaCl (pH 7). The proteins were eluted at a flow-rate of 0.5 ml/min and detected at 280 nm. Calibration of the column was performed by injection of a mixture of standard proteins (ferritin, M_r 450 000; catalase, 240 000; aldolase, 158 000; bovin serum albumin, 68 000; chymotrypsin, 25 000). The peaks were integrated with Maxima 810 software.

Capillary electrophoresis

Protein separation was performed with an automated capillary electrophoresis system (Model 270A; Applied Biosystems, San Jose, CA, USA) in a fused-silica capillary (72 cm \times 50 μ m I.D.) thermostated at 30°C. Before each injection, 0.1 M sodium hydroxide and the running buffer were passed through the capillary for 2 and 4 min, respectively. Samples were diluted to 100 μ g/ml in water and injected at the anodic side for 1 s under vacuum (5 in.Hg). The absorbance at 200 nm was detected on-line at the cathodic side and recorded on a Spectra-Physics SP 4400 integrator (chart speed 1 cm/min) with a signal attenuation of 8.

The mobility (μ) was calculated according to the following equation:

$$\mu = (L_d L_t / V) [(1/t_m) - (1/t_{co})]$$

where L_d is the length of the capillary from the anode to the detector, L_t is the total length of

the capillary, V is the applied voltage, t_m and t_{eo} are the migration times of the sample and the electroosmotic flow, respectively.

Isoelectric focusing (IEF)

The gels (PAGplates 3.5–9.5; Pharmacia) were run at 50 mA for 1.5 h and stained with Coomassie Brilliant Blue. pI markers (pI 3–10) were used for calibration (Pharmacia).

Preparative chromatofocusing

The column (mono P HR 5/20; Pharmacia) was equilibrated with two column volumes using 10 mM 2-(N-cyclohexylamino)ethanesulphonic acid (CHES) buffer (pH 9) and the proteins (0.5 mg) were eluted with a pH gradient using Polybuffer 96 diluted eightfold in 10 mM CHES buffer (pH 6) (flow-rate 0.1 ml/min). The absorbance at 280 nm and the pH were monitored on-line. Each fraction collected was dialysed against 20 mM phosphate buffer (pH 6.8).

RESULTS AND DISCUSSION

IgG and $F(ab')_2$ characterization

The products obtained after pepsin proteolysis of the purified antibody were characterized by

SDS-PAGE (Fig. 1). A major band of M_r 150 000 (lane A) corresponding to the M_r of the IgG1 was seen before pepsination, whereas after 20 min of incubation with the enzyme, only one band of M_r 100 000 (lane B), corresponding to the $F(ab')_2$ fragment, was observed. The homogeneity of both preparations was determined by gel filtration. The two peaks (peaks 1 and 2) corresponded to polypeptides of M_r 150 000 and 100 000, respectively. The purity of each product, measured by peak integration, was 98%.

Discrimination of $F(ab')_2$ isoforms by FSCE

Effect of pH. At pH 2.5 the $F(ab')_2$ were positively charged and migrated toward the cathode, with a negligible electroosmotic flow, in a unique peak detected 78.47 min after injection (Fig. 2A). At pH 8.3, when the electrophoretic mobility of the protein and the electroosmotic flow were opposite, three peaks were detected 28.36 min after injection (Fig. 2B). The negative peak observed was due to the electroosmotic flow. At pH 9.5 five peaks characterized the $F(ab')_2$ (18 min, Fig. 2C), and a preceding peak corresponded to the sample buffer (16.8 min). Compared with the previous electropherograms,

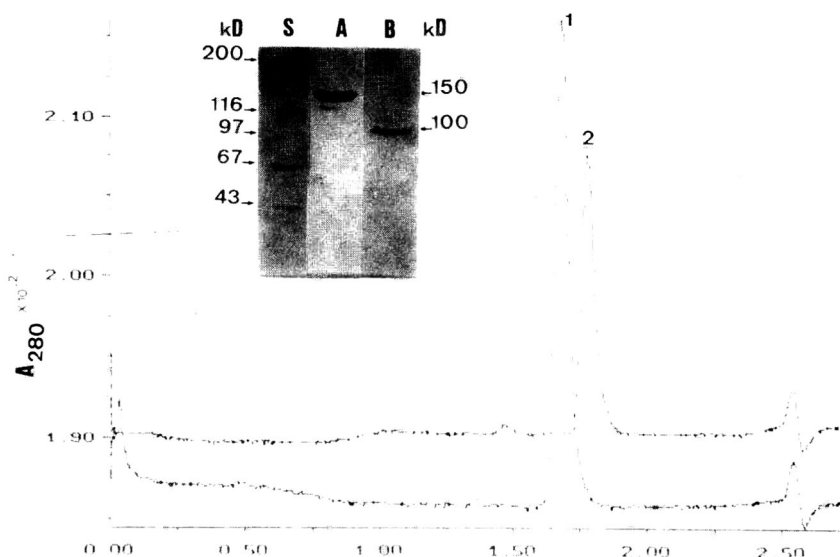


Fig. 1. SDS-PAGE and HPSEC characterization of purified IgG and $F(ab')_2$. SDS-PAGE: lane S = molecular mass standards; A = purified IgG diluted fourfold; B = pepsinated product. HPSEC: Peak 1 = purified IgG diluted fourfold; 2 = pepsinated product. kD = kilo dalton.

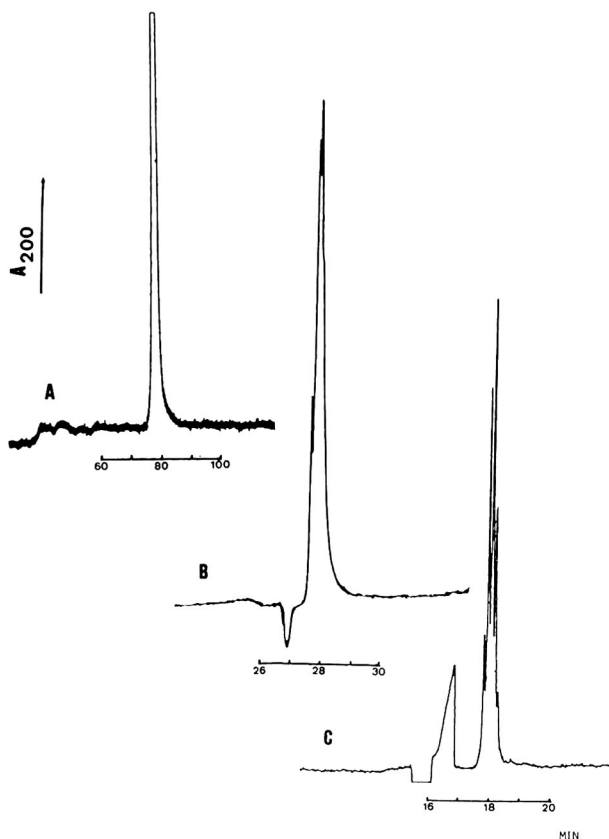


Fig. 2. Electropherograms of the purified $F(ab')_2$ at different buffer pH values. The applied voltage was 5 kV (70 V/cm). (A) 20 mM citrate buffer (pH 2.5) (chart speed 0.1 cm/min); (B) 20 mM borate buffer (pH 8.3); (C) 20 mM CHES buffer (pH 9.5). The horizontal axis is the migration time in minutes and the vertical axis is the absorbance at 200 nm.

this result indicated an increase in selectivity at pH 9.5.

Effect of buffer concentration. Fig. 3 shows that the migration times of the $F(ab')_2$ were 30, 25 and 20 min for tricine buffer concentrations of 100, 50 and 20 mM, respectively (Fig. 3A, B and C). These results suggest that a decrease in buffer concentration increased the apparent mobility of the protein. The mobility of the electroosmotic flow, characterized by the negative peak (Fig. 3), also increased when the buffer concentration decreased. Further, the true mobility of the protein, which is the difference between its apparent mobility and the mobility of the electroosmotic flow, decreased.

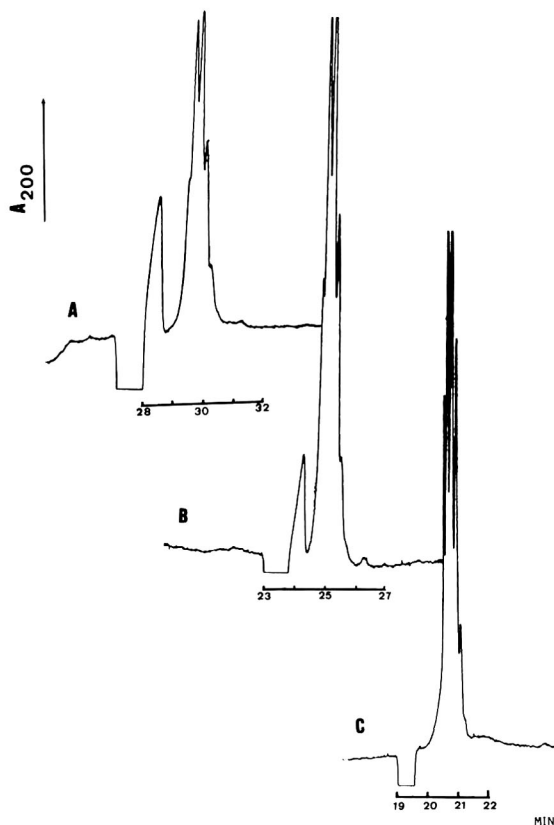


Fig. 3. Electropherograms of the purified $F(ab')_2$ at different buffer concentrations. Migration buffers: tricine of (A) 100, (B) 50 and (C) 20 mM (pH 8). The applied voltage was 5 kV (70 V/cm).

These results suggest that variations in buffer concentration had a greater effect on the endosmotic flow than on the mobility of the protein. At each buffer concentration, the $F(ab')_2$ was characterized by five peaks. Some sign of separation was observed at a buffer concentration of 100 mM and clearly improved at 20 mM. Under these conditions, the decrease in the electroosmotic flow, which is characterized in Fig. 3C by a sharp negative peak, should affect the difference of mobility between the isoforms, increasing the resolution.

Effects of voltage and injection time. Fig. 4A represents the electropherogram obtained with a lower voltage (3 kV). The five peaks were clearly visible and, compared with the previous electropherograms, the resolution was improved. Nevertheless, the product was eluted 34 min

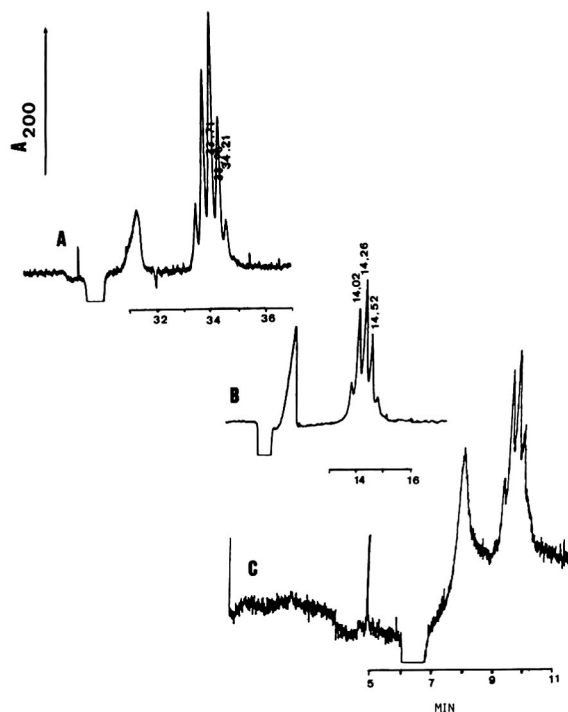


Fig. 4. Optimization of voltage and injection time in 20 mM CHES buffer (pH 9.5). (A) Applied voltage, 3 kV (42 V/cm); injection time, 1 s; capillary length, 72 cm; (B) electrophoresis at 208 V/cm for the first 5 min and 42 V/cm for the remainder; (C) protein diluted to 20 $\mu\text{g}/\text{ml}$ and injection time 0.1 s, which corresponded to 8 pg of protein (80 amol). Capillary length, 69 cm.

after injection. In order to decrease this migration time, the electrophoresis was carried out at 15 kV for the first 5 min and at 3 kV for the remainder. Under these conditions, the $\text{F}(\text{ab}')_2$ was observed after 14 min without a significant modification of the resolution (Fig. 4B). The electropherogram obtained after injection of only 80 amol of $\text{F}(\text{ab}')_2$ (Fig. 4C) indicated that, despite the very small amount of protein injected, the different isoforms were still clearly detectable.

Kinetics of pepsination of IgG: comparison between IEF and FSCE

The kinetics of pepsination of the IgG were followed by IEF and FSCE analysis. In IEF, purified IgG was characterized by different bands corresponding to pI values ranging from 6.3 to 6.5 (Fig. 5, T_0). After 10 min of pepsina-

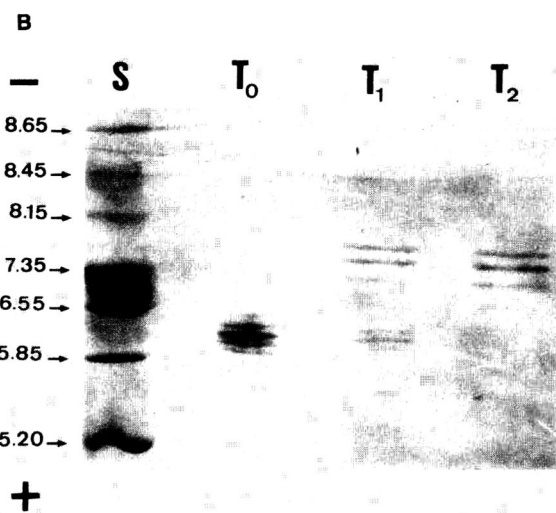
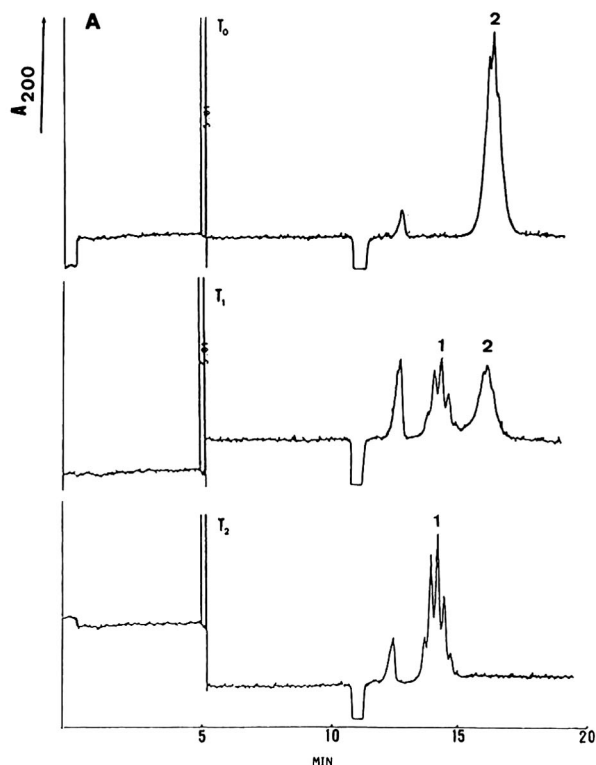


Fig. 5. (A) FSCE analysis of the kinetics of pepsination of the IgG. 20 mM CHES buffer (pH 9.5); applied voltage, 15 kV (208 V/cm) for 5 min and then 3 kV (42 V/cm). T_0 = starting material diluted fourfold before injection; T_1 = after 10 min of pepsination; T_2 = after 20 min of pepsination. (B) Isoelectric focusing at different times of the kinetics. Lane S = pI markers 3–10; T_0 = starting material; T_1 and T_2 = protein after 10 and 20 min of pepsination, respectively.

tion (Fig. 5, T_1), both IgG and the $F(ab')_2$ were visible. The $F(ab')_2$ was characterized by different bands ranging from pI 7.1 to 7.55. After 20 min (Fig. 5, T_2), the intensity of $F(ab')_2$ had increased whereas no residual IgG was detectable, suggesting total digestion of the antibody. In FSCE, purified IgG was characterized by different peaks eluted 16 min after injection (Fig. 5, T_0 , peak 2). After 10 min (Fig. 5, T_1), the previous peaks decreased while new peaks corresponding to the $F(ab')_2$ appeared 14 min after injection (Fig. 5, T_1 , peak 1). After 20 min of pepsination, no IgG was visible while the concentration of the $F(ab')_2$ increased. No contaminating peaks were visible.

These techniques allowed a clear discrimination of the IgG from the $F(ab')_2$ and confirmation that the heterogeneity of the $F(ab')_2$ was not due to unproteolysed IgG. The presence of these isoforms should be attributed to post-translational modifications of the IgG [20] and the microheterogeneity observed with the $F(ab')_2$ indicates that these modifications were not due only to the Fc fragment.

Preparative separation of the isoforms

The $F(ab')_2$ obtained after pepsination of the IgG were purified by chromatofocusing (Fig. 6). The protein bound to the gel was eluted between pH 7.5 and 6.5 in different peaks, confirming the presence of isoforms. Some eluted fractions

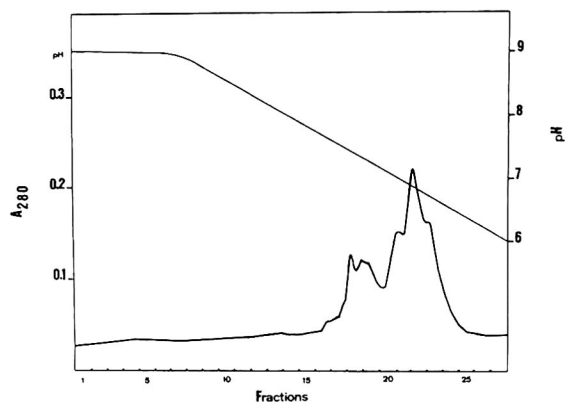


Fig. 6. Chromatofocusing separation of the $F(ab')_2$ isoforms. The chromatofocusing was performed using a Mono P column (HR 5/20). Elution was effected with a linear pH gradient from 9 to 6. The flow-rate was 0.1 ml/min.

corresponding to the different peaks observed in Fig. 6 were characterized by IEF and FSCE.

Characterization of the separated isoforms by FSCE: comparison with IEF

Fig. 7 shows the overlaid electropherograms obtained after FSCE analysis of the $F(ab')_2$ (Fig. 7F) and of fractions 18, 20, 22 and 24 (Fig. 7A, B, C and D, respectively) eluted from the chromatofocusing column. Fraction 18 was characterized by one major peak (Fig. 7A, peak 1) and a second protein more retained in the capillary (peak 2). These products corresponded to the first and second isoforms identified in the $F(ab')_2$ (peaks 1 and 2, Fig. 7F). In Fig. 7B the same isoforms are seen in inverted ratio and a

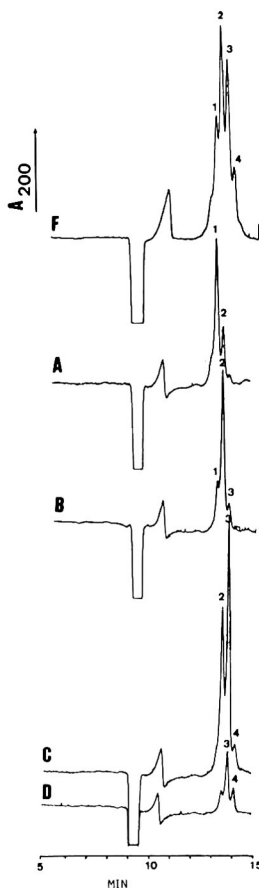


Fig. 7. FSCE characterization of each isoform. The analysis was performed with the Mono P fractions 18, 20, 22, 24 (A, B, C and D, respectively). Experimental conditions as in Fig. 4B. The $F(ab')_2$ was diluted fourfold before injection.

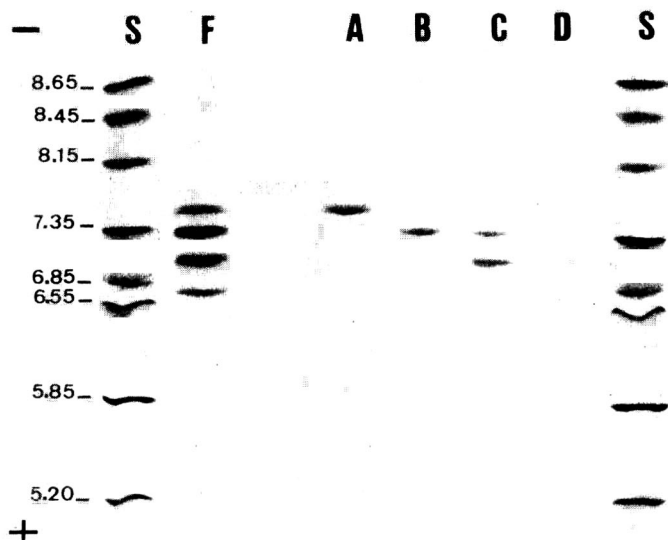


Fig. 8. Isoelectric focusing of the Mono P fractions (Fig. 6). Lane F = F(ab')₂; lane A–D = Mono P fractions 18–24; S = pI standards.

third peak is slightly detectable (peak 3). FSCE analysis of fraction 22 shows two significant peaks (Fig. 7C, peaks 2 and 3) indicating that the two isoforms were present at similar concentrations. These peaks corresponded to the second and third forms of the purified F(ab')₂ (Fig. 7F, peaks 2 and 3). In contrast to the previous fractions, the most electropositive form (peak 1) was absent whereas a fourth peak was visible (peak 4). In fraction 24 (Fig. 7D), the major isoform was the third one and the second and fourth isoforms were still detectable. These results show that the different F(ab')₂ isoforms could be separated by chromatofocusing and that each peak characterized by FSCE corresponded to one of those present in the starting material.

Compared with the FSCE pattern (Fig. 7F), the IEF characterization of the F(ab')₂ (Fig. 8F) shows similar repartitioning of the different isoforms. After chromatofocusing, fraction 18 (lane A) contained two forms characterized by one major band (pI = 7.56) and a more acidic band (pI = 7.35). In lane B, the concentration of the second form increased whereas the previous one decreased. Fraction 22 (lane C) contained a mixture of two isoforms with pI = 7.35 and 7.1. In contrast, in lane D, only the third form (pI =

7.1) was slightly visible and the most acidic form, identified in the starting material (lane F), was not detectable. The isoforms whose ΔpI differed by 0.23 pH unit were identified by FSCE with a Δt between each isoform of 0.24 min (Figs. 7 and 8).

These results show a qualitative and quantitative correlation between IEF and FSCE techniques which can be explained by the fact that the isoforms have the same molecular mass (Fig. 1) and were thus separated in FSCE only by their differences in charge.

CONCLUSIONS

The identification of different forms of a monoclonal F(ab')₂ by FSCE has been achieved. Optimization of the experimental conditions (20 mM CHES buffer at pH 9.5 and lowering the voltage to 3 kV) led to the identification of five isoforms. The presence of these isoforms was first confirmed by the different bands observed after isoelectric focusing analysis. Further, the kinetics of pepsination of the purified IgG, also characterized by FSCE, indicated that the heterogeneity described above was not due to the presence, with the F(ab')₂, of residual anti-

bodies. In order to characterize each isoform, chromatofocusing was successfully used for a preparative separation of the F(ab')₂ isoforms. The reproducibility of the capillary electrophoresis analysis allowed each isoform to be identified and to be correlated with the F(ab')₂ polypeptides previously defined. Capillary electrophoresis represents an attractive complement to conventional analytical techniques for the characterization of subtle differences in charge of proteins, with the advantage that it is quicker, more sensitive and requires very small sample amounts.

REFERENCES

- 1 E. Wenisch, A. Jungbauer, C. Tauer, M. Reiter, G. Gruber, F. Steindl and H. Katinger, *J. Biochem. Biophys. Methods*, 18 (1989) 309.
- 2 R.G. Nielsen, E.C. Rickard, P.F. Santa, D.A. Sharknas and G.S. Sittampalam, *J. Chromatogr.*, 539 (1991) 177.
- 3 B.J. Moellering, J.L. Tedesco, R. Reid Townsend, M.R. Hardy, R.W. Scott and C.P. Prior, *BioPharm*, 3 (1990) 30.
- 4 H.H. Lauer and D. McManigill, *Anal. Chem.*, 58 (1986) 166.
- 5 R.I. Hecht, J.C. Morris, F.S. Stover, L. Fossey and C. Demarest, *Prep. Biochem.*, 19 (1989) 201.
- 6 R.G. Nielsen, G.S. Sittampalam and E.C. Richard, *Anal. Biochem.*, 177 (1989) 20.
- 7 P.G. Pande, R.V. Nellore and H.R. Bhagat, *Anal. Biochem.*, 904 (1992) 103.
- 8 N.A. Guzman and L. Hernandez, in T.E. Hugli (Editor), *Techniques in Protein Chemistry*, Academic Press, San Diego, New York, 1989, pp. 456–467.
- 9 J.W. Jorgenson and K.D.A. Lukacs, *Science*, 222 (1983) 226.
- 10 P.D. Grossman, J.C. Colburn, H.H. Lauer, R.G. Nielsen, R.M. Riggin, G.S. Sittampalam and E.C. Rickard, *Anal. Chem.*, 61 (1989) 1186.
- 11 G.H. Bolt, *J. Phys. Chem.*, 61 (1957) 1166.
- 12 P.D. Grossman, K.J. Wilson, G. Petrie and H.H. Lauer, *Anal. Biochem.*, 173 (1988) 265.
- 13 A.D. Tran, S. Park, P.J. Lisi, O.T. Huynh, R.R. Ryall and P.A. Lane, *J. Chromatogr.*, 542 (1991) 459.
- 14 M. Taverna, A. Baillet, D. Biou, M. Schlüter, R. Werner and D. Ferrier, *Electrophoresis*, 13 (1992) 359.
- 15 B.J. Compton, *J. Chromatogr.*, 559 (1991) 357.
- 16 A. Jungbauer, C. Tauer, E. Wenisch, K. Uhl, J. Brunner, M. Purtscher, F. Steindl and A. Buchacher, *J. Chromatogr.*, 512 (1990) 157.
- 17 M.W. Fanger, R.F. Graziano, L. Shen and P.M. Guyre, *Chem. Immunol.*, 47 (1989) 214.
- 18 F. Dhainaut, N. Bihoreau, J.L. Meterreau, J. Lirochon, R. Vincentelli and G. Mignot, *Cytotechnology*, 10 (1992) 33.
- 19 U. Laemmli, *Nature*, 227 (1970) 680.
- 20 D.R. Hoffman, in N. Catssimpoolas and J. Drysdale (Editors), *Biological and Biomedical Applications of Isoelectric Focusing*, Plenum Press, New York, 1977, p. 121.

Short Communication

New graph of binary mixture solvent strength in adsorption liquid chromatography

Veronika R. Meyer*

Institute of Organic Chemistry, University of Berne, Freiestrasse 3, CH-3012 Berne (Switzerland)

Mariana D. Palamareva

Department of Chemistry, University of Sofia, Sofia 1126 (Bulgaria)

(First received February 17th, 1993; revised manuscript received March 23th, 1993)

ABSTRACT

A graph that allows the determination of the composition of a binary solvent mixture if a given eluent strength is needed is presented. It is suited for adsorption (*i.e.* normal-phase) liquid chromatography on silica and includes the twelve binary mixtures possible with hexane, dichloromethane, *tert.*-butyl methyl ether, tetrahydrofuran, ethyl acetate and isopropanol.

INTRODUCTION

In 1974, Saunders presented a graph for the determination of binary eluent strength in adsorption liquid chromatography [1]. It found widespread use and was reprinted in many books about column liquid chromatography. Fig. 1 is a reproduction of this diagram; it is included here because it was important in the development of adsorption chromatography and because it is the model for the new graph described in this paper. It allows the quick determination of the eluent composition if a certain solvent strength is needed. The graph was inspired by an earlier figure by Neher [2].

The uppermost bar in the drawing represents the solvent strength parameter ϵ^0 after Snyder [3] (in this volume, the concept of solvent strength is developed in Chapter 8, pp. 185–240). In most tables of the eluotropic series, ϵ^0 values are given for alumina, but the graph is for silica with $\epsilon^0(\text{silica}) = 0.77 \epsilon^0(\text{alumina})$. The other horizontal lines represent the volume per cent composition of the following solvent mixtures, from top to bottom: isopropyl chloride in pentane, dichloromethane in pentane, diethyl ether in pentane, acetonitrile in pentane, methanol in pentane, dichloromethane in isopropyl chloride, diethyl ether in isopropyl chloride, acetonitrile in isopropyl chloride, methanol in isopropyl chloride, diethyl ether in dichloromethane, acetonitrile in dichloromethane, methanol in dichloromethane, acetonitrile in diethyl ether, methanol in di-

* Corresponding author.

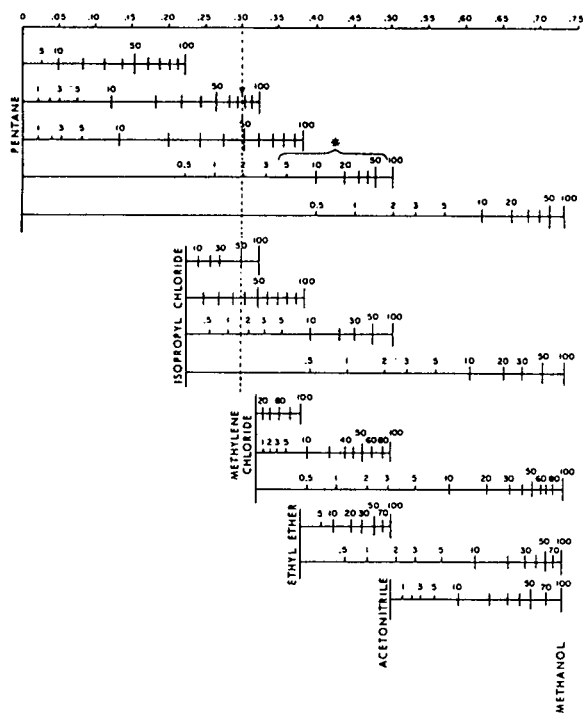


Fig. 1. Graph of mixed solvent strengths ϵ^0 on silica by Saunders (reprinted with permission from ref. 1, copyright American Chemical Society 1974). It considers the solvents pentane, isopropyl chloride, dichloromethane (methylene chloride), diethyl ether (ethyl ether), acetonitrile and methanol. The asterisk marks the region where pentane and acetonitrile are not miscible; Saunders recommends adding some carbon tetrachloride. The dashed vertical line was added for explanatory purposes: to obtain a mixture with $\epsilon^0 = 0.30$ it is possible to use, for example, 2% acetonitrile in pentane or 50% dichloromethane in isopropyl chloride.

ethyl ether, and methanol in acetonitrile.

In the paper [1] it is not explained how the graph was calculated, but this is clear from Snyder's book [3]. There the following equation can be found (eqns. 8–10 on p. 208 of that volume):

$$\epsilon_{ab} = \epsilon_a + \frac{\log(N_b 10^{\alpha n_b (\epsilon_b - \epsilon_a)} + 1 - N_b)}{\alpha n_b}$$

where ϵ_a is the eluent strength of the weaker solvent (=solvent a), N_b is the mole fraction of

the stronger solvent (=solvent b), α is the activity of the adsorbent surface ($\alpha = 1$ if the adsorbent is higher active; $\alpha = 0$ in the case of full deactivation), n_b is the reduced (*i.e.* relative) cross-section of a molecule of the stronger solvent (dimensionless) and ϵ_b is the eluent strength of the stronger solvent.

For three reasons we found it appropriate to calculate and draw a new graph:

(1) Whereas the ϵ^0 values of pure pentane (=0 by definition), isopropyl chloride (0.22), dichloromethane (0.32), acetonitrile (0.50) and methanol (0.73) are in accordance with the values given by Snyder [3] (p. 195) if corrected by the silica factor of 0.77, the value for diethyl ether as given in the graph is wrong. ϵ^0 (alumina) is 0.38, therefore ϵ^0 (silica) is 0.29. In error the alumina value of 0.38 was used for the drawing. However, this is a historical remark as some of the ϵ^0 values have undergone revision in the meantime.

(2) The choice of solvents does not represent the most used eluents by today's experience.

(3) The weakest point of the graph is that it does not include an important concept in adsorption chromatographic theory which has been developed in the meantime, that is solvent localization [4,5]. The localization parameter, m , is a measure of the ability of the solvent molecule to interact with the adsorbent which is used as stationary phase. In the case of silica, the adsorptive sites responsible for retention are its silanol groups. Molecules that can interact with these sites by means of their polar functional group, such as ethers, esters, alcohols, nitriles and amines, will prefer a specific position with respect to a nearby silanol group. Silica surrounded with such a localizing solvent or sample is covered with a well-defined layer of molecules. In contrast to this, a non-localizing solvent or sample such as dichloromethane or benzene will interact with silica to a much weaker extent and the coverage is random. It is obvious that even a small amount of a strongly localizing solvent, such as an alcohol, will have a distinct influence on sample retention.

THE NEW GRAPH

Choice of solvents

For the calculation of a new graph the following six solvents were chosen.

Hexane. As pentane, the solvent has $\epsilon^0 = 0$, but it is cheaper (as a mixture of isomers) and has a suitable boiling point of 69°C, whereas pentane with a boiling point of 36°C is less convenient (but can be useful for special purposes).

Dichloromethane. Of the medium polar solvents, this is a weak one because it is non-localizing. In the course of the optimization of a separation it offers a distinct selectivity as it is the representative eluent with dipole properties [6]. Despite its interesting and useful properties it should be avoided whenever possible because it is toxic and environmentally harmful.

tert.-Butyl methyl ether (tBME). This solvent has now replaced diethyl ether in many applications because it does not form peroxides and offers the same boiling point advantage as in the case of hexane vs. pentane: 55°C for tBME and 35°C for diethyl ether [7]. It is the representative eluent with proton-accepting properties [6] and is localizing.

Tetrahydrofuran (THF). Although it is not cheap, THF is often used. It offers the same strength as tBME and is localizing but it is much weaker a proton acceptor [6].

Ethyl acetate. This solvent also has the same strength as tBME and THF. Its polarity properties are quite similar to THF [6]. Its drawback is the missing UV transparency; it cannot be used below 260 nm.

Isopropanol (IPA). This is a strong (polar and localizing) solvent that is fully miscible with hexane.

In any case all six solvents are fully miscible with each other. Acetonitrile and methanol are not miscible with hexane and for this reason they are not included in the graph. In compositions with hexane, acetonitrile and methanol, as well as water, play an important role as modifiers to deactivate the adsorbent surface [8] but not as mobile phase strength adjusters. For toxicological and ecological reasons chloroform was not considered, although it is the representative solvent as proton donor [6].

Calculations

The calculation of solvent strength ϵ^0 according to Snyder's theory [4,5] is demanding because it involves iterative mathematics and for this reason cannot be done without an appropriate program run on a personal computer. This program is described in detail in a previous paper [9].

The parameters used for the calculations here are listed in Table I. The program failed to calculate ϵ^0 values of mixtures of hexane con-

TABLE I
SOLVENT PARAMETERS USED FOR THE CALCULATIONS

d/M_r = solvent density (g/ml) divided by molecular mass; n = reduced molar cross-section; ϵ' = elution strength on silica when the molar fraction of the solvent in the mobile phase approaches 0; ϵ'' = elution strength on silica when the molar fraction of the solvent in the mobile phase approaches 1; $f_1(C)/n$ = parameter describing the influence of strong solvent concentration on elution strength.

Solvent	$100d/M_r$	n	ϵ'	ϵ''	$f_1(C)/n$
Hexane	0.77	—	0	0	0
Dichloromethane	1.57	4.1	0.30	0.30	0
<i>tert.</i> -Butyl methyl ether	0.84	4.1	1.01	0.48	1.10
Tetrahydrofuran	1.23	5.0	0.73	0.48	1.30
Ethyl acetate	1.02	5.2	0.94	0.48	1.60
Isopropanol	1.34	4.4	1.80	0.60	4.10

taining less than 3% IPA, so these values were taken from a paper by Snyder and Glajch [10]. Indicating these extreme mixture ratios, the graph shows the drastic increase in solvent strength if a minute amount of a strong component is added to a weak eluent; however, the numeric value of ϵ^0 should not be taken for granted in this region.

The graph

Fig. 2 presents the new solvent strength graph for binary mixtures on silica. It is used in identical manner as the Saunders graph. The possible range of ϵ^0 values offered by a certain mixture is indicated by the horizontal bars. The numbers below these bars indicate the amount of stronger solvent in volume per cent that is needed to obtain the desired strength of the mixture. The use of the graph is illustrated by an example:

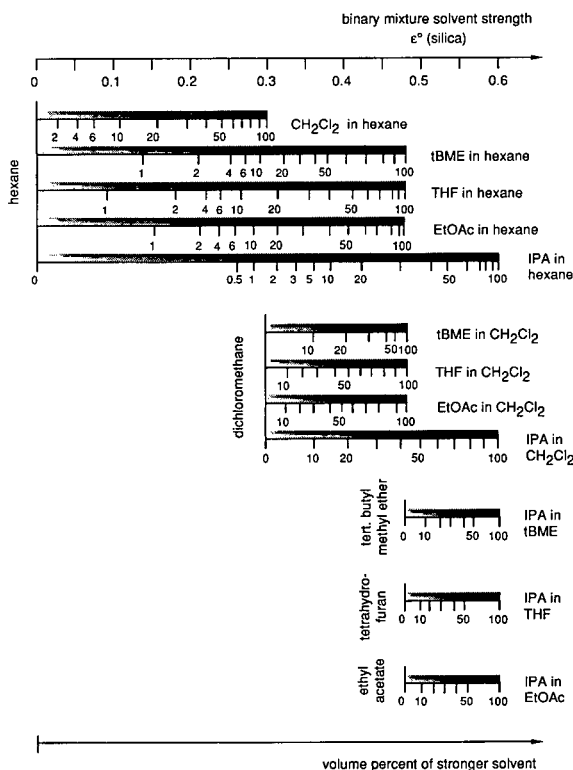


Fig. 2. Solvent strength graph for binary mixtures of hexane, dichloromethane, *tert*-butyl methyl ether, tetrahydrofuran, ethyl acetate and isopropanol used in adsorption liquid chromatography on silica.

If a solvent strength of 0.4 is needed, this can be obtained by the following mixtures:

approximately 60% *tert*-butyl methyl ether in hexane; 45% tetrahydrofuran in hexane; 50% ethyl acetate in hexane; 15% isopropanol in hexane; 20% *tert*-butyl methyl ether in dichloromethane; 45% tetrahydrofuran in dichloromethane; 50% ethyl acetate in dichloromethane; or 20% isopropanol in dichloromethane.

Although all of these eight mixtures have the same strength, their selectivity for a given separation problem can be rather different. "Selectivity" means that the strength, as determined by the capacity factor k' of a certain individual solute, is not constant but can vary. For the solution of complex separation problems it can be useful to try several of these mixtures, as separation factors, resolutions and even elution orders may change. Thus, it has been shown [4,5,11,12] that solvent selectivity varies depending on whether the strong (polar) solvent is non-localizing, localizing and basic or localizing and non-basic. Of the polar solvents shown in Fig. 2, dichloromethane is non-localizing. The solvents *tert*-butyl methyl ether and THF are localizing and basic, and they should be similar in terms of selectivity (but different from dichloromethane). Ethyl acetate is a localizing, non-basic solvent whose selectivity is expected to be different from the other solvents of Fig. 2. Finally, isopropanol is a localizing, basic solvent. But it should differ somewhat in selectivity because of its proton-donating ability. Thus the solvents in Fig. 2 encompass a wide range of possible selectivity and they should be useful for optimizing band spacing and resolution. Unfortunately, it is still difficult to predict elution orders, and today's research interest is not directed towards this type of problem [13]. Nevertheless, the effect of ϵ and two other parameters of Snyder's theory on various separations has been studied in detail [14].

CONCLUSIONS

The graph presented in Fig. 2 can be useful for the determination of the composition of a binary mixture if a certain elution strength is needed in adsorption chromatography on silica. An alter-

native approach is the use of the microcomputer program permitting an easier choice of mobile phases containing two or more solvents [9,14].

ACKNOWLEDGEMENTS

We are grateful for most helpful advice obtained from Dr. L.R. Snyder. Thanks are due to the National Research Fund, Bulgaria, for a grant to one of us (M.D.P.).

REFERENCES

- 1 D.L. Saunders, *Anal. Chem.*, 46 (1974) 470.
- 2 R. Neher, in G.B. Marini-Bettolo (Editor), *Thin Layer Chromatography*, Elsevier, Amsterdam, 1964, p. 75.
- 3 L.R. Snyder, *Principles of Adsorption Chromatography*, Marcel Dekker, New York, 1968.
- 4 L.R. Snyder, J.L. Glajch and J.J. Kirkland, *J. Chromatogr.*, 218 (1981) 299.
- 5 L.R. Snyder, in Cs. Horváth (Editor), *High-Performance Liquid Chromatography — Advances and Perspectives*, Vol. 3, Academic Press, New York, 1983, p. 157–223.
- 6 L.R. Snyder, *J. Chromatogr. Sci.*, 16 (1978) 223.
- 7 C.J. Little, A.D. Dale, J.A. Whatley and J.A. Wickings, *J. Chromatogr.*, 169 (1979) 381.
- 8 D.L. Saunders, *J. Chromatogr.*, 125 (1976) 163.
- 9 M.D. Palamareva and H.E. Palamarev, *J. Chromatogr.*, 477 (1989) 235.
- 10 L.R. Snyder and J.L. Glajch, *J. Chromatogr.*, 248 (1982) 165.
- 11 J.L. Glajch, J.J. Kirkland and L.R. Snyder, *J. Chromatogr.*, 238 (1982) 269.
- 12 L.R. Snyder, J.L. Glajch and J.J. Kirkland, *Practical HPLC Method Development*, Wiley-Interscience, New York, 1988, pp. 114–120.
- 13 N. Volpe and A.M. Siouffi, *Chromatographia*, 34 (1992) 213.
- 14 M.D. Palamareva and I.D. Kozekov, *J. Chromatogr.*, 606 (1992) 113.

Short Communication

Time- and cost-saving approach for liquid chromatography–mass spectrometry vacuum systems

Joseph T. Snodgrass, Mark J. Hayward* and Michael L. Thomson

*American Cyanamid Company, Agricultural Research Division, Analytical, Physical and Biochemical Research Section,
P.O. Box 400, Princeton, NJ 08543-0400 (USA)*

(First received January 21st, 1993; revised manuscript received April 15th, 1993)

ABSTRACT

A refrigerated trap system is described for recovering the mobile phase utilized with popular liquid chromatography–mass spectrometry interfaces. By efficiently freezing the excess LC effluent, vacuum system components are protected from rapid wear and scheduled maintenance intervals can be substantially extended. The modest cost of the system is easily justified based on the increased lifetime afforded to expensive vacuum pumps and the added convenience, time savings and the safety gained by the elimination of dry ice–solvent or liquid nitrogen bath systems.

INTRODUCTION

In LC systems, the analytes of interest typically comprise only a very minor proportion of the flowing mobile phase. When a mass spectrometer operating under high vacuum is utilized for LC detection, provisions must be made to accommodate the high mass transfer rates associated with removal of the mobile phase from the vacuum chambers. For some early LC–MS interfaces such as direct liquid injection or moving belt devices, simply increasing the effective pumping speed of the mass spectrometer's vacuum system was usually adequate because mass transfer was reduced prior to reaching the vacuum system. In the more modern LC–MS interfaces where the vacuum system must accept the full flow of the LC effluent, such as thermospray [1] and particle

beam systems [2], the load on the vacuum mechanical pumps is much greater. The situation is often exacerbated by the use of solvents ill-suited for pumping by standard vacuum pumps. Water, for example, is a very common mobile phase component that is exceedingly corrosive to the internal parts of mechanical vacuum pumps.

The typical method for accommodating the LC mobile phase flows associated with modern LC–MS interfaces employs one or more additional mechanical pumps, which are usually protected by an in-line dry ice solution cold trap. The pumps either remove most of the solvent mixture before it arrives at the ion source in a differential pumping configuration, or pumps away the entire solvent stream from the ion source after a small fraction has been sampled by the mass spectrometer. These two configurations are commonly used in particle beam and thermospray interfaces, respectively [2]. The weak link in using these systems is usually the cold trap used

* Corresponding author.

TABLE I
TEMPERATURES OF DRY ICE BATHS

Values from ref. 3. Note: isopropanol value approximated based on melting point.

Solvent	Temperature (°C)
Ethylene glycol	-15
Carbon tetrachloride	-23
3-Heptanone	-38
Acetonitrile	-42
Cyclohexanone	-46
Chloroform	-61
Ethanol	-72
Acetone	-77
Isopropanol	-90
Diethyl ether	-100
Savant RTV4104 Refrigerated Trap	-104 ^a

^a Included for comparison.

to recover the mobile phase. As shown in Table I, the dry ice slurries prepared for these traps provide cooling to temperatures that are only marginally lower than the freezing point of the mobile phase components. (Acetonitrile, for example, has a freezing point of approximately -46°C.) These slurries only maintain their temperature for a few hours before requiring the addition of dry ice. After a few days, the entire slurry must be discarded because contamination by water condensing from the air causes the temperature of the slurry to rise substantially. Dry ice baths tend to bubble and froth when the coolant is first admitted to the dewar. Furthermore, the solvents commonly used in these cold traps are often flammable, and may also pose other safety concerns, such as exposure hazards. Liquid nitrogen traps offer a lower temperature alternative but share the remainder of the disadvantages of dry ice traps. In practice, it is rare that dry ice or liquid nitrogen traps are adequately maintained. As a consequence, a considerable fraction of the mobile phase is pumped all the way into the mechanical vacuum pump, where it condenses, collects, and corrodes the pump's internal parts. Unless the pump oil is drained and replaced each time it is contaminated, which may be on a daily basis, it is likely

that the mechanical vacuum pump will need rebuilding or replacement every three to six months.

In this note, we describe a refrigerated solvent recovery system which replaces the dry ice-solvent cold trap. All the components of this system are commercially available at a cost low enough that the system quickly pays for itself in savings for dry ice and solvents. The system also affords superior protection against mobile phase induced damage to the mechanical vacuum pumps, which leads to the greatest cost savings, since rebuilding or replacing these pumps can be quite expensive. Most importantly, the system can result in considerable time savings for the personnel involved by minimizing routine start-up and shut-down time and by reducing instrument down time.

EQUIPMENT

The refrigerated solvent recovery system is illustrated in Fig. 1. The refrigerated trap and mechanical vacuum pump are shown in the configuration we have used extensively, with a thermospray type LC-MS interface (TSP1) on a triple stage quadrupole mass spectrometer (Finnigan MAT TSQ-46).

The refrigerated solvent recovery trap is a model number RVT4104 trap supplied by Savant Instruments (Farmingdale, NY, USA) at a cost of US \$2500. A silicone heat transfer fluid is

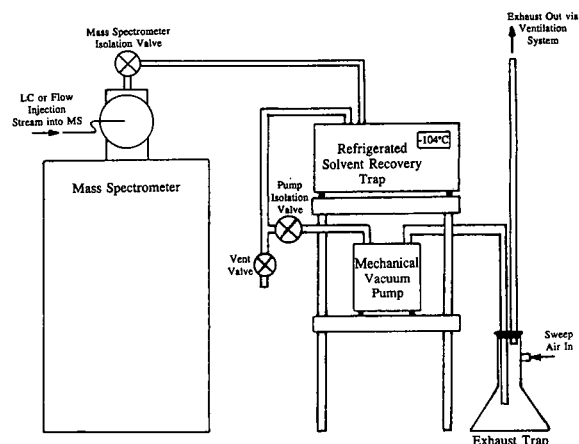


Fig. 1. The refrigerated trap mobile phase recovery system for LC-MS.

cooled to -103°C to -112°C by a low-temperature refrigeration system. This fluid remains a liquid, insuring good thermal contact with a 4-l glass vessel that collects the condensed solvent. Both the refrigeration system and the glass solvent collection vessel are enclosed in a square metal cover. Temperature monitoring is provided via a digital display. The glass collection vessel can be easily removed when it is filled by disconnecting the vacuum hoses (equipped with quick-disconnect fittings) and raising it through a large hole on the top of the unit. The three vacuum valves shown in the figure make it possible to perform this operation without breaking vacuum for the mechanical vacuum pump or the mass spectrometer. The mechanical vacuum pump is kept running and at full operating temperature at all times in order to prevent the condensation of corrosive solvents in the lubricating oil.

The mechanical vacuum pump is a Balzers UNO-016B single stage direct drive pump with a pumping speed of 360 l/min, designed expressly for LC-MS applications. During operation, the ballast is opened slightly. The pump is raised off the ground on the shelving shown in Fig. 1 in order to achieve the following two advantages: First, the exhaust line descends to the exhaust trap, allowing any condensable vapors expelled by the pump to collect in the ambient temperature exhaust trap. This prevents any contaminated liquids from refluxing back into the pump oil and minimizes their build up in the ventilation system. Second, routine maintenance for the mechanical vacuum pump is facilitated by locating it above the lab floor. One oil drain is located on the front of the pump, which projects out slightly from the shelf. A 3-in. (7.6 cm) diameter hole cut in the shelf, allows easy access to the other oil drain plug under the base of the pump.

RESULTS AND CONCLUSIONS

In a recent paper, we described techniques developed to carry out automated routine sample analyses using flow injection thermospray mass spectrometry [4] with the system shown in Fig. 1. As a result of our successful efforts in

automation, this instrument is used quite heavily (over 4000 samples analyzed per year). Before installation of the refrigerated solvent recovery trap, a 1-l glass trap cooled in a dry ice-isopropanol bath was used in-line, just before the same mechanical vacuum pump. During operation, the pressure measured at the intake to the pump would typically rise to 1 Torr (133 Pa) or more, for a mobile phase flow-rate of 1.4 ml/min. The pressure in the mass spectrometer was approximately $2 \cdot 10^{-5}$ Torr (2.7 mPa). For a recently rebuilt or new mechanical pump, the pump oil would typically require replacement every 2–4 weeks. After a few months of service, even more frequent oil changes were required. On average, a full rebuilding of the pump was necessary every 6 months.

After installation of the new refrigerated trap system, the pressure rise at the mechanical pump intake became barely discernable when the same mobile phase flow was initiated. With the pump ballast open, the typical pressure during operation is less than 100 mTorr (13 Pa). The pressure in the mass spectrometer remains at $2 \cdot 10^{-5}$ Torr (2.7 mPa). The maintenance interval between pump oil changes was extended to once every 3 months, and the need to rebuild pumps should be reduced to a frequency approaching that of pumps operating in far less demanding applications (once every 3 to 5 years). In addition to these benefits, the new system is much easier to use than the messy

TABLE II
KEY FEATURES OF REFRIGERATED AND DRY ICE SOLVENT RECOVERY TRAPS

Feature	Dry ice	Refrigerated
Operating pressure	>1000 mTorr (>130 Pa)	<100 mTorr (<13 Pa)
Oil change frequency	2 weeks	3 months
Pump rebuild frequency	6 months	3–5 years ^a
Required attention frequency	4 h	1 week

^a Estimated lifetime.

solvent bath trap. Instead of the daily preparation and hourly attention required by a solvent–dry ice bath, the only requirement is replacing the glass vessel with a clean one, which takes *ca.* 1 min. At our usage rate this is required only once a week. The comparative features of the refrigerated and dry ice types of vapor traps are given in Table II. Although, the refrigerated system has not been tested with particle beam LC–MS, we expect similar performance improvements for systems where the mechanical pumping system is required to accept liquid mobile phase flow-rates on the order of 1 ml/min.

In summary, the refrigerated trap system represents a significant improvement that can benefit many laboratories using LC–MS on a routine basis. The main benefits include better protec-

tion and less frequent maintenance intervals for mechanical vacuum pumps, no daily preparation and periodic attention to cold baths, and the elimination of flammable and potentially hazardous solvents. The net result is considerable savings in both time and money.

REFERENCES

- 1 A.L. Yergey, C.G. Edmonds, I.A.S. Lewis and M.L. Vestal, *Liquid Chromatography/Mass Spectrometry Techniques and Applications*, Plenum Press, New York, 1990.
- 2 W.M.A. Niessen and J. van der Greef, *Liquid Chromatography–Mass Spectrometry: Principles and Applications*, Marcel Dekker, New York, 1992.
- 3 A.J. Gordon, *The Chemists Companion: A Handbook of Practical Data, Techniques, and References*, Wiley, 1972.
- 4 M.J. Hayward, J.T. Snodgrass and M.L. Thomson, *Rapid Comm. Mass Spectrom.*, 7 (1993) 85.

Short Communication

4-(Trifluoromethyl)-2,3,5,6-tetrafluorobenzyl bromide as a new electrophoric derivatizing reagent

Manasi Saha, Jayanta Saha and Roger W. Giese*

Department of Pharmaceutical Sciences in the Bouve Pharmacy and Health Sciences, and Barnett Institute, Northeastern University, 360 Huntington Avenue, Boston, MA 02115 (USA)

(First received February 1st, 1993; revised manuscript received April 7th, 1993)

ABSTRACT

4-(Trifluoromethyl)-2,3,5,6-tetrafluorobenzyl bromide (TTBB) was synthesized in a single step from $\alpha,\alpha,\alpha,2,3,5,6$ -heptafluoro-*p*-xylene. The purpose of TTBB is to function as an analogue of pentafluorobenzyl bromide (PFBB) in electrophoric derivatization reactions prior to detection by gas chromatography–electron-capture negative ion mass spectrometry (GC–ECNI-MS). In more detail, it was anticipated that TTBB could be used along with, or as a substitute for, PFBB to help control some interferences and confirm results. This is because a TTBB-product (of an analyte) would have different retention and sometimes *m/z* characteristics than a corresponding PFBB product in GC–ECNI-MS, while the two products should be similar in their ease of formation and yields. Results demonstrating these expectations were achieved by derivatizing and detecting two analytes with these reagents: N7-(2-hydroxyethyl)xanthine, and 2,3-pyrenedicarboxylic acid.

INTRODUCTION

Pentafluorobenzyl bromide (PFBB) is used as a derivatizing reagent to enhance the detectability of susceptible compounds by gas chromatography–electron-capture negative ion mass spectrometry (GC–ECNI-MS) and GC with electron-capture detection (ECD). Examples of such compounds are some of the normal and modified DNA nucleobases [1–3], arachidonic acid metabolites [4–5], drugs [6–9], phenols [10], plant metabolites [11], indole-amine metabolites [12], fatty acids [13], herbicides [14], inorganic anions [15] and histamine [16]. A low detection

limit can be achieved especially when a derivative is formed which gives essentially a single ion in GC–ECNI-MS. However, this compromises the specificity by making it difficult to know whether an interference is present. When GC–ECNI-MS is used for environmental analysis, it is useful to monitor more than one ion to help confirm results [17]. Increased demands are therefore placed on prior sample cleanup in chemical analysis when pentafluorobenzyl derivatives are formed that give single ions in GC–ECNI-MS. Use of a second GC column can help to confirm a result but is not always practical.

Along these lines, it can be useful to derivatize a given analyte with 2,3,5,6-tetrafluorobenzyl bromide. By producing a different but analogous product (having a different GC retention time,

* Corresponding author.

m/z or both), the use of this reagent can overcome a persistent interference or help to confirm peak identity [18]. For the latter purpose, it may be attractive to use the two reagents separately (on two aliquots of the sample), or as a mixture on a single sample.

We considered that it would be useful to have a third reagent of this type for additional flexibility in coping with interferences and confirming results. Partly this is because interferences tend to become increasingly random as analytical methods are progressively applied to smaller amounts of trace analytes. Thus, as reported here, we have prepared and tested a second analog of pentafluorobenzyl bromide, in which a trifluoromethyl group rather than a hydrogen atom replaces the *para* fluorine atom in pentafluorobenzyl bromide. The chemical and physical properties of the trifluoromethyl group have been reviewed [19].

EXPERIMENTAL

Reagents

Pentafluorobenzyl bromide, potassium hydroxide and tetrabutyl ammonium hydrogen sulphate (Bu_4NHSO_4) were purchased from Aldrich (Milwaukee, WI, USA). HPLC-grade organic solvents were purchased from Doe and Ingalls (Medford, MA, USA). $\alpha,\alpha,\alpha,2,3,5,6$ -Heptafluoro-*p*-xylene and benzoylperoxide were from Aldrich. Gases for GC-ECNI-MS were from Med-Tech (Medford, MA, USA). 2,3-Pyrene-dicarboxylic acid was synthesized as described [20], as was N7-(2-hydroxyethyl)xanthine [3].

Equipment

A Model 5988A mass spectrometer from Hewlett-Packard (Palo Alto, CA, USA) was used. The gas chromatograph, a Hewlett-Packard 5890 Series II, was connected to the mass spectrometer with the capillary interface kept at 290°C and the ion source at 250°C. A Hewlett-Packard 59970 MS Chemstation data system was used to record the data. Methane (2 Torr; 1 Torr = 133.322 Pa) and He (20 p.s.i.; 1 p.s.i. = 6894.76 Pa) were used as reagent and carrier gases respectively. Injections were made in an on-column mode onto an HP Ultra 1 (dimethyl-

polysiloxane), 25 m × 0.2 mm I.D., 0.11 μm film thickness capillary column, and the oven was programmed from 110 to 250°C at 70°C/min (then 10 min hold) for compounds 1 to 3, and from 140 to 300°C at 70°C/min for 4, with a hold of 13 min.

Methods

4-(Trifluoromethyl)-2,3,5,6-tetrafluorobenzyl bromide (TTBB). A mixture of $\alpha,\alpha,\alpha,2,3,5,6$ -heptafluoro-*p*-xylene (5 g, 21.5 mmol), N-bromosuccinimide (3.45 g, 19.4 mmol) and benzoylperoxide (500 mg, 2.0 mmol) in 50 ml of CCl_4 was refluxed under nitrogen for 10 h. The hot reaction mixture was filtered through a Buchner funnel (Celite). The solvent was evaporated and the crude product was purified by silica flash chromatography (bed volume: 15 cm × 2 cm) with isoctane, yielding a colorless oil (2.7 g, 40%). $^1\text{H NMR}$ (300 MHz, C^2HCl_3) δ 4.55 (2H, s). This reagent is now available from Aldrich.

N1,N3-Bis-[4-(trifluoromethyl)-2,3,5,6-tetrafluorobenzyl]-N7-{2-[4-(trifluoromethyl)-2,3,5,6-tetrafluorobenzoyloxy]ethyl}xanthine (3). To a stirred solution of N7-(2-hydroxyethyl)xanthine (N7-HEX; 2 mg, 0.01 mmol) in 100 μl of 1 N KOH were added CH_2Cl_2 (300 μl), Bu_4NHSO_4 (10 mg, 0.0027 mmol) and TTBB (10 mg, 3.2 μmol). After stirring for 48 h at room temperature the reaction mixture was partitioned between 1 ml each of water and CH_2Cl_2 . The organic layer was separated and the aqueous layer was extracted 3× with 1 ml of CH_2Cl_2 . The combined CH_2Cl_2 fractions were dried over Na_2SO_4 , and the filtered solution was evaporated under vacuum. The crude product was purified on an analytical silica TLC plate with ethyl acetate-hexane (1:1), to give a white solid (2 mg, 22%). $^1\text{H NMR}$ (300 MHz, C^2HCl_3): δ 7.30 (s, 1H), 5.20 (s, 2H), 5.06 (s, 2H), 4.26 (s, 2H), 4.13 (t, 2H), 3.60 (t, 2H).

1,2-Bis[4-(trifluoromethyl)-2,3,5,6-tetrafluorobenzyl]pyrene dicarboxylate (4). To a stirred solution of 2,3-pyrene dicarboxylic acid (2.01 mg, 6.9 μmol) in 200 μl of CH_3CN was added K_2CO_3 (25 mg, 0.17 mmol) and TTBB (10 μl, 0.065 mmol). The reaction mixture was stirred for 20 h at room temperature and filtered

(paper). The filtrate was evaporated under vacuum, and the product was purified by silica TLC using an analytical plate (ethyl acetate–hexane, 5:95) for development; $R_f = 0.45$, followed by ethyl acetate for band extraction, giving 1.34 mg (26%). $^1\text{H NMR}$ (C^2HCl_3): δ 8.73 (s, 1H), 8.35–8.12 (m, 7H), 5.71 (s, 2H); 5.56 (s, 2H).

Trace reactions (each in duplicate)

Derivatization of N7-HEX with PFBB. Step 1: N7-HEX (95 pg, 0.49 pmol) in 10 μl of acetic acid–water (1:1), was evaporated under nitrogen. Potassium carbonate (5 mg, 36 μmol), acetonitrile (100 μl) and PFBB (1 μl , 0.38 μmol) were added. After stirring for 20 h at room temperature, the reaction mixture was evaporated under nitrogen.

Step 2: The residue obtained in step 1 was treated with a mixture of 50 μl of 1 M KOH containing 50 μg of Bu_4NHSO_4 , 150 μl of CH_2Cl_2 and 10 μl (3.8 μmol) of PFBB. After stirring for 20 h at room temperature, the product, N1,N3-bis(pentafluorobenzyl)-N7-[2-(pentafluorobenzoyloxy)ethyl]xanthine (**1**), was isolated and quantified by GC–ECNI-MS as described [21].

Derivatization of N7-HEX with PFBB and then TTBB. After step 1 as above, TTBB was used in step 2. The product N1,N3-bis-(pentafluorobenzyl)-N7-[2-[4-(trifluoromethyl)tetrafluorobenzoyloxy]ethyl]xanthine (**2**) was isolated and quantified by GC–ECNI-MS.

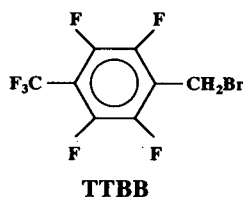
Trace derivatization of N7-HEX with PFBB and then a 1:1 mixture of pentafluorobenzyl bromide and TTBB. After step 1 as above, a 1:1 mixture of pentafluorobenzyl bromide and TTBB was used in step 2. The product mixture of **1** and **2** was isolated and quantified by GC–ECNI-MS.

Trace derivatization of N7-HEX with TTBB. The same procedure was used as above in steps 1 and 2, except TTBB was substituted for pentafluorobenzyl bromide, and the product (**3**) was quantified by GC–ECNI-MS.

RESULTS AND DISCUSSION

In order to establish a new analogue of pentafluorobenzyl bromide (PFBB) for derivatization

purposes, we converted $\alpha,\alpha,\alpha,2,3,5,6$ -heptafluoro-*p*-xylene to 4-(trifluoromethyl)-2,3,5,6-tetrafluorobenzyl bromide (TTBB).

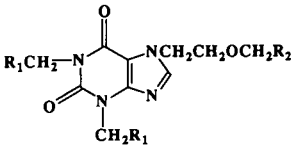
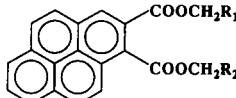


PFBB is a useful reagent both in terms of its reactivity as an alkylating agent, and the GC–ECD or GC–ECNI-MS properties of the derivatives it forms with a diversity of target compounds [1–16]. Thus, in order to test the usefulness of TTBB, we compared it in these two respects with representative compounds. For convenience, we selected two analytes from our current work on the detection of DNA adducts by pentafluorobenzoylation/GC–ECNI-MS: N7-(2-hydroxyethyl)xanthine [21] and 2,3-pyrenedicarboxylic acid [22]. Together these two compounds provide three types of functional groups for derivatization: ring NH, hydroxyethyl OH, and carboxyl.

The derivatives that we formed are shown in Table I, along with reaction yields (preparative starting from 2 mg of N7-HEX, and analytical from 95 pg) and relative molar responses by GC–ECNI-MS. No effort was made to optimize the reaction yields with TTBB (arbitrarily the conditions currently in use with PFBB were adopted). Yet the analytical yields for products **1–3** are all reasonable (as absolute yields at the picogram level), as are the preparative yields of **3** and **4**. These latter reactions were conducted with only 2 mg of starting material in each case. A co-injection of **1**, **2** and **3** gave GC retention times of 7.67, 7.40 and 7.27 min, respectively.

Molar responses in GC–ECNI-MS depend on both the recoveries and electron capture characteristics of the compounds tested in the system. Active sites in the injector, column, and ion source can all contribute to the former, and many parameters can influence the yield of ions from the source [23]. Thus one should be careful not to over-interrupt relative molar response

TABLE I
YIELD AND RESPONSE OF ELECTROPHORIC PRODUCTS

Structure	Yield		Response by GC-ECNI-MS ^a
	Preparative	Analytical	
			
1: R ₁ = R ₂ = C ₆ F ₅	—	27, 45 ^b	1.0
2: R ₁ = C ₆ F ₅ ; R ₂ = (CF ₃)C ₆ F ₄	—	66, 84 ^c	— ^d
3: R ₁ = R ₂ = (CF ₃)C ₆ F ₄	27	40, 66	0.2
			
4: R ₁ = R ₂ = (CF ₃)C ₆ F ₄	26		1.5

^a Molar response relative to 1 based on peak area.

^b This yield is from prior work [18], and the structure of this compound was established previously [2].

^c Analytical yield assuming that 1 and 2 have the same relative molar response.

^d The molar response is not available since this product was not prepared preparatively.

values. We conclude, from the molar response values presented in Table I, that TTBB is similar to pentafluorobenzyl bromide in its ability to provide sensitive derivatives of the compounds tested for GC-ECNI-MS.

The chromatograms A and B in Fig. 1 were obtained by derivatizing 95 µg of N7-(2-hydroxyethyl)xanthine on the N1 and N3 positions with PFBB, followed by derivatization of the hydroxyethyl OH with a 1:1 molar mixture of PFBB and TTBB. Chromatograms of corresponding blank reactions (no analyte) are shown in Fig. 1A' and B'. As seen, a peak with nearly same retention time as 2, but with 1/4 of the abundance, is present in A' but not in B'. For the individual sample leading to chromatogram B, more background peaks are seen, but the corresponding blank chromatogram B' is the cleanest of all. This kind of variation in background peaks as a function of *m/z*, or even one vial vs. another, is encountered sometimes at this level of sensitivity by GC-ECNI-MS in our ex-

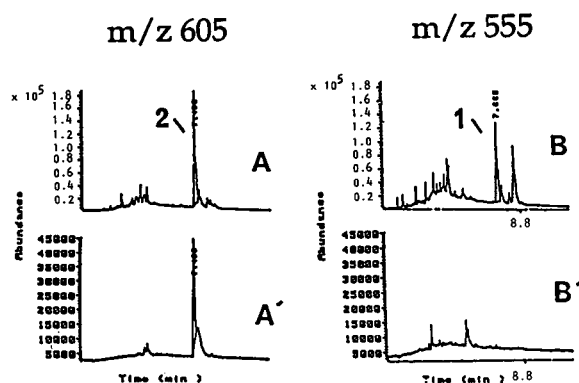


Fig. 1. GC-ECNI-MS chromatograms from the derivatization of N7-(2-hydroxyethyl)xanthine (95 µg) in two steps (see Experimental): step 1 with PFBB, step 2 with PFBB-TTBB, 1:1. Corresponding chromatograms from blank reactions (no analyte) are shown (A', B'). Retention times (min): 1 = 7.67 min; 2 = 7.40 min; highest peak in A', 7.43 min. Note that the abundance scale is expanded by 4× in A', B' relative to A, B.

perience, and supports the usefulness of forming more than derivative.

In conclusion, the availability now of two analogues of pentafluorobenzyl bromide (H or CF₃ at the *para* position instead of F) provides additional flexibility in this area of derivatization to cope with both consistent and random interferences, helping to confirm results. Conveniently, the same column and conditions can be used to quantify these products. Their similar chemical and physical characteristics also allow them to be formed together and co-purified.

ACKNOWLEDGEMENT

This work was supported by Grant OH02792 from the National Institute for Occupational Safety and Health, Centers for Disease Control. Contribution No. 581 from the Barnett Institute of Chemical Analysis.

REFERENCES

- 1 R.M. Kok, A.P.J.M. de Jong, C.J. van Groeningen, G.J. Peters and J. Lankelma, *J. Chromatogr.*, 343 (1985) 59.
- 2 M. Saha, G.M. Kresbach, R.W. Giese, R.S. Annan and P. Vouros, *Biomed. Environ. Mass Spectrom.*, 18 (1989) 958.
- 3 K. Allam, M. Saha and R.W. Giese, *J. Chromatogr.*, 499 (1990) 571.
- 4 R.J. Strife and R.C. Murphy, *J. Chromatogr.*, 305 (1984) 3.
- 5 H. Schweer, G. Mackert and H.W. Seyberth, *Biomed. Environ. Mass Spectrom.*, 19 (1990) 94.
- 6 A. Arbin and P.O. Edlund, *Acta Pharm. Suec.*, 12 (1975) 119.
- 7 S.B. Martin and M. Rowland, *J. Pharm. Sci.*, 61 (1972) 1235.
- 8 O. Gyllenhaal and P. Hartvig, *J. Chromatogr.*, 189 (1980) 351.
- 9 J.E. Greving, J.H.G. Jonkman and R. A. de Zeeuw, *J. Chromatogr.*, 148 (1978) 389.
- 10 J.M. Rosenfeld and J.L. Crocco, *Anal. Chem.*, 50 (1978) 701.
- 11 A.G. Netting and B.V. Milborrow, *Biomed. Environ. Mass Spectrom.*, 17 (1988) 281.
- 12 J.M. Rosenfeld, G.M. Brown, C.H. Walker and C. Sprung, *J. Chromatogr.*, 325 (1985) 309.
- 13 O. Gyllenhaal, H. Brotell and P. Hartvig, *J. Chromatogr.*, 129 (1976) 295.
- 14 E.G. Cotterill, *J. Chromatogr.*, 171 (1979) 478.
- 15 H.L. Wu, S.H. Chen, S.J. Lin, W.R. Hwang, K. Funazo, M. Tanaka and T. Shono, *J. Chromatogr.*, 269 (1983) 183.
- 16 L.J. Roberts and J.A. Oates, *Anal. Biochem.*, 136 (1984) 258.
- 17 R.E. Clement and H.M. Tosine, in B.K. Afghan and A.S.Y. Chau (Editors), *Analysis of Trace Organics in the Aquatic Environment*, CRC Press, Boca Raton, FL, 1989, p. 151.
- 18 S. Abdel-Baky, K. Allam and R.W. Giese, *Anal. Chem.*, 64 (1992) 2882.
- 19 M.A. McClinton and D.A. McClinton, *Tetrahedron*, 48 (1992) 6555.
- 20 C. Sotiriou, W. Li and R.W. Giese, *J. Org. Chem.*, 55 (1990) 2159.
- 21 M. Saha and R.W. Giese, *J. Chromatogr.*, 629 (1993) 35.
- 22 W. Li, C. Sotiriou-Leventis, S. Abdel-Baky, D. Fisher and R.W. Giese, *J. Chromatogr.*, 588 (1991) 273.
- 23 S. Abdel-Baky and R.W. Giese, *Anal. Chem.*, 63 (1991) 2986.

Book Review

Chromatographic retention indices—an aid to identification of organic compounds, by V. Pacáková and L. Feltl, Ellis Horwood, Chichester, 1992, 285 pp., price US\$ 115.00, ISBN 0-13-772328-8.

It is well known that published retention data are given in many forms, and therefore their usefulness in different laboratories is limited. The Kováts retention index solves the problem of the uniform expression of retention data. The retention index according to Kováts is the only retention value in GLC in which the three fundamental quantities, *viz.*, the relative retention, the specific retention volume and the Kováts coefficient, are united. This book deals with chromatographic retention indices, in most instances with the retention index according to Kováts (about 95%).

According to the Preface, dated September 1991, the book is a modernized and enlarged variant of the Czech publication (SNTL, Prague) issued in 1986. This circumstance has caused a break in the scientific level of the book, since the review and the evaluation of papers published after 1986 do not reach the level for the previous period. This 5-year period merits special attention because significant advances have occurred in the field of the retention index system (RIS). Unfortunately, the authors obtained knowledge of considerable research projects, *e.g.*, the solvation parameters according to Abraham *et al.* [*J. Chromatogr.*, 594 (1992) 229] already after closing the manuscript. Similarly, the authors have not covered at all retention index reviews and important papers by different authors (*e.g.*, M.B. Evans and J.K. Haken, R.V. Golovnya *et al.*, G. Tarján *et al.*, Á. Bata *et al.*, J. Bermejo *et al.*, C.J.W. Brooks *et al.*, L. Szepesy *et al.*, F. Wang and Y. Sun and De Zeeuw). It has also escaped their attention that the RIS is becoming more and more a connecting link between retention data and theoretical aspects, especially thermodynamic relationships, in addition to its

original role in the identification of organic compounds.

In the second retention index review by our research group [G. Tarján *et al.*, *J. Chromatogr.*, 472 (1989) 1] we drew attention to the fact that the introduction of the Kováts coefficient created new possibilities for the investigation of the linkage between molecular structure and retention data, as the data for the *n*-alkanes used as reference material pairs do not shield the data to be employed. However, I cannot understand why the retention polarity, occurring in both retention index reviews by our research group, and well established in practice, was not used in the evaluation of the stationary phases as a reference basis. Similarly, our last retention index paper [*J. Chromatogr. Sci.*, 29 (1991) 382] would have helped the present authors with this field of the RIS. The limited extent of the book (which is not the authors' fault) is not commensurate with the significance and results in the special field of GLC. Also, the authors cannot be blamed for the only brief survey of certain non-GLC topics.

After the above general comments, a detailed critical evaluation is presented below, with the remark that the severity of my comments must be attributed to my intense appreciation of and affection for the RIS.

Although a list of references in the Introduction would have covered the history of the subject, its absence is regretted because it would not only have cleared up certain priority questions but would also have drawn attention to the outstanding personalities of the RIS, from Altenburg via Korhonen till Vigdergauz.

In eqns. 1.12 and 1.13 in Chapter 1, the V_g designation is incomplete because the superscript

on V_g^0 has been omitted; this is fundamental because it relates to 0°C . Although the references given cover the essential literature, the basic equation of the retention index and the various equations derived from it using equivalent mathematical transformations appear in a separate chapter.

The title of section 1.2.1 is incomplete; the correct title should have been "Relative retention and relative volatility".

In section 1.2.2, in the first line on p. 20 the designation \cong is correct because any of the reference n -alkanes can be eluted together with the investigated substance. Here the b value in eqn. 1.17, *i.e.*, the slope of the n -alkane plot, should have received much more attention (a separate chapter) from both theoretical and practical respects. This expression is not only the fundamental parameter of the RIS but is also one of the key factors in the qualification and classification of stationary phases in GLC.

At the bottom of p. 20 there is an unfortunate error in eqn. 1.19, where the + sign has been omitted before the $100z$ at the end of the right-hand side of the equation.

In the discussion at the top of p. 21, it should certainly have been mentioned that both methane and ethane do not follow entirely the linear relationships for the homologues and from propane to n -heptane technical measurement problems can affect the linearity.

In section 1.2.3 the MU system according to Vandenhoevel *et al.* [*Biochim. Biophys. Acta*, 64 (1962) 416] has been omitted. It is also important to note the lack of mention of the introduction of the possibility of how these results obtained by means of "other retention index systems" in GLC can be transformed into retention index value, *e.g.*, linear retention index value, MU value.

Section 1.3.1 is the best written part of the book, and it is difficult to see why the other chapters are not as good. The paper by H.C. Furr [*J. Chromatogr. Sci.*, 27 (1989) 216] on simulation possibilities would have deserved mention because of its practical usefulness.

The title of section 1.4 is erroneous. It would have been better to use the original title (ref. 199), as there is no question of a newer RIS,

only the good application of the temperature-programmed retention index.

Chapter 2 is also good. It is unfortunate that the authors have been hindered in the presentation of several comparative tables, applications, etc., just as in the illustration of the close connections between isothermal and temperature-programmed retention indices, owing to the restricted dimensions of the book. Similarly, the lack of explanation of questions connected with the influence of pressure and flow-rate programming and double temperature and carrier gas flow-rate programming on retention indices can also be attributed to size limitations.

Although the inclusion of the indices connected with the constants applied (A_1 , A_2 , etc.) would have complicated the presentation of the equations, their absence is disturbing. Surely, *e.g.*, A is not the same constant in eqns. 2.23 and 2.26?

The relationship between molecular structure and retention index is the most interesting research field in GLC, although size limitations in its discussion can be felt here also. I specially missed retention index tables for steroids, alkoxysilanes, pyrazines, etc., which would have stimulated further research in this field.

In Chapter 4, I cannot understand why the authors have written nothing about the relatively newer results of our research group, although they know of them (ref. 53). However, we have referred many times to the fact that the differences in retention indices at an isothermal column temperature can be considered to be a first approximation in research on molecular structures. The only expedient way is to consider the chemical bonds in the molecule examined with due regard for the primary and secondary atomic environments.

Chapter 5 deals with the stationary phases used in GLC. Size limitations are obvious here also, as the prediction of retention indices receives little attention. The material presented is excellent but the omitted aspects are unfortunate, *e.g.*, papers on Rohrschneider's concept and calculation method, McReynolds' system and the Tekler equation.

In Chapter 6, which deals with retention indices on selected stationary phases, we have to

accept the selection of the authors, but it should be noted that the retention index tables would have been more valuable if they had contained the *b* value and the Kováts coefficients at different isothermal column temperatures.

To summarize, the authors have endeavoured to overcome the problems caused by the limitations on space in a laudable manner. The material presented is of high level and the background literature is comprehensive in most instances.

The book is well presented typographically with few errors. The book covers well the various aspects of both GLC and the RIS, and it should be on the bookshelves of all advanced gas chromatographic laboratories.

Budapest (Hungary)

J.M. Takács

Author Index

- Ahnoff, M., see Witte, D.T. 641(1993)39
- Altria, K.D., Harden, R.C., Hart, M., Hevizi, J., Hailey, P.A., Makwana, J.V. and Portsmouth, M.J.
Inter-company cross-validation exercise on capillary electrophoresis. I. Chiral analysis of clenbuterol 641(1993)147
- Andersson, P.E., Demirbükler, M. and Blomberg, L.G.
Characterization of fuels by multi-dimensional supercritical fluid chromatography and supercritical fluid chromatography-mass spectrometry 641(1993)347
- Armstrong, D.W., see Pawlowska, M. 641(1993)257
- Aue, W.A. and Sun, X.-Y.
Quenching in the flame photometric detector 641(1993)291
- Bald, E. and Sypniewski, S.
Reversed-phase high-performance liquid chromatographic determination of sulphide in an aqueous matrix using 2-iodo-1-methylpyridinium chloride as a precolumn ultraviolet derivatization reagent 641(1993)184
- Beckers, J.L.
Isotachophoresis superimposed on capillary zone electrophoresis 641(1993)363
- Betts, T.J.
Capability of a carbon support to improve the gas chromatographic performance of a liquid crystal phase in a packed column for some volatile oil constituents 641(1993)189
- Bihoreau, N., see Vincentelli, R. 641(1993)383
- Birkenmeier, G., see Walter, H. 641(1993)279
- Blomberg, L.G., see Andersson, P.E. 641(1993)347
- Bonifaci, L. and Ravanetti, G.P.
Thermodynamic study of polystyrene-*n*-alkane systems by inverse gas chromatography 641(1993)301
- Borák, J., see Macka, M. 641(1993)101
- Brites, M.J., Guerreiro, A., Gigante, B. and Marcelo-Curto, M.J.
Quantitative determination of dehydroabietic acid methyl ester in disproportionated rosin 641(1993)199
- Burke, J.A., see Pirkle, W.H. 641(1993)21
- Camacho-Torralba, P.L., Vigh, Gy. and Thompson, D.H.
High-performance chiral displacement chromatographic separations in the normal-phase mode. I. Retention and adsorption studies of potential displacers developed for the Pirkle-type naphthylalanine silica stationary phase 641(1993)31
- Camps, F., see Marco, M.-P. 641(1993)81
- Caruso, J.A., see Vela, N.P. 641(1993)337
- Chen, S., see Pawlowska, M. 641(1993)257
- Choma, I. and Dawidowicz, A.L.
Siliceous sorbents with immobilized Carbowax 20M as column packings for liquid chromatography. I. Application in high-performance liquid chromatography 641(1993)211
- Choma, I., Dawidowicz, A.L., Dobrowolski, R. and Pikus, S.
Siliceous sorbents with immobilized Carbowax 20M as column packings for liquid chromatography. I. Physico-chemical properties of siliceous materials with immobilized Carbowax 20M layer 641(1993)205
- Coll, J., see Marco, M.-P. 641(1993)81
- Dankers, J., Groenenboom, M., Scholtis, L.H.A. and Van der Heiden, C.
High-speed supercritical fluid extraction method for routine measurement of polycyclic aromatic hydrocarbons in environmental soils with dichloromethane as a static modifier 641(1993)357
- Dawidowicz, A.L., see Choma, I. 641(1993)205
- Dawidowicz, A.L., see Choma, I. 641(1993)211
- Delgado, C., see Selisko, B. 641(1993)71
- Demirbükler, M., see Andersson, P.E. 641(1993)347
- De Zeeuw, R.A., see Witte, D.T. 641(1993)39
- Dobrowolski, R., see Choma, I. 641(1993)205
- Ehwald, R., see Selisko, B. 641(1993)71
- Erni, F., see Keller, H.R. 641(1993)1
- Excoffier, J.L., see Keller, H.R. 641(1993)1
- Fingas, M., see Wang, Z. 641(1993)125
- Fischbeck, G., see Schewes, R. 641(1993)89
- Fisher, D., see Selisko, B. 641(1993)71
- Franke, J.-P., see Witte, D.T. 641(1993)39
- Fritz, J.S., see Schmidt, L. 641(1993)57
- Gescher, A., see Mráz, J. 641(1993)194
- Giese, R.W., see Saha, M. 641(1993)400
- Gigante, B., see Brites, M.J. 641(1993)199
- Groenenboom, M., see Dankers, J. 641(1993)357
- Guerreiro, A., see Brites, M.J. 641(1993)199
- Hagel, L., Hartmann, A. and Lund, K.
Analytical gel filtration of dextran for study of the glomerular barrier function 641(1993)63
- Hagen, D.F., see Schmidt, L. 641(1993)57
- Hailey, P.A., see Altria, K.D. 641(1993)147
- Hamana, K., see Niitsu, M. 641(1993)115
- Harden, R.C., see Altria, K.D. 641(1993)147
- Hartmann, A., see Hagel, L. 641(1993)63
- Hart, M., see Altria, K.D. 641(1993)147
- Hayward, M.J., see Snodgrass, J.T. 641(1993)396
- Hevizi, J., see Altria, K.D. 641(1993)147
- Hong, J., see Kim, K.-R. 641(1993)319
- Iwasaki, M., see Yonekura, S. 641(1993)235
- Janoš, P.
Determination of stability constants of metal complexes from ion chromatographic measurements 641(1993)229
- Jhecta, P., see Mráz, J. 641(1993)194
- Jump, W.G., see Wilson, T.D. 641(1993)241
- Kai, M., see Yonekura, S. 641(1993)235
- Kaida, Y. and Okamoto, Y.
Optical resolution by high-performance liquid chromatography on benzylcarbamates of cellulose and amylose 641(1993)267

- Karlsson, K.-E., see Witte, D.T. 641(1993)39
- Keller, H.R., Kiechle, P., Erni, F., Massart, D.L. and Excoffier, J.L.
Assessment of peak homogeneity in liquid chromatography using multivariate chemometric techniques 641(1993)1
- Kibbey, C.E. and Meyerhoff, M.E.
Shape-selective separation of polycyclic aromatic hydrocarbons by reversed-phase liquid chromatography on tetraphenylporphyrin-based stationary phases 641(1993)49
- Kiechle, P., see Keller, H.R. 641(1993)1
- Kim, K.-R., Shim, W.-H., Shin, Y.-J., Park, J., Myung, S. and Hong, J.
Capillary gas chromatography of acidic non-steroidal antiinflammatory drugs as *tert*.-butyldimethylsilyl derivatives 641(1993)319
- Koistinen, J., see Sinkkonen, S. 641(1993)309
- Kolehmainen, E., see Sinkkonen, S. 641(1993)309
- Krstulović, A.M., see Lesellier, E. 641(1993)137
- Lahtiperä, M., see Sinkkonen, S. 641(1993)309
- Lepschy von Gleissenthall, J., see Schewes, R. 641(1993)89
- Lesellier, E., Krstulović, A.M. and Tchaplá, A.
Specific effects of modifiers in subcritical fluid chromatography of carotenoid pigments 641(1993)137
- Levesque, J., see Rey, J.-P. 641(1993)180
- Lund, K., see Hagel, L. 641(1993)63
- Macka, M. and Borák, J.
Chromatographic behaviour of some platinum(II) complexes on octadecylsilica dynamically modified with a mixture of a cationic and an anionic amphiphilic modifier 641(1993)101
- Maidl, F.X., see Schewes, R. 641(1993)89
- Makwana, J.V., see Altria, K.D. 641(1993)147
- Marasas, W.F.O., see Shephard, G.S. 641(1993)95
- Marcelo-Curto, M.J., see Brites, M.J. 641(1993)199
- Marco, M.-P., Sánchez-Baeza, F.J., Camps, F. and Coll, J.
Phytoecdysteroid analysis by high-performance liquid chromatography-thermospray mass spectrometry 641(1993)81
- Markell, C.G., see Schmidt, L. 641(1993)57
- Massart, D.L., see Keller, H.R. 641(1993)1
- Matsuzaki, S., see Niitsu, M. 641(1993)115
- Meyer, V.R. and Palamareva, M.D.
New graph of binary mixture solvent strength in adsorption liquid chromatography 641(1993)391
- Meyerhoff, M.E., see Kibbey, C.E. 641(1993)49
- Morita, I. and Sawada, J. I.
Capillary electrophoresis with on-line sample pretreatment for the analysis of biological samples with direct injection 641(1993)375
- Mráz, J., Jheeta, P., Gescher, A. and Threadgill, M.D.
Unusual deuterium isotope effect on the retention of formamides in gas-liquid chromatography 641(1993)194
- Murray, P.G., see Pirkle, W.H. 641(1993)11
- Murray, P.G., see Pirkle, W.H. 641(1993)21
- Myung, S., see Kim, K.-R. 641(1993)319
- Nakajima, M., Wakabayashi, H., Yamato, S. and Shimada, K.
New labelling agent, 2-[2-(isocyanate)ethyl]-3-methyl-1,4-naphthoquinone, for high-performance liquid chromatography of hydroxysteroids with electrochemical detection 641(1993)176
- Nakazato, T. and Yoza, N.
Detection systems with a photodiode-array detector for flow-injection and high-performance liquid chromatographic determination of phosphinate, phosphonate and diphosphonate 641(1993)221
- Neumann, W.C., see Wilson, T.D. 641(1993)241
- Niitsu, M., Samejima, K., Matsuzaki, S. and Hamana, K.
Systematic analysis of naturally occurring linear and branched polyamines by gas chromatography and gas chromatography-mass spectrometry 641(1993)115
- Ohkura, Y., see Yonekura, S. 641(1993)235
- Okamoto, Y., see Kaida, Y. 641(1993)267
- Palamareva, M.D., see Meyer, V.R. 641(1993)391
- Park, J., see Kim, K.-R. 641(1993)319
- Pawlowska, M., Chen, S. and Armstrong, D.W.
Enantiomeric separation of fluorescent, 6-aminoquinolyl-N-hydroxysuccinimidyl carbamate, tagged amino acids 641(1993)257
- Perry, R.L., see Tindall, G.W. 641(1993)163
- Pikus, S., see Choma, I. 641(1993)205
- Pirkle, W.H. and Murray, P.G.
Chiral stationary phase design. Use of intercalative effects to enhance enantioselectivity 641(1993)11
- Pirkle, W.H., Murray, P.G. and Burke, J.A.
Use of homologous series of analytes as mechanistic probes to investigate the origins of enantioselectivity on two chiral stationary phases 641(1993)21
- Portsmouth, M.J., see Altria, K.D. 641(1993)147
- Pousset, J.-L., see Rey, J.-P. 641(1993)180
- Ravanetti, G.P., see Bonifaci, L. 641(1993)301
- Reinhold, N.J., Tjaden, U.R. and Van der Greef, J.
Automated isotachophoretic analyte focusing for capillary zone electrophoresis in a single capillary using hydrodynamic back-pressure programming 641(1993)155
- Rey, J.-P., Levesque, J. and Pousset, J.-L.
Analytical studies of *dl*-stylopine in *Chelidonium majus* L. using high-performance liquid chromatography 641(1993)180
- Reynolds, D.L., see Sly, L.A. 641(1993)249
- Roth, M.
Thermodynamic pitfalls in chromatography revisited: supercritical fluid chromatography 164(1993)329
- Saha, J., see Saha, M. 641(1993)400
- Saha, M., Saha, J. and Giese, R.W.
4-(Trifluoromethyl)-2,3,5,6-tetrafluorobenzyl bromide as a new electrophoric derivatizing reagent 641(1993)400
- Samejima, K., see Niitsu, M. 641(1993)115
- Sánchez-Baeza, F.J., see Marco, M.-P. 641(1993)81
- San Martin, T., see Wilson, T.D. 641(1993)241
- Sawada, J.-I., see Morita, I. 641(1993)375

- Schewes, R., Maidl, F.X., Fischbeck, G., Lepschy von Gleisenthall, J. and Süss, A.
Trace determination of weathered atrazine and terbuthylazine and their degradation products in soil by high-performance liquid chromatography–diode-array detection 641(1993)89
- Schmidt, L., Sun, J.J., Fritz, J.S., Hagen, D.F., Markell, C.G. and Wisted, E.E.
Solid-phase extraction of phenols using membranes loaded with modified polymeric resins 641(1993)57
- Scholtis, L.H.A., see Dankers, J. 641(1993)357
- Selisko, B., Delgado, C., Fisher, D. and Ehwald, R.
Analysis and purification of monomethoxy-polyethylene glycol by vesicle and gel permeation chromatography 641(1993)71
- Shephard, G.S., Thiel, P.G., Marasas, W.F.O., Sydenham, E.W. and Vleggaar, R.
Isolation and determination of AAL phytotoxins from corn cultures of the fungus *Alternaria alternata* f. sp. *lycopersici* 641(1993)95
- Shim, W.-H., see Kim, K.-R. 641(1993)319
- Shimada, K., see Nakajima, M. 641(1993)176
- Shin, Y.-J., see Kim, K.-R. 641(1993)319
- Sinkkonen, S., Kolehmainen, E., Koistinen, J. and Lahtiperä, M.
High-resolution gas chromatographic–mass spectrometric determination of neutral chlorinated aromatic sulphur compounds in stack gas samples 641(1993)309
- Sly, L.A., Reynolds, D.L. and Walker, T.A.
Isomeric separation of Beraprost sodium using an α -acid glycoprotein column 641(1993)249
- Snodgrass, J.T., Hayward, M.J. and Thomson, M.L.
Time- and cost-saving approach for liquid chromatography–mass spectrometry vacuum systems 641(1993)396
- Sun, J.J., see Schmidt, L. 641(1993)57
- Sun, X.-Y., see Aue, W.A. 641(1993)291
- Süss, A., see Schewes, R. 641(1993)89
- Sydenham, E.W., see Shephard, G.S. 641(1993)95
- Sypniewski, S., see Bald, E. 641(1993)184
- Takács, J.M.
Chromatographic retention indices—an aid to identification of organic compounds (by V. Pacáková and L. Felt) (Book Review) 641(1993)405
- Tchapla, A., see Lesellier, E. 641(1993)137
- Thiel, P.G., see Shephard, G.S. 641(1993)95
- Thompson, D.H., see Camacho-Torrallba, P.L. 641(1993)31
- Thomson, M.L., see Snodgrass, J.T. 641(1993)396
- Threadgill, M.D., see Mráz, J. 641(1993)194
- Tindall, G.W., Wilder, D.R. and Perry, R.L.
Optimizing dynamic range for the analysis of small ions by capillary zone electrophoresis 641(1993)163
- Tjaden, U.R., see Reinhoud, N.J. 641(1993)155
- Van der Greef, J., see Reinhoud, N.J. 641(1993)155
- Van der Heiden, C., see Dankers, J. 641(1993)357
- Vela, N.P. and Caruso, J.A.
Comparison of flame ionization and inductively coupled plasma mass spectrometry for the detection of organometallics separated by capillary supercritical fluid chromatography 641(1993)337
- Vigh, Gy., see Camacho-Torrallba, P.L. 641(1993)31
- Vincentelli, R. and Bihoreau, N.
Characterization of each isoform of a F(ab')₂ by capillary electrophoresis 641(1993)383
- Vleggaar, R., see Shephard, G.S. 641(1993)95
- Wakabayashi, H., see Nakajima, M. 641(1993)176
- Walker, T.A., see Sly, L.A. 641(1993)249
- Walter, H., Widen, K.E. and Birkenmeier, G.
Immobilized metal ion affinity partitioning of erythrocytes from different species in dextran–poly(ethylene glycol) aqueous phase systems 641(1993)279
- Wang, Z. and Fingas, M.
Quantitative analysis of polyethoxylated octylphenol by capillary supercritical fluid chromatography 641(1993)125
- Widen, K.E., see Walter, H. 641(1993)279
- Wilder, D.R., see Tindall, G.W. 641(1993)163
- Wilson, T.D., Jump, W.G., Neumann, W.C. and San Martin, T.
Validation of improved methods for high-performance liquid chromatographic determination of phenylpropanolamine, dextromethorphan, guaifenesin and sodium benzoate in a cough-cold formulation 641(1993)241
- Wisted, E.E., see Schmidt, L. 641(1993)57
- Witte, D.T., Ahnoff, M., Karlsson, K.-E., Franke, J.-P. and De Zeeuw, R.A.
Liquid chromatographic chiral separations of the N-6-(endo-2-norbornyl)-9-methyladenine enantiomers 641(1993)39
- Wu, G.
Determination of proline by reversed-phase high-performance liquid chromatography with automated pre-column *o*-phthalaldehyde derivatization 641(1993)168
- Yamato, S., see Nakajima, M. 641(1993)176
- Yeung, E.S.
A practical guide to HPLC detection (by D. Parriott) (Book Review) 641(1993)203
- Yonekura, S., Iwasaki, M., Kai, M. and Ohkura, Y.
High-performance liquid chromatography of guanine and its nucleosides and nucleotides by pre-column fluorescence derivatization with phenylglyoxal reagent 641(1993)235
- Yoza, N., see Nakazato, T. 641(1993)221

PUBLICATION SCHEDULE FOR THE 1993 SUBSCRIPTION

Journal of Chromatography and Journal of Chromatography, Biomedical Applications

MONTH	1992	J	F	M	A	M	J	J	
Journal of Chromatography	Vols. 623–627	628/1 628/2 629/1 629/2	630/1 + 2 631/1 + 2 632/1 + 2 633/1 + 2	634/1 634/2	635/1 635/2 636/1 636/2	637/1 637/2 638/1 638/2	639/1 639/2 640/1 + 2	641/1 641/2 642/1 + 2 643/1 + 2 644/1	The publication schedule for further issues will be published later.
Cumulative Indexes, Vols. 601–650									
Bibliography Section				649/1			649/2		
Biomedical Applications		612/1	612/2	613/1	613/2 614/1	614/2 615/1	615/2 616/1	616/2 617/1	

INFORMATION FOR AUTHORS

(Detailed *Instructions to Authors* were published in Vol. 609, pp. 437–443. A free reprint can be obtained by application to the publisher, Elsevier Science Publishers B.V., P.O. Box 330, 1000 AH Amsterdam, Netherlands.)

Types of Contributions. The following types of papers are published in the *Journal of Chromatography* and the section on *Biomedical Applications*: Regular research papers (Full-length papers), Review articles, Short Communications and Discussions. Short Communications are usually descriptions of short investigations, or they can report minor technical improvements of previously published procedures; they reflect the same quality of research as Full-length papers, but should preferably not exceed five printed pages. Discussions (one or two pages) should explain, amplify, correct or otherwise comment substantively upon an article recently published in the journal. For Review articles, see inside front cover under Submission of Papers.

Submission. Every paper must be accompanied by a letter from the senior author, stating that he/she is submitting the paper for publication in the *Journal of Chromatography*.

Manuscripts. Manuscripts should be typed in **double spacing** on consecutively numbered pages of uniform size. The manuscript should be preceded by a sheet of manuscript paper carrying the title of the paper and the name and full postal address of the person to whom the proofs are to be sent. As a rule, papers should be divided into sections, headed by a caption (e.g., Abstract, Introduction, Experimental, Results, Discussion, etc.) All illustrations, photographs, tables, etc., should be on separate sheets.

Abstract. All articles should have an abstract of 50–100 words which clearly and briefly indicates what is new, different and significant. No references should be given.

Introduction. Every paper must have a concise introduction mentioning what has been done before on the topic described, and stating clearly what is new in the paper now submitted.

Illustrations. The figures should be submitted in a form suitable for reproduction, drawn in Indian ink on drawing or tracing paper. Each illustration should have a legend, all the *legends* being typed (with double spacing) together on a *separate sheet*. If structures are given in the text, the original drawings should be supplied. Coloured illustrations are reproduced at the author's expense, the cost being determined by the number of pages and by the number of colours needed. The written permission of the author and publisher must be obtained for the use of any figure already published. Its source must be indicated in the legend.

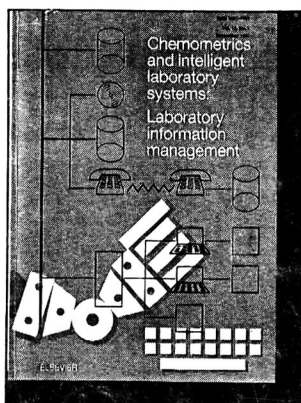
References. References should be numbered in the order in which they are cited in the text, and listed in numerical sequence on a separate sheet at the end of the article. Please check a recent issue for the layout of the reference list. Abbreviations for the titles of journals should follow the system used by *Chemical Abstracts*. Articles not yet published should be given as "in press" (journal should be specified), "submitted for publication" (journal should be specified), "in preparation" or "personal communication".

Dispatch. Before sending the manuscript to the Editor please check that the envelope contains four copies of the paper complete with references, legends and figures. One of the sets of figures must be the originals suitable for direct reproduction. Please also ensure that permission to publish has been obtained from your institute.

Proofs. One set of proofs will be sent to the author to be carefully checked for printer's errors. Corrections must be restricted to instances in which the proof is at variance with the manuscript. "Extra corrections" will be inserted at the author's expense.

Reprints. Fifty reprints will be supplied free of charge. Additional reprints can be ordered by the authors. An order form containing price quotations will be sent to the authors together with the proofs of their article.

Advertisements. The Editors of the journal accept no responsibility for the contents of the advertisements. Advertisement rates are available on request. Advertising orders and enquiries can be sent to the Advertising Manager, Elsevier Science Publishers B.V., Advertising Department, P.O. Box 211, 1000 AE Amsterdam, Netherlands; courier shipments to: Van de Sande Bakhuyzenstraat 4, 1061 AG Amsterdam, Netherlands; Tel. (+31-20) 515 3220/515 3222, Telefax (+31-20) 6833 041, Telex 16479 els vi nl. UK: T.G. Scott & Son Ltd., Tim Blake, Portland House, 21 Narborough Road, Cosby, Leics. LE9 5TA, UK; Tel. (+44-533) 753 333, Telefax (+44-533) 750 522. USA and Canada: Weston Media Associates, Daniel S. Lipner, P.O. Box 1110, Greens Farms, CT 06436-1110, USA; Tel. (+1-203) 261 2500, Telefax (+1-203) 261 0101.



Audience

Chemists, pharmacists, computer scientists and managers working in academic, clinical, industrial and government laboratories.



Elsevier Science Publishers

Attn. Carla G.C. Stokman
P.O. Box 330, 1000 AH Amsterdam
The Netherlands

Fax: (+31-20) 5862 845

In the USA & Canada

Attn. Judy Weislogel
P.O. Box 945, Madison Square Station
New York, NY 10160-0757, USA
Fax: (212) 633 3880

LABORATORY INFORMATION MANAGEMENT

Section of CHEMOMETRICS AND INTELLIGENT LABORATORY SYSTEMS

Editor:

R.D. McDowall, *The Wellcome Research Laboratories, Beckenham, Kent, UK*

Coordinating Editor:

D.L. Massart, *University of Brussels, Brussels, Belgium*

Editor for North America:

R.R. Mahaffey, *Eastman Chemical Company, Kingsport, TN, USA*

Associate Editor:

R.E. Dessy, *Virginia Polytechnic Institute, Blacksburg, VA, USA*

AIMS AND SCOPE

The journal covers all aspects of information management in a laboratory environment, such as information technology, storage, processing and flow of data. The following topics are covered:

- ❖ **Laboratory Information Management Systems (LIMS):** Systems architecture, database design, novel aspects of interfacing, methods of data acquisition and integration with other computer applications and instruments.
- ❖ **Means of integrating and merging laboratory information:** Document preparation using chemical structures, spectra, results and text; corporate communication.
- ❖ **Networks:** Novel technology for the dissemination, storage and retrieval of information.
- ❖ **Regulatory Aspects:** Development and implementation of governmental guidelines and regulations and industry standards, and their effect on information management.
- ❖ **Electronic Laboratory Notebooks.**
- ❖ **Human aspects of laboratory automation:** The application of chemometrics and expert systems to handle laboratory information is within the scope of the journal. The application of robotics or dedicated automation systems is of interest where these systems form part of an integrated solution for information management. The journal aims to cover micro-, mini-, and mainframe applications and systems, both those designed in-house or available commercially.

The journal publishes five types of papers: **Original research papers, Tutorial articles, Case studies, State-of-the-art review articles, and Short communications.** A **Monitor Section** provides news on meetings, book and software reviews, a calendar of forthcoming events, etc.

ABSTRACTED/INDEXED IN: ASCA, Analytical Abstracts, BioSciences Information Service, Cambridge Scientific Abstracts, Chromatography Abstracts, Current Contents, Current Index to Statistics, Excerpta Medica, INSPEC, SCISEARCH.

1993: SUBSCRIPTION INFORMATION

Volume 21 In 3 Issues

Dfl. 448.00 / US \$ 256.00 (including postage) ISSN 0925-5281

- I would like a free sample copy of Laboratory Information Management.
- Instructions to Authors.
- to enter a subscription for 1993.
Please send me a Proforma Invoice.

Name _____

Address _____

The Dutch Guilder price (Dfl.) is definitive. US\$ prices are for your convenience only and are subject to exchange fluctuations. Customers in the European Community should add the appropriate VAT rate applicable in their country to the price(s).

71141411430065



0021-9673(19930709)641:2;1-Y